

PROCEEDINGS



EurCOLD

Dear EURCOLD Members and Colleagues of Dam Sector

On behalf of the EURCOLD Board and on my behalf, it is a great honour for me to invite our European National Committees, dam experts, engineers, and researchers, young professional and students to participate in the 13 th EURCOLD Symposium, which will be held in Bydgoszcz, Poland, from the 21st to the 25th of September 2026.

I invite you to come to the EURCOLD 2026 in Poland, not only to discuss the professional topics and sharing of knowledge, also to meet friends and colleagues of EURCOLD family.

Polish Committee on Large Dams POLCOLD is hosting the 13th ICOLD European Club Meeting and Symposium. I am sure that POLCOLD will arrange a high -quality technical content for the symposium along with an unforgettable cultural and social programme. Bydgoszcz, located in northern Poland, is a charming city known for its historic architecture, picturesque canals and vibrant cultural life. With this unique blend of history, nature and culture, this city provides an inspiring setting for our scientific and technical discussions.

The Symposium will bring together dam experts, researchers, engineers, and young professionals and decision makers from across Europe and beyond to exchange knowledge and European experience on topics related to dam engineering, Leeves and Tailing dams, Dam and Reservoir safety management for people, Risk assessment, Dams legal conditions and technical requirements, and sustainable infrastructure development.

Additionally, the networking opportunities available during this event can facilitate new partnerships and enhance your professional connections.

This symposium will also be marked by the celebration of the 100 th anniversary of CFBR, highlighting a century of achievements in Dam engineering.

Your professional background and experience make your participation particularly valuable and we would be honoured to welcome you as a participant in this important scientific and technical event.

We sincerely hope you will be able to join us in Bydgoszcz, Poland and contribute to the success of the 13th EURCOLD Symposium.

Yours Sincerely

Arjan JOVANI

President of EURCOLD

Polski Komitet Wielkich Zapór
POLCOLD

Dear Friends, EURCOLD members, colleagues in hydroengineering!

It is a great honour for me to welcome you to a historic moment for our European community of dam engineers and experts. Polish Committee on Large Dams POLCOLD is hosting the 13th ICOLD European Club Meeting and Symposium, which will be held from the 21st to the 25th of September 2026 in Bydgoszcz, Poland.

I direct this invitation to all national committees in Europe and to persons involved in dam engineering and water management in the world.

Bydgoszcz, the city of the Symposium, is located on the watershed of the Wisła and Odra rivers, connecting two basins and becoming the capital of Polish hydroengineering in a certain sense. For ages, Bydgoszcz has been situated near rivers and hydroengineering infrastructure. I hope our meeting in Bydgoszcz will be a breathtaking event, not only because of the Symposium programme but because of the beauty of the city as well.

A visit to significant dams in the surrounding area of Bydgoszcz is planned for all participants. It will be a pleasure to present to you some examples of dams constructed in 1930's as part of a development programme realised after regaining independence.

The seminar will focus particularly on water management conditions, the most common operational problems, maintenance, failures and other events, including extreme weather phenomena. It will be a great opportunity to exchange and share European experience and knowledge of dam engineering and levees.

One of the afternoon sessions will be devoted to CFBR/French-COLD history and achievements. Together with our French friends, we will celebrate the 100th anniversary.

We keep on building our relationship between all people involved in dam care, from designers through executors to users, continuing the tightening of cooperation.

I look forward to seeing you in Bydgoszcz; it will be an unforgettable experience.

Yours,

Piotr Śliwiński

President
Polish Committee on Large Dams

Organising Committee

Piotr Śliwiński - Chairman

Agata Lethel – French Day

Krzysztof Wrzosek – publications

Dagmara Zelaya Wziątek – Young Professionals

Maciej Sieinski – sponsors

Ludgarda Iłowska-Smietana – ENEA field trip

Scientific Committee

Paweł Falaciński – Chairman

Paweł Popielski – Vice-chairman

Zbigniew Kledyński – Member

Subjects and topics

A. Dams and reservoir safety management for people

- dam safety assessment, inspection and monitoring
- water management for people, drought and flood control
- risk assessment due to climate and social changes
- legal conditions and technical requirements for safe dams
- tourism, irrigation and other benefits of dams and reservoirs
- warning systems for dam surrounding
- failures - lessons learnt

B. Dams and Energy

- pump storage plants – construction and exploitation
- new technologies and solutions in waterpower
- exploitation of dams for waterpower

C. Dam Engineering and Construction

- dam aging problems and solutions applied – case studies
- construction repair technologies and materials
- reconstructions, expansions and development of old dams
- development of design methods

D. Levees and tailing dams

- levees and tailing dams monitoring and safety evaluation
- design methods development for levees
- tailing dam seismic resilience monitoring
- slurry and water management

SESSION A (part I). Dams and reservoir safety management for people		
1	Tomasz Howiacki	Practical Implementation of Distributed Fibre Optic Sensing in Earth Dams: From Laboratory Models to Field Applications
2	Alexandre Jean Pachoud	Wind-wave contributions to freeboard determination in Swiss Alpine reservoirs: A systematic analysis
3	Laurent Peyras	European BECCA project: Solutions for safe reservoirs, integrated into their environment and respectful of biodiversity, as part of climate change adaptation in mountain areas
4	Daniel Gaftoi	Behaviour Monitoring and Safety Assessment of a Very High Arch Dam during Reservoir Drawdown
5	Krzysztof Zamiar	Experimental investigation of earth dam breaching – latest research results
6	Ludivine Saint-Mard	Reassessing Seismic Risk for Hydraulic Dams Through Worldwide Experience Feedback

Practical Implementation of Distributed Fibre Optic Sensing in Earth Dams: From Laboratory Models to Field Applications

Tomasz Howiacki

tomasz.howiacki@pk.edu.pl

authorsList

1. Rafał Sieńko
2. Łukasz Bednarski
3. Tomasz Howiacki
4. Katarzyna Zuziak

affiliationsList

1. PhD, Eng., Faculty of Civil Engineering, Cracow University of Technology, Warszawska 24, 31-155 Kraków, Poland, 0000-0002-2751-7558

2. PhD, Eng., Faculty of Mechanical Engineering and Robotics, AGH University of Kraków, Mickiewicza 30, 30-059 Kraków, Poland, 0000-0002-5404-9921

3. PhD, Eng., Faculty of Civil Engineering, Cracow University of Technology, Warszawska 24, 31-155 Kraków, Poland, 0000-0002-6833-7203

4. Msc, MBA, SHM System | Nerve-Sensors, Libertów, Jana Pawła II 82A, 30-444 Kraków, Poland, 0000-0002-3577-399X

keywords

distributed fibre optic sensing, earth dams, dam monitoring, geotechnical instrumentation, structural safety

Abstract:

Earth dams require monitoring systems capable of identifying spatially localised changes that may remain undetected between conventional point sensors. Distributed fibre optic sensing (DFOS) addresses this limitation by providing continuous measurements along the full length of an installed sensing element. Depending on the interrogation technique, the same monitoring concept can be applied to strain, temperature, vibration or displacement assessment.

This paper examines the practical use of DFOS in earth-dam monitoring, with emphasis on the transition from laboratory investigations to full-scale engineering applications. The discussion covers sensor selection, installation procedures and the relationship between sensor-soil interaction and the quality of recorded data. Particular attention is paid to sensor routing, anchorage, protection against installation damage and the achievement of adequate mechanical coupling with the surrounding soil. These factors determine whether measured responses can be interpreted as representative of the actual behaviour of the dam body.

Selected examples derived from experimental and field measurements are used to illustrate differences between controlled small-scale conditions and operating earth dams. Laboratory models allow installation parameters and loading conditions to be examined systematically, whereas field implementation introduces variable soil properties, construction tolerances, environmental effects and constraints associated with existing infrastructure. The paper identifies the principal challenges arising from this scale transition and discusses their consequences for data processing and interpretation.

The study demonstrates how laboratory experience can support the design of reliable field monitoring schemes while also showing why installation procedures must be adapted to site-specific conditions. The findings provide practical guidance for incorporating DFOS into dam-safety assessment and long-term monitoring programmes.

Chloé Lehmann

Dam Safety Intern

Dam Safety Unit

Swiss Federal Office of Energie SFOE, 3003 Bern, Switzerland

Alexandre Jean Pachoud

Dam Safety Specialist

Dam Safety Unit

Swiss Federal Office of Energie SFOE, 3003 Bern, Switzerland

Corresponding author: alexandre.pachoud@bfe.admin.ch

Marius Bühlmann

Team Lead Dam Analytics

Axpo Power AG, Parkstrasse 23, 5401 Baden, Switzerland

Wind-wave contributions to freeboard determination in Swiss Alpine reservoirs: A systematic analysis

Wind-generated waves and run-up are a crucial component of freeboard for dam safety, yet input uncertainties persist when applying wind-wave run-up estimation methods. This paper reviews the Swiss regulatory framework for freeboard and evaluates empirical methods for wave run-up. By applying these approaches to all large Swiss dams using public wind data, the study critically compares results against current directives. It concludes with recommendations for a comprehensive safety freeboard determination framework while addressing key practical uncertainties.

KEYWORDS: Dam safety; Wind-waves; Run-up; Freeboard; Alpine reservoirs

INTRODUCTION

The impact of wind-generated waves in reservoirs plays a major role in defining the safety freeboard for Alpine dams, particularly for embankment dams. Numerous quantitative methods are available, but the data required for their application – especially regarding wind – are often difficult to obtain. Furthermore, the scopes of application for these various methods are not always clear to practitioners. While the dam community widely considers approaches that limit freeboard allowance based on wave run-up estimates, more recent approaches from the coastal community regarding overtopping discharge limits have yet to be systematically applied to reservoirs (Pullen et al., 2018).

In this paper, the regulatory framework in Switzerland regarding flood safety and safety freeboard determination is first presented. Salient empirical, equation-based approaches for estimating wind-waves, run-up, and overtopping discharge are then reviewed. A systematic application of a selection of approaches is performed for all large dams in Switzerland using publicly available wind data. The various approaches are critically compared, and the aggregated results are assessed from a high-level perspective against the current Swiss directive for dam safety against floods. Finally, recommendations are provided for developing a comprehensive framework for freeboard allowance in Switzerland, highlighting the main uncertainties in practice.

REGULATORY FRAMEWORK AND CHALLENGES IN SWITZERLAND

In Switzerland, dam safety is regulated under the Federal Act on Water Retaining Facilities (WRFA, SR 721.101) and the Water Retaining Facilities Ordinance (WRFO, SR 721.101.1), where the Swiss dam safety concept is detailed: (1) structural safety (including safety against flood); (2) surveillance and maintenance; and (3) emergency planning. According to the regulation, dams are classified into three classes as a function of the water storage height and the storage capacity, as a proxy for the potential consequences in case of dam breach. The dams in classes I and II are *large* dams under *direct* federal supervision, while dams in Class III are mostly smaller dams under the supervision of the Swiss cantons, subject an *indirect* federal supervision. The Swiss Federal Office of Energy (SFOE) is the federal authority responsible for the safety supervision. Approximately 225 large dams (mostly built between 1940s and 1970s, see Schwager et al., 2023) are under direct supervision for SFOE

in Switzerland, and some 200 dams under indirect supervision. The spread of dams under direct and indirect safety supervisions as a function of storage capacity and storage height in Switzerland is depicted in Fig. 1. The distribution of large dams under direct supervision per dam type is shown in Fig. 2.

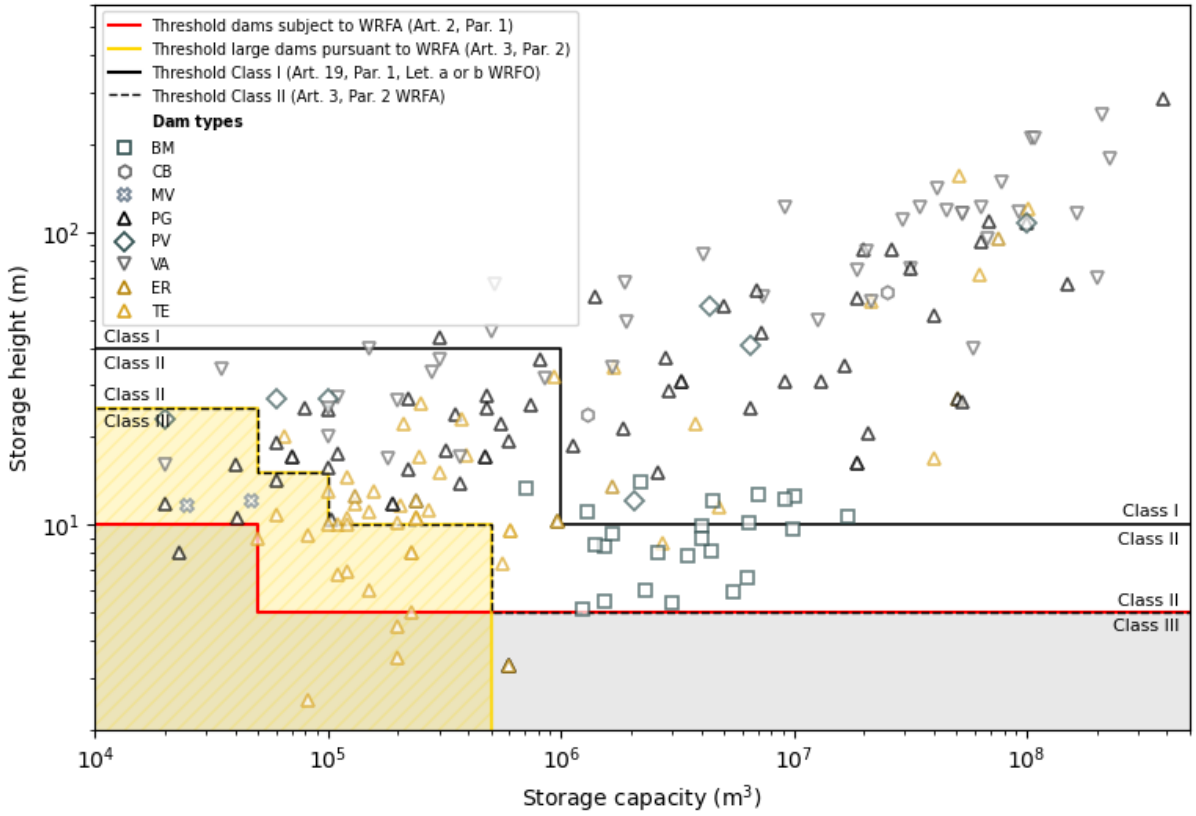


Fig. 1. Distribution of dams under direct federal supervision per dam class (from Pachoud et al., 2025). BM: weir; CB: buttress dam; MV: multiple arch dam; PG: gravity dam; PV: gravity arch dam; VA: arch dam; ER: rockfill dam; TE: earth dam

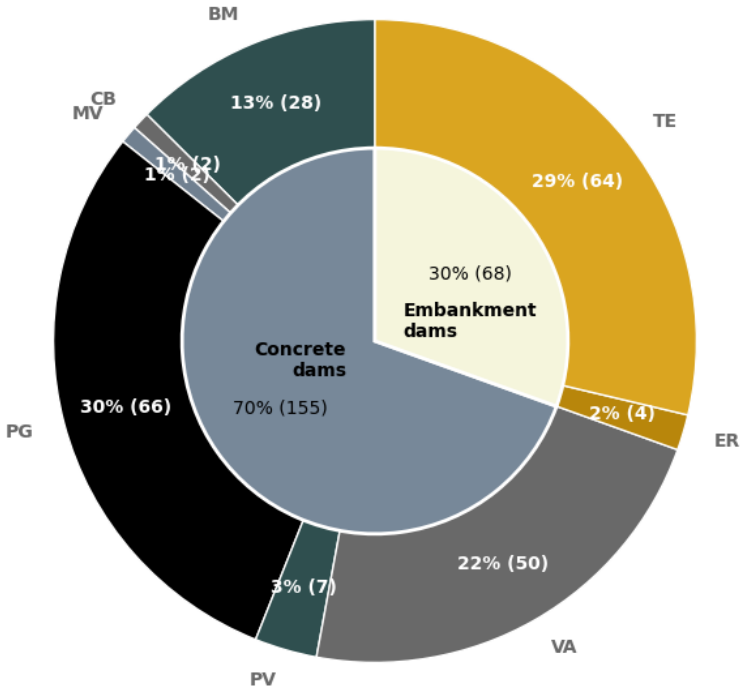


Fig. 2. Distribution of dams under direct federal supervision per dam type (from Pachoud et al., 2025). BM: weir; CB: buttress dam; MV: multiple arch dam; PG: gravity dam; PV: gravity arch dam; VA: arch dam; ER: rockfill dam; TE: earth dam

The Swiss regulation is implemented under the guidance of the *Directive on the safety of water retaining facilities* (referred to the *Swiss directive* hereinafter), enacted by the SFOE and published in 5 parts (A to E). The Swiss directive materialises the dam safety concept and prescribes minimum safety requirements. The safety requirements for dam safety against flood are prescribed in the Part C2 of the Swiss directive (SFOE, 2018). Pursuant to the latter, dams under direct federal supervision must be checked against a *design flood* (extraordinary situation) and a *safety check flood* (extreme situation), corresponding to 1'000-year return period, and a *much larger return period* (typically greater than 10'000-year, or the Probable Maximum Flood), respectively. In the extreme situation, water level must not exceed the *danger level*, defined in the directive as the level above which dam safety is compromised. Without special studies, it typically corresponds to the highest watertight elevation of the dam (in general, dam crest or parapet elevation for concrete dams; and the highest level of watertightness element for embankment dams). In the Swiss directive, the *safety freeboard* is defined as the distance between the highest water level reached in the extraordinary situation and the danger level. The safety freeboard aims at ensuring that there is no damage due to possible waves. During a flood event, this typically refers to wind-waves. Components of the total freeboard (in relation to the operation level) may also account for impacts such as

impulse waves or seismic-induced oscillations (*Seiche*), but these are out of the scope of this study.

The Part C2 of the Swiss directive (SFOE, 2018) provides standard values for minimum required safety freeboard, as a function of dam type and dam height, see Tab. 1. These values may be reduced only if substantiated by facility-specific studies. However, the directive does not provide general requirements or guidance for such studies. Moreover, the determination of relevant wind velocities is subject to large uncertainties, particularly in Alpine territories where topography may also play a major role, making wind station data transfer difficult. In this context, it may be challenging both for operators and dam safety authorities to define admissible safety concepts. The actual level of conservativeness (or lack of conservativeness) of the minimum required safety freeboard of Tab. 1 was also not systematically analysed. In this study, these challenges are discussed through a systematic application of wind-induced waves and run-up estimation methods at all dams under direct federal supervision, including a critical selection of wind inputs.

Tab. 1. Standard values for minimum required freeboard according to the Swiss directive (SFOE, 2018)

Dam height	$\boldsymbol{H \geq 10\ \mathrm{m}}$	$\boldsymbol{10\ \mathrm{m} < H < 40\ \mathrm{m}}$	$\boldsymbol{H \leq 40\ \mathrm{m}}$
Concrete dams	0.5 m	linear interpolation	1.0 m
Embankment dams			
- without u/s riprap	1.0 m	linear interpolation	3.0 m
- with u/s riprap	1.0 m	linear interpolation	2.5 m

REVIEW OF WIND-WAVES AND RUN-UP ESTIMATION METHODS

Wind-wave calculation methods were originally developed for coastal protection. Various empirical methods have been developed based on measurement campaigns in the course of the 20th century. Numerical modelling is an alternative to empirical methods to calculate wind-waves, more accurately accounting for the reservoir shape, the geometry of the dam crest and the wind fields.

In this study, the use of numerical modelling has been excluded due to the large resources it would have required to be applied at approximately 200 Swiss reservoirs. For the systematic analysis, empirical methods have been considered more suitable, particularly with

the objective to provide insights to the dam engineers for proportionate practical applications. Various empirical methods are the basis of standards or guidelines for freeboard determination at dams. For this study, three salient standards and guidelines have been considered:

1. (DVWK, 1997): a guide for freeboard determination at dams published by the German Association for Water Management and Irrigation Engineering (DVWK), which is based on the Krylow II parametrically structured spectral method for the wave height;
2. (ICE, 2015): a guide for floods and reservoir safety published by the Institution of Civil Engineers (UK), which is based on the methodologies for predicting waves and wave overtopping in the first edition of the EurOtop manual (now superseded by the second edition, EurOtop II, 2018); the wave height determination is based on the simplified Donelan/JONSWAP method; and
3. (USBR, 2021): design standard for embankment dams published by the U.S. Bureau of Reclamation (USA), based on the guidelines of the Coastal Engineering Manual (USACE, 2015).

These guidelines have the advantage to provide a dam-specific framework for freeboard determination and are based on different methods for waves and run-up estimate. (DVWK, 1997) and (USBR, 2021) are commonly used by practitioners in Switzerland and prescribe a freeboard allowance based on wave run-up estimate. Application of the methodologies of the EurOtop manual in the frame of (ICE, 2015) was to date more seldom but is gaining attention due to the interesting change of paradigm by embracing approaches that rather allow estimating overtopping against admissible values. The three selected methods are briefly described hereinafter, where only the run-up equations are presented. The reader shall refer to the references for the complete description of the approaches.

Method of (DVWK, 1997)

In the method of (DVWK, 1997), a mean wave height H_{We} is calculated accounting for the contributions of partial mean waves from different sectors of the reservoir (illustrated in Fig. 4). The mean wave height is then converted to a wave height with given exceedance probability $H_{We,x\%}$ assuming a Rayleigh distribution.

For vertical walls (e.g., gravity and arch dams), the wave run-up $R_{x\%}$ of a x exceedance probability (%) corresponds to the wave height of the corresponding exceedance probability:

$$R_{x\%} = H_{We,x\%} \tag{1}$$

For inclined walls (e.g., embankment dams) with slopes lower than 1.6H:1.0V, $R_{x\%}$ is estimated according to Eq. (2):

$$R_{x\%} = k_D k_R \cdot k_x \cdot \sqrt{(H_{We} \cdot L_m)} \cdot \tan\alpha \tag{2}$$

where $k_D k_R$ is a roughness coefficient characterising the upstream face of the dam; k_x is a conversion factor to a certain probability of exceedance x; L_m is the mean wave length and α is the upstream face slope. In the (DVWK, 1997) guide, values for k_x are suggested based on dam type (i.e., lower probabilities of exceedance are suggested for dams more sensitive to overtopping). To cope with the limit of application of Eq. (2) in relation to the slope, more recent developments can be considered (Bornschein & Pohl, 2012; Pohl, 2019) to account for steeper slopes.

Method of (ICE, 2015)

In the guide of (ICE, 2015), the significant wave height H_S is calculated according to the simplified Donelan/JONSWAP method. The reservoir fetch to be used in the empirical equations is longest straight line from the dam axis (illustrated in Fig. 5), possibly extended by one directional change in case of bent or "banana"-shape of the reservoir.

The approach of (ICE, 2015) is based on the concept of permissible overtopping discharge, resulting in a minimum freeboard. The approach is based on the developments of the EurOtop manual. In this study while the general framework of (ICE, 2015) is considered to determine freeboards, the updated empirical equations to estimate the overtopping discharge q as a function of freeboard R_C are taken from the latest version of the EurOtop manual (EurOtop II, 2018). For vertical and steep walls, the average discharge cam be estimated via Eq. (3):

$$\frac{q}{\sqrt{g \cdot H_S^3}} = 0.047 \cdot \exp\left[-\left(2.35 \cdot \frac{R_C}{H_S}\right)^{1.3}\right] \tag{3}$$

where g is the acceleration of gravity. For embankment slopes, the average discharge q follows an analogous formulation, see Eq. (4):

$$\frac{q}{\sqrt{g \cdot H_S^3}} = \frac{0.023}{\sqrt{\tan\alpha}} \cdot \gamma_b \cdot \xi_{m-1,0} \cdot \exp\left[-\left(2.7 \cdot \frac{R_C}{\xi_{m-1,0} \cdot H_S \cdot \gamma_b \cdot \gamma_f \cdot \gamma_\beta \cdot \gamma_v}\right)^{1.3}\right] \tag{4}$$

with $\xi_{m-1,0}$ is the wave breaking parameter estimated by means Eq. (5)

$$\xi_{m-1,0} = \frac{\tan\alpha}{\left(\frac{H_s}{L_{m-1,0}}\right)^{0.5}} \tag{5}$$

and where:

- α is the slope of the upstream face of the structure in degrees from the horizontal;
- $L_{m-1,0}$ is the (nominal) deep-water wave length;
- γ_b is the influence factor for a berm (1.0 for simple slope);
- γ_f is the roughness factor (tabulated in ICE, 2015, for various typical cover of embankment dam upstream faces);
- γ_β is the influence factor for wave obliquity (1.0 for normal wave attack);
- γ_v is the influence factor for a small wall on the slope (expression provided in ICE, 2015).

The maximum value of the overtopping discharge from Eq. (4) is limited by the value issued from Eq. (6):

$$\frac{q}{\sqrt{g \cdot H_S^3}} = 0.09 \cdot \exp\left[-\left(1.5 \cdot \frac{R_C}{H_S \cdot \gamma_f \cdot \gamma_\beta \cdot \gamma_*}\right)^{1.3}\right] \tag{6}$$

where γ_* is an overall influence factor of a storm wall on the embankment, generally taken to 1.0, otherwise according to (EurOtop II, 2018).

The (ICE, 2015) guide suggests limits for allowable mean wave overtopping over embankment dams (typically between 0.1 and 1.0 l/s/m depending on the dam crest and downstream face cover) or depending on the crest usage and occupation.

Method of (USBR, 2021)

In the method of (USBR, 2021), the significant wave height H_S is calculated based on an empirical equation in which the fetch must be estimated as the average value of a fan of nine radiales issued from dam crest, typically offset by 3° from one another, see the illustration in Fig. 6. The i^{th} percent exceedance run-up $R_{i\%}$ is estimated as a function of the i^{th} percent exceedance wave $H_{i\%}$ (converted from H_S) by Eq. (7) as

$$\frac{R_{i\%}}{H_{i\%}} = \left(A \cdot \xi_p + C\right) \cdot \gamma_r \cdot \gamma_b \cdot \gamma_h \cdot \gamma_\beta \tag{7}$$

with ξ_p the surf-similarity factor (slope greater than 5.0H:1.0V) defined by Eq. (8)

$$\xi_p = \frac{\tan \alpha}{\sqrt{s_p}} \tag{8}$$

and where:

- s_p is the peak waves steepness (ratio of $H_{i\%}$ over wave length);
- α is the slope angle of the upstream face of the embankment dam with the horizontal;
- A and C are coefficients that depends on ξ_p and the i^{th} percent exceedance probability (tabulated in USBR, 2021);
- γ_r is a reduction factor accounting for surface roughness (tabulated in USBR, 2021, for various typical cover of embankment dam upstream faces);
- γ_b is a reduction factor accounting for the possible influence of berms ($\gamma_b = 1.0$ for nonbermed profiles);
- γ_h is a reduction factor accounting for shallow-water conditions, where the wave height distribution may deviate from the Rayleigh distribution ($\gamma_h = 1.0$ for Rayleigh-distributed waves);
- γ_β is a reduction factor accounting for the angle of incidence β (angle between the central radial that was used to calculate the fetch and the normal to the dam axis, graphically provided in USBR, 2021).

WIND DATA IN SWITZERLAND

The wave estimation empirical methods generally require a wind velocity input 10 m above ground, with an averaged velocity over a fetch-limited duration, for which wave heights reach equilibrium with the wind velocity. For Alpine reservoirs, this fetch-limited duration typically ranges from the order of few minutes to one hour. In this study, the following wind data in Switzerland have been explored:

- Maps of gust velocities, provided by the Federal Office for the Environment FOEN (see Dierer et al., 2014);
- The Wind Atlas of Switzerland, provided by the Swiss Federal Office of Energy SFOE (see Koller & Humar, 2019); and
- Wind measurement stations of MeteoSwiss (see, e.g., Ceppi et al., 2008). Other measurement networks may also be available in Switzerland. Most dams in Switzerland are not equipped with wind measurement stations.

A short description, together with advantages and drawbacks for this study, is provided in Tab. 2 below.

Tab. 2. Description of available wind data in Switzerland

Source	**Description**	**Advantages**	**Drawbacks**
Map of gust velocities (FOEN)	Generated for extreme events, with return periods from 30 to 300 years. Gust velocities (1-s) provided 10 m above ground, including uncertainties; spatial resolution 3 x 3 km.	Suited for automatised and systematic analysis (grid results). Developed for high-return periods. No need for elevation transfer. Publicly available.	Resolution raises caution in mountainous regions. Velocity conversion to fetch-limited duration required.
Wind Atlas (SFOE)	Generated for wind power under normal operating conditions. Wind velocities provided from 50 to 150 m above ground; spatial resolution 100 x 100 m. Results provided under the form of Weibull distributions, for every 30°-sector.	Suited for automatised and systematic analysis (grid results). High spatial resolution. Directional results available.	Distributions not suitable for extreme analyses, even for yearly maximum that may be underestimated. Some wind regimes influenced by thermal effects and daily wind cycles are also poorly represented by the distributions. Need for elevation transfer to 10 m above ground.

Wind measurement stations of MeteoSwiss (part of SwissMetNet network)	Time series of wind measurements. Point data; usually 10 m above ground; usually 1-s and 10-s averages provided.	Direct measurement, locally representative of the wind climatology. Long time series available. Flexible extreme value analyses. No need for elevation transfer.	Heterogeneous spatial coverage. Expert-knowledge required for data transfer to other sites or performance of site-specific studies.

From Tab. 2, the use of Wind Atlas (SFOE) has been excluded in this study as the dataset is not fit for the purpose of estimating large return period wind velocities, typically required for dam flood safety. Wind measurement stations are highly valuable sources but are in general merely available in the vicinity of dams and therefore not representative of local conditions without performing tailored site-specific analyses. The map of gust velocities has therefore been adopted for the systematic analysis conducted in this study. The example of 50-year return period gust velocities over Switzerland is shown in Fig. 3.

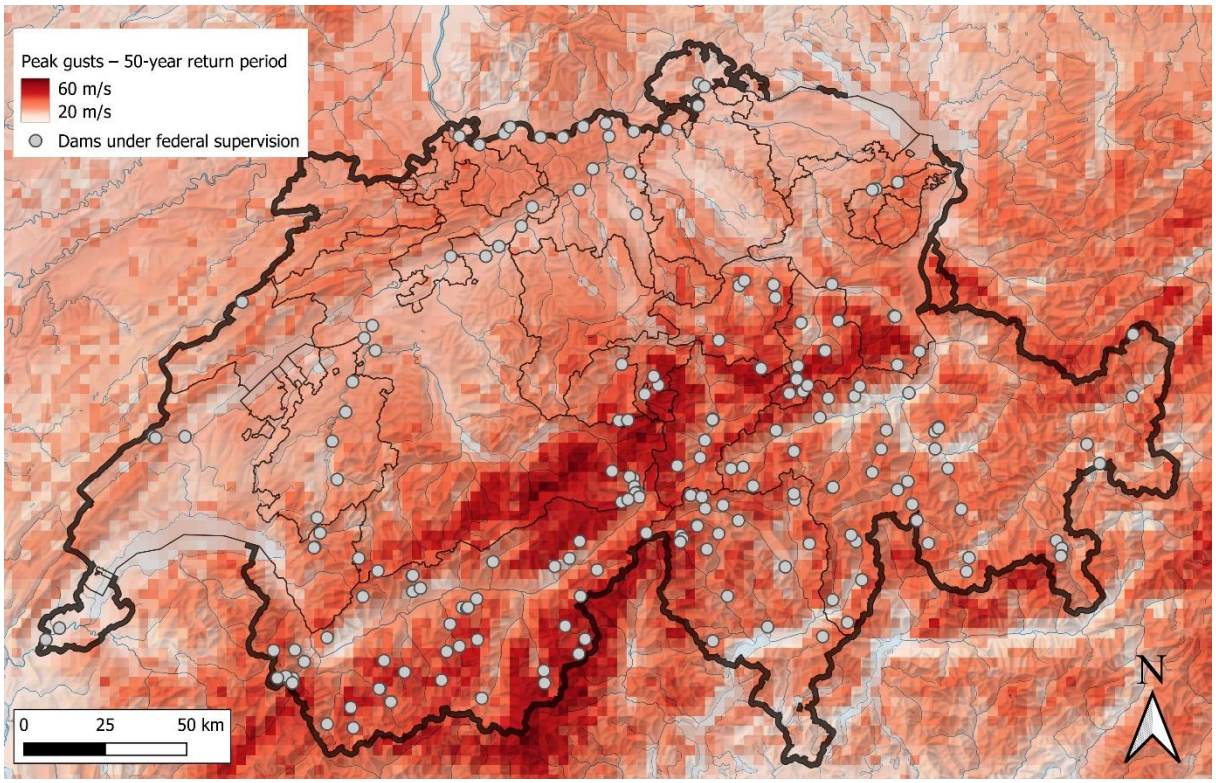


Fig. 3. Example of the map of 50-year return period gust velocities, replotted with the data provided by the Federal Office for the Environment FOEN on https://map.geo.admin.ch/ (last accessed on 29.05.2026), status 07.11.2024 (dataset explained in Dierer et al., 2014).

The use of the map of gust velocities requires to convert the 1-s gust velocities to the required fetch limited duration (or the duration required as an input into each specific wind wave estimate estimation method). To that purpose, the possible relevance of the conversion equation published by the U.S. Army Corps of Engineers USACE (USACE, 1984; USACE, 2015), mentioned for example in dam safety publications in France (Naaim et al., 2010; Cfbr, 2013) and in South Africa (WRC, 2011a; WRC, 2011b), has been investigated. The formulation is as follows in Eq. (9), for a wind velocity duration t lower than 3'600 s (typically sufficient for Alpine reservoirs):

$$\frac{U_t}{U_{3600}} = 1.277 + 0.296 \cdot \tanh\left[0.9 \cdot log\left(\frac{45}{t}\right)\right] \quad (9)$$

where U_t is the wind velocity (m/s) over duration t (s), and U_{3600} is the reference hourly duration (m/s). The advantage of Eq. (9) is that it is continuous, which is an advantage for a systematic application.

Equation (9) has been developed in the frame of ocean engineering and shore protection. To assess its suitability in regions of Switzerland, it has been compared to gust factors from

literature, see, e.g., Fallot & Hertig, 2008 for typical values in Switzerland, and the conversion factors provided in (Herbert et al., 1995; DVWK, 1997). It was concluded (not shown herein) that Eq. (9) provides converted wind velocity values which are relevant and on the safe side for a systematic application in Switzerland.

Finally, it is noteworthy that the use of the Swiss map of gust velocities (FOEN) requires some caution in some regions, were provided values may not be on the safe side. Some recommendations in (Dierer et al., 2014), not reported herein, were followed in the frame of this study. They were complemented with further comparisons with extreme value estimates at selected wind measurement stations of MeteoSwiss, also not reported herein, in order to assess the performance of the map of gust velocities against point values.

SYSTEMATIC APPLICATION TO SWISS DAMS

The three methods (DVWK, 1997; ICE, 2015; USBR, 2021) have been applied systematically to the more than 200 dams under direct federal supervision in Switzerland. The application was kept as close as possible to each original method, to the extent that this is applicable under Swiss conditions (for example, the map of wind velocities in the United Kingdom and associated conversion factors provided in ICE, 2015, were disregarded). Wind data were extracted from the map of gust velocities (FOEN) for all available return periods (30, 50, 100 and 300 years) and converted to the required durations for each method. The wind velocity was systematically assumed to be in the most conservative direction in terms of freeboard determination for all dams (wind orientation is not provided by the map of gust velocities). The method-specific parameters (all coefficients and factors) were determined at best for each specific dam. The exceedance percentages for the run-up estimates (DVWK, 1997; USBR, 2021) and the admissible discharges (ICE, 2015) were defined following the recommendations of each approach for each specific dam.

The fetches required by each method were calculated automatically and systematically using a routine implemented in the QGIS-software (QGIS.org, 2026) and reservoir shapefiles made available by swisstopo (*swissTLM3D Hydrographical network*, available at opendata.swiss: https://opendata.swiss/de/dataset/swisstlm3d-gewassernetz, last accessed on 25.04.2025). Examples of application of the three methods (DVWK, 1997; ICE, 2015; USBR, 2021) to a specific Swiss dam are shown in Fig. 4 to 6, respectively.

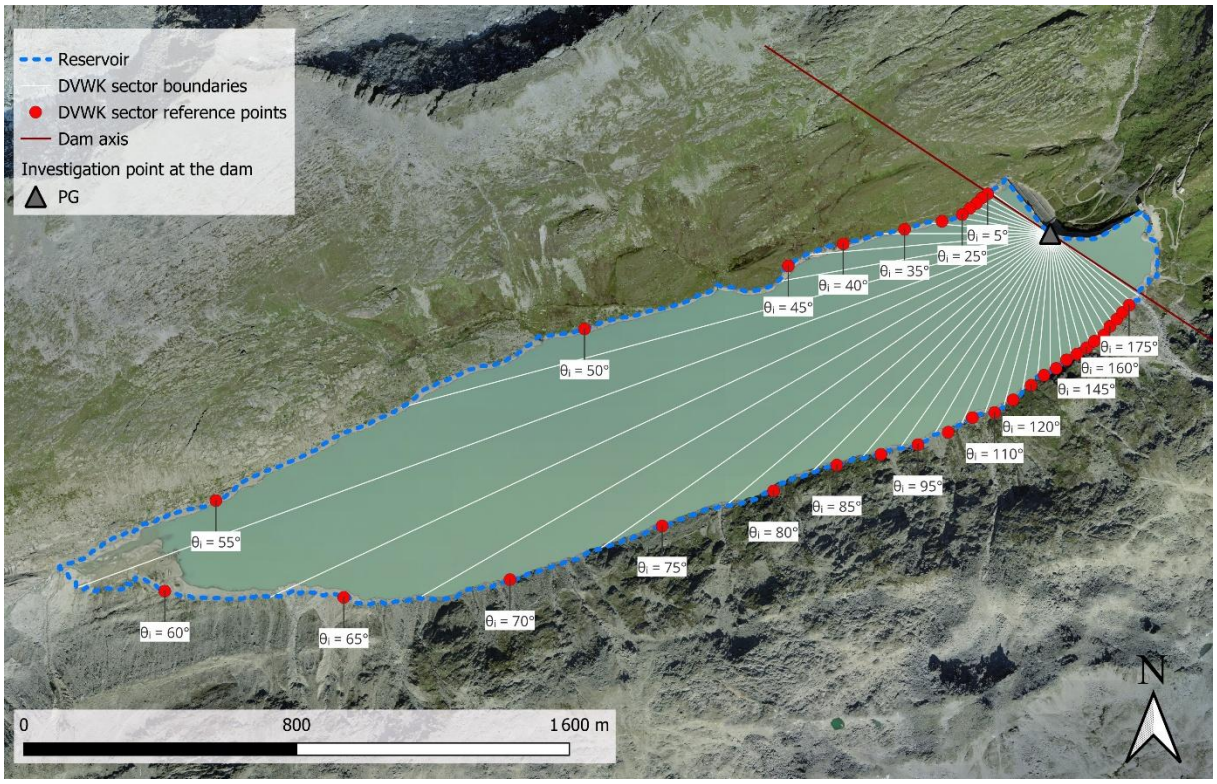


Fig. 4. Reservoir sectors determined based on (DVWK, 1997). Map background: Federal Office of Topography swisstopo

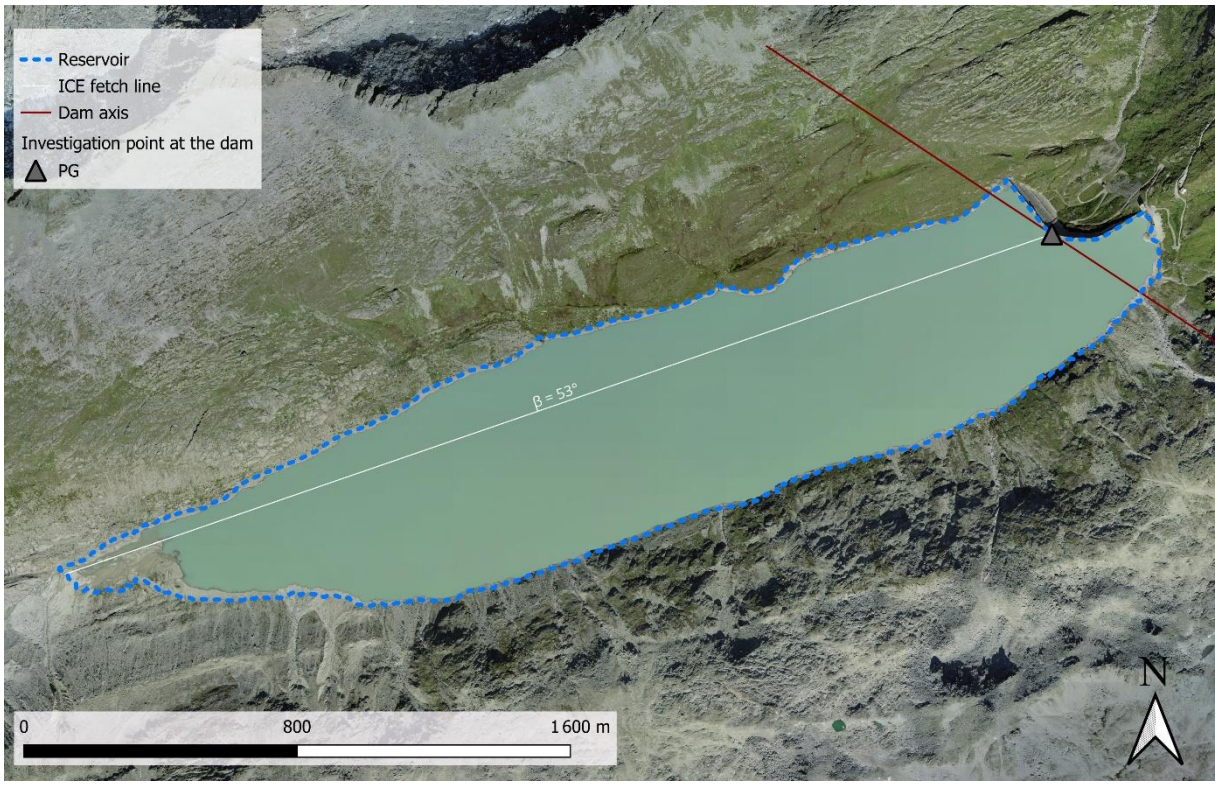


Fig. 5. Longest straight fetch determined according to (ICE, 2015), Map background: Federal Office of Topography swisstopo

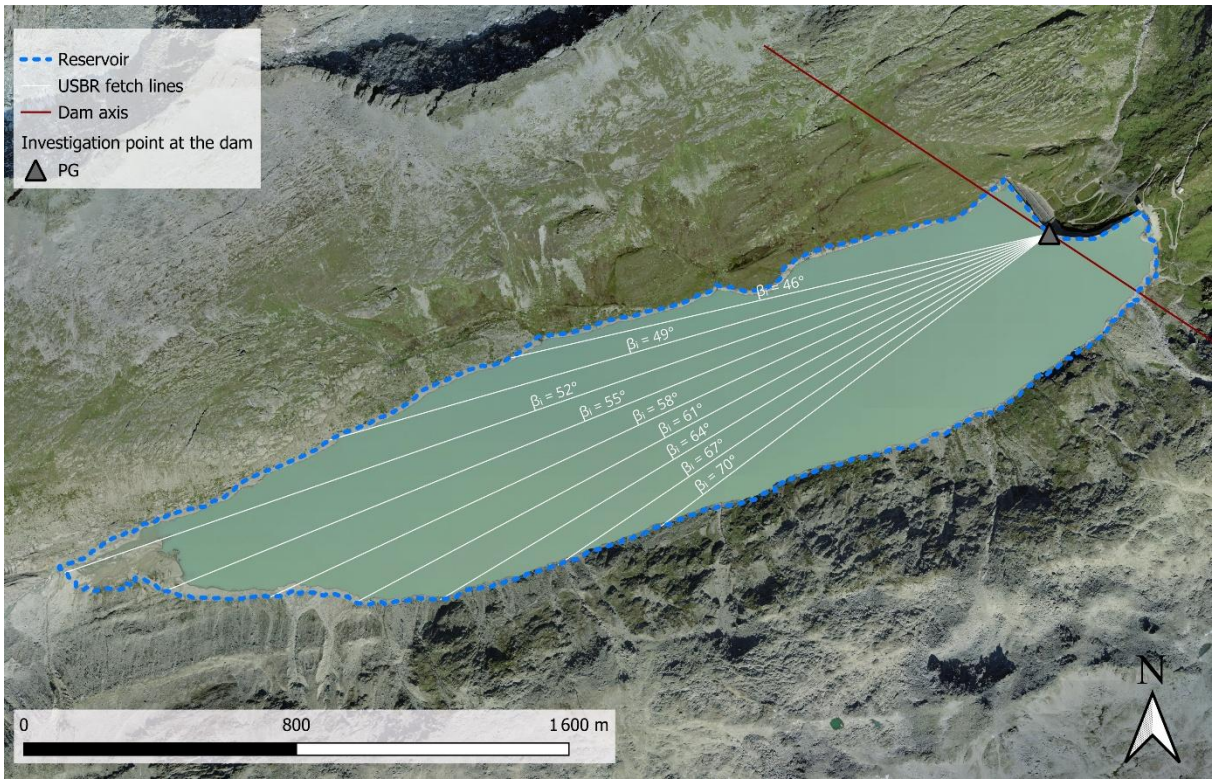


Fig. 6. Fan of radiales determined according to (USBR, 2021). Map background: Federal Office of Topography swisstopo

The results of the systematic application of the three methods (DVWK, 1997; ICE, 2015; USBR, 2021) are represented in Fig. 7 against the standard values of the Swiss directive (SFOE, 2018) reported in Tab. 1, for a 50-year wind return period. For each dam, only the most conservative run-up height estimate of the three methods is plotted. The following observations can be made, only applicable to wind-wave component of the freeboard:

- The standard values of the Swiss directive (SFOE, 2018) are not always conservative, both for embankment and concrete dams. A group of c. 15 smaller dams (roughly with height lower than 30 m) would require higher minimum safety freeboard requirements under the hypothesis of an extraordinary flood event combined with a 50-year return period wind event.
- For most dams, facility-specific studies would allow reducing the minimum safety freeboard standard value under the previously mentioned load case.

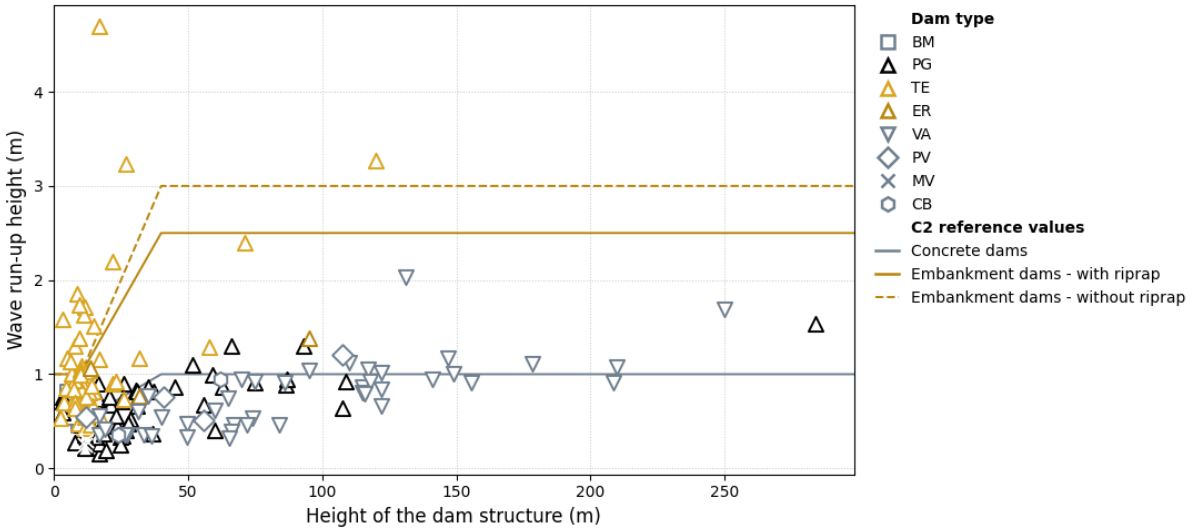


Fig. 7. Most conservative estimates of wave run-up height for a 50-year return period wind at all Swiss dams under direct federal supervision from the three methods (DVWK, 1997; ICE, 2015; USBR, 2021), plotted against the standard values of the Swiss directive (SFOE, 2018). BM: weir; CB: buttress dam; MV: multiple arch dam; PG: gravity dam; PV: gravity arch dam; VA: arch dam; ER: rockfill dam; TE: earth dam

DISCUSSION

The results of the systematic wave run-up height estimation at all Swiss dams under direct federal supervision and their comparison with the minimum safety freeboard standard values of the Swiss directive (SFOE, 2018) outlines the potential need to update this aspect of the directive. As of today, the standard values of the Swiss directive are a function of the dam height only. However, as shown in Fig. 7, some reservoirs may feature long fetches for relatively low dam height, leading to an underestimation of the minimum requirement on the safety freeboard depending on the load case (extraordinary flood situation combined with a certain wind return period). In the case of a high dam combined with a small reservoir area, the opposite situation may occur.

In Fig. 8, the most conservative estimates of wave run-up height from the three methods (DVWK, 1997; ICE, 2015; USBR, 2021) for a 50-year return period wind are replotted against the longest straight fetch in the reservoir from dam axis. One can observe a better correlation with the estimates of wave run-up height. The results for embankment dams are more spread; this is because various geometrical and material parameters influence the

run-up estimate, such as the upstream face slope and cover. The moderate spread observed for concrete dams is due to the fact that wind input remains site-specific.

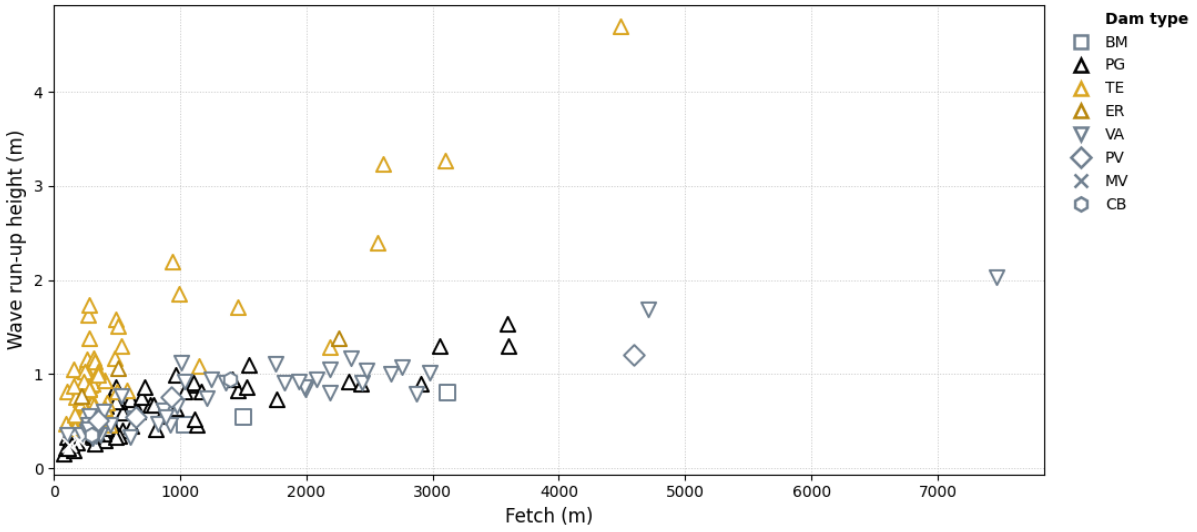


Fig. 8. Most conservative estimates of wave run-up height for a 50-year return period wind at all Swiss dams under direct federal supervision from the three methods (DVWK, 1997; ICE, 2015; USBR, 2021), plotted against the longest straight fetch in the reservoir (from dam axis). BM: weir; CB: buttress dam; MV: multiple arch dam; PG: gravity dam; PV: gravity arch dam; VA: arch dam; ER: rockfill dam; TE: earth dam

A future update of the Swiss directive would also need to tackle the challenge of defining relevant load cases, i.e., the correlation between flood and wind events. This aspect, to the best of the authors' knowledge, is not studied in Switzerland, and was out of the scope of this study. However, it is opined that the results of this study will represent a sound basis to edict updated and more detailed recommendations to assess wind-wave contributions to the determination of safety freeboard at Swiss dams.

SUMMARY AND OUTLOOK

This paper systematically analyses wind-wave contributions to safety freeboards in Swiss Alpine reservoirs. It reviews the Swiss regulatory framework and applies three major empirical run-up/overtopping estimation methods (DVWK, 1997; ICE, 2015; USBR, 2021) to over 200 large dams in Switzerland. The study demonstrates that the map of gust velocities provided by the Federal Office for the Environment can be used without complex analyses for estimating wind-waves when combined with a conservative gust conversion procedure to determine fetch-limited wind durations. The proposed methodology is a relatively

straightforward approach which, in general, can be used for safety freeboard calculation in Switzerland without extensive site-specific studies, as it was assessed to stand on the side of safety if the necessary caution is exercised when using the map of gust velocities. Where conservativeness should be reduced, alternative site-specific studies can be explored.

This study outlines potential directions to update the Swiss directive for dam safety against floods, calling for updated requirements and new technical recommendations tailored to Alpine reservoir conditions. The definition of minimum admissible freeboards based on overtopping limits should also be explored. This could be particularly relevant for concrete dams, which may be less sensitive to wind-wave overtopping under some conditions. Defining relevant load cases – namely, combined flood and wind events – remains a challenge to be addressed by future research. The integration of updated requirements into the Swiss directive must also be conducted within a comprehensive flood safety evaluation framework accounting for other aspects, such as extreme flood estimation (Pachoud et al, 2025).

REFERENCES

[1] Bornschein, A. & Pohl, R. 2012 "Wave run-up of breaking and non-breaking waves with longshore current". In *Book of Proceedings of the International Conference of the Application of Physical Modelling to Port and Coastal Protection (CoastLab 12)*, Gent, Belgium, 17-20 September 2012.

[2] Ceppi, P., Della-Marta, P.M., Appenzeller, C. 2008. "Extreme value analysis of wind speed observations over Switzerland." *Arbeitsberichte der MeteoSchweiz* 219.

[3] Cfbr 2013. *Recommandations pour le dimensionnement des évacuateurs de crues de barrages*. Comité français des barrages et réservoirs (Cfbr).

[4] Dierer, S., Müller, S., Stucki, P., Brönnimann, S., Romppainen-Martius, O. 2014. *Karten der Sturmgefährdung in der Schweiz: Flächendeckende Darstellung der Böenspitzen in der Schweiz für verschiedene Wiederkehrperioden*. Bern: Meteotest und Geographisches Institute der Universität Bern. DOI:10.7892/boris.62780.

[5] DVWK 1997. "Freibordbemessung an Stauanlagen." In *Merkblätter zur Wasserwirtschaft* 246/1997, Deutscher Verband für Wasserwirtschaft und Kulturbau e.V., Bonn.

[6] EurOtop II 2018. *Manual on wave overtopping of sea defences and related structures - An overtopping manual largely based on European research, but for worldwide application*, Second Edition.

[7] Fallot, J. M., & Hertig, J. A. 2008. "Détermination des vents extrêmes à l'aide d'analyses statistiques et de modélisations numériques dans une topographie accidentée en Suisse. " *Bulletin de la Société géographique de Liège* 51:31-47.

[8] Herbert, D.M., Lovenbury, H.T., Allsop, N.W.H., Reader, R.A. 1995. *Performance of blockwork and slabbing protection for dam faces*. HR Wallingford.

[9] ICE 2015. *Floods and reservoir safety*, Fourth edition. Institution of Civil Engineers ICE. Westminster, London, UK: ICE Publishing. DOI:10.1680/frs.60067.

[10] Koller, S. & Humar, T. 2019. *Atlas of Swiss Winds – Final Report*. Meteotest AG and Swiss Federal Office of Energy SFOE.

[11] Naaim, M., Degoutte, G., Delorme, F. 2010. "Les vagues dans les retenues d'altitudes: analyse et méthodes pour la prévention. " *Sciences Eaux & Territoires* (2):102-113. DOI:10.14758/SET-REVUE.2010.2.13.

[12] Pachoud, M.J., Viviroli, D., Frauchiger, R., Brocard, E., Côté, M. 2025. "New approach to estimate extreme floods for Swiss dams by means of continuous hydrological simulations." In *Twenty-Eighth International Congress on Large Dams/Vingt-Huitième Congrès International des Grands Barrages*. CRC Press. DOI:10.1201/9781003642428.

[13] Pohl, R. 2019 "Freibordberechnung an Talsperren". In *Talsperrensicherheit - Aktuelle Entwicklungen und Herausforderungen*, Innsbruck, Austria, 8 April 2019.

[14] Pullen, T. et al. 2018. "Wave and overtopping predictions on reservoirs and inland waterways". In *Proceedings of the 3rd International Conference on Protection against Overtopping*, UK, 6-8 June 2018.

[15] QGIS.org 2026. QGIS Geographic Information System. QGIS Association. http://www.qgis.org

[16] Swiss Federal Office of Energy SFOE (Ed.) 2018. *Directive on the safety of water retaining facilities, Part C2: Safety against flood and lowering of the reservoir water level*. Version 2.02. Bern, Switzerland.

[17] Schwager, M.V., Askarinejad, A., Friedli, B., Oberender, P.W., Pachoud, A.J., Pfister, L. 2023. “Swiss dam safety regulation: Framework, recent changes and future perspectives.” In *Role of Dams and Reservoirs in a Successful Energy Transition*. Boes, R., Droz, P., Leroy, R. (Eds.). London, UK: CRC Press. DOI:10.1201/9781003440420.

[18] Swiss Confederation. Federal Act on Water Retaining Facilities (WRFA, SR 721.101) of 1 October 2010 (Status as of 1 July 2023).

[19] Swiss Confederation. Water Retaining Facilities Ordinance (WRFO, SR 721.101.1) of 23 November 2022 (Status as of 1 January 2023).

[20] USACE 1984. *Shore Protection Manual*. Coastal Engineering Research Center. Washington, D.C.: U.S. Army Corps of Engineers.

[21] USACE 2015. *Coastal Engineering Manual – Part II*. Washington, D.C.: U.S. Army Corps of Engineers.

[22] USBR 2021. "Design standards No. 13 - Embankment Dams", Chapter 6: Freeboard. In *Reclamation Design Standards*, DS-13(6)-2.1: Phase 4 Final.

[23] WRC 2011a. Guidelines on freeboard for dams - Volume I: Literature review and case studies. WRC Report No. K5/1759/1, Water Research Commission, Gezina, South Africa.

[24] WRC 2011b. Guidelines on freeboard for dams - Volume II. WRC Report No. K5/1759/1, Water Research Commission, Gezina, South Africa.

European BECCA project: Solutions for safe reservoirs, integrated into their environment and respectful of biodiversity, as part of climate change adaptation in mountain areas

Laurent PEYRAS, Guillaume STOLTZ, Samuel WESTRELIN, Pierre BERTELOOT, Virginie DIOULOUFET, Hamza TAHIR
INRAE UMR RECOVER Aix en Provence, France
laurent.peyras@inrae.fr

Giulia BODRATO, Salvatore LA MONICA, Davide PATROCCO
REGIONE PIEMONTE, Turin, Italie

Monica BARBERO, Daniele GANORA, Fabrizio BARPI
Politecnico di Torino, Turin, Italie

Florent ARTHAUD, Benjamin GERFAND
USMB, Chambéry, France

André EVETTE, Stéphanie GAUCHERAND
INRAE LESSEM, Grenoble, France

Dominique LAIGLE, Guillaume PITON
INRAE IGE, Grenoble, France

Paolo ROPELE, Franco COLLE
Regione Autonoma Valle d'Aosta, Aoste, Italie

Key words

reservoirs, climate change, BECCA, biodiversity, France, Italy

Abstract

The European BECCA project - Sustainable and Safe Basins for Ecology, designed for adaptation to Climate Change -, funded by Europe in Alcotra Program France-Italia, aims to address the design of safe reservoirs and the rehabilitation of existing reservoirs, adopting nature-based techniques. In particular, the BECCA project plans to defining technical recommendations for the design, construction, rehabilitation, and management of small and medium-sized, simple, low-cost dams that guarantee an adequate level of safety for downstream populations, protect against natural hazards, and pay close attention to environmental aspects. The article presents the BECCA project's proposals and operational

techniques for the naturalisation and revitalisation of reservoirs using nature-based solutions.

1. Introduction

In 2022, all climate indicators point to drier-than-average conditions across much of Europe. The combined effects of low rainfall and high temperatures have led to widespread and prolonged drought, affecting many sectors of society. The greatest rainfall deficits were recorded in the Alpine arc (Source: Copernicus), with significant consequences for the population and economy of mountain areas. The critical conditions observed in 2022 merely confirm the trend of climate change over recent decades, with serious impacts on Alpine regions: severe summer droughts detrimental to agriculture in rural mountain areas, to drinking water supplies, to fire risk and to hydroelectric power generation; and, with rising temperatures, a lack of snow in winter detrimental to winter sports resorts.

Local stakeholders are working to identify effective and sustainable solutions for adapting to climate change. One of the preferred solutions involves the creation of small and medium-sized reservoirs to store water, thereby helping mountain regions adapt to climate change by ensuring the continuation of economic activities and an adequate level of safety for the communities living there. However, regulatory authorities in France and Italy have noted that these small and medium-sized reservoirs in the cross-border region can pose risks to the population in the event of failure, as well as having significant impacts on the environment and natural habitats. The European BECCA project – Sustainable and Safe Basins for Ecology, designed for Adaptation to Climate Change – funded by the European Interreg ALCOTRA France-Italy programme, aims to provide the tools to design safe reservoirs and rehabilitate existing ones using nature-based techniques. This project focuses specifically on the France–Italy cross-border area corresponding to the Alpine arc, but the results are widely applicable beyond this to other mountainous or foothill regions. In particular, the BECCA project aims to establish technical recommendations for the design, construction, rehabilitation and management of small and medium-sized, simple, low-cost reservoirs that guarantee an adequate level of safety for downstream populations, protect against natural hazards, and place a strong emphasis on environmental considerations by taking the environment into account from the design stage to minimise ecological impacts. Through a guidance

document [1], the BECCA project proposes operational techniques for the naturalisation and revitalisation of reservoirs using nature-based solutions.

2. Mountain and high-altitude water retention in the face of climate challenges

The mountainous regions of the French and Italian Alps are undergoing significant climate change, with increasingly dry summers and winters with less snowfall. These changes have a direct impact on water resources, agriculture, and hydroelectric power generation and artificial snow production. Against this backdrop, hillside and high-altitude reservoirs, which enable water to be stored during periods of high flow, regulate floods and safeguard local areas, have been developed.

The BECCA project proposes, in a guidance document [1], a technical framework for the design, construction and rehabilitation of these structures, incorporating nature-based solutions (NBS), whilst balancing safety, hydraulic performance, protection against natural hazards, sustainability and respect for the environment, using local materials and ensuring careful integration into the landscape.

This new set of recommendations [1] updates the current technical reference that established best practice [4], and also incorporates recommendations on the risks and impacts of high-altitude reservoirs [5].

3. Site selection – Design principles

The first step in designing a hillside or high-altitude reservoir is to select a site that minimises environmental impacts. The **Avoid > Reduce > Offset** principle guides this approach: the aim is to avoid outstanding environments, wetlands or protected natural habitats, to reduce the ecological footprint by prioritising sites that have already been developed, and to offset any remaining impacts through ecological measures.

The chosen sites must allow for harmonious integration into the landscape. The cut-and-fill technique enables the re-use of excavated materials to construct the embankment, thereby reducing costs and the carbon footprint. This approach is particularly suited to mountainous areas, where access is often difficult and where material volumes must be optimised. The slopes of the embankments are designed to promote vegetation growth and stability, with gradients generally ranging from 1:3 to 1:2.5.

Particular attention is paid to creating ecological refuge zones covering at least 30% of the perimeter of the upstream embankments. These areas, maintained at a constant water level of 20 to 30 cm, allow the development of hydrophytic and helophytic plants, thus providing a permanent habitat for local wildlife, such as amphibians, insects, small mammals and birds. These features also help to stabilise the embankments and limit erosion.

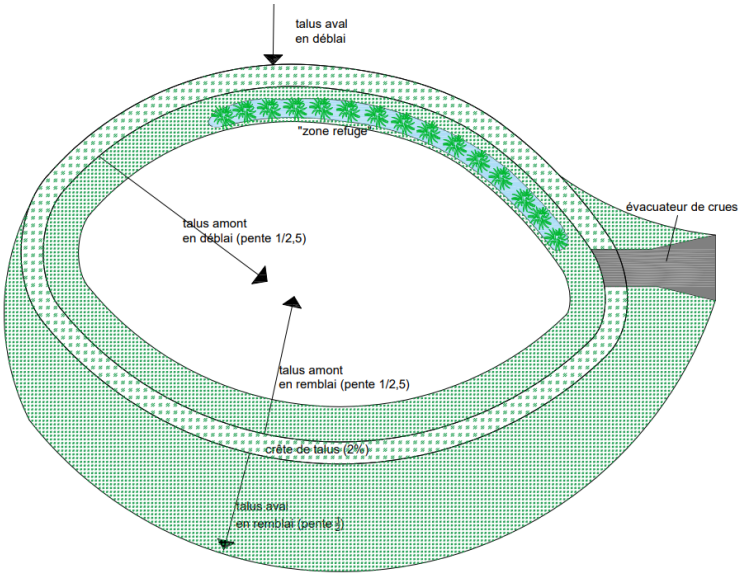


Fig. 1. *General development of a reservoir with a refuge area*

4. integration into the landscape

To ensure optimal integration into the landscape, and where the reservoir is situated within an existing vegetated environment, the BECCA guide recommends that the downstream slopes and the crest of the reservoir be vegetated with local herbaceous species that are resistant to the site's climatic conditions. This vegetation provides protection against surface erosion whilst improving the visual and environmental integration of the structure.
However, planting shrubs or trees on the embankments is prohibited, as their root systems could compromise the stability of the slopes, degrade the DEG by penetrating deeply into the embankment, and make it more difficult to inspect the dams. On the cuttings overlooking the reservoir or in its vicinity, vegetation may include woody plants or small trees as it is not in direct contact with the waterproofing or structural elements.
The guide recommends the use of local materials to minimise visual and ecological impact: rock and soil excavated on site are reused for riprap and embankments, thereby reducing costs and the carbon footprint. Concrete is avoided as far as possible, except for critical hydraulic structures such as spillways.



Fig. 2. *An example of successful integration into the landscape – Manigod Resort (74 – France)*

5. Ecological integration : creating functional ecosystems for biodiversity

The environmental integration of retention basins is a key objective of the BECCA project [3]. It is based on the creation of ecological refuge areas for biodiversity, which are permanently flooded and promote the development of biodiversity. They are designed using self-filtering materials to allow plants to grow whilst protecting the waterproofing system. These refuge zones allow water to be retained and are not drained, in order to preserve aquatic ecosystems. The drainage system is designed to prevent the accumulation of stagnant water whilst allowing for natural renewal.

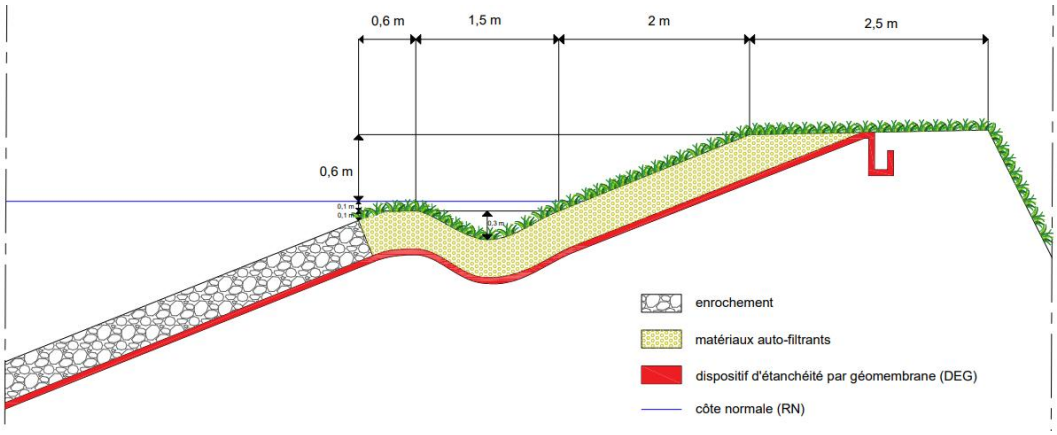


Fig. 3. *Design of a refuge zone in the upper part of the reservoir*

The creation of functional habitats represents an innovation compared to the traditional design of reservoirs. The BECCA guide recommends that these areas be maintained at a constant water level of 20 to 30 cm, thereby allowing the growth of hydrophytic and helophytic plants and providing a permanent habitat for local wildlife, such as amphibians, insects, small mammals and birds. These features also help to stabilise embankments and limit erosion, whilst promoting biodiversity.

Refuge zones are designed using self-filtering materials (0–125 mm), as detailed in the guide. These materials provide erosion resistance, retention of fine particles, support for plant growth and protection of the geomembrane waterproofing system (DEG). The presence of vegetation, which may include woody plants or small trees in the cut, helps prevent degradation of the self-filtering material layer. Filling the voids with fine materials creates a substrate that promotes root growth and stabilises the materials.

The design of the DEG must be adapted to the presence of ecological refuge zones. In particular, the positioning of the geogrid anchors must be carefully considered to avoid a 'drum effect' that could occur where the DEG is positioned over the ecological refuge zone. The guide proposes two solutions to counter this drum effect, whilst ensuring the continuity of the waterproofing provided by the geomembrane. These are based on the principle of increasing the load exerted on the geogrid in order to weigh down the entire DEG.

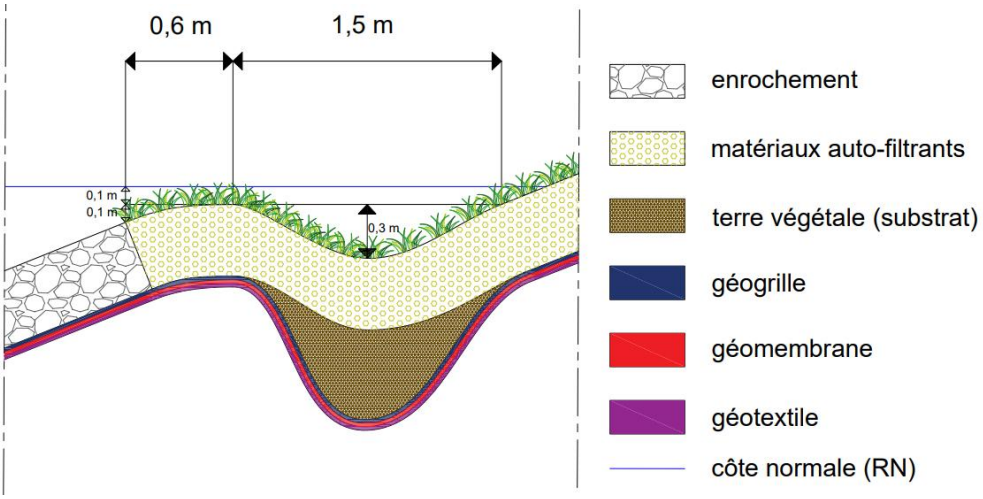


Fig. 4. *Cross-section of a narrow refuge zone with containment*

6. Assessment of the compatibility of vegetation with geomembrane waterproofing system

An experimental study was conducted to assess the interaction between the underground systems of helophyte plants (roots and rhizomes) and the waterproofing geomembranes used in high-altitude reservoirs [3]. The aim was to verify that the proposed vegetation techniques do not pose any additional risk to the safety of the structures. Experiments in rhizotrons (Figure 9) enabled the underground development of three helophyte species to be monitored over a 10-month period in contact with a 1.5 mm PVC-P geomembrane commonly used in reservoirs.

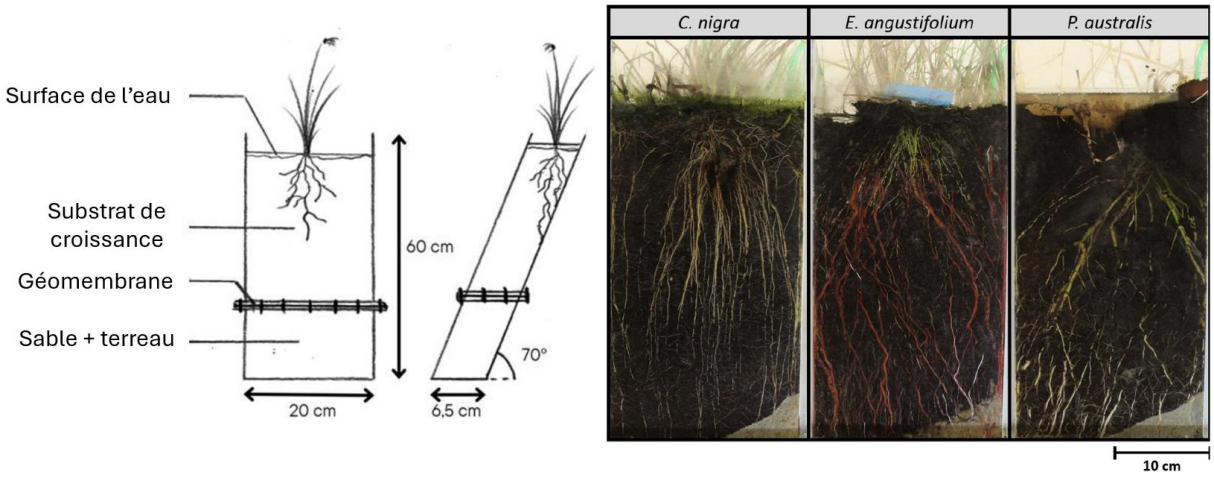


Fig. 5. *Diagram of the rhizotrons used in the experiment and photographs of the underground systems of the three helophyte species studied at the end of the experiment. The waterproof geomembrane is visible at the bottom of each photograph.*

Two of the species tested, Carex nigra and Eriophorum angustifolium, are already being used in experiments to revegetate reservoirs. A third species, Phragmites australis, known for the vigorous growth of its rhizomes and its ability to penetrate certain waterproofing materials, was included as a more aggressive reference species. Observations revealed contrasting root architectures depending on the species, with a theoretical degradation potential increasing from Carex nigra to Phragmites australis. Following a contact period of 100 to 200 days with the geomembrane, visual, mechanical and chemical analyses were carried out. The results showed no degradation of the geomembrane under the experimental conditions, including for Phragmites australis. This work suggests that the use of suitable herbaceous plants can be considered in reservoir revegetation projects, with no identified impact on the integrity of the waterproofing system.

7. Floating rafts to promote biodiversity in reservoirs with significant tidal ranges

A floating vegetated raft was assembled and installed in a high-altitude reservoir to encourage colonisation by the local biodiversity (Figure 6). Helophytes (Carex nigra and Eriophorum angustifolium covering an area of 21.2 m²) and hydrophytes (Chara globularis and Chara vulgaris covering an area of 5.4 m²), all collected from ponds and wetlands within a 10 km radius of the reservoir, were transplanted onto the raft. Thanks to a suitable anchoring system, the raft follows even the most extreme fluctuations in water level.



Fig. 6. *A floating plant-covered raft (A) with helophytes (B, D) and a submerged central section covered with hydrophytes (C).*

One year after planting, in the summer of 2025, the vast majority of plants had survived (Figures 5B and C); the helophytes showed significant root development. At the same time, monitoring of faunal biodiversity was established, including an inventory of amphibians, aquatic invertebrates, adult odonates and zooplankton. The macro-invertebrate communities on the raft are dominated by chironomids but also host other taxa such as odonate larvae. No amphibians have been observed on the raft to date. In 2026, the continuation of these monitoring activities will enable an assessment of the effectiveness of the structures in terms of fauna colonisation and their ability to provide resources and shelter.

8. Waterproofing and stability : solutions tailored to the challenges of mountain sites

In mountainous areas, soils are often poorly impermeable due to their heterogeneous grain size or high permeability. Foundations may also be at risk of dissolution, particularly in karst or gypsum-rich areas. To address these challenges, waterproofing solutions rely on geomembrane waterproofing systems, supplemented by nature-based solutions for better environmental integration.

Geomembrane waterproofing systems (GWS) are chosen for their high-performance waterproofing and durability. The presence of the geomembrane requires systematic covering to limit the impacts of UV radiation, frost or mechanical impacts. This covering can be achieved using various protective layers, topped with locally sourced riprap. A layer of topsoil may be incorporated into the riprap in the area above the normal operating level to improve landscape integration. For older high-altitude or hillside reservoirs that have not been lined (which is to be avoided), it is recommended that their banks be re-profiled to achieve gentler slopes, compatible with full lining. Finally, it is generally recommended to use light-coloured geomembranes (grey or beige) rather than black ones, to avoid excessively high temperatures that are detrimental to biodiversity.

Drainage is another key aspect of the design. Drains, constructed from local granular materials (gravel, sand), are combined with geotextiles to prevent clogging. Perimeter ditches at the foot of the embankment help to limit sediment inflow into the reservoir and preserve water quality.

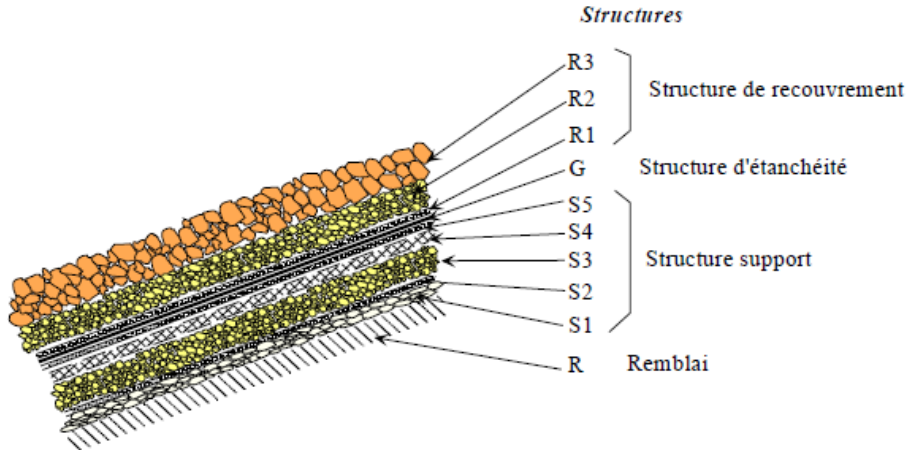


Fig. 7. *Example of a DEG with a support structure suitable for aggressive subgrade materials and semi-permeable backfill materials*

9. Engineering firms with multidisciplinary expertise in the design of retention systems integrated into their surroundings

The design of hillside and high-altitude reservoirs that are integrated into their surroundings requires two distinct areas of expertise:

- Dam engineering: this involves a wide range of interrelated skills, including the fundamentals of civil and geotechnical engineering, as well as hydrology, hydraulics, monitoring, etc.
- Ecological engineering: this involves skills relating to restoration ecology and engineering, often referred to as ecological engineering. The aim here is to restore and rehabilitate natural or man-made environments, drawing on natural processes.

10. Conclusions

The mountainous regions of the French and Italian Alps are undergoing significant climate change, with increasingly dry summers and winters with less snowfall. These changes have a direct impact on water resources, agriculture and hydroelectric power generation. In this context, hillside and high-altitude reservoirs can offer solutions to mitigate these socio-economic impacts, provided they meet certain criteria during their development.

In this context, the European BECCA project – Sustainable and Safe Basins for Ecology, designed for Adaptation to Climate Change – funded by the European Interreg ALCOTRA France-Italy programme, proposes design elements for safe reservoirs and the rehabilitation of existing reservoirs using nature-based techniques. This project focuses particularly on the France–Italy cross-border area corresponding to the Alpine arc, but the results are widely applicable beyond this to other mountainous or foothill regions.

As its main deliverable, the BECCA project presents, in a guide of recommendations [1], a technical framework for the design, construction and rehabilitation of these structures, incorporating nature-based solutions (NBS), whilst balancing safety, hydraulic performance, protection against natural hazards, sustainability and environmental respect, using local materials and ensuring careful integration into the landscape.

11. ACKNOWLEDGEMENTS

This work forms part of the BECCA project – ID BECCA 20148 – funded by the European Union under the INTERREG ALCOTRA France–Italy programme. The authors would therefore

like to express their deep gratitude to the European Union for giving them the opportunity to carry out this project and for providing the necessary funding.

12. REFERENCES

[1] Guide BECCA (2026). *Retenues collinaires et d'altitude : Recommandations pour la conception, la réalisation, la surveillance, l'entretien et la réhabilitation*.

[2] CFBR (2015). *Guidelines for the justification of embankment dams and levees*.

[3] GERFAND Benjamin (2026). *Biodiversité et solutions de végétalisation des retenues d'altitude : vers des écosystèmes nouveaux ?* Thèse de doctorat USMB/INRAE – ADS/Compagnie des Alpes

[4] PEYRAS L., MERIAUX P. (2009). *Retenues d'altitude*. Ed. Quae

[5] EVETTE A., PEYRAS L., LAIGLE D. (2009). Risques et impacts des retenues d'altitude. Ed. Quae

Behavior Monitoring and Safety Assessment of a Very High Arch Dam during Reservoir Drawdown

D. Gaftoi, D. Stematiu, C. Popescu, L. Laurentiu, Gh. Boian

Abstract:

The drawdown of the Vidraru Reservoir is required to carry out the rehabilitation works associated with the bottom outlets. In the case of very high arch dams, such as Vidraru Dam (166.60 m), this operational condition generates structural effects significantly different from those occurring under normal operating conditions. As the water level decreases, the upstream face becomes exposed to ambient temperature, leading to modifications in the thermal regime of the structure and consequently affecting displacements and stress distribution. During the cold season, direct exposure to air temperature fluctuations may cause joint opening, reducing the three-dimensional structural interaction and potentially increasing seepage.

This atypical operational condition required the intensification and extension of the existing monitoring program. In addition, two complementary investigation programs were implemented: (1) ambient vibration measurements aimed at the indirect assessment of the global structural stiffness, and (2) geodetic monitoring of the dam's adjacent slopes using 3D laser scanning technology.

The interpretation of the recorded data is essential for assessing structural safety under atypical loading conditions. Validation of the measured displacements during drawdown was performed using a deterministic finite element model. This approach enables the evaluation of stress distribution within the structure and provides a reliable basis for assessing the safety level.

The paper presents the general context of the reservoir drawdown, the intensified and extended monitoring strategy, and the results of the safety assessment conducted during this operational phase.

Keywords:

Very high arch dam, Reservoir drawdown, Structural monitoring, Dam safety assessment, Finite element analysis

1. INTRODUCTION

The drawdown of reservoirs associated with high dams represents a rare operating condition, with significant implications for the structural behavior and safety assessment of the structure. In the case of very high arch dams (such as the Vidraru Dam), the substantial reduction of the water level leads to changes in both the hydrostatic loading conditions and the thermal regime of the structure, generating effects that differ from those corresponding to normal operation. The drawdown of the Vidraru Reservoir is required by the rehabilitation works of the Vidraru Hydropower Plant, particularly those involving the hydromechanical equipment associated with the bottom outlets.

Considering the atypical nature of this operating condition, the routine structural monitoring program was intensified and extended. The frequency of observations and measurements increased throughout the entire drawdown period, while the conventional monitoring system was supplemented by two additional investigation programs: ambient vibration measurements for the indirect assessment of the global structural stiffness, and monitoring of the adjacent slopes through 3D laser scanning (LiDAR).

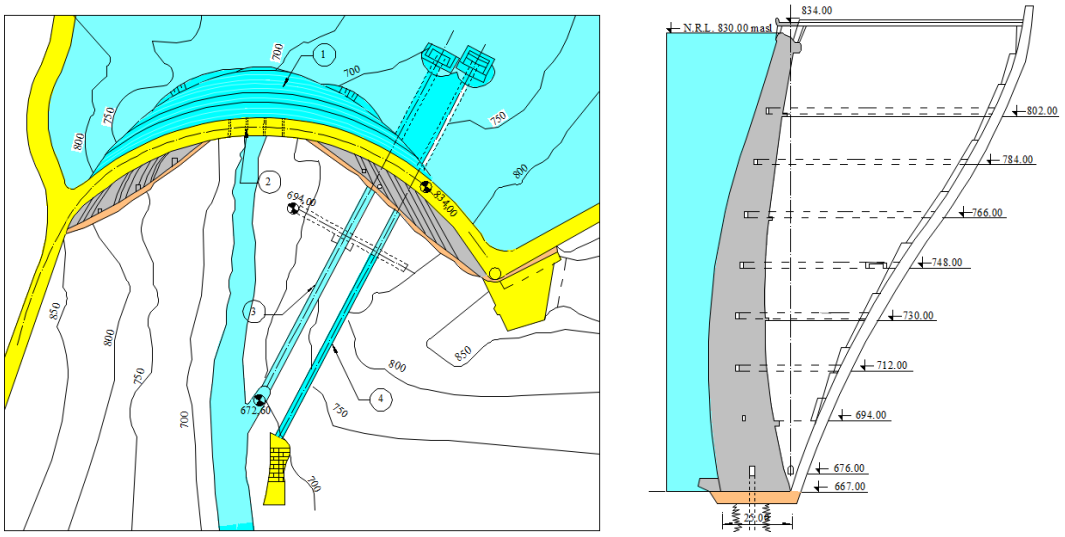
The interpretation of the monitoring data obtained during reservoir drawdown required the use of complementary analysis methods in addition to the conventional monitoring tools. To validate the measured displacements and to assess the stress distribution within the structure, a deterministic finite element model was developed, capable of reproducing the mechanical and thermal effects associated with this atypical operating condition.

This paper presents the technical context of the Vidraru Reservoir drawdown, the adopted monitoring strategy, and the results of the structural behavior and safety assessment performed during this special operating condition.

2. DATA REGARDING THE DAM

Vidraru Dam is located on the Argeș River, forming a reservoir with a total storage capacity of 465 million m³ of water. The dam is a double-curvature concrete arch dam, with a height of 166.60 m, a crest length of 314 m, and a total concrete volume of approximately 470,000 m³. The thickness of the dam varies from 25.0 m at the base to 6.0 m at the crest. According to the Romanian legislation, Vidraru Dam is classified as a Class I dam and assigned to Importance Category A (dam of exceptional importance).

The dam is composed of 22 monoliths separated by spiral contraction joints. The width of the monoliths is variable, ranging between 10 m and 14 m each. Figure 1 presents the typical cross-section of the dam together with the plan view highlighting the main structural components.



(a) *(b)*

Figure 1 – Vidraru dam (a) plan view, b(central monolith cross section)
1. dam body, 2. frontal spillway, 3. bottom outlet no. 1, 4. bottom outlet no. 2

For flood discharge and reservoir level control, Vidraru Dam is equipped with a central spillway with a discharge capacity of 260 m³/s and two bottom outlets located in the left abutment, each capable of discharging up to 160 m³/s. The ongoing refurbishment program includes the modernization of the hydromechanical equipment associated with the bottom outlets.

Water is conveyed to the underground hydropower plant through an intake located on the right abutment. The refurbishment program also includes the replacement of the electromechanical equipment of the hydropower plant.

The monitoring system installed at Vidraru Dam complies with the requirements for special monitoring imposed by the exceptional importance category of the structure. The monitoring system includes pendulums (4 pendulum sections – P2, P7, P12 and P17 – figure 2), joint deformation measurements, foundation deformation instruments, piezometers, temperature sensors, seepage monitoring devices, seismic instrumentation, and a local meteorological station.

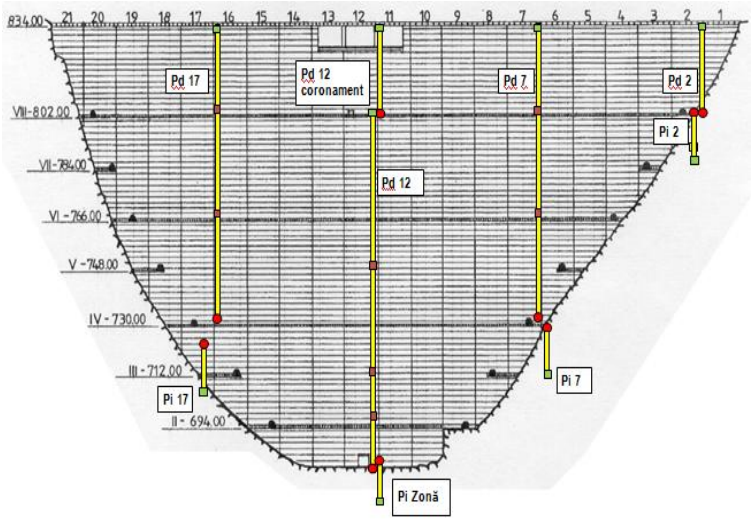


Figure 2 - Direct and inverted pendulum sections for Vidraru dam

3. RESERVOIR DRAWDOWN PROGRAM

In order to carry out the rehabilitation works of the hydromechanical equipment associated with the bottom outlets, it is necessary to lower the Vidraru Reservoir water level down to elevation 688.00 masl.

The last complete drawdown of the Vidraru Reservoir was carried out during 1974–1975 following an incident involving bottom outlet no. 2 [7]. The event was caused by the instability of a rock wedge located upstream of the Johnson valve, resulting in local damage to the outlet system. The phenomenon had a local character and did not affect the overall stability or safety of the dam. The reservoir level was subsequently lowered from elevation 823.00 masl to a minimum level of 690.25 masl, reached in March 1975.

The drawdown strategy adopted for the present operation was based on both the observations obtained during the 1974–1975 drawdown and the known structural response of the dam during the cold season. Under normal winter operating conditions, the dam typically exhibits significant downstream displacements caused by the combined effects of concrete thermal contraction and the hydrostatic pressure associated with high reservoir levels. Reservoir drawdown during this period reduces the hydrostatic load, generating an upstream displacement tendency. As a result, the effects of the two governing factors — air temperature decrease and reservoir level reduction — partially compensate each other, leading to a significantly smaller variation of the overall displacement response.

Based on these considerations, the August–February period was considered favorable for reservoir drawdown from the structural safety point of view. During this interval, the main

factors governing the dam behavior act in opposite directions, limiting the predicted displacement amplitudes. The proposed reservoir drawdown schedule is presented in figure 3.

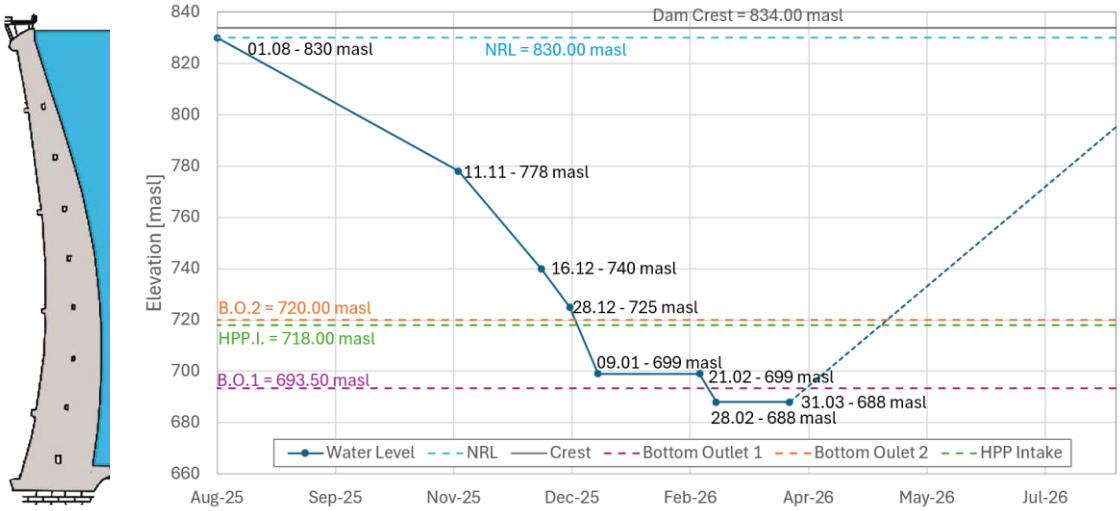


Figure 3 - Proposed drawdown schedule for Vidraru Reservoir

The reservoir drawdown started on August 10, 2025, from elevation 814.26 masl, following the predefined drawdown schedule. The operation was performed progressively in order to limit rapid variations of the hydrostatic loading conditions and to allow continuous assessment of the structural response throughout the process. The main drawdown stages considered in the present analysis are summarized in table 1.

Table 1 - Main drawdown stages considered for Vidraru Reservoir

Date	Reservoir level	30-day moving average air temperature	Obs.
	[masl]	[°C]	
01.08.2025	814.50	18.10	Starting of the drawdown process
31.10.2025	778.00	6.70	Minimum operating reservoir level
31.01.2026	699.00	-2.20	Minimum reservoir level

Reservoir drawdown and subsequent refilling may influence both the structural behavior of the dam and the response of the adjacent abutments. The most significant effects are associated with modifications of the hydrostatic loading, thermal field, and seepage regime. During drawdown, exposure of the upstream face to atmospheric conditions alters the thermal regime of the structure and may promote the opening of contraction joints during the cold season, resulting in a reduction of global structural stiffness and an increase in seepage through the joints.

At the same time, reservoir level variations modify pore-water pressures and seepage conditions within the abutment rock mass. The dissipation of pore pressures during drawdown may induce valley-opening tendencies, while seasonal thermal effects may produce localized rock expansion or contraction near exposed surfaces. These mechanisms can influence the deformation of the arch supports and consequently affect the structural response of the dam. Reservoir refilling may additionally reveal long-term changes in structural stiffness associated with dam aging, as displacements recorded under increasing hydrostatic load may differ from those observed during earlier filling phases.

Considering the atypical nature of the Vidraru reservoir drawdown, the monitoring program was intensified throughout the operation period. In addition to the conventional monitoring system, ambient vibration measurements and 3D LiDAR surveys were implemented to assess changes in global structural stiffness and abutment stability. Furthermore, a deterministic finite element model was developed and calibrated to validate the measured displacements and evaluate the stress distribution within the structure.

4. Structural Response During Reservoir Drawdown

4.1 Structural response evaluated using data provided by the monitoring system

This chapter summarizes the evolution of the main factors governing the structural response of the dam during the reservoir drawdown period analyzed (August 1, 2025 – January 31, 2026). Figure 4 presents the evolution of the reservoir water level, while figure 5 shows the variation of the daily air temperature together with the corresponding 30-day moving average temperature. During the reservoir drawdown period, no significant seismic or hydrological events were recorded. Consequently, the observed structural response can be primarily attributed to the combined effects of reservoir level variations and thermal loading.

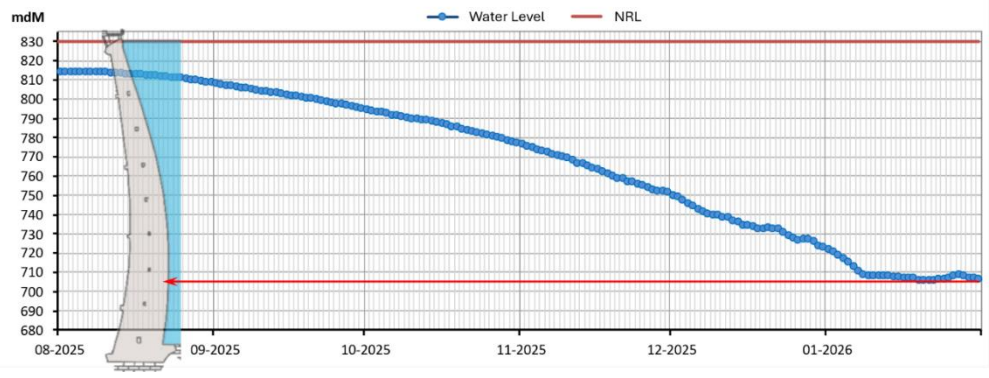


Figure 4 - Evolution of the reservoir water level during the analyzed drawdown period

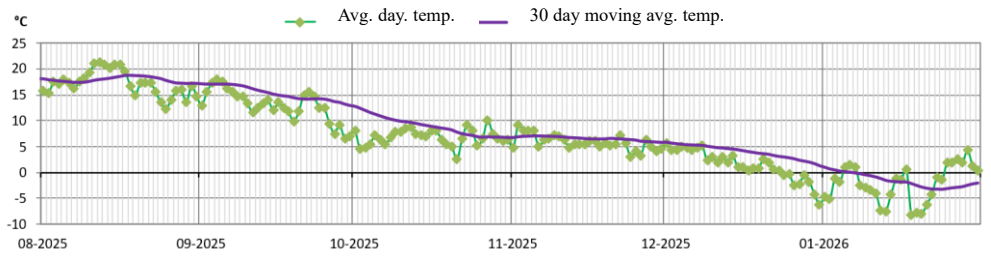


Figure 5 - Evolution of air temperature during the analyzed reservoir drawdown period

The structural response was evaluated using data provided by the monitoring system, focusing on: (1) horizontal displacements measured by the pendulum system, (2) horizontal displacements measured at the micro-triangulation reference points, (3) relative displacements recorded across the contraction joints, and (4) seepage discharge measurements.

The horizontal displacements of the dam are monitored in both the radial direction (upstream–downstream) and the tangential direction (left abutment–right abutment) using direct and inverted pendulums installed in monoliths P2, P7, P12, and P17. The reference measurements used for displacement evaluation were established on September 2, 2010, following the rehabilitation of the monitoring system.

Since the radial direction represents the dominant component of the structural response, the following discussion focuses on the displacements measured along this direction. Figure 6 presents the time evolution of the crest displacement relative to the dam foundation.

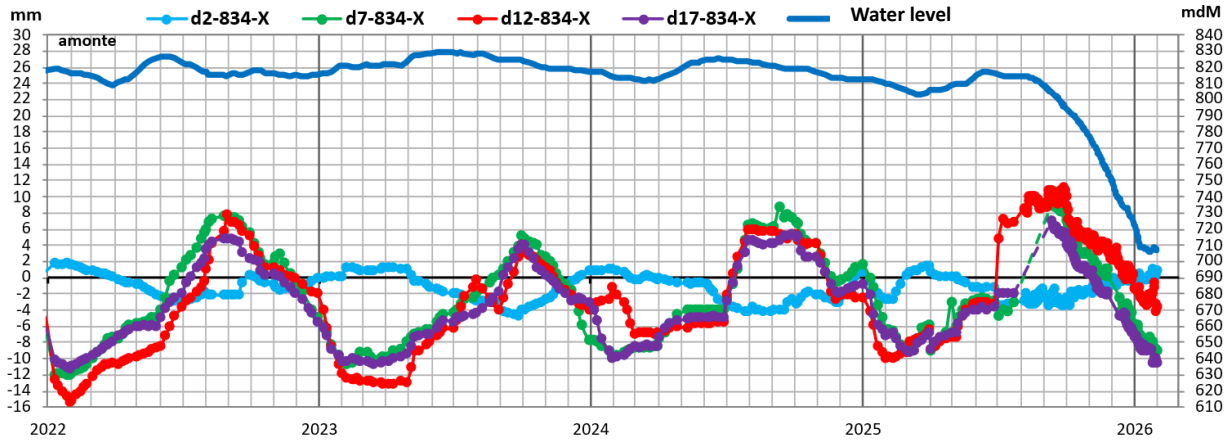


Figure 6 - Time evolution of the dam crest displacement relative to the foundation

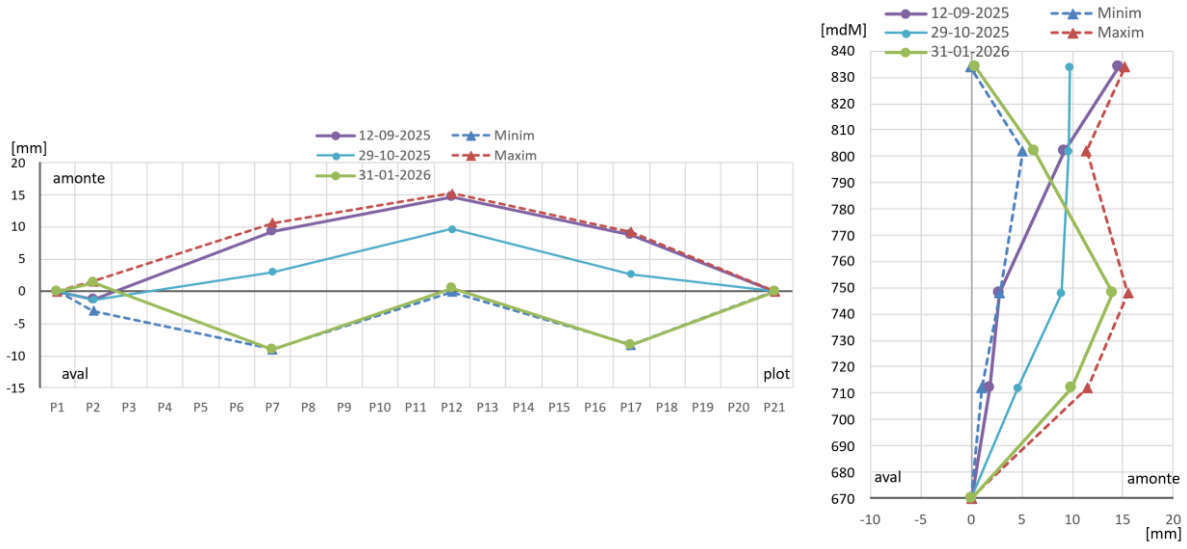
The analysis of the pendulum measurements indicates that the dam exhibited normal behavior throughout the drawdown period. The measured displacements were consistent with the governing loading factors, namely the seasonal thermal field and the hydrostatic pressure

associated with the reservoir water level. As expected, the largest displacement amplitudes were recorded in the central monolith (P12), while progressively smaller values were observed in the monoliths located closer to the abutments.

The spatial distribution of displacements was also consistent with the expected behavior of an arch dam. Along the arch direction, the maximum displacements occurred in the central region of the structure and gradually decreased toward the abutments. Similarly, along the cantilever direction, the largest displacements were recorded at the crest and progressively decreased toward the foundation.

Following reservoir drawdown, a pronounced downstream displacement tendency was observed. This behavior is attributed primarily to the decrease in air temperature during the cold season, whose influence becomes more significant as an increasing portion of the upstream face is exposed to atmospheric conditions. The results therefore confirm that thermal actions represent the dominant factor governing the displacement response of the dam.

The crest displacement profiles derived from the pendulum measurements during the reservoir drawdown period, together with the minimum and maximum displacement envelopes, are presented in figure 7 - a. The measured profiles exhibit the expected structural response, with the deformation shape recorded at the minimum reservoir level (January 31, 2026) lying close to the lower envelope and corresponding to the largest downstream displacements. This behavior is primarily governed by thermal loading. Under the cold-season thermal field, the contraction of the concrete induces a downstream displacement of the dam crest. As the reservoir level decreases, the influence of hydrostatic loading is progressively reduced, while the exposure of the upstream face to atmospheric conditions increases, further enhancing the effect of air temperature on the structural response.



(a) (b)

Figure 7 - Horizontal displacements [mm]
(a) crest displacement profiles, (b) monolith P12 displacement profiles

The displacement profiles of the maximum-height cantilever section (monolith P12), derived from the pendulum measurements, are presented in Figure 7 – b together with the minimum and maximum displacement envelopes. Compared to the conditions recorded at the beginning of the reservoir drawdown, the deformation profile measured at the end of the drawdown period (January 31, 2026) indicates downstream displacements at elevations 834 m (crest) and 802 m, and upstream displacements at elevations 748 m and 712 m.

Statistical behavior models were developed using the crest displacements measured by the pendulums installed in monoliths P7, P12, and P17. For the upstream–downstream direction, the following explanatory variables were considered:

- the reservoir water level at the time of measurement;
- the air temperature, represented by the 90-day moving average preceding the measurement date.

As an example, figure 8 presents the statistical model developed for the crest displacement of monolith P12. The calculated response closely follows the measured values, with the residuals remaining within the expected statistical range, including during the reservoir drawdown period.

Since the vast majority of measurements remained within the range associated with normal structural behavior, it can be concluded that, from the perspective of pendulum measurements, the dam exhibited a response fully consistent with the applied loading conditions throughout the analyzed period.

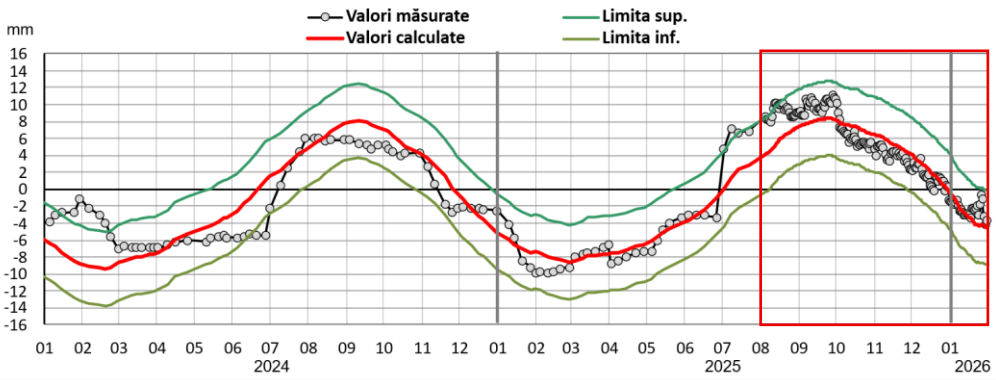


Figure 8 - Statistical model of crest displacements for monolith P12

The results obtained from the micro-triangulation network, contraction joint measurements, seepage monitoring system, and visual inspections confirmed the conclusions derived from the pendulum measurements. The measured displacements remained consistent with the applied loading conditions, while relative joint displacements were negligible, generally remaining below 0.1 mm. Seepage discharge progressively decreased during drawdown and reached zero when the reservoir level dropped below elevation 710.00 masl. No evidence of abnormal structural behavior, such as cracking, concrete deterioration, excessive seepage, or instability of the adjacent abutments, was observed during the monitoring period. Figure 9 illustrates the condition of the upstream and downstream faces of the dam at the end of the drawdown operation.


(a)



(b)

Figure 9 – Visual inspection performed using drones
(a) right abutment - downstream face, (b) upstream face

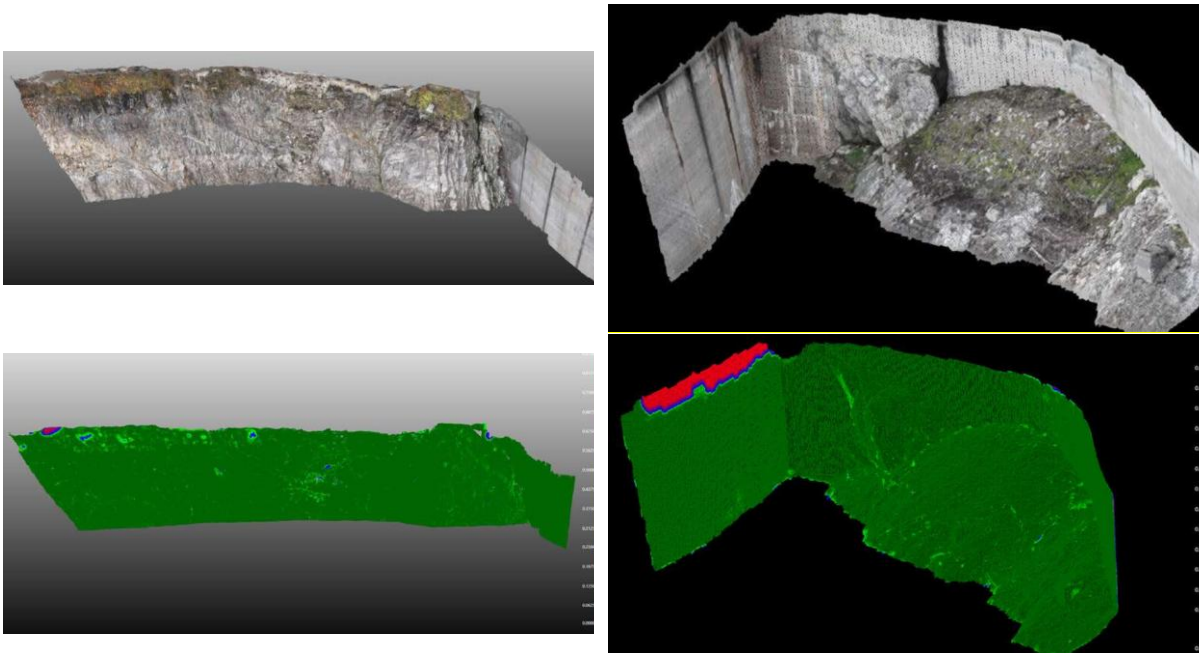
4.2 Slope Stability Monitoring Using 3D Laser Scanning

Particular attention was paid to the stability of the abutments located upstream of the dam during the reservoir drawdown process. A potential concern associated with rapid reservoir

level reduction is the delayed dissipation of pore water pressures within the rock mass, which may adversely affect slope stability. To detect any abnormal behavior at an early stage, a dedicated monitoring program based on 3D laser scanning was implemented.

In order to assess possible slope displacements and deformations in the vicinity of the dam abutments, four geodetic survey campaigns were scheduled using 3D laser scanning technology. The first survey was performed at the beginning of the reservoir drawdown, followed by additional surveys at the minimum operating reservoir level and at the minimum reservoir level. A final survey is planned during the reservoir refilling stage, when the water level reaches the minimum operating level.

To date, 3 of the 4 LiDAR survey campaigns have been carried out using a DJI Matrice 350 platform equipped with a Zenmuse L2 sensor. Following each survey, the resulting point clouds and Digital Surface Models (DSM) were compared in order to identify elevation differences. Color-coded difference maps were subsequently generated to facilitate the visual identification of potentially unstable areas. Figure 10 presents the three-dimensional comparison of the mesh surfaces generated from the LiDAR point clouds acquired during the August and November 2025 surveys for both abutments of the dam.



(a) *(b)*

Figure 10 – Comparison of the mesh surfaces generated from the LiDAR point clouds

The direct comparison of the point clouds indicates that the areas exhibiting apparent displacements in the range of 50–100 cm are restricted to locations where the LiDAR filtering

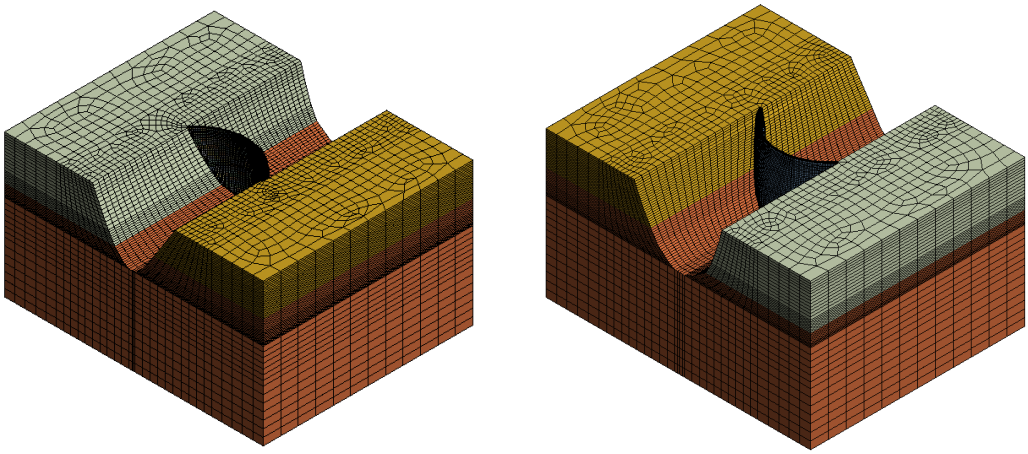
process resulted in the complete removal of points from one of the datasets. This effect is associated with the point cloud comparison algorithm, which computes elevation differences by searching, for each point in the reference cloud, for neighboring points located within a sphere of 100 cm radius in the comparison cloud. In areas where one of the point clouds contains no valid LiDAR points, the computed differences may artificially approach the search radius, resulting in apparent displacements of up to 100 cm. Consequently, these localized differences should be interpreted as processing artifacts rather than actual ground movements.

The analysis did not identify any significant displacements of the upstream abutment surfaces that could adversely affect the safety of the Vidraru Dam as a result of the reservoir drawdown operation. Additional comparisons performed using the datasets acquired during the winter survey confirmed this interpretation. An important consideration in the analysis of the LiDAR data is the influence of seasonal snow and ice cover, which may generate apparent elevation differences unrelated to actual ground movements. Most of the differences identified between successive surveys were associated with snow accumulation on the upper parts of the abutments. After accounting for this effect, no significant deformations of the upstream abutments attributable to reservoir drawdown were identified.

5. Static Analysis Using the Deterministic Finite Element Model

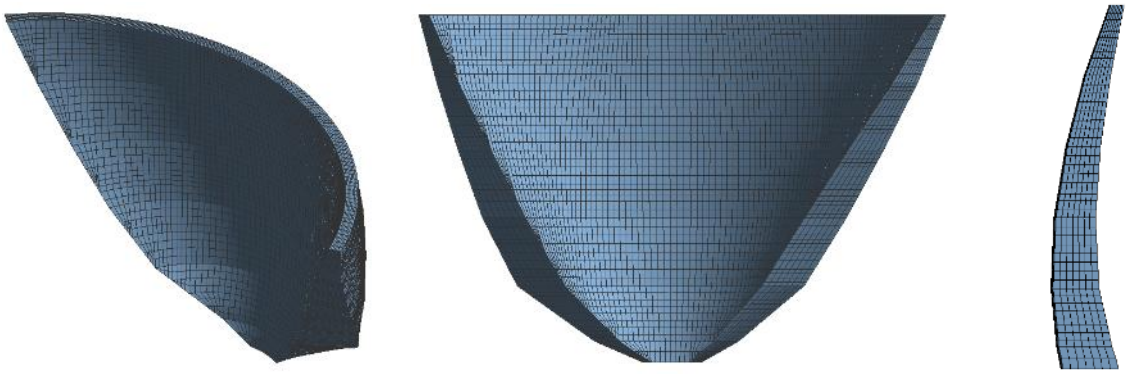
A deterministic finite element model of the dam–foundation system was developed to simulate the structural response of the dam under the loading conditions corresponding to the different reservoir drawdown stages (figure 11 and 12). Both the dam body and the foundation rock mass were discretized using three-dimensional quadratic isoparametric finite elements with incompatible modes and three translational degrees of freedom per node (ux, uy, uz). Particular attention was given to achieving a regular mesh for all model components. Contraction joints were not explicitly represented and the dam was assumed to behave as a monolithic structure.

The foundation rock mass was discretized using 20-node solid elements following the valley geometry. To obtain a regular discretization and to facilitate mesh compatibility at the dam–foundation interface, bonded contact elements were employed. The foundation domain was extended approximately 1.5 times the dam height in all directions from the dam–foundation interface, which was considered sufficient to minimize boundary effects and adequately represent foundation flexibility.



(a) *(b)*

Figure 11 – Axonometric Views of the Vidraru Dam Finite Element Model (a) downstream view, (b) upstream view



(a) *(b)* *(c)*

Figure 12 - Adopted mesh for dam structure (a) Axonometric view from downstream, (b) downstream view, (c) maximum height section

The material properties assigned to the various discretized domains are presented in Table 2. For the purpose of the analysis, both the concrete and the foundation rock mass were assumed to be homogeneous, isotropic, and linearly elastic materials.

Static calibration of the finite element model was performed using displacement measurements recorded at the instrumentation installed within the central cantilever (P12), including the inverted pendulum and the direct pendulums. Two independent analyses were carried out in order to reproduce the structural response corresponding to the maximum and minimum temperatures recorded during the last five years. Both extreme thermal conditions occurred during 2022.

Table 2 - FEM model material properties

Material		Static Young's Modulus E	Poisson's Ratio μ	Density ρ
		[MPa]	[-]	[t/m^3]
Dam Concrete		3.20 E4	0.20	2.45
Left Abutment Rock Mass		1.85 E4	0.24	0
Central Foundation Rock Mass		3.45 E4	0.24	0
Right Abutment Rock Mass		2.45 E4	0.24	0

The calibration procedure considered two material parameters as calibration variables: the coefficient of thermal expansion of concrete (α) and the static modulus of elasticity of concrete. The coefficient of thermal expansion was varied between 5×10^{-6} and 12×10^{-6} °C^{-1}, while the static modulus of elasticity was varied between 27.000 MPa and 37.000 MPa. The best agreement between the numerical predictions and the measured displacements was obtained for a coefficient of thermal expansion of $\alpha = 5\times10^{-6}$ °C^{-1} and a static modulus of elasticity of E_c =32.000 MPa. These values were subsequently adopted for all static analyses presented in this study.

For each drawdown stage considered in the analysis, the corresponding boundary conditions were applied, including the reservoir water level and the air temperature represented by the 30-day moving average preceding the analyzed date.

The temperature field within the dam body was determined through a heat transfer analysis. The thermal boundary conditions consisted of the air temperature applied to all exposed surfaces of the dam (downstream face, crest, and exposed portion of the upstream face), together with a depth-dependent water temperature distribution applied to the submerged upstream face. The latter was defined according to the formulation proposed by Priscu [9]:

$$\theta_r = \bar{\theta_r} + A_r cos\left(\frac{2\pi t}{T} - \beta\right) \quad (1)$$

$$\bar{\theta_r} = 4.50 + (k\bar{\theta_a} - 4.50)\left(1 - \frac{z}{H}\right)^2 \quad (2)$$

where:

θ_r: reservoir water temperature at time t

$\overline{\theta_r}$: mean annual reservoir water temperature at elevation z below the water surface level H

$\overline{\theta_a}$: mean annual air temperature

A_r: amplitude of the annual reservoir water temperature fluctuations

T: period of one annual cycle (T = 8760 h)

β: phase shift (radians)

k: coefficient equal to 1.6 for reservoir depths greater than 60 m

The resulting temperature field was subsequently transferred to the structural model and combined with the remaining loads, namely self-weight and hydrostatic pressure, for the stress–strain analysis.

The numerical analyses focused on the following response quantities:

- radial displacements of the nodes belonging to monolith P12, used for comparison with the displacement measurements obtained from the pendulum system – figure 13;
- tangential displacements along three representative arch rings located at elevations 730 masl, 794 masl, and 834 masl;
- maximum and minimum principal stresses (σ_1 and σ_3);
- arch stresses evaluated along four representative arch rings located at elevations 690 masl, 730 masl, 794 masl, and 834 masl – figure 14;
- cantilever stresses evaluated in three characteristic sections corresponding to the instrumented monoliths P7, P12, and P17 – figure 15;
- stress distribution at the dam–foundation interface – figure 16.

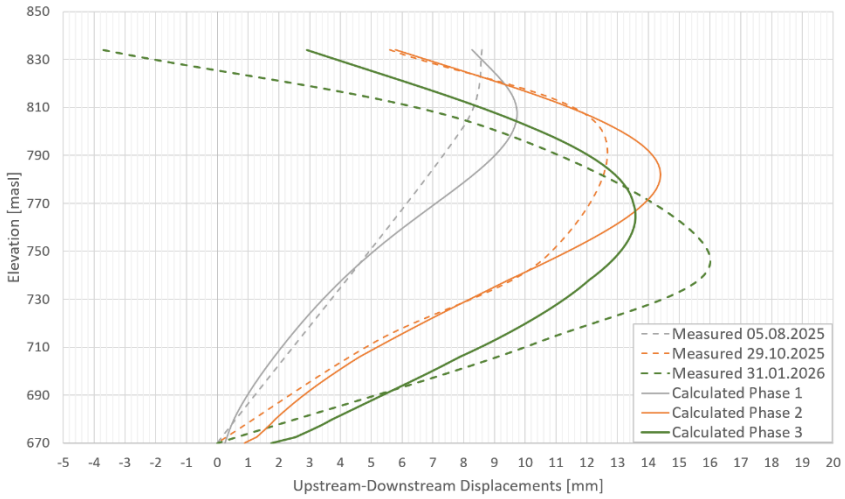


Figure 13 - Calculated and measured radial displacements for monolith P12 [mm]

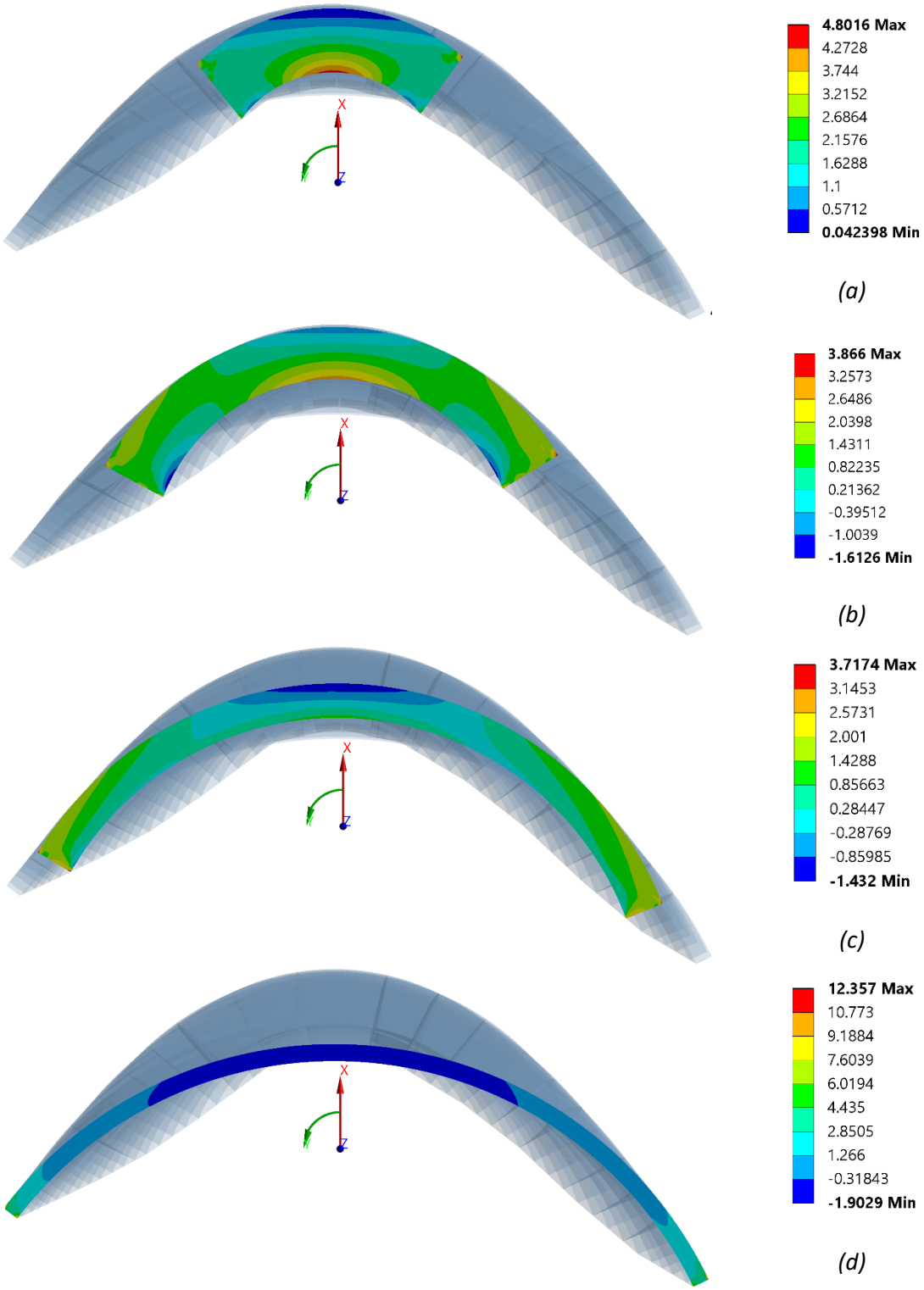
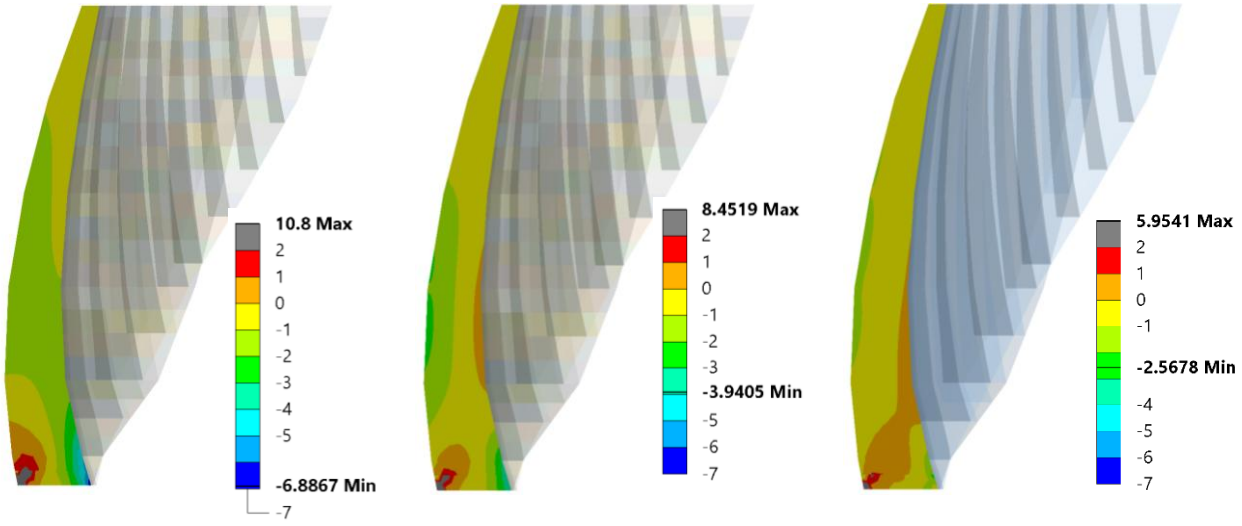
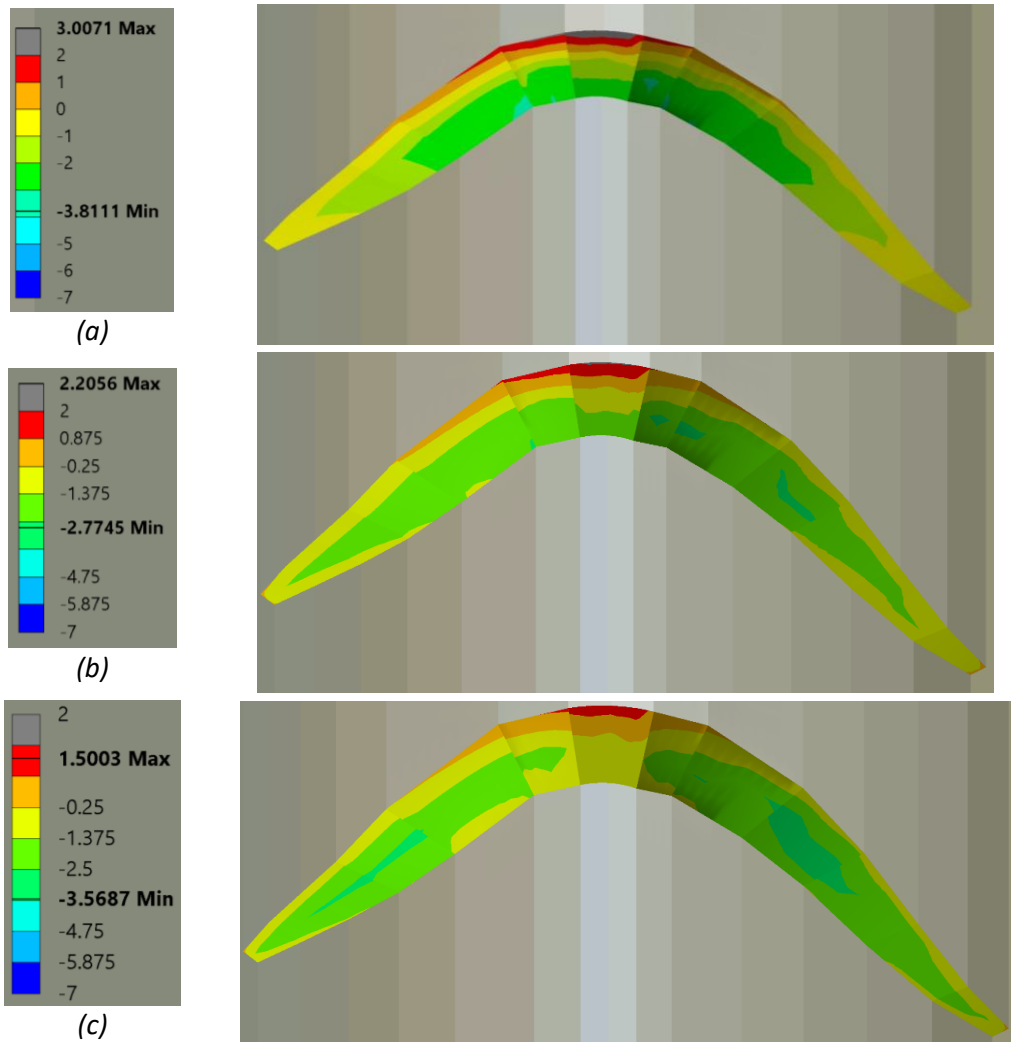


Figure 14 - Arch stresses evaluated for third phase [MPa]
(a) arch ring 690 masl, (b) arch ring 730 masl, (c) arch ring 794 masl, (d) arch ring 834 masl



(a) *(b)* *(c)*

Figure 15 - Cantilever stresses – central monolith (P12) [MPa]
(a) first phase, (b) second phase, (c) third phase



(a)

(b)

(c)

Figure 16 - stress distribution at the dam–foundation interface [MPa]
(a) first phase, (b) second phase, (c) third phase

The results obtained for the three drawdown stages considered in the static analyses allow several observations to be made:

- A good agreement was observed between the finite element predictions and the displacement measurements provided by the monitoring system. The highest level of correlation was obtained for the maximum-height section (P12), where the calculated radial displacements fall within the range recorded by the direct and inverted pendulums.
- For all analyzed stages, the shape of the deformed structure was consistent with the applied loading conditions, indicating a predictable mechanical response in accordance with the expected behavior of high concrete arch dams.
- From the stress analysis perspective, the computed stress levels remained within the elastic range of mass concrete for almost the entire structure. Local stress concentrations exceeding 2 MPa were identified in the central region of the lower arch rings, near the downstream face. However, under actual structural conditions, local stress redistribution mechanisms are expected to occur, resulting in lower effective stress levels than those predicted by the linear-elastic model. Such effects cannot be captured by the present linear elastic analysis.
- The stresses evaluated in the cantilevers and at the dam–foundation interface showed a gradual reduction as the reservoir level decreased. Stress values exceeding 2 MPa were limited to the maximum-height section and were confined to a relatively small area near the upstream toe of the structure.
- Both the monitoring data interpretation and the deterministic finite element analyses lead to the same conclusion: the displacement response of the Vidraru Dam is controlled predominantly by thermal actions, while the influence of hydrostatic loading variations is comparatively smaller. The displacement amplitudes induced by air temperature changes are significantly greater than those associated with reservoir level fluctuations. This behavior has been consistently observed throughout the operational life of the dam and is not limited to the reservoir drawdown conditions investigated in the present study.

6. AMBIENT VIBRATION MONITORING

As part of the monitoring program implemented during the reservoir drawdown and refilling operations, an additional ambient vibration measurement campaign was carried out. The program was motivated by the fact that the modal parameters of the structure, namely the

natural frequencies and vibration periods, provide an indirect measure of its global stiffness. The main objective was to identify possible changes in structural integrity resulting from the significant variations in loading conditions associated with the drawdown and refilling processes. For comparable reservoir levels and thermal conditions, the preservation of the modal characteristics may be regarded as evidence of structural integrity, whereas an increase in the natural periods may indicate a reduction in structural stiffness.

The results of ambient vibration testing characterize the global dynamic behavior of the structure within the linear-elastic range associated with low-amplitude vibrations. The identified modal parameters provide a global representation of the structural condition at the time of testing and constitute an objective indicator of the in-situ behavior of the dam. Such measurements can be used both for the calibration of numerical models and for the long-term assessment of structural behavior through comparison with future measurements. [1 – 5, 11, 12]

Two measurement layouts were considered, each consisting of three acquisition channels, with sensors installed at monoliths P5, P8, P10, P12, P15, and P17, as shown in figure 17. For each scheme configuration, several records with a duration of five minutes were acquired, corresponding to 30,000 samples per record at a sampling frequency of 100 Hz (time step of 0.01 s). The measurement system consisted of a GeoSIG GMSplus data acquisition unit and VE-51-H horizontal uniaxial sensors manufactured by GeoSIG, Switzerland.

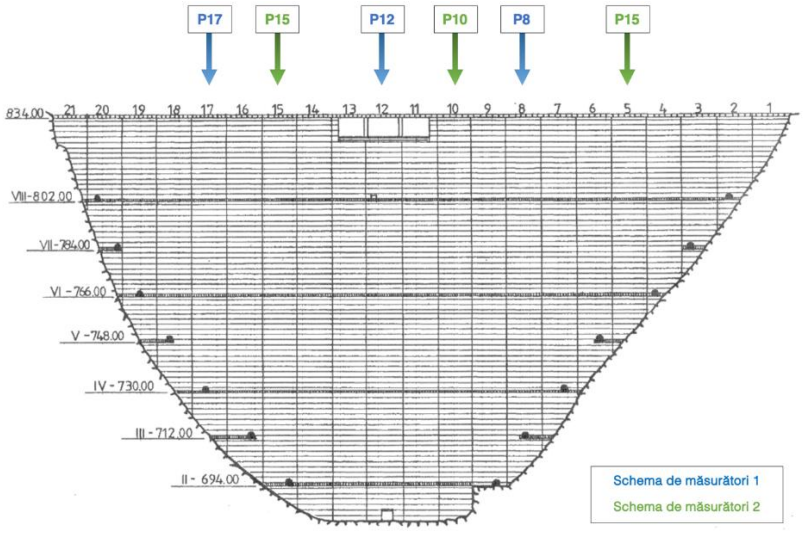


Figure 17 - Measurement schemes for AVM

The monitoring program includes three ambient vibration measurement campaigns: (a) at the beginning of the reservoir drawdown, (b) at the minimum reservoir level, and (c) after completion of the reservoir refilling process. At the time of writing, two of these campaigns have been completed: the first at the beginning of the drawdown operation, under thermal

conditions representative of the warm season, and the second at the minimum reservoir level, under thermal conditions representative of the cold season.

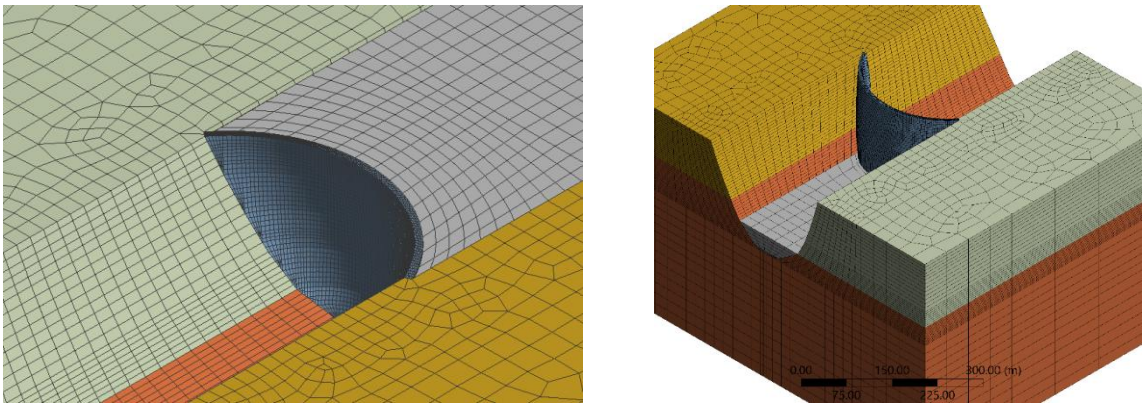
The analysis of the recorded signals identified the natural frequency associated with the fundamental vibration mode (within the low-amplitude vibration range) at approximately 2.6 – 2.7 Hz (T_1 = 0.37 – 0.385 s) during the first measurement campaign, performed under warm-season conditions with the reservoir level at elevation 814 masl. For the second measurement campaign, conducted during the cold season with the reservoir level at elevation 699 masl, the identified fundamental frequency ranged between 2.44 and 2.49 Hz (T_1 = 0.40 – 0.41 s). The first 5 recorded frequencies and periods for both measurement campaigns are presented in table 3.

Table 3 - First 5 recorded frequencies and periods for both measurement campaigns

Vibration mode	First campaign		Second campaign	
	Frequency [Hz]	Period [s]	Frequency [Hz]	Period [s]
1	2.60	0.385	2.44	0.410
2	3.65	0.274	3.25	0.308
3	4.25	0.235	3.91	0.256
4	6.30	0.159	5.86	0.171
5	8.10	0.123	8.23	0.122

The first measurement campaign provided the modal parameters required for the dynamic calibration of the finite element model. The dynamic calibration results were consistent with both the static calibration procedure and the conclusions of previous investigations [8, 10], providing additional confidence in the adopted material properties and overall model representation.

The dynamic calibration procedure was performed using a modal analysis based on the same finite element model employed for the static analyses. In contrast to the static model, the reservoir was explicitly represented using acoustic fluid elements characterized by four degrees of freedom per node (three displacements and pressure) – figure 18. The physical properties assigned to the reservoir water were adopted from the literature [13]: modulus of elasticity E = 1308 MPa, Poisson's ratio ν = 0.499, density ρ = 1000 kg/m³, and sound velocity v = 1438.6 m/s.



(a) *(b)*

Figure 18 - FEA models for (a) warm season and (b) cold season

The dynamic elastic moduli assigned to the different rock volumes were obtained by geophysical in situ investigations done in 1993 [8]. Calibration of the numerical model was performed by matching the experimentally identified fundamental vibration period obtained during the first measurement campaign. For the average fundamental period of 0.38 s, the calibrated global dynamic modulus of elasticity of the dam concrete was found to be approximately 47,500 MPa. It should be noted that the calibrated value is in very good agreement with the results of the geophysical investigations carried out in 1993, which yielded a dynamic modulus of elasticity of E_{dyn} = 49,800 MPa [8]. This consistency provides additional confidence in the adopted dynamic properties and the overall validity of the numerical model.

The comparison between the modal parameters identified during the second measurement campaign (empty reservoir, cold season) and those obtained at the beginning of the drawdown operation (reservoir elevation 814 masl, warm season) reveals an increase in the fundamental vibration period and a corresponding reduction in the identified natural frequencies. This behavior indicates a decrease in the global stiffness of the dam–foundation system. Such a trend is particularly significant because the disappearance of the reservoir effect would normally be expected to increase the natural frequencies due to the reduction of the hydrodynamic added mass. The observed decrease in frequency therefore suggests that the stiffness reduction associated with the cold-season thermal field and the partial opening of contraction joints is more significant than the stiffening effect resulting from reservoir drawdown.

Using the modal parameters identified during the second ambient vibration campaign, the dynamic calibration procedure was repeated following the same methodology adopted for the first campaign. For the average fundamental period of 0.41 s, corresponding to the minimum

reservoir level condition (reservoir elevation 699.00 masl.), the calibrated global dynamic modulus of elasticity of the dam concrete was found to be approximately 32,000 MPa.

This value is significantly lower than the global dynamic modulus obtained from the first measurement campaign conducted under warm-season conditions (E_{dyn} = 47,500 MPa). The reduction in the calibrated global stiffness is attributed to the cold-season thermal field, which promotes the opening of contraction joints and consequently reduces the overall stiffness of the structure. Since the finite element model adopted in the present study is based on a linear-elastic formulation and does not explicitly represent the contraction joints, this seasonal stiffness variation can only be reproduced indirectly through modifications of the adopted global modulus of elasticity.

Figure 19 illustrates the influence of the reservoir water level on the modal characteristics of the dam–reservoir system for both the warm-season and cold-season calibrations. From a dynamic perspective, variations in reservoir level modify the total mass of the system through changes in the hydrodynamic interaction between the reservoir and the structure, resulting in corresponding changes in the natural frequencies, vibration periods, and mode shapes. Establishing a relationship between reservoir level and modal parameters enables meaningful comparisons between numerical predictions and measurements performed under different operating conditions.

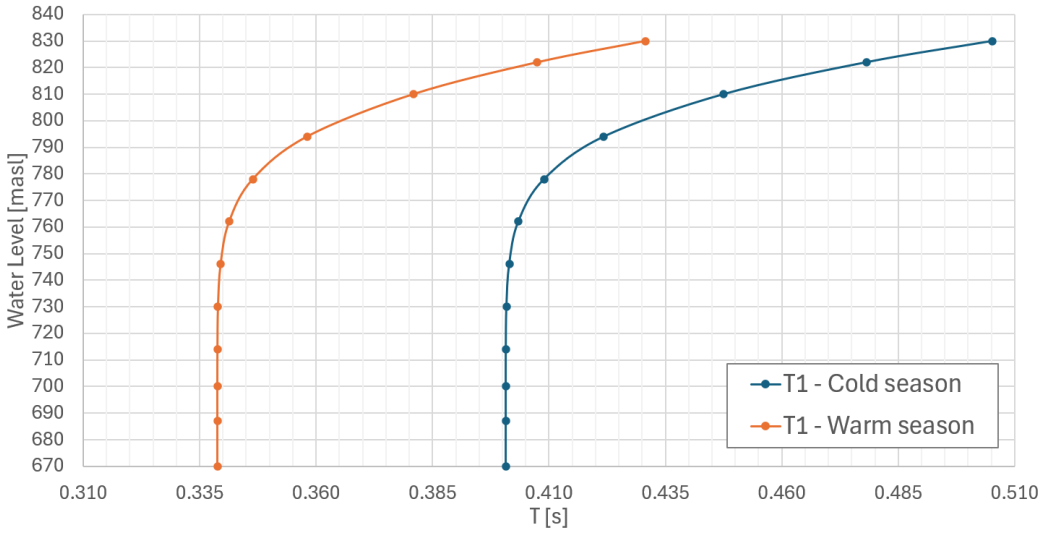


Figure 19 - Variation of the Fundamental Vibration Period as a Function of Reservoir Water Level for Warm- and Cold-Season Conditions

The modal parameters identified during the cold-season campaign indicate that thermally induced joint opening has a greater influence on the global structural stiffness than

the reservoir drawdown itself, consistent with the conclusions obtained from the monitoring data and the numerical analyses.

7. CONCLUSIONS

The drawdown of the Vidraru Reservoir constituted an atypical operating condition that significantly modified both the hydrostatic loading and the thermal regime acting on the dam. Despite these changes, all monitoring systems indicated a normal structural response throughout the analyzed period.

The interpretation of pendulum measurements, micro-triangulation surveys, seepage discharge records, and visual inspections consistently showed that the dam behavior remained within the expected range associated with the applied loading conditions.

The separation of the hydrostatic and thermal components of the response demonstrated that air temperature is the dominant factor governing the displacement behavior of the Vidraru Dam. This conclusion was independently confirmed by both statistical behavior models and deterministic finite element analyses.

The deterministic finite element model provided a very good agreement with the measured displacements and enabled a detailed evaluation of the stress distribution within the structure. The computed stress levels remained within the elastic range of mass concrete, with only limited local stress concentrations identified in specific areas of the lower arch rings.

Ambient vibration measurements revealed a significant seasonal variation in the global stiffness of the dam–foundation system. The calibrated equivalent dynamic modulus decreased from approximately 47.5 GPa under warm-season conditions to approximately 32 GPa under cold-season conditions, indicating a substantial reduction in global stiffness associated with thermally induced joint opening.

No significant deformations of the adjacent abutments were identified by the LiDAR monitoring program. The observed differences between successive surveys were primarily associated with point-cloud processing limitations and seasonal snow cover rather than with actual slope movements.

Reservoir drawdown did not compromise the safety of the Vidraru Dam; however, ambient vibration measurements revealed a significant seasonal reduction in global stiffness associated with thermally induced joint opening, an effect that cannot be directly captured by a conventional monolithic linear-elastic FE model.

REFERENCES

[1] Abdulamit, A., A. Aldea, S. Demetriu, C. Neagu, and D. Gaftoi. 2017. “Ambient Vibration Tests at Some Buttress Dams in Romania.” In Proceedings of the X International Conference on Structural Dynamics (EURODYN 2017). Procedia Engineering 199: 2196–2201.

[2] Abdulamit, A., D. Stematiu, and D. Gaftoi. 2016. “An Alternative Method to Evaluate the Health Status for Concrete Dams.” Environmental Engineering and Management Journal 15 (6): 1397–1407.

[3] Darbre, G. R., C. A. M. de Smet, and C. Kraemer. 2000. “Natural Frequencies Measured from Ambient Vibration Response of the Arch Dam of Mauvoisin.” Earthquake Engineering & Structural Dynamics 29 (5): 577–586.

[4] Gaftoi, D., A. Abdulamit, A. Aldea, R. Sârghiuță, and C. Popescu. 2021. “Assessing Structural Safety of an Arch Dam Using In Situ Vibration Tests.” IOP Conference Series: Materials Science and Engineering 1203. DOI:10.1088/1757-899X/1203/2/022122

[5] Gaftoi, D., A. Abdulamit, and D. Stematiu. 2016. “Assessment of Gura Râului Dam Safety Using Measurements of Structural Response to Ambient Vibrations.” Procedia Engineering 161: 722–728. Presented at the World Multidisciplinary Civil Engineering–Architecture–Urban Planning Symposium (WMCAUS 2016), Prague, Czech Republic.

[6] ICOLD Committee on Concrete Dams. 2024. Arch Dam Design: Structural Analysis Methodologies and Criteria, December 2024. http://www.icold-cigb.org./

[7] Institutul de Studii și Proiectări Hidrotehnice. 1984. Accidente la Construcții Hidrotehnice. București. (in Romanian)

[8] Popovici, A., R. Sârghiuță, I. Toma, and T. Moldoveanu. 1996. “Reevaluation of the Seismic Safety of a Large Arch Dam Commissioned Thirty Years Ago.” Paper no. 1706. In Proceedings of the Eleventh World Conference on Earthquake Engineering.

[9] Prișcu, R. 1973. Construcții Hidrotehnice. Volumul 1. București: Editura Didactică și Pedagogică. (in Romanian)

[10] Prișcu, R., A. Popovici, D. Stematiu, L. Ilie, and C. Stere. 1980. Ingineria Seismică a Marilor Baraje. București: Editura Academiei Republicii Socialiste Romania. (in Romanian)

[11] Sârghiuță, R., and A. Abdulamit. 2014. “Diagnosis of the Structural Evolution of Dams Using Dynamic Monitoring Data.” In Proceedings of the International Symposium Dams in a Global Environmental Challenges, Bali, Indonesia.

[12] Sârghiuță, R., A. Abdulamit, and T. Bugnariu. 2007. “Safety Assessment of Arch Dams Using Global Elastic Modulus Concept.” In Proceedings of the International Symposium Thirty Years from the Romanian Earthquake of March 4 1977.

[13] State of Practice for the Nonlinear Analysis of Concrete Dams at the Bureau of Reclamation. 2006. Denver, CO: U.S. Department of the Interior, Bureau of Reclamation.

Experimental investigation of earth dam breaching – latest research results

authorsList

1. Krzysztof Zamiar
2. Stanisław Kostecki

affiliationsList

1. Master of Science, Politechnika Wrocławska, Wybrzeże Stanisława Wyspiańskiego 27, 50-370 Wrocław, Poland, ORCID: 0000-0001-5988-1066
2. Associate Professor, Politechnika Wrocławska, Wybrzeże Stanisława Wyspiańskiego 27, 50-370 Wrocław, Poland, ORCID: 0000-0001-5002-6119

keywords

overtopping, dam failure, laboratory tests, breach mechanism,

abstract

Dam failures are highly hazardous events with severe impacts and far-reaching consequences. In Poland, two major dam disasters occurred in the 21st century as a result of overtopping, which led to progressive erosion and breaching of the structures. These include the failure of the dam in Niedów in 2010 and the failure in Stronie Śląskie in 2024. The ability to predict the consequences of such failures in advance is crucial for the protection of areas located downstream of the reservoir. This requires a thorough understanding of the processes governing dam erosion and breach development, which determine the rate of water outflow through the breach. This topic was addressed by the authors in a previous publication entitled "Understanding Geotechnical Embankment Washout Due to Overtopping: Insights From Physical Tests" (Studia Geotechnica et Mechanica, 2024), where the previous stage of experimental research on this phenomenon was presented. In 2025, the next stage of the research was carried out. The experimental setup, consisting of a 50 cm high and 200 cm long dam and a reservoir with a capacity of 14.4 m^3, was extended by adding concrete slabs to the upstream slope of the dam. This solution is commonly used as a sealing and protective lining in many earth dams. The main objective of this new experiment was to investigate the influence of the slabs on the breaching process The paper presents the results of the latest experiment and compares them with the results from previous tests, focusing on similarities and differences. The most important elements include video recordings documenting the breaching process and an analysis of the outflow rate. The study also summarizes the successful and unsuccessful aspects of the conducted experiment and outlines directions for further research.

Reassessing Seismic Risk for Dams and Hydromechanical Equipment Through Worldwide Experience Feedback

Ludivine SAINT-MARD, Nicolas HUMBERT**,** David GRAVELEINE**,** Philippe KOLMAYER**,** Federic LAUGIER

EDF-HYDRO-CIH La Motte-Servolex, France

Ludivine.saint-mard@edf.fr

Key words

Seismic risk assessment, Dam performance, International database, Earthquake experience feedback

Abstract

This paper reassesses seismic risk for dams and hydromechanical equipment through worldwide earthquake experience feedback. International databases, largely focused on damaged or failed structures, show that seismic-induced failures are exceptionally rare, particularly for modern hydraulic dams. The study highlights the importance of positive seismic feedback, which is often absent from existing analyses. An international framework is proposed to standardize post-earthquake data collection and to develop a shared database supporting observation-based and proportionate seismic risk assessment.

1. Introduction

The safety of dams -including the civil engineering structures, appurtenant works, and hydromechanical equipment- constitutes a central issue in risk assessment studies. Among the hazards considered, earthquakes are given a level of attention and analytical complexity comparable to flooding, although their associated risk level is significantly lower.

Current state-of-the-art practice increasingly relies on advanced analysis numerical methods, often demanding substantial engineering resources. However, the earthquake feedback accumulated since the early operation of hydraulic dams -through synthesis bulletins, post-earthquake reconnaissance missions, and inspection reports- leads to a robust conclusion: dam and gate structural failures directly attributable to earthquakes are exceptionally rare. This observation is particularly striking when contrasted with the large number of significant earthquakes occurring each year in the vicinity of dams, and when compared with the much higher frequency of failures associated with non-seismic causes. Societal perception of seismic risk therefore appears to introduce a fundamental bias in the way seismic risk for dams is assessed.

Considering these findings, a graduated approach to seismic risk is proposed, placing observation at the core of justification methods. For a well-designed dam without known pathologies, an argumentation primarily based on earthquake feedback may be sufficient. Such an approach would be further strengthened by the existence of a comprehensive earthquake feedback database. At present, most publicly available syntheses focus mainly on reported damage and failures, whereas positive earthquake feedback -which represents the great majority of observed cases- remains largely undocumented, despite being essential for quantitative risk assessment. To address this limitation, a dedicated tool is proposed to collect this information through standardized data-collection forms, triggered by alert mechanisms notifying relevant seismic events. The tool would allow systematic archiving and classification of observations, enabling statistical analysis of seismic performance within a consolidated international database co-developed with the hydraulic community.

2. Earthquake feedback

Seismic earthquake feedback provides essential insight into the behavior of dams, appurtenant structures, and hydromechanical equipment, when subjected to earthquake loading. Existing syntheses and technical reports document most major seismic-related incident affecting dams worldwide. In this context, an incident is defined as an unintentional event, of internal or external origin, that affects or may affect the normal operation (for example loss of maneuverability for a flood spillway gate), safety, or security of a dam, potentially resulting in failure or damage. A failure is a catastrophic incident characterized by an uncontrolled release of impounded water and/or a total loss of integrity of the dam body, its foundation, or its

abutments. By contrast, damage refers to an observable degradation of structural integrity or functionality that may require repair or enhanced monitoring, without constituting a failure in itself.

The main sources of publicly accessible seismic feedback consist of synthesis studies, post-earthquake reconnaissance missions, and post-seismic inspections. An overview of these sources and the key conclusions drawn from them is presented in the following sections.

2.1. International synthesis

The ICOLD Incident Database, initially published as Bulletin 99 in 1995 (ICOLD, 1995) and updated through Bulletin 188 in 2025 (ICOLD, 2025), provides a global inventory of dam failures together with a statistical analysis of their causes. According to this database, only 2 % of the 311 documented dam failures are attributed to seismic events, whereas floods account for 42 % of the failures. This highlights the marginal contribution of earthquakes to dam failures in the worldwide earthquake feedback compared with hydrological loading (**Figure *1***).

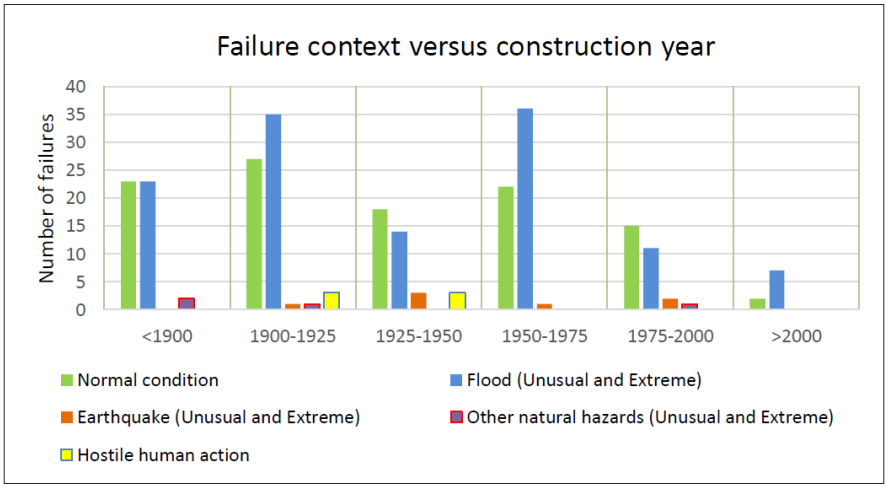


Figure 1 Failure context versus construction year (ICOLD, 2025)

The bulletin further indicates that embankment dams are more frequently affected by seismic incidents than concrete dams (**Figure *2***), with eight embankment dams involved in seismic related failures compared to only one concrete dam. It is noteworthy that the only documented case of failure of a concrete dam occurred as a result of fault rupture directly beneath the structure.

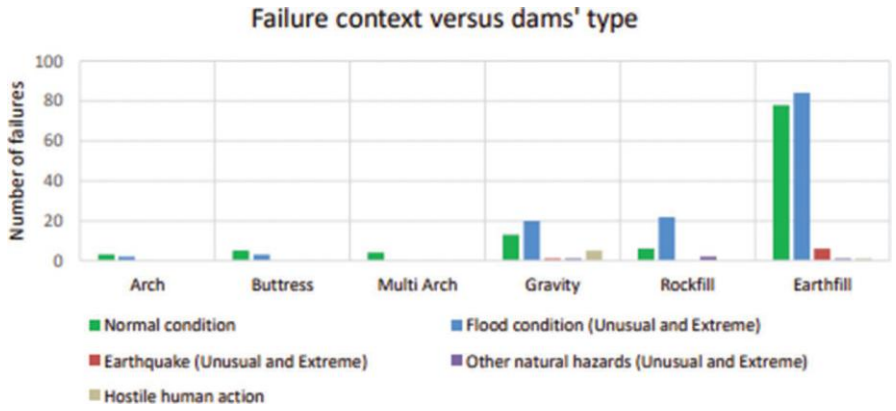


Figure 2 Failure context versus dam's type (ICOLD, 2025)

For embankment dams, the dominant failure mechanism is structural, whereas the single concrete dam case corresponds to a foundation-related failure mode due to the rupturing fault. The seismic failure cases identified in the ICOLD database are summarized in **Table *1***.

Dam name	**Country**	**Year of construction**	**Dam type**	**Height (m)**	**Year of failure**	**Reservoir volume (hm^3)**
Tappar	India	1976	Embankment	15.5	2001	25–50
Fujinuma-ike	Japan	1949	Embankment	18.5	2011	1–5
Shih-Kang	Taiwan	1997	Gravity	25	1999	1–5
Austrian Dam (Lake Elsman)	USA	1950	Embankment	56.4	1989	5–10
Lower San Fernando Dam	USA	1921	Embankment	43	1971	25–50
Baihe (Paiho)	China	1960	Embankment	66.4	1976	>1000
Douhe	China	1956	Embankment	16	1976	Empty
Lliu-Lliu	Chile	1934	Embankment	20	1985	1-5

Table 1 List of rupture dams due to earthquake (ICOLD, 2025)

While the ICOLD Incident Database provides a failure-oriented global overview of dam breakdowns, a complementary perspective is offered by the USSD reports, which focus on the observed performance of dams subjected to seismic loading, including the large body of cases where no rupture occurred.

Since 1992, the United States Society on Dams (USSD) has published the report series Observed Performance of Dams During Earthquakes (Volumes I (USCOLD, 1992), Volume II (USCOLD, 2000) and Volume III (USSD, 2014)), which compiles several hundred historical case studies and constitutes a comprehensive synthesis of actual dam performance under seismic loading. Decades of worldwide experience reported by USSD show that seismic-induced dam failures are exceptionally rare. Across several thousand dams exposed to earthquake ground motions, approximately twelve seismic failures are reported worldwide, none of which involve modern hydroelectric dams. The documented failures primarily concern hydraulic fill embankment dams, tailing dams, and small, older earth dams, which do not reflect current design, construction, nor operational standards.

For concrete dams, the USSD reports document no cases of rupture caused by seismic loading alone, even in situations where peak crest accelerations exceeded 1.7 g, such as at Pacoima Dam during the 1994 Northridge earthquake. Reported damage is generally limited to cracking, joint movements, and minor permanent displacements, typically ranging from millimeters to a few centimeters, without loss of reservoir retaining capacity.

For well-designed embankment dams, seismic effects are mainly expressed through permanent deformations rather than instability or breach, including crest settlements from a few centimeters up to approximately 1 % of dam height, cracking, and localised seepage, while maintaining water retention. Notable examples include the response of Aratozawa Dam under a Peak Ground Acceleration of 1.03 g. In some cases, dams have even experienced seismic loading exceeding their design level without suffering excessive damage, such as Aratozawa, Concerto Viejo, Ishibuchi, and Shapai dams.

The 2011 Tōhoku earthquake led to approximately 400 immediate post-seismic dam inspections, with only one reported failure, the Fujinuma-ike Dam, a small, old irrigation dam outside modern engineering standards. Observations generally reported crest cracking, settlements, and temporary increases in seepage. Similarly, the 1994 California earthquake subjected 105 dams within 75 km of the epicenter to strong ground motion; no failures were observed, although 11 dams exhibited damage.

The synthesis of the USSD reports on the observed performance of dams during earthquakes consistently indicates that no structural rupture of gates or spillway systems, nor any uncontrolled reservoir release, has been documented across the range of analysed seismic events. This represents a key conclusion given the diversity of contexts, dam typologies, and loading conditions considered. Where impacts on hydromechanical equipment have been reported, they are generally limited to secondary effects, such as temporary loss of power supply, constraints on gate operability, or disturbances resulting from damage to surrounding civil structures. These effects remain operational in nature and do not compromise the structural integrity or the fundamental safety functions of the equipment.

For hydromechanical gate systems, (Graveleine, et al., 2024) conducted an analysis based on an extensive literature review of approximately 250 information sources. This synthesis shows that, based on the available data, no dam facility has experienced a reservoir drawdown because of major direct damage to a gate system. The analysis highlights several key findings. First, the impact observed on gate systems can generally be considered limited. Several of the analyzed cases involve gate facilities subjected to major earthquakes (magnitude > 8), for which the literature neither reports damage to bottom outlet gates nor any associated reservoir drawdown. Structural damage to structures and equipment is only reported for strong earthquakes (magnitude > 7) and is systematically linked to external factors. Indeed, recorded disorders consistently originate from the immediate environment of the equipment, such as movements of the civil-engineering structures, problems affecting fixed components, impacts from external projectiles or aggressors, or loss of power supply. Importantly, the reviewed documentation does not report any case of direct structural failure of gate components. Furthermore, no voluntary or uncontrolled reservoir drawdown resulting from the failure of a gate system is identified in the analyzed sources.

2.2. Post-earthquake reconnaissance

Post-earthquake reconnaissance involves on-site investigations conducted from a few days to several weeks after the occurrence of a major seismic event. These missions mobilize multidisciplinary teams, including expertise in seismology, civil engineering, and geotechnical engineering, to collect field data, document observed damage through visual inspection and photographic records, and analyze the response of structures and soils subjected to seismic loading.

For several decades, the French association of earthquake engineering (AFPS) has organized post-seismic reconnaissance, accounting to date for nearly half hundred deployments. In recent years, these missions have increasingly integrated specialists from hydraulic domain to better document the post-earthquake behavior of dams. This contribution began with the 2023 Kahramanmaraş seismic sequence in Türkiye (AFPS, 2023) and continued with the 2024 Noto earthquake in Japan (AFPS, 2024), for which publicly available reports have been produced and are summarized just after.

Türkiye 2023. The February 6, 2023 seismic sequence, including a Mw 7.8 event, affected approximately 140 dams, most of them located within 50 km of the fault rupture. Estimated peak ground accelerations ranged from 0.1 to 1.3 g during the Pazarcık earthquake and from 0.15 to 0.45 g during the Elbistan earthquake (Humbert, et al., 2025). Although all dams maintained their reservoir-retention capability, moderate to significant permanent deformations were observed, mainly on earth and rockfill embankment dams, whereas concrete dams displayed a better overall performance. Permanent displacements increased systematically with dam height, while reinforced-concrete appurtenant structures, such as spillways, generally exhibited a satisfactory response. As part of the emergency response measures, the reservoir levels of the Sultansuyu and Arıklıkaş dams were controlledly lowered, demonstrating the proper post-seismic functioning of the gates.

The 1 January 2024, Noto earthquake (Mw 7.5) resulted in the inspection of 94 dams in Japan, none of which exhibited damage affecting safety, according to the Japanese Ministry of Land, Infrastructure, Transport and Tourism (MLIT). Three dams recorded accelerations exceeding 0.3 g, including Oya and Hakkagawa, which were visited during the AFPS mission. The Oya rockfill dam showed minor damage without impact on safety functions and illustrates repeated resistance to strong earthquakes (in 1993 with local magnitude 6.6; in 2007 with local magnitude 6.9). The reservoir water level was precautionarily lowered, demonstrating the proper functioning of the bottom outlet gate. By contrast, the Hakkagawa gravity dam, despite a measured crest acceleration of 1.63 g, showed no notable damage. Reservoir levels observed during the mission indicated a rapid return to normal operating conditions, within less than two months, or even the absence of a significant transitional phase.

At the international level, the Earthquake Engineering Research Institute (EERI) operates the Learning from Earthquakes (LFE) program, which, similarly to AFPS missions, deploys reconnaissance teams, produces reports, and archives observations in online databases. Dams are only rarely included in these missions; however, the involvement of hydraulic specialists

would allow for broader integration of dam inspections. In addition, the Geo-Engineering Extreme Events Reconnaissance (GEER) Association conducts post-disaster reconnaissance focused on geotechnical effects induced by extreme events. Some GEER reports include post-earthquake dam inspections, notably following the 2010 Maule earthquake in Chile (GEER, 2010) and the 1989 Loma Prieta earthquake (GEER, 1990).

2.3. Post-seismic inspection

In the same way as post-earthquake reconnaissance missions, post-seismic inspections focus specifically on dams and are primarily embedded within a regulatory and operational framework. ICOLD has issued recommendations on this topic through Bulletin 62 in 1988 (ICOLD, 1988), which were subsequently updated in Bulletin 166 in 2016 (ICOLD, 2016).

ICOLD Bulletin 166 states that any felt seismic shaking, or any earthquake likely to have produced significant intensity at a dam site, shall immediately trigger a post-seismic inspection, without waiting for a complete seismological characterization of the event. The initial inspection, essentially visual and conducted by trained operating personnel, aims to rapidly identify any condition that could lead to an immediate or delayed failure. It systematically covers the dam body, foundations, drainage systems, appurtenant structures, hydromechanical equipment, as well as the upstream and downstream environment. When damage is observed, or when the seismic event is considered sufficiently severe, a more detailed engineering inspection must be carried out, including enhanced use of monitoring data and, where necessary, delayed inspections to detect time-dependent damage. The bulletin also emphasizes systematic written documentation of inspections, including in the absence of damage, through structured reports ensuring traceability and contributing to earthquake feedback.

As an example, in Japan, post-earthquake inspections are conducted in accordance with MLIT inspection guidelines. When an earthquake occurs and ground acceleration exceeds predefined thresholds, the dam operator is required to perform an immediate visual inspection and submit an initial report to the supervisory authority within hours. A second, more detailed inspection is generally required thereafter and formally reported.

These post-seismic inspection reports represent a highly valuable source of information for seismic feedback, providing systematic and structured observations of dam behavior following earthquake loading.

3. Analyses of seismic dam's risk

3.1. Seismic vulnerability of dams

International syntheses converge toward a robust conclusion: dams -and concrete dams in particular- exhibit a low structural sensitivity to seismic loading. Using a conservative approach, the data reported by the USSD of twelve historical seismic induced dam failures worldwide can be retained, although this number largely includes tailings dams. When compared with the global dam inventory, currently amounting to 62,362 dams listed in the ICOLD World Register of Dams (September 2025), this represents approximately 0.02 % of dams having experienced seismic failure. Considering that most of these dams have been in operation for several decades -about 55 years on average for concrete dams (ICOLD, 2023)- this corresponds to roughly 3.1 million cumulative dam years of exposure to seismic loading.

Assuming a Poissonian framework (rare, independent events with a constant rate), the seismic earthquake feedback yields a failure rate on the order of 10^{-6} per dam-year ($\approx 4 \times 10^{-6}$). In other words, an individual dam has on average less than a one-in-250 000 annual probability of seismic failure. Although empirical in nature, this estimate clearly illustrates the very low seismic vulnerability of dams. Among the twelve documented failure cases, a significant proportion concerns tailings dams, old or severely under-designed structures, the real probability is even lower when considering hydraulic dams as it should. Moreover, this assessment does not explicitly account for dam age, typology, or seismic context. This indicates that, for a recent, properly designed dam, built in geological conditions consistent with its design assumptions, the empirical risk of seismic failure is close to zero. Consistently, seismic-induced dam failures clearly belong to the category of extremely rare events, which also explains why national-scale observation alone is insufficient and justifies reliance on long-term, international seismic earthquake feedback.

3.2. Relative seismic risk of dams

At the global scale, and over approximately 120 years of systematic observation, seismic-induced dam failures remain an extreme exception. Other causes clearly dominate the statistics of dam failures. For instance, (ICOLD, 2025) indicates that, among the 311 dam failures analysed, only 2 % are attributed to earthquakes, whereas 42 % are caused by floods. This implies that a dam failure is about twenty times more likely to be caused by a flood than by a seismic event.

Moreover, the consolidated analysis presented in (Humbert, et al., 2025) shows that, across all dams, failure causes are overwhelmingly non-seismic, primarily related to overtopping, internal erosion, design deficiencies, or ageing processes. In global failure statistics, earthquakes therefore appear as a marginal cause of dam failure.

3.3. Societal perception of seismic risk for dams

In a paper presented at the 27th ICOLD Congress in 2022 (Bremen, 2022), Roger Bremen (Lombardi Engineering) reaches a similar conclusion: the risk of dam failure due to earthquakes is low, and significantly lower than that associated with other causes such as floods. This observation leads to a questioning of the current prioritization in dam safety and to a call for rebalancing attention toward risks that are far more likely, notably overtopping and internal erosion. Under these conditions, further increasing the seismic resistance of dams would have only a marginal impact on dam failure statistics and on the overall societal risk associated with dams.

The question therefore arises: if seismic dam failure is such a marginal phenomenon, why have requirements continued to increase and methodologies become more complex? (Bremen, 2022) attributes this trend largely to the societal perception of seismic risk among the public and authorities, shaped by recent catastrophic earthquakes that have left a strong imprint on collective memory. He highlights an evolution in the dominant causes of fatalities from natural disasters: while droughts and floods were predominant in the early twentieth century, earthquakes now dominate fatality statistics, influencing risk perception disproportionally (**Figure *3***).

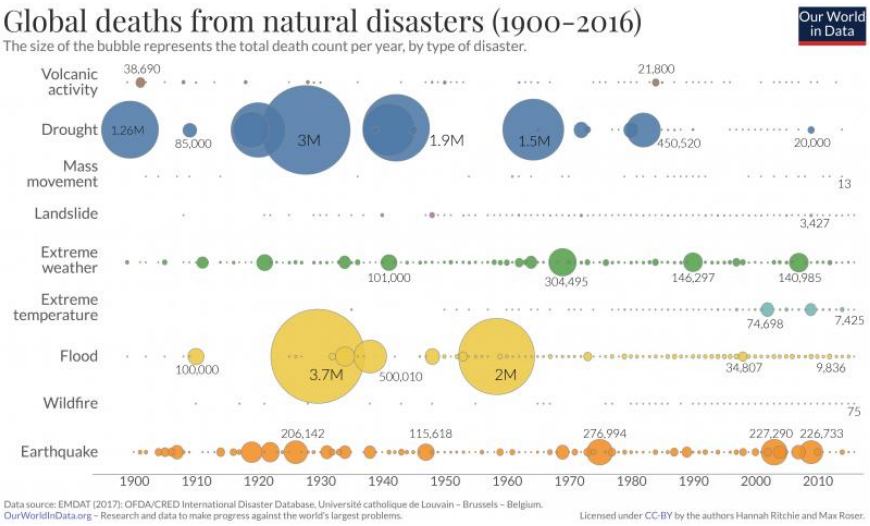


Figure 3 Global deaths from natural disasters (Bremen, 2022)

Also, we often can see in the media destroyed buildings after large earthquakes. (Humbert, et al., 2025) further explains that many existing buildings and infrastructures are highly vulnerable to earthquakes because they were designed without seismic provisions and rely primarily on vertical load-bearing mechanisms. Horizontal seismic forces therefore exceed their resistance capacity. By contrast, dams are inherently designed to withstand large horizontal loads, and, in some cases, upward forces associated with uplift pressures. For low to moderate earthquakes, seismic actions are therefore absorbed by the existing design margins developed for normal and exceptional loading conditions.

In light of these observations, Bremen advocates a revision of current practices and safety effort prioritization, encouraging greater focus on risk factors that represent more probable causes of failure, such as flood-related external erosion and internal erosion under normal operating conditions for embankment dams. He also introduces the concepts of vulnerability and uncertainty into dam safety assessment, arguing for an approach centered on the specific weaknesses of each dam in order to better target safety measures.

3.4. Toward a graduated approach to seismic risk

Ultimately, earthquake hazard represents a low level of risk for dams, particularly when compared with other failure mechanisms. Risk analysis efforts should therefore be proportionate to the actual level of risk and associated consequences. Priority should be given to hydraulic studies, while complex seismic analyses should be reserved for specific cases, such as dams presenting known pathologies, design deficiencies, or unfavorable geological conditions. In many situations, a well-structured argumentation based on seismic feedback may be appropriate, and in some cases sufficient, to support dam safety assessments. Placing observation back at the core of justification frameworks amounts to recognizing the legitimacy of experience.

Furthermore, (Graveleine, et al., 2024) shows that for low-to-moderate seismicity countries such as France, hydromechanical equipment whose gate systems are broadly comparable at first order to those operated in high-seismicity regions in terms of design principles, geometry, materials, mass, inertia, and layout. Therefore, they questioned the legitimacy of the actual risks involved. This question is more relevant given that post-seismic feedback does not appear to highlight any clear evidence of gate major structural disorder, including for relatively old equipment.

The use of seismic experience feedback to demonstrate the adequacy of structures with respect to seismic risk could help avoid the systematic reliance on finite element numerical analyses (currently the standard approach) and could alleviate the difficulties encountered by hydraulic engineering practitioners in demonstrating the seismic stability of structures and equipment through numerical methods. These difficulties are partly methodological but are also amplified by the current trend in seismic hazard assessments, which tend to increase over time.

These challenges can be partly attributed to the available computational tools, which, for concrete dams, remain largely based on stress-based approaches (pseudo-static, modal spectral, or linear transient analyses), while displacement-based methodologies are more commonly applied to embankment dams. Even when accounting for ductility, the application of advanced non-linear or displacement-based approaches remains more complex for structures such as concrete dams, which are predominantly composed of unreinforced materials with limited deformation capacity.

Furthermore, the development of complex nonlinear transient models is both time-consuming and resource-intensive, and their justification to safety authorities can be challenging. In addition, seismic studies tend to monopolize available engineering resources, which could be more effectively allocated to failure modes that are more frequently represented in the global dam experience feedback, such as flooding.

It should be noted that experience-based approaches are already implemented in other industries to demonstrate the seismic adequacy of installations. For instance, the Seismic Qualification Utility Group method (SQUG, 2001) demonstrates the seismic capacity of equipment through walkdown inspections, by comparing their configuration to reference equipment that has performed successfully during past earthquakes—particularly using seismic experience databases —based on similarity and empirical robustness criteria, without resorting to detailed calculations. These methods have served as a reference for the present work and for the experience feedback framework proposed in Section 5.

4. Argumentation based on seismic feedback

The previous analysis leads to the conclusion that an argumentation based on seismic feedback can constitute a relevant and robust approach for seismic risk assessment. Such an approach is particularly strong when it relies on observations from high-seismicity countries. This raises the question of its applicability to low-seismicity countries, such as France. In this context, can the seismic feedback from countries like Japan be considered representative?

4.1. Observation time: low- versus high-seismicity countries

Using the comparison between France and Japan presented in Humbert et al. (2024), the question is raised whether one year of Japanese seismic feedback is equivalent to one year of French seismic feedback. The study analyses Gutenberg–Richter relationships for two seismic contexts: a low-seismicity environment (France) and a high-seismicity environment (Japan), over equivalent surface areas and observation periods.

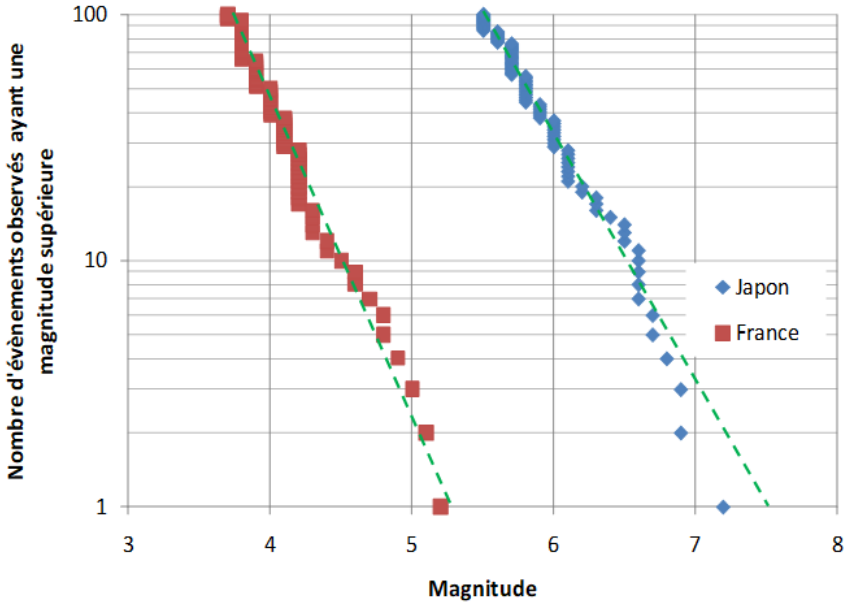


Figure 4 Comparison of cumulative Gutenberg–Richter curves for regions of equal area and observation period in Japan and France (Humbert, et al., 2025)

The results show that one year of seismic observation in Japan is equivalent to approximately one hundred years of observation in metropolitan France. Furthermore, the offset of about two magnitude units between the two contexts implies that an earthquake of magnitude M in France has a return period comparable to that of an earthquake of magnitude M + 2 in Japan.

In this context, Japan represents a highly accelerated and extensive source of seismic earthquake feedback for assessing dam robustness. The country hosts approximately 1 900 large dams (ICOLD definition) with an average age of about 50 years, representing nearly 110 000 cumulative dam-years of observation. When transposed to the French seismic context, which is roughly one hundred times less active, this corresponds to several million theoretical years of exposure. Consequently, a detailed analysis of Japanese dam performance over the last five decades provides a key basis for a realistic and proportionate assessment of seismic risk for French dams, relying on experience that cannot be achieved at the national scale alone.

4.2. Limitations of the existing earthquake feedback

The synthesis of seismic feedback highlights several key observations. First, the seismic risk level for dams appears globally low, particularly for properly designed and well-maintained structures without known pathologies. Available data show that, even when earthquakes lead to damage, the observed effects are generally limited and compatible with the preservation of fundamental safety functions.

However, this assessment relies on intrinsically incomplete earthquake feedback. International databases are mainly populated by cases involving sufficient damage to justify formal reporting and dissemination, whereas cases of good seismic performance without noticeable damage are rarely documented, despite representing the majority of situations. This asymmetry leads to a partial view of actual dam behavior under seismic loading. While existing analyses demonstrate that damage remains limited even in affected cases, a comprehensive risk evaluation would require answering a critical question: for a given dam type subjected to an earthquake of given magnitude and distance, what proportion of dams exhibits good or very good seismic performance? This proportion is likely high but remains largely unknown due to the lack of systematic data. Explicitly accounting for positive seismic feedback would enable a more accurate quantification and prioritization of seismic risk and support more proportionate, observation-based assessment methods.

In addition, existing earthquake feedback predominantly documents the behavior of dam bodies, while providing more limited information on appurtenant structures and hydromechanical gate systems. These components are less frequently reported in post-earthquake inspection reports, despite their importance for overall dam safety.

4.3. Positive seismic feedback

Post-earthquake earthquake feedback from major seismic events such as the 2011 Tōhoku earthquake and the 1994 Northridge earthquake provides a particularly valuable dataset, not only through observed damage, but also through the systematic absence of dam failures across large populations of exposed structures. With several hundred dams inspected under severe ground motion levels and no rupture observed for modern dams, these events represent large-scale full-system tests that significantly constrain the plausible frequency of seismic-induced dam failure. This positive earthquake feedback, often undervalued, is essential to support a proportionate and evidence-based seismic risk assessment. A well-known example is the seismic qualification of nuclear plant equipment, where prior fragility estimates are

substantially reduced after incorporating earthquake positive experience data showing no observed failures under significant ground motion levels (Kennedy & Ravindra, 1984).

Large post-earthquake inspection campaigns offer a unique opportunity to enhance positive earthquake feedback: when many dams are subjected to strong seismic excitation and systematically inspected without failure, the absence of rupture becomes statistically informative. Under minimal and explicit assumptions, this allows the derivation of conservative upper bounds on conditional failure probability. Positive earthquake feedback should therefore be systematically collected and analyzed in relation to dam characteristics, in order to properly assess the empirical seismic risk for dams, appurtenant structures, and mechanical components subjected to a given intensity level.

5. Harmonized international post-earthquake feedback tool

Based on the above observations, it appears relevant to develop a tool dedicated to the formalization and valorization of earthquake feedback, particularly at the international level. Such a tool would enable the exploration, collection, classification, analysis, and objective interpretation of earthquake feedback related to the actual behavior of dams, appurtenant structures, and hydromechanical gate systems, as well as the seismic loadings to which they were effectively exposed. It would also allow identification of components or subsystems that performed well and those that experienced difficulties.

This approach would make it possible to build a database more comprehensive than existing international syntheses, as it would explicitly integrate positive earthquake feedback, which is too often neglected. Based on an alert system, designated focal points would be notified when a major earthquake occurs near a dam. A standardized data-collection form would then be shared with operators and completed through a user-friendly interface.

In parallel, complementary actions could be implemented. For instance, the involvement of the hydraulic engineering community in post-earthquake reconnaissance missions could be encouraged to ensure dam coverage during these missions and allow direct completion of earthquake feedback forms. Another promising approach would involve the use of data extraction using artificial intelligence of post-earthquake inspection reports from high-seismicity countries, to extract and classify information related to damage—or the absence of damage—at dams.

Once a robust database is established, it will be possible to quantitatively demonstrate the seismic robustness of dams, appurtenant structures, or individual components based on observation and statistics, thereby supporting a graduated approach to seismic risk assessment.

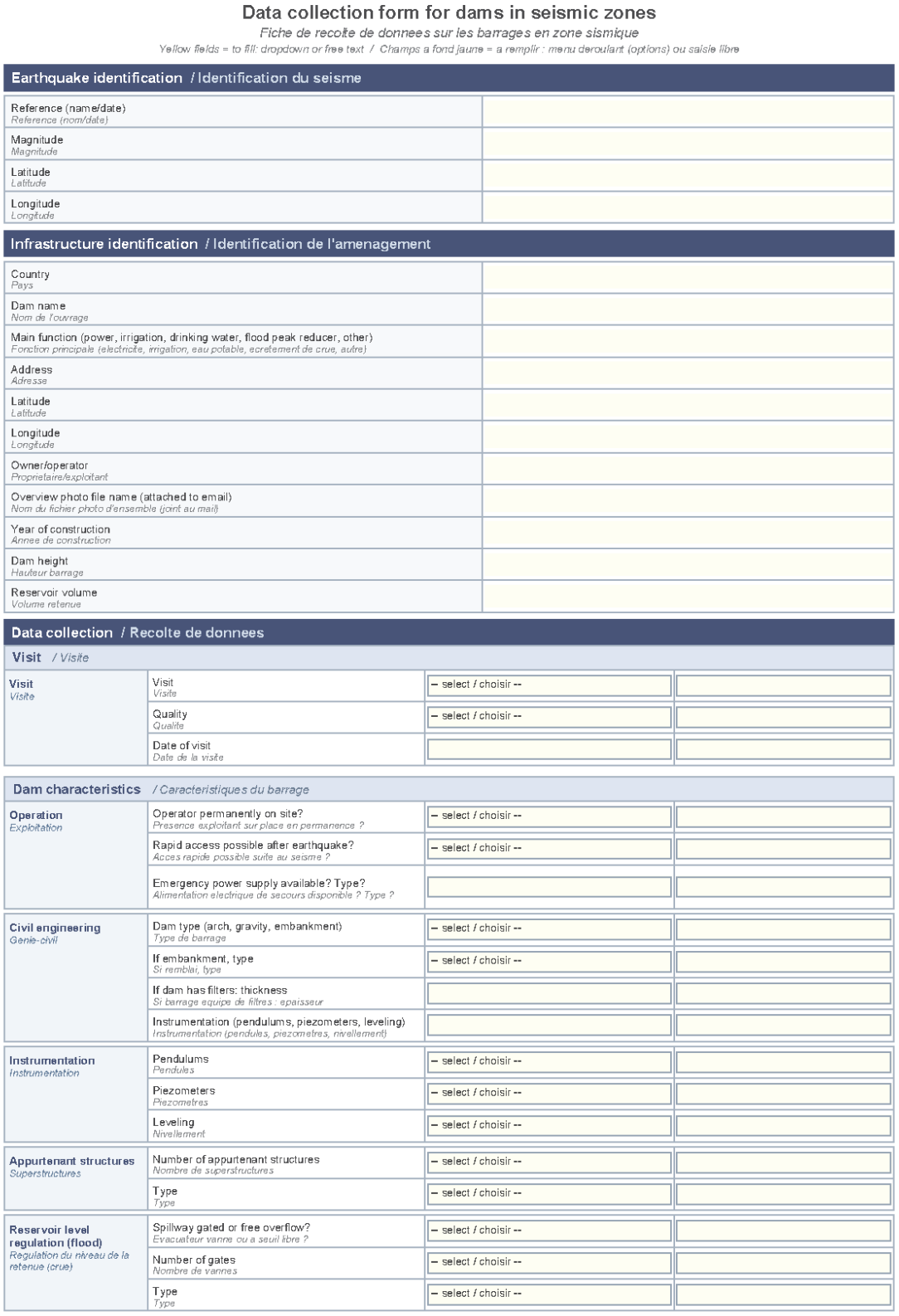
5.1. Alert system

An alert tool would allow rapid notification of relevant focal points following an earthquake occurring near a dam. By coupling an online earthquake database with the ICOLD World Register of Dams, the alert system could identify dams subjected to significant seismic intensity and initiate data collection. Focal points would then contact operators and invite them to complete the data-collection form, which would subsequently be archived in the database.

5.2. Data-collection form for future events

(Graveleine, et al., 2024) has developed a standardized data-collection form for use during AFPS post-earthquake missions. This form constitutes a structuring tool for earthquake feedback collection on dams, aiming to document dam behavior in a homogeneous and comprehensive manner. It gathers information across complementary domains, including civil engineering (dam typology, foundations, deformations, cracking, monitoring systems), hydromechanical equipment and gates (gate types, operating systems, functional status, leakage, drawdown capacity), and operational conditions (reservoir level, power supply availability, accessibility, operational continuity).

The form also incorporates seismic characterization (magnitude, distance, accelerations), enabling correlation between observed seismic loading and dam response. Finally, it records the pre-earthquake condition, post-earthquake condition, and condition at the time of inspection, providing a coherent temporal view of safety evolution. Through its multidisciplinary and operational nature, the form serves as a central support for comparative and capitalizable analysis of dam behavior under seismic loading.



Data collection form for dams in seismic zones

Fiche de recolte de donnees sur les barrages en zone sismique

Yellow fields = to fill: dropdown or free text / Champs a fond jaune = a remplir : menu deroulant (options) ou saisie libre

Earthquake identification / Identification du seisme

Reference (name/date) *Reference (nom/date)*	
Magnitude *Magnitude*	
Latitude *Latitude*	
Longitude *Longitude*	

Infrastructure identification / Identification de l'amenagement

Country *Pays*	
Dam name *Nom de l'ouvrage*	
Main function (power, irrigation, drinking water, flood peak reducer, other) *Fonction principale (electricite, irrigation, eau potable, ecretement de crue, autre)*	
Address *Adresse*	
Latitude *Latitude*	
Longitude *Longitude*	
Owner/operator *Proprietaire/exploitant*	
Overview photo file name (attached to email) *Nom du fichier photo d'ensemble (joint au mail)*	
Year of construction *Annee de construction*	
Dam height *Hauteur barrage*	
Reservoir volume *Volume retenue*	

Data collection / Recolte de donnees

Visit / *Visite*

Visit *Visite*	Visit *Visite*	-- select / choisir --	
	Quality *Qualite*	-- select / choisir --	
	Date of visit *Date de la visite*		

Dam characteristics / *Caracteristiques du barrage*

Operation *Exploitation*	Operator permanently on site? *Presence exploitant sur place en permanence ?*	-- select / choisir --	
	Rapid access possible after earthquake? *Acces rapide possible suite au seisme ?*	-- select / choisir --	
	Emergency power supply available? Type? *Alimentation electrique de secours disponible ? Type ?*		
Civil engineering *Genie-civil*	Dam type (arch, gravity, embankment) *Type de barrage*	-- select / choisir --	
	If embankment, type *Si remblai, type*	-- select / choisir --	
	If dam has filters: thickness *Si barrage equipe de filtres : epaisseur*		
	Instrumentation (pendulums, piezometers, leveling) *Instrumentation (pendules, piezometres, nivellement)*		
Instrumentation *Instrumentation*	Pendulums *Pendules*	-- select / choisir --	
	Piezometers *Piezometres*	-- select / choisir --	
	Leveling *Nivellement*	-- select / choisir --	
Appurtenant structures *Superstructures*	Number of appurtenant structures *Nombre de superstructures*	-- select / choisir --	
	Type *Type*	-- select / choisir --	
Reservoir level regulation (flood) *Regulation du niveau de la retenue (crue)*	Spillway gated or free overflow? *Evacuateur vanne ou a seuil libre ?*	-- select / choisir --	
	Number of gates *Nombre de vannes*	-- select / choisir --	
	Type *Type*	-- select / choisir --	

Figure 5 Page 1 of the post-earthquake feedback collection form for a dam structure and its equipment (Graveleine, et al., 2024)

5.3. Database and data exploitation

Another key component is the accessibility and exploitation of the collected data. The tool should readily provide answers to questions such as: for a certain type of concrete dam built in the 1970s, how many similar dams have experienced a PGA of 0.5 g? What proportion exhibited damage, failure, or gate malfunction? Beyond simple querying, the database should allow filtering and cross-analysis based on dam typology, age, seismic intensity, distance to fault, and observed performance. Such capabilities would support benchmarking of observed behavior, identification of dominant response patterns, and objective comparison between expected and observed performance, thereby enabling a more quantitative, experience-based and proportionate assessment of seismic risk.

6. Conclusion

The synthesis of international seismic feedback clearly shows that seismic-induced dam or gate failures are extremely rare events, particularly for modern hydraulic structures designed and operated in accordance with current standards. Statistical analyses, combined with several decades of large-scale post-earthquake observations, demonstrate that earthquakes represent a marginal cause of dam failure when compared with more frequent mechanisms such as flooding, overtopping, or internal erosion. For concrete dams in particular, no rupture attributable solely to seismic loading has been documented, except in highly specific geological configurations.

On the other hand, existing syntheses are largely limited to failure-based feedback and therefore do not provide an exhaustive representation of dam behavior under strong seismic loading. A dam that performs satisfactorily during severe earthquakes constitutes valuable information in itself. Furthermore, most syntheses focus primarily on the dam body, while appurtenant structures and hydromechanical gate systems -although equally critical to dam safety- are seldom addressed. Systematically documenting their seismic feedback would significantly enhance the overall assessment of dam safety.

The analysis further highlights that the apparent discrepancy between the low empirical seismic risk and the growing complexity of assessment methodologies is largely driven by risk perception, shaped by the societal impact of catastrophic earthquakes affecting vulnerable buildings and infrastructures. Unlike many other structures, dams are inherently designed to withstand significant horizontal and uplift forces, allowing moderate to strong seismic loading to be absorbed by existing design margins.

In this context, seismic safety assessments should evolve toward a risk-proportionate and observation-driven framework, where analytical effort is commensurate with actual vulnerability and consequences. Greater consideration of positive seismic feedback, including systematic documentation of satisfactory performance during major earthquakes, is essential to support such an approach. The development of harmonized international feedback tools and databases would significantly enhance the ability to quantify seismic robustness and to justify safety levels based on real behavior rather than theoretical conservatism.

Finally, these observational elements will also serve as a basis for revisiting, if necessary, the sizing and design rules applicable to dams and gates, ensuring that these rules always prioritize safety without being overly conservative, and that they are proportionate and adapted to each specific situation. Simplicity of the methods (leading to robust implementation) must also be a key focus in the long term.

References

AFPS, 2023. *Report of the post-seismic mission launched by the AFPS following the earthquakes of 6 February 2023 in Turkey,* s.l.: s.n.

AFPS, 2024. *Report of the post-seismic mission launched by the AFPS following the earthquake of january1, 2024, in the Noto region (Japan),* s.l.: s.n.

Bremen, R., 2022. Consequences on the design practice of worldwide dam accidents. *ICOLD 27th congress*.

GEER, 1990. *Preliminary report on the principal geothechnical aspects of the October 17, 1989 Loma Prieta earthquake - Report No. UCB/EERC-90/05,* s.l.: s.n.

GEER, 2010. *Geo-engineering reconnaissance of the 2010 Maule, Chile earthquake - Report No GEER-022,* s.l.: s.n.

Graveleine, D., Pollier, R., Boulat, L. & Cuby, S., 2024. Vanne de barrage et séismes : éléments de l'état de l'art et perspectives pour la France et les pays faiblement à modérément sismiques.

Humbert, N., Kolmayer, P. & Laugier, F., 2025. Analyse de risque proportionnée des barrages vis-à-vis du séisme en France métropolitaine, zone faiblement à modérément sismique - valorisation du retour d'expérience.

ICOLD, 1988. Inspection of dams following earthquake-guidelines.

ICOLD, 1995. Dam failures - Statistical analysis - Bulletin 99.

ICOLD, 2016. Inspection of dams following earthquake guidelines - Bulletin 166.

ICOLD, 2023. Ageing of concrete dams.

ICOLD, 2025. ICOLD incident database bulletin 99 update: statistical analysis of dam failures.

Kennedy, R. & Ravindra, M., 1984. Sesimic fragilities for nuclear power plant risk studies.

SQUG, 2001. Generic Implementation Procedure (GIP) for seismic verification of nuclear plant equipment.

USCOLD, 1992. Observed performance of Dams during earthquakes, Volume I.

USCOLD, 2000. Observed Performance of dams during earthquakes.

USSD, 2014. Observed performance of dams during earthquakes, Volume III.

SESSION A (part II). Dams and reservoir safety management for people		
1	Bettina Geisseler	Procurement process - Contract design - Dam safety Panel of Experts
2	Arjan Jovani	VAU I DEJES - Dam Safety Monitoring, Reservoirs Management and Renewable Energy Integration, ALBANIA
3	Rune Øynes	Web-Based Software for Stability Analysis of Concrete Gravity Dams, Buttress Dams and Masonry Dams
4	Jyoti Prakash Hati	Flow regulation and nutrient dynamics in a Polish lowland reservoir catchment: Implications from SWAT hydrological modelling
5	Vanja Verdel	Exposed Geomembranes in Pumped Storage Schemes

Paper submitted for the 13th ICOLD European Club Symposium in Bydgoszcz, Poland

Dam construction projects:
Procurement process - Contract design – Multi-Party Agreements

Author: Geisseler, Bettina, Lawyer, GEISSELER LAW, Im Rebstall 1, 79112 Germany, geisseler@geisseler-law.com

Abstract

The choice of the right partner (Contractor), the procurement process and last, but not least, an adapted structure and "design" of the dam construction/ erection contract are as important as the choice of the site, the choice of the type and the design of the dam or the adapted mixture of the concrete used to build the dam.

Various ideas have been developed in the construction industry during the last decades to improve the whole process from the selection of the Contractors over the construction/ erection period until the first filling/ Provisional Acceptance and the end of the warranty period. The purpose of those ideas is to eliminate weaknesses in the process, to balance potentially conflicting interests of different stakeholders and to focus on the construction/ erection instead of lengthy discussions on changed circumstances or hindrances resulting in a request for compensation of additional costs or discussions on the causes of a time for completion exceeding the agreed one.

The ideas range from the so-called early Contractor involvement to the (recommended or even compulsory) involvement of a Panel of independent Dam Safety Experts to the question which contract model shall be chosen.

The paper will start by demonstrating the some [1] essentials of a dam construction contract which can be considered as critical success factors such as

- an unambiguous wording of the description of the Scope of Works, including technical norms (such as ICOLD Bulletins, DIN norms) to be complied with
- managing interfaces
- the relationship between the Employer and the Contractor
- the allocation of risks
- the monitoring of the project: quality assurance and reporting obligations.

In the second part of the paper the development of more collaborative contracts models will be shown. Whereas so-called Alliance contracts are already widely used – and as it seems with success – in the hydropower business, there is a new contract model, developed in Australia some years ago and now starting to be used e.g. in the Swiss and German railway sector, but suitable for other infrastructure projects: the Multi-Party Agreement on Integrated Project Delivery in a Partnership Model. The key elements as well as the advantages or potential disadvantages will be shown.

Keywords: Contract design – Employer's Requirements - Allocation of Risks – Interface Management – Quality Assurance - Multi-Party Agreements

INTRODUCTION

A thoroughly drafted construction contract will not only help to balance the mutual interests of the Owner/ Operator ("Employer") [2] and the Contractor as well as of the other stakeholders such as statutory regulatory authorities (permitting authorities, surveilling authorities) or the financing institutions, but help to avoid disputes. Special attention should be paid to clearly drafting the Scope of Works clause/ Employer's Requirements.

History shows that in a considerable number of cases there have been disputes on cost overruns or non - compliance with the milestone plan and the Time for completion. Often this is due to the occurrence of unforeseen events, which to overcome costs money and time. The question arising is, who of the contractual parties shoulders those risks. Thus, the parties are advised to clearly and as detailed as possible allocate typical risks to either party or even both parties.

Another typical problem in the execution of large-scale and complex infrastructure projects results from the fact that usually the Employer splits the Works into various lots and mandates specialised firms, which among each other do not have any contractual relationship. In a classical multi – contracting structure the coordination of various lots is a very challenging task for the Employer, who in my opinion is the best one if not to say only one being in the position to manage the interfaces between the different Contractors accordingly and to align the different works.

The above mentioned issues have led to discussions within the community of Employers, Contractors and Consultants dealing with large – scale infrastructure construction projects. The question was, how to find a more cooperative way of project execution instead of submitting claims to each other and losing time in discussing claims. The answer was in the hydropower and dam construction business the so-called Alliance Contract. A further step in this development towards a more cooperative way of project execution is another new contract model, used in multi-contracting structures: a Multi-Party Agreement on Integrated Project Delivery , combining the principles of the Alliance Contract with the fact that all Contractors – executing the different lots – are bound together with the Employer by *one* contract as if they were – but though they are not – in a Consortium Agreement.

This Contract model has first been used for projects in Australia and is currently more and more used in the Swiss and German railway / tunnelling sector. In case it proofs to be a considerable amelioration in the project execution, the author is convinced that it will be used as well in the hydropower / dam construction sector.

1. THE ESSENTIALS OF A DAM ERECTION CONTRACT

1.1. The Scope of Works clause and the Employer's Requirements

The definition of the Scope of Works is *the core* provision of the contract. While drafting the Scope of Works clause and setting up the so-called Employer's Requirements, the contractual parties need to avoid ambiguous expressions such as "of superior quality", which can be interpreted in different ways. Other expressions like "state of the art" or even "proven good industry practice" have – among experts – a clear meaning and can thus be used. The contractual parties should keep in mind: the level of detail in specifying the

Employer's Requirements goes hand in hand with taking responsibility for ensuring that the requirements result in the desired functionality ("fit for purpose"). A Contractor realising that the specified requirements might result in defects / mal – functioning of the dam, must immediately – in a traceable form – inform the Employer on his observations, to be exempted from his own liability.

The Scope of Works clause serves as reference for evaluating whether the dam delivered by the Contractors has deficiencies or not. And, it is the benchmark in disputes between the Employer (future Owner and Operator of the dam) and the Contractor if the latter asserts a claim for "EOT" (extension of time) and compensation of additional costs, alleging that works requested by the Employer are "Extra Work" requiring a so-called "Change Order".

There are different approaches to define the Scope of Works. There might be more functional descriptions such as the definition of the capacity of the spillways. But other than in pure hydropower plant projects , where , as the case may be, a more functional definition of the Scope of Works might be preferred leaving it up to the Contractor how to fulfil the requirements, Employers in dam construction projects seem to prefer to specify their requirements to the smallest detail, e.g. down to the properties of the construction material (e.g. concrete) to be used and the determination of the laboratory in which the suitable material mix will be determined.

An important part of the definition of the Scope of Works are the quality standards the Contractor must comply with. If not already resulting from the applicable law those standards are often reflected in norms / Bulletins from private norming associations such as the ICOLD Bulletins or DIN norms. To avoid discussions whether the adherence to those standards is sufficiently covered by the state of the art requirement, which each Contractor must follow, those standards should – and this cannot be said often enough – be incorporated into the construction contract by explicitly declaring them to be an integrated part of the contract and applicable intra partes.

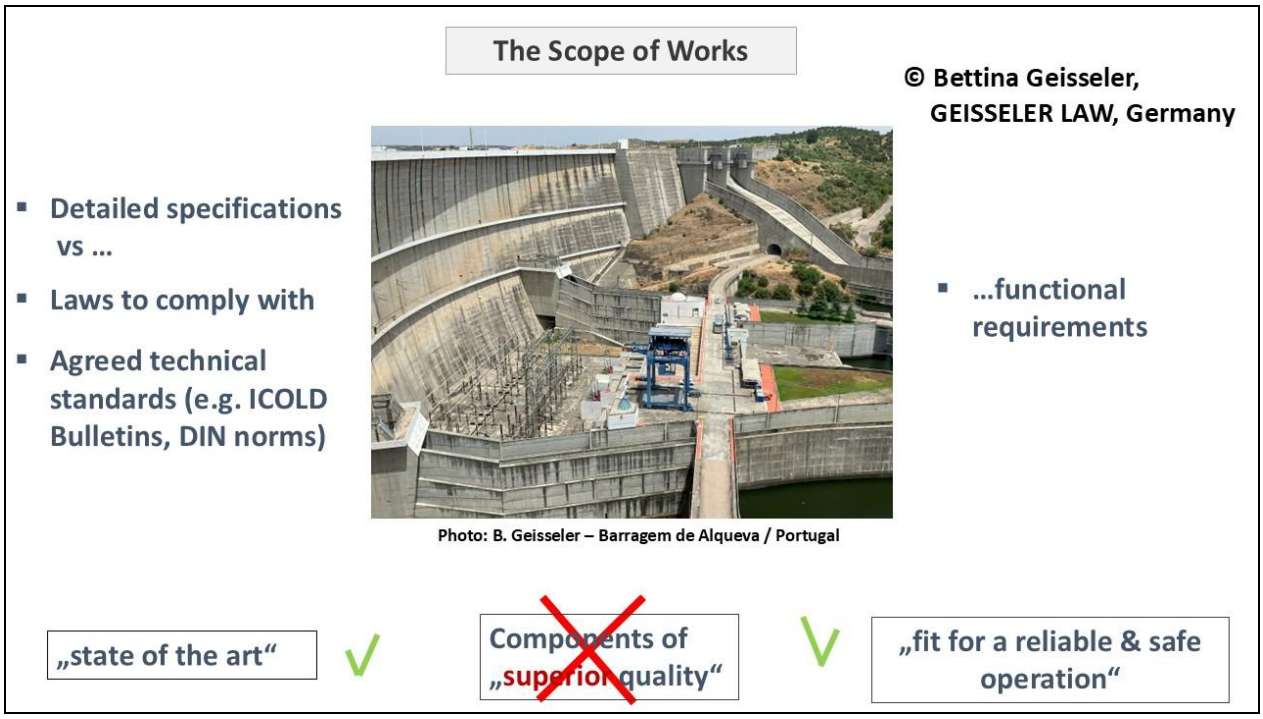


Fig. 1 – The definition of the Scope of Works

Whereas the body of the contract will in most cases contain the major commercial provisions , the Contract will include various more technical annexes such as the technical specifications ("Employer's Requirements") , the milestone plan, specific safety requirements to be observed by the Contractor during the project execution etc.

The author recommends to determine the order of precedence of the documents in case of a possible contradiction and to name the date and version of issuance of the annexed documents. Special attention should be paid to the fact that sometimes liability extensions (mostly) respectively restrictions might be hidden in some annexes. In some cases specific technical guarantees, expressed in technical formula and having legal consequences might be agreed upon in the annexes.

General recommendation: the Contractor's responsible project engineer and the advising lawyer should work in close cooperation and *not* each of them isolated in their "ivory tower" by studying either only the contractual/ commercial provisions in the body of the contract and on the other hand the technical annexes stipulating the prerequisites for the legal consequences of non-compliance.

1.2. Interface Management and mutual obligations/ duties of the contractual parties

In a dam construction project with typically various lots, i.e. a multi-contracting structure there are many interfaces: the interfaces between the contractual parties, i.e. the Employer (Owner) and the Contractor, the interfaces to the other stakeholders and the interfaces between different Contractors for different parts (lots) of the whole works. The role of the contract is to clearly attribute the respective responsibilities and to define the mutual obligations regarding the interfaces. Coping with interfaces first of all requires both from a technical point of view as well as from a contractual point of view to identify the interfaces.

While the Scope of Works determines the limits of supply, and thus determines which works/ services at the interfaces fall within the Contractor's responsibility, the interface management relates to the question of which of the parties is responsible for coordinating the different lots. The parties need to decide who shoulders the risk if one lot upon which another lot is dependent is poorly performed or delivered too late.

Sometimes Employers try to overwhelm the interface risk to the contractors either by stipulating in the contract two obligations, which the Contractor(s) has/ have to fulfil: (i) the Contractor must deliver – within the limits of his Scope of Works - a complete work and he is obliged to perform all supplies and services which are necessary for the functioning of the entire Works (the dam) even if they are not explicitly mentioned in the Employer's Requirements; and (ii) the Contractors have to coordinate themselves and to cope with the interfaces (!). The author doubts whether such a clause stipulated in such a general way is valid. Furthermore it should be noted, that in case (i) this clause still requires Employers to clearly stipulate the limits of supplies or, differently spoken, the "Excluded Works" for each lot and that regarding case (ii) only the Employer has the possibility to effectively influence the interface management, as his Contractors among themselves do not have any contractual relationship. This means: he must draft the contracts in a way that he can use the compensation for delayed performance of a lot to compensate another contractor who is waiting to carry out his works and who may need to keep staff and machinery on standby – or in case that the info provided by one contractor, on which another contractor depends is inaccurate leading to a mal-performance and remedying costs. Generally spoken: the

Employer must assure that a contractor depending on another lot receives all necessary information he needs to perform his own works.

Often it is helpful to establish a detailed “Interface Matrix” in the annexes to the contract.

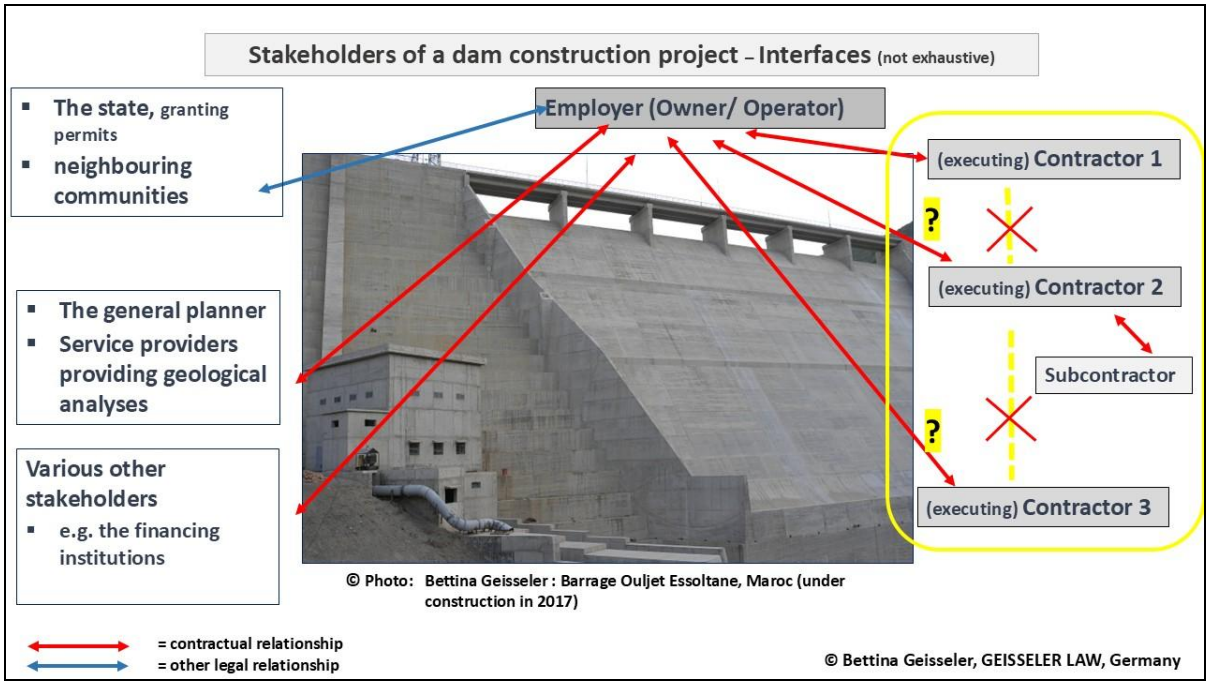


Fig. 2 – Managing interfaces

A particular interface is the one between the Employer and the Contractor. The contractual parties should thoroughly determine, who bears to which extent the design responsibility and whether the Contractor can rely (“rely upon information”) on the data and documents provided to him by the Employer or whether he is obliged not only to countercheck them roughly for more or less evident discrepancies and inaccuracies , but to carefully review them.

An essential point are the cooperation and other duties to be complied with by the Employer. The contract should clearly stipulate at what moment the Employer must comply with his duties (e.g. granting access to the site! Or – as the case may be – handing over the concept design) to enable the Contractor to perform his works in time. In case of direct dependencies between the Employer’s duties and the Contractor’s obligations it is - from the Contractor’s point of view - essential to agree with the Employer that the timely and correct fulfilment of these Employer’s duties is prior condition for the Contractor to perform. This is to avoid discussions, if the Contractor runs into a penalised delay in case he cannot perform because of non-performance of Employer’s duties.

Regarding the approval rights (duties) of the Employer: here again the contract should determine the deadline, within which the Employer has to give his approval.

1.3. Unforeseen event – legal consequences

In large-scale projects risks can materialise, which might jeopardize the milestone and overall time schedule as well as the price targets and consequently endanger the whole project.

One of the major risks in connection with dam construction projects typically is the geology for the foundations.

A well-drafted contract has to provide for a detailed risk allocation and has to stipulate which of the Parties bears the negative impacts if such typical risks materialise. The allocation of risks between the Employer and the Contractor and the balancing of the risks in view of the calculated and offered contract price is one of the most challenging and difficult tasks while drafting and negotiating a dam construction contract.

A Contractor who accepts a clearly identified risk cannot claim EOT (extension of time) and/ or compensation for higher costs in case of hindrances during the project execution due to the occurrence of that risk.

The more complex a project is, and the more stakeholders in the project exist, the more difficult it will be to balance the risks because the provisions of all the other agreements have to be considered. The financing banks have a vital interest that the Owner/ Employer does not assume risks which would endanger his possibility to comply with his obligations under the terms of the financing agreements and thus jeopardize the whole project.

The contractual parties should identify and discuss in detail the major and typical project-related risks, then carefully evaluate these risks and allocate them to one of the parties.

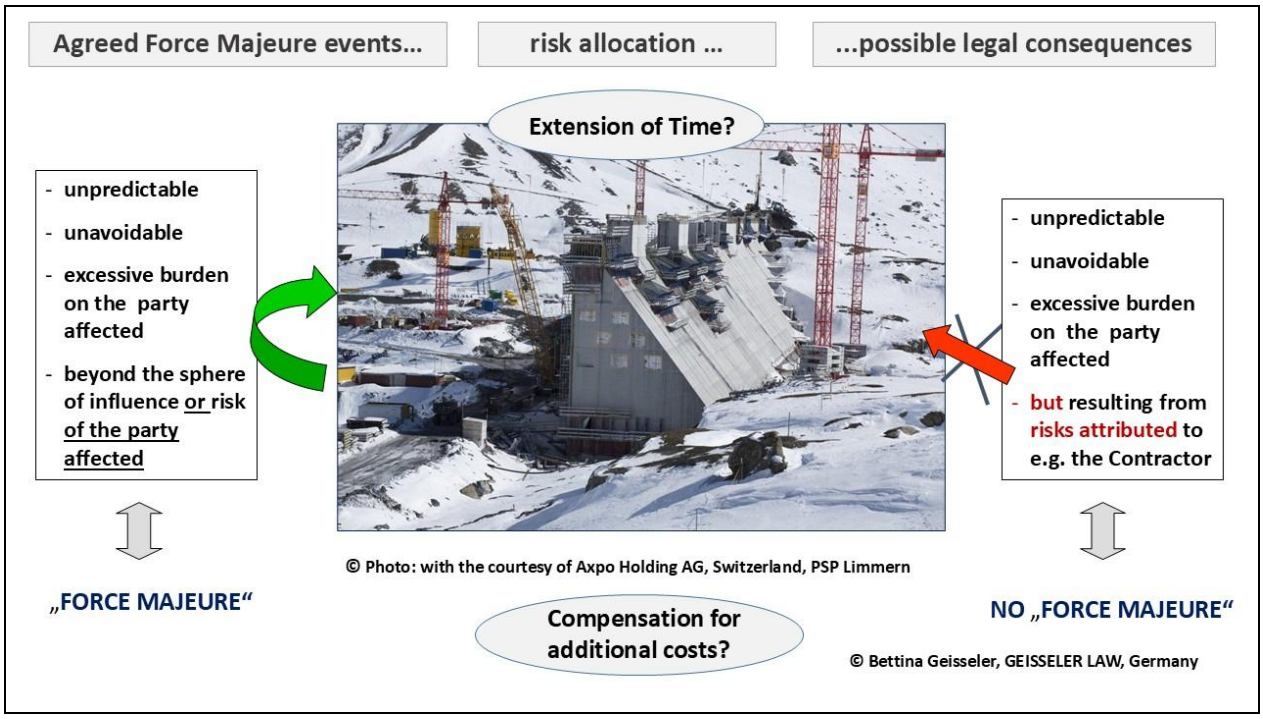


Fig. 3 – Allocation of risks

It might be very tempting for an Employer to shift all the risks to his Contractor. But if at the same time he expects the Contractor to offer the Works at – what he considers to be – a "competitive price", he risks the Contractor's bankruptcy in case of a major unforeseen event which will cost enormous sums of money to overcome.

In a well negotiated, balanced contract, the taking over of major risks with at least a medium probability of occurrence will normally lead to a proportionate increase of the contract price.

There exist many contractual variations to reflect this issue – from one contractual party assuming all risks to the concept of risk sharing, totally or at least above a certain level, under so-called "Alliance Agreements". Often the parties allocate the risks to that party, which better can control the situation.

The parties should be aware of the fact, that the contract law, i.e. the applicable law governing the contract, sometimes provides for solutions which the contractual parties do not like. In this case they explicitly have to derogate from the otherwise applicable provisions and stipulate provisions reflecting their intentions in the contract.

1.4. Monitoring: quality assurance and reporting obligations

The implementation of a good quality assurance system is of utmost importance. Part of this program will be the approval and inspection rights of the Employer.

For quality assurance reasons an Employer will always reserve the right to approve the design documents drafted by the Contractor as well as the engagement of major subcontractors. The later one can be done already as pre-agreement in an annex to the contract or – if suitable – already in the tender documents.

A delicate issue is the question to what extent an Employer has/ should have instruction rights. There are legal systems / Civil Codes, which already provide for such rights. If the parties do want to exclude these rights, they derogate from the applicable law and must do so explicitly by writing it down into the contract. If the applicable Code does not provide for such instructions rights, it is up to the contractual parties whether they would like to agree on such instruction rights or not. It should ne noted, that a Contractor following the Employer's instructions will be exempted from liability if those instructions result in defects.

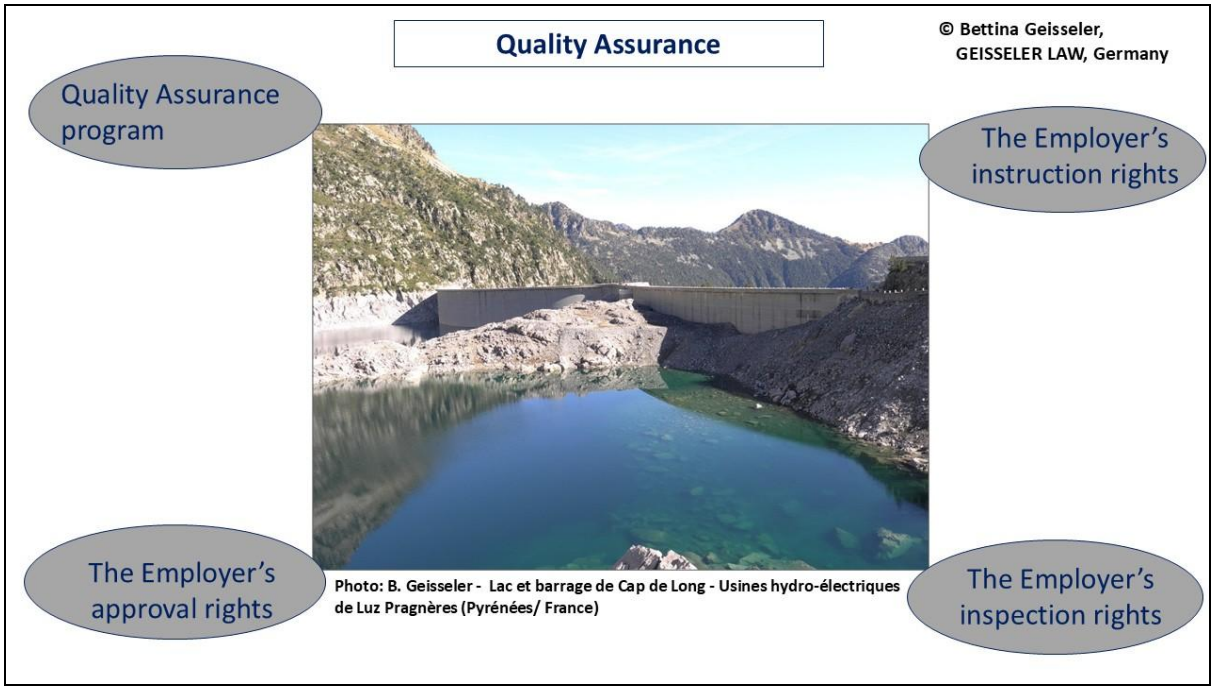


Fig. 4 – Quality Assurance

The implementation of an adapted reporting system is standard. This should be done on a regular basis respectively ad hoc – in case of serious defects, delays or when other obstacles

to the implementation of the project become predictable. The Contractor must report promptly , comprehensively and truthfully . Only such reporting will enable the Employer to monitor the project and to react accordingly , e.g. by suspending the whole project executing for a certain time and aligning the execution of the various lots depending on each other.

2. ALLIANCE AGREEMENTS; MULTI-PARTY AGREEMENTS ON INTEGRATED PROJECT DELIVERY

In order to speed up the project delivery and avoid lengthy discussions about the justification for cost overruns and hindrances with a Contractor's request for compensation of additional costs and time extensions, various contractual approaches and models have been developed in recent years and decades.

Alliance and Integrated Project Delivery contract models have – as it seems successfully – been used in recent decades. They promote early Contractors' involvement and lead to a collaborative problem-solving execution, as the Employer and the Contractor share the chances and risks of the project.

However, one major issue remained in large-scale projects with a multi – contracting structure: the handling of interfaces between the various engaged Contractors, whose supplies and services are interdependent and whose non-performance, time- or quality–wise, might have a negative impact on the performance of another lor by another Contractor.

Recently the model of Multi-Party Agreements ("MPA") using the method of an Integrated Project Delivery ("IPD") in a Partnership Model has been introduced on the European market and is currently being used occasionally , mainly by Employers in the railway sector [3].

2.1. Project Phases – Partners' duties – organisation

One major characteristic of this model is the fact , that the contract ties the Employer and his various Contractors such as the Planner, the other executing Contractors (civil works et al.) together in *one* Agreement without those Contractors being bound by a Consortium Agreement. And: it is the Employer who chooses the Partners and invites them to sign the MPA !

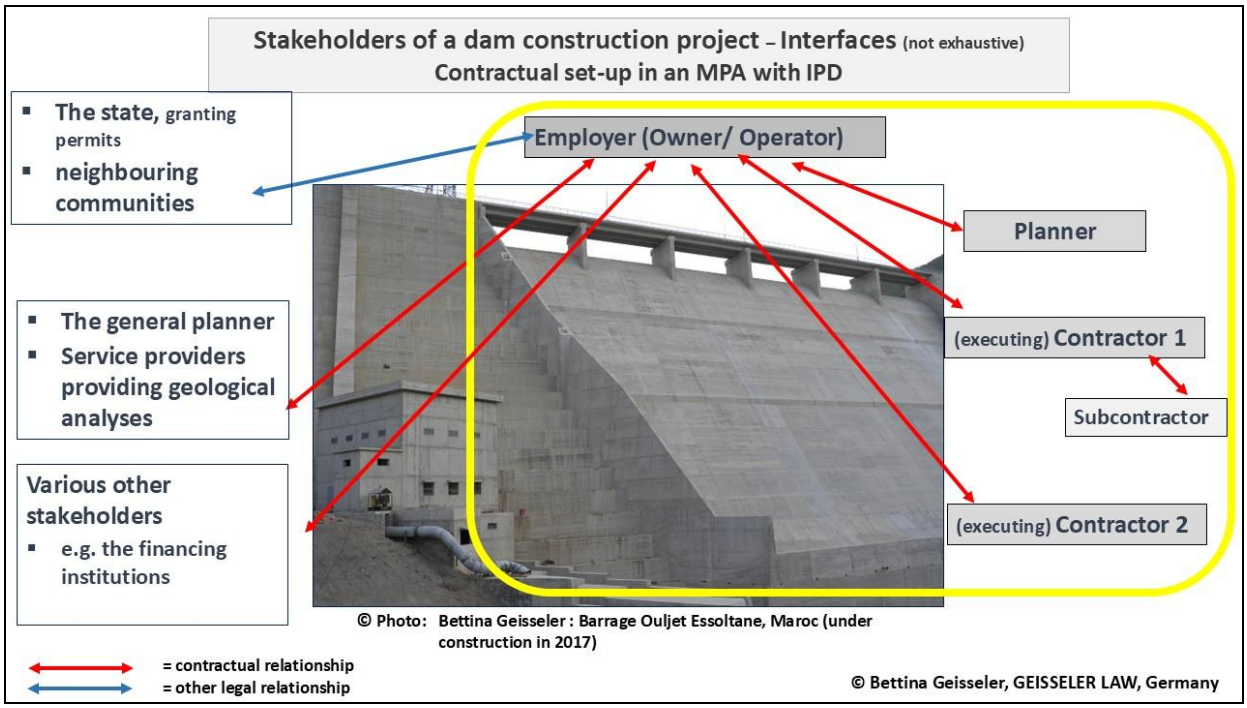


Fig. 5 – contractual set-up in a MPA with IPD

A typical contract (such as used by an European Employer with respect to a large–scale infrastructure project) provides for two phases:

during Phase 1, all Partners - including the Employer - are responsible for the entire planning process (a detailed execution programme for the works with specifications and a detailed planning and construction schedule).

A key element within Phase 1 is the calculation of the costs by each Contractor resulting in the establishment of a document with the project's overall target construction costs as well as the identification and evaluation of potential project-related risks. As in traditional contract models those will be assessed – with the probability of their materialisation - within the forecasted costs and attributed to one of the Contractors, who will then bear the burden to potentially provide his services to overcome this risk. They will be listed in a so–called opportunity and risk table (in German "CRT") – together with their calculated costs and corresponding risk provisions; exempted are the "Employer risks" to be borne by the Employer. At the end of Phase 1, the target construction costs for the execution of the entire project shall have been jointly defined and the those planning-services, to be delivered by the Planner up to the end of phase 1, performed.

Based upon this the Employer (reflecting in particular whether the target costs are within his budget) will call the option for Phase 2 (execution of the project).

Mutual transparency and a collaborative approach are the main characteristics of such a MPA:

- all Partners must disclose all information that is relevant to the project or a Partner, without reservation and exchange such transparently with each other. Exempted is only confidential company information that requires confidentiality, which must be disclosed to the auditor mandated by the Employer only.
- Though each Partner provides his services in his own responsibility, all provide their services in coordination with each other and each Partner must enable the other Partners to optimise their advisory functions with regard to the task they are responsible for.
- The planning, realisation and execution of the entire project is carried out jointly by all Partners.

The project usually is managed by the following bodies: the Project Realisation Team (PRT) for the day-to-day realisation, the Project Management Team (PMT) as core decision body, and – as escalation level - the Senior Management Team (SMT). In the contracts, the author has seen, each of the Partners has one vote in those bodies and the decision making process will be done by unanimity in the PMT respectively with a majority of 75% in the SMT, which means that – depending on the number of Partners – one Contractor can be overruled.

2.2. Target costs – Scope of Works - remuneration – Participation Pool

The target costs, called target costs II to be determined by the Contractors in Phase 1 consist of the production costs (target costs I, made of base costs and provisions for risk costs) plus the contribution margin. The target costs II are the overall reference value for the calculated costs of the project to be borne by the Employer and the basis for the remuneration of each Contractor under the conditions (incentives/ loss of the share in the so-called Participation Pool) as agreed upon in the Contract. Unless the Scope of Works will be modified the target costs remain unchanged, e.g. in case of deviations from the execution Programme, but with an unchanged performance target in accordance with the project Programme.

The Contractors will be remunerated for their services performed as follows: the remuneration due to the Contractors is the compensation for the reimbursable actual costs (i.e. the actual costs incurred for the services provided, to be demonstrated/proven) plus – in principle, up to the originally calculated amount of target costs I - the individual contribution margin (as indicated by each Contractor in its proposal), but reduced by the individual part of the Participation Pool related to the services performed/ supplies delivered.

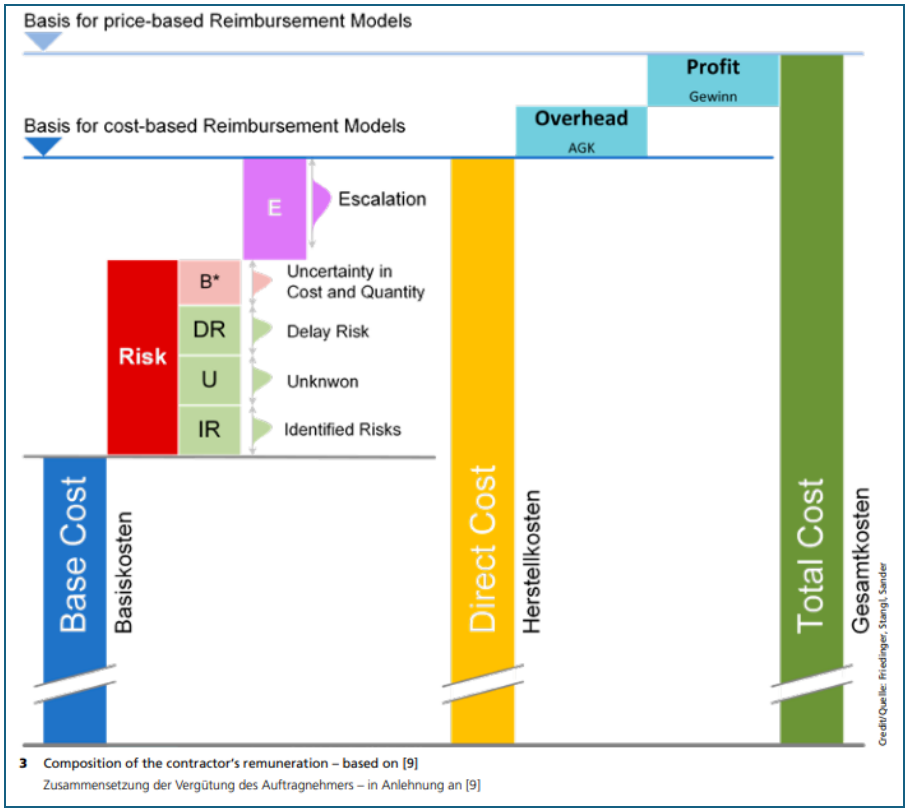


Fig. 6 – cost calculation in IPD contract models, with the courtesy of © tunnel (official Journal of STUVA e.V.) no. 4-5, 2025

Together with the offer each Contractor (at that moment not knowing whether he will be engaged by the Employer and in particular, who will be his Co-Contractors) has to mention a certain amount (in % of his calculated and offered costs) , which he is willing to put into a so-called Participation Pool. The expectations of an Employer regarding the percentage varies from project to project and might depend on the fact whether the Contractor is the Planner or an executing Contractor. The sum of all amounts calculated per Contractor according to

the quoted percentage of the respective target costs I per Contractor builds the overall sum of the Participation Pool.

The Participation Pool will be distributed only at the end of the project – each Contractor receiving his pars pro toto.

The risk sharing in such an MPA/ IPD project is reflected by the fact that in case the total reimbursable costs exceed the calculated target costs the Participation Pool will be reduced accordingly; in the worst case it is exhausted. Usually the Employer and the Contractors share the risk of reimbursable costs exceeding the target costs. Causes for target cost overruns might be risks materialising which not have been identified/ calculated in the CRT or planning defects which materialise in the execution phase. In this case that the execution Partner is asked to remedy those defects and is remunerated for the actual costs incurred for remedying.

On the other hand these contracts provide for incentives, be it in case of completion before the agreed time for completion , be it in case of a cost *under*runs.

CONCLUSION

A balanced contract with carefully drafted provisions will help to minimise project-related risks.

Regarding the recently developed contract model of the MPA with IPD in a Partnership Model, so far mainly used by Employers in the railway sector, the model is certainly as well suitable for large-scale dam projects.

However the Parties should be aware of the fact that a thorough drafting of the Scope of Works clause as well as of the opportunities and risk table by identifying and evaluating potential risks cannot be avoided. Additionally, a Contractor should consider, whether he wishes to be tied to Co-Contractors he has not chosen. And – up to a certain extent , depending on the provisions of the contract – he is forced to commonly share the risks with his Co–Contractors in case of a reduction/ exhaustion of the Participation Pool in case the target costs overrun is not caused by executing his own Scope of Works. This is – and the Contractors must be aware of this legal consequence (!) - a sort of joint and several liability

usually known only in Consortium situations. The fact that in the SMT in the contracts known to the author a 75% majority rule applies leads to the risk that one Contractor – depending on the number of Contractors - can be overruled in the STM decision body.

Thus, the contract model still has to prove its overall advantages. At the moment it is too early to evaluate the overall impacts.

Notes and References

[1] The paper can only deal with some important contractual issues. Other important issues such as questions of the *applicable law* (not a "quantité négligeable", because it will e.g. decide upon the available remedies and might contain mandatory legal provisions which the parties must consider while balancing their mutual interests!), or the *dispute resolution mechanism* (state courts vs. arbitration) could not be taken into consideration. The questions of the *Employer's remedies in case of delay, defects* or other non-compliance committed by the Contractor could not be addressed in this paper. Neither the consequences of a (declared) suspension.

The aim of this paper is to alert Owners/ Employers or Contractors of critical issues potentially having a major (financial) impact on the execution of a dam project, and to suggest, which critical issues should be considered and taken into account when drafting the contract. In no way shall it constitute and substitute a specific legal advice, which will depend inter alia on the applicable law.

[2] According to legal drafting standards some typical legal terms with an established meaning such as "Owner", "Contractor", "Scope of Works" are written in capital letters in the construction contracts and this paper.

[3] *Rieker, Klaus* and *Geisseler, Bettina* , proceedings for the conference "Underground Construction 2026 Prague"

Prof. Sundermeier et al. , TU Berlin : Partnerschaftliche Projektabwicklung für die Schienenverkehrsinfrastruktur – «Partnerschaftsmodell Schiene»

https://www.bauindustrie-bayern.de/fileadmin/Webdata/Themen/20200213_Tagung_Bauen_statt_Streiten/2002_02_13_Vortrag_Prof._Sundermeier_Praesentation_PPA_final__TUB_.pdf

VAU I DEJES - Dam Safety Monitoring, Reservoirs Management and Renewable Energy Integration, ALBANIA

Authors: 1- Ermal NURI, Technical Division Director of A.P.C sh.a, Albania.

2- Ermal KACURRI, Director of DSD, A.P.C sh.a & ALBCOLD Member, Albania

3- Arjan JOVANI, ALBCOLD, Albania

Keyword: ViD HPP-Vau i Dejes Hydropower Plant, APC sh.a-Albanian Power Corporation sh.a, ADAS - Automated Data Acquisition System, Ashta HPP - Ashta Hydropower plant, Spillway, Qyrsaqi Dam, Zadeja Dam

ABSTRACT

The ViD HPP constitutes the strategic downstream terminus of the Drin River Cascade, operating in a high-stakes hydraulic sequence following the Fierza and Koman HPPs and regulating outflows for the Ashta HPP. Commissioned between 1967 and 1971, this complex utilizes a 52-meter rated head to drive an installed capacity of 250 MW, generating a critical annual average of 878 GWh for the Albanian power grid. The structural integrity of the 580 million m^3 reservoir is maintained by a sophisticated system of four large dams: the Qyrsaqi Dam, a massive composite structure integrating the power intake works, high-pressure penstocks, and primary regulated spillways; the Zadeja Dam, a rock fill embankment providing critical storage containment and auxiliary spillway capacity; and the Rragam and Gjoci Dams, which serve as essential embankment closures to the reservoir perimeter. These structures enable a formidable flood-defense capability, with a combined regulated spillway discharge capacity of 6,900 m^3/s, functioning as the final safety valve for the entire cascade and protecting the Shkodra area from maximum hydrological events.

To manage this aging yet strategic infrastructure, APC sh.a. has transitioned to the **Sentinel 2.0** system, a sophisticated ADAS platform. This platform integrates over **194 monitoring instruments**:

- **Geodetic Systems:** High-precision 3D monitoring to detect horizontal deflections and vertical settlements.
- **Structural & Geotechnical:** Utilizing inclinometers, and joint meters to track internal pore pressure and deformation.
- **Advanced Hydraulic Monitoring:** Features automated piezometers to monitor internal pore water pressure and phreatic levels, integrated with pressure gauges and an extensive network of measurement of seepage rates across the dam structures.
- **Seismic:** Strong-motion accelerographs analyze structural responses to seismic events.
- **Hydrometeorological system.** Real -time hydro-meteorological stations enable proactive inflow forecasting

Beyond hydroelectric generation, the ViD reservoir is a vital socio-economic engine for Northern Albania, supporting a diverse ecosystem of services:

- **Flood Mitigation & Irrigation:**
- **Aquaculture & Transport:**
- **Tourism & Environment:**
- **Renewable Energy Hybridization:**

This article will be focused in Modern Monitoring systems, Reservoir integrated management, Multi use purposes, and Photovoltaic integration as next step in the future for sustainable energy system. The digitalization proces enhances operational efficiency, extends asset lifespan, and ensures the socio-economic resilience of the Drin River Cascade against climate and seismic risks.

PAPER TITLE

Web-Based Software for Stability Analysis of Concrete Gravity Dams, Buttress Dams and Masonry Dams

RELEVANT SYMPOSIUM TOPICS:

A. Dams and reservoir safety management for people
   Dam safety assessment, inspection and monitoring
C. Dam Engineering and Construction
   - Development of design methods

AUTHORS:
Contact Author
- Rune Øynes, Software Developer, DamSolutions AS, Solstadveien 36b, 1395 Hvalstad, Norway, Phone: +47 92820785, E-mail: roynes@askerdata.no

Co-Author
- Thomas Konow, Dam Safety Specialist, DamSolutions AS, Brusetveien 73, 1395 Hvalstad, Norway, Phone: +47 45401617, E-mail: thomas.konow@gmail.com

KEYWORDS:
Concrete gravity dams, Buttress dams, Masonry dams, Stability analysis, Dam design software, Safety factors, Limit state design, Web-based engineering tools

ABSTRACT:

Background and Purpose
Dam safety assessment requires rigorous stability calculations for concrete gravity, buttress, and masonry structures. Traditional desktop software generally not tailored to dams, and the quality of calculations may vary.. We have developed a modern, web-based software solution that makes dam stability analysis more accessible to engineers, dam owners, and regulators while maintaining rigorous calculation standards compliant with Norwegian Dam Safety Regulations and Eurocode principles.

Software Overview
The software calculates the stability of concrete gravity dams (with and without drainage systems), masonry dams, and buttress dams. It can be used for both new dam design and assessment of existing structures. Built on a modern .NET 9 Blazor architecture, the system can be deployed either in Microsoft Azure or within a company's own IT environment. This enables organizations to benefit from cloud-based collaboration and accessibility or maintain complete control of sensitive data through on-premises deployment.

The application supports multiple languages (Norwegian/English) and provides real-time calculation feedback during design iterations.

Key Features and Functionality
The program is functional and user-friendly, offering the following features:

- **Dam Cross-Section Module**: Interactive canvas-based drawing tools for defining dam cross-sections with multiple segment types (upstream, downstream, middle, foundation, parapet, void).

automatically calculates geometric properties including cross-sectional area, center of gravity, and foundation width. Support for inclined foundations is included.

- **Interactive Visualization**: Real-time graphical display of the dam cross-section, pore pressure distribution zones , and water pressure polygons on upstream/downstream faces. The visualization updates continuously as input parameters are modified, enabling immediate feedback during design iterations. The canvas uses a sophisticated 41+ module TypeScript runtime for responsive interaction.

- **Pore Pressure Analysis**: Automatic generation of pore pressure profiles beneath the dam based on limit state (SLS/ULS/ALS) and dam type (gravity, drained gravity, buttress, masonry). Table-driven default parameters (drainage distance Dx, zone widths D1/D2/D3, drain factor k) with automatic adjustments. Manual adjustment capability for site-specific conditions. Iterative pore pressure calculation to determine drainage efficiency required for force equilibrium. Dam type-specific pore pressure geometry (e.g., buttress dams use pillar width only, not total foundation width).

- **Comprehensive Load Modeling**: Automatic loads include self-weight, upstream/downstream water pressure (horizontal and vertical components), and pore pressure (vertical and horizontal). User-defined loads include ice pressure, rock anchors, post-tensioned tendons, and additional custom loads. Load combination according to limit state requirements with separate tracking of stabilizing and destabilizing moments.

- **Stability Calculations:** The program evaluates stability against sliding and overturning using two methods. Global Safety Method (factors of safety) calculates Sliding = Capacity/Destabilizing Loads and Overturning = Stabilizing Moment/Destabilizing Moment. Partial Factor Method (Eurocode approach) evaluates resultant force location relative to foundation middle-third (kern) limits with resultant safety factor based on eccentricity limits.

- **Limit State Design**: Safety is calculated for three limit states: Serviceability (SLS) for normal operating conditions, Ultimate (ULS) for extreme design conditions, and Accidental (ALS) for emergency scenarios. Each limit state uses appropriate partial factors and safety requirements according to dam type.

- **Safety Assessment**: Predefined safety factors and partial factors according to Norwegian Dam Safety Regulations and Eurocode. Dam type-specific requirements (gravity, drained gravity, buttress, masonry). Manual adjustment capability for project-specific requirements or alternative standards. Validation warnings for failed safety requirements (factor < 1.0).

Technical Implementation

The software is built on .NET 9 Blazor framework using a hybrid rendering approach: Server-side rendering for initial page load and administrative functions, and WebAssembly (WASM) for interactive calculation pages, providing desktop-like responsiveness without server round trips. The architecture includes Azure cloud hosting with SQL Server database backend, REST API for data access and calculation services, Entity Framework Core for data persistence, and multi-language localization (Norwegian/English) with resource-based translation system.

The calculation pipeline, processes dam geometry through multiple stages: pre-calculation (water heights, drainage defaults), water pressure segment calculations, pore pressure zone calculations, load summation, and safety factor evaluation. A comprehensive logging system captures all intermediate calculation steps for validation and debugging. Calculation results and geometric data can be exported for documentation and regulatory submissions.

Conference Demonstration

A production-ready version of the program will be demonstrated during the presentation, showcasing the complete workflow:

- Dam project creation and configuration
- Interactive cross-section drawing with segment geometry definition
- Real-time visualization of water pressure and pore pressure distributions
- Water level and limit state scenario configuration
- Automatic calculation execution and results display
- Safety factor evaluation using both Global Safety and Partial Factor methods
- Comparison of results across different limit states
- We will present the key design assumptions, calculation methodologies based on Norwegian Dam Safety Regulations and Eurocode, and practical applications for different dam types (gravity, drained gravity, buttress, masonry).

FIGURES

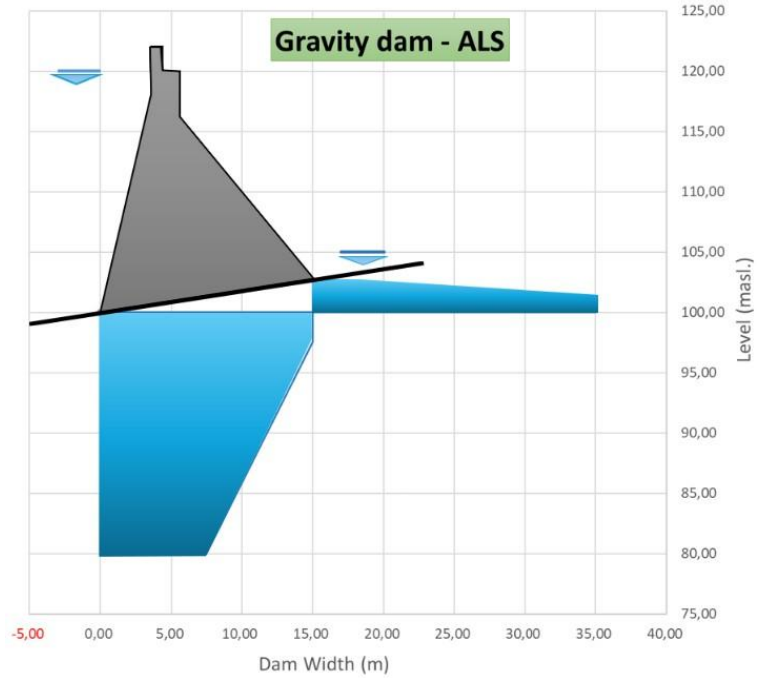


Figure 1: Gravity concrete dam with inclined foundation - illustrating segment geometry (upstream, middle, downstream segments), self-weight distribution, and upstream/downstream water pressure polygons on sloped faces.

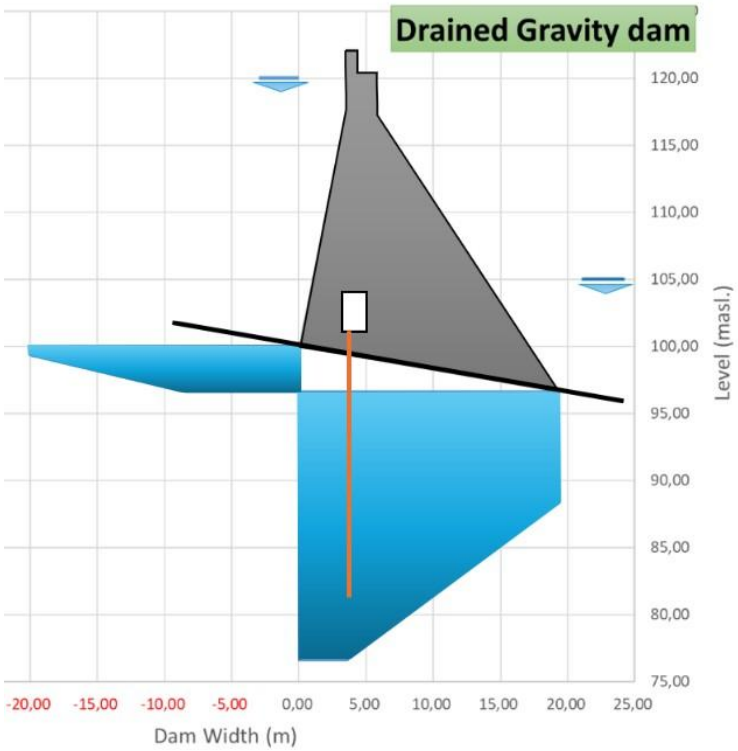


Figure 2: Drained gravity concrete dam with inclined foundation - showing pore pressure zone distribution (Pu, P1, P2, P3) beneath the foundation, with drainage system reducing pore pressure according to drain factor k and drainage distance Dx.

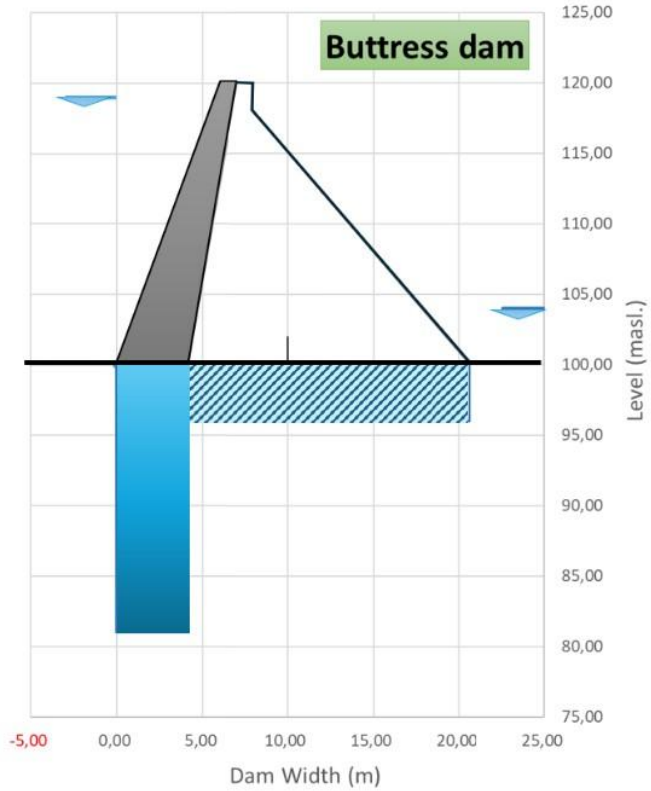


Figure 3: Buttress dam - demonstrating stability analysis for complex geometry including pillar segments and upstream slab. Pore pressure zones use pillar width only (not total foundation width) for buttress-specific calculations.

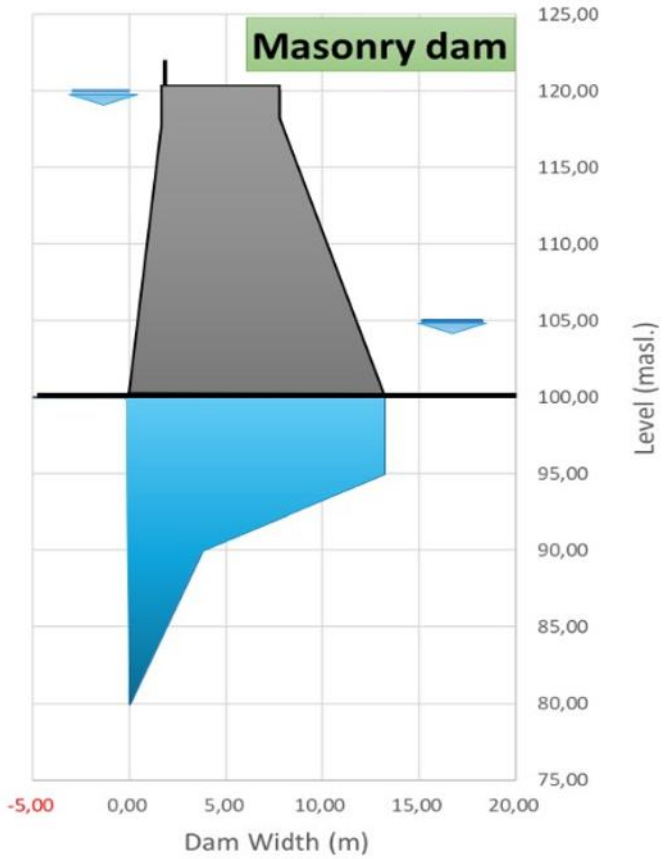


Figure 4: Masonry dam - illustrating material property handling, limit state analysis with masonry-specific partial factors, and safety factor evaluation using both Global Safety Method and Partial Factor Method.

Flow regulation and nutrient dynamics in a Polish lowland reservoir catchment: Implications from SWAT hydrological modelling

1. Jyoti Prakash Hati, 2. Halina Kaczmarek, 3. Bogumił Nowak, 4. Mikołaj Matela, 5. Krystian Obolewski

affiliationsList

1.Jyoti Prakash Hati M.Sc, Wydział Nauk Geograficznych, Uniwersytet Kazimierza Wielkiego w Bydgoszczy, Poland. Orcid 0000-0002-7635-6439
2. Halina Kaczmarek, PhD, Wydział Nauk Geograficznych, Uniwersytet Kazimierza Wielkiego w Bydgoszczy, Poland. Orcid 0000-0002-0650-8134
3. Bogumił Nowak, PhD, Wydział Nauk Geograficznych, Uniwersytet Kazimierza Wielkiego w Bydgoszczy, Poland. Orcid 0000-0002-6963-770X
4. Mikołaj Matela, M.Sc, Katedra Hydrobiologii, Uniwersytet Kazimierza Wielkiego w Bydgoszczy, Poland. Orcid 0000-0001-5839-512X
5. Krystian Obolewski, PhD, Katedra Hydrobiologii, Uniwersytet Kazimierza Wielkiego w Bydgoszczy, Poland. Orcid 0000-0001-9361-0286

keywords

SWAT, Jeziorsko Reservoir, hydrological modelling, nutrient transport, water resource management.

abstract

The Jeziorsko Reservoir, built in 1986 on the Warta River in central Poland, serves as a flood regulation, provides water for irrigation, and generates hydropower. The reservoir with a catchment area of more than 9000 km2 has experienced significant seasonal flow and water level variability. High nutrient load due to intensive agriculture in the upstream region, and changes in rainfall and evaporation patterns due to climate change poses threat to water quality and the long-term ecological health of the reservoir. Therefore, in this research, the Soil and Water Assessment Tool (SWAT) model was simulated to identify the point and non-point sources of pollutants (nitrogen and phosphorus) in the Jeziorsko Reservoir basin. The SWAT model uses high-resolution inputs like digital elevation model, CORINE Land Cover, detailed soil maps, and daily weather data to simulate hydrological response and flow regime, which was validated from the daily discharge data acquired from weather stations. The watershed was divided into sub-basins and hydrological response units (HRUs) so that surface runoff, groundwater recharge, evapotranspiration, sediment yield, and nitrogen/phosphorus transport could be simulated on a daily to yearly basis. The model was calibrated with a warm-up period, then simulated and validated against daily discharges, reservoir water levels, and regulated outflows. The model performance showed that it could reproduce the effects of flow regulation, such as reducing flood peaks, and estimate sediment and nutrient yield in the sub-basins. Sensitivity analysis found that the soil evaporation compensation factor and the groundwater delay were the most important factors for model accuracy. Scenario analyses further illustrate that optimal agricultural management practices could diminish nutrient loads significantly, thereby alleviating eutrophication risks. This research framework was proven to be a strong decision-support tool for improving climate resilience, optimising multi-objective reservoir management, and supporting sustainable water resources planning in regulated Central European basins.

Advanced geomembrane systems for dams and reservoirs of new pumped storage schemes

Gabriella Vaschetti, Carpi Tech, gabriella.vaschetti@carpitech.com
Vanja Verdel, Carpi Tech, vanja.verdel@carpitech.com

The first applications of geomembranes in pumped storage schemes date back to the beginning of the 1990s and aimed to restore the watertightness of ageing dams forming one of the reservoirs. A few of such projects were alread discussed at several ICOLD conferences .

Construction of pumped storage schemes is now booming thanks to the acceleration towards clean energies: pumped hydro storage is the “clean battery” that can balance the alternating energy shortage and surplus characteristic of wind and solar sources. In these schemes, watertightness of the upper and lower reservoirs is important not only for structural safety, but also to minimise maintenance, which often involves outage and heavy revenue losses. Geomembranes therefore started in the middle of the 2010ies to be used also in new construction, to provide the water barrier to the dams forming the reservoirs, or to the entire reservoirs, as effective alternative to conventional facings such as concrete or bituminous concrete, that are less effective in accepting settlements and differential displacements and in sealing joints at boundaries, and are more sensitive to temperature variations, with subsequent frequent need for maintenance. Advanced geomembrane systems, based on the experience acquired in applications in embankment dams and reservoirs, were developed to meet the requirements of these demanding schemes. Portugal, with the Pico da Urze reservoir, part of the Calheta pumped storage schemes, was a pioneer in these applications.

Scope of the paper is to amplify what had been discussed the previous conference, outlining the characteristics and design of advanced geomembrane systems in dams and reservoirs of new pumped storage schemes, discussing their advantages, and presenting the state-of-the-art solutions by three projects: Gandhi Sagar and Pinnapuram in India, with an exposed flexible geomembrane lining respectively the upper reservoir and the dams forming both reservoirs, and Pico da Urze in Portugal where upper reservoir is lined with an exposed flexible PVC-P geomembrane - to enhance durability in an environment with particularly high UV radiation.

SESSION B. Dams and energy		
1	Alexandre Jean Pachoud	EURCOLD bulletins on penstocks, pressure shafts and tunnels: Selected aspects of fatigue evaluation of welded steel parts
2	Agata Léthel	Pumped storage power plants in Poland
3	Nicolas Ulrich	Checking the vibration risks in civil works structures of PSP powerhouses: leveraging on–site investigations to support numerical analysis
4	Alireza Farhadi	Numerical Optimization of an Integrated Fish Passage System in a High-Capacity Run-of-River Hydropower Plant

Alexandre Pachoud

Dam Safety Specialist

Dam Safety Unit

Swiss Federal Office of Energie SFOE, 3003 Bern, Switzerland

Corresponding author: alexandre.pachoud@bfe.admin.ch

Claudia Pollak-Reibenwein

Lead Engineer

Penstock and Gates Department

ANDRITZ HYDRO GmbH, Lunzerstraße 78, 4030 Linz, Austria

ORCID 0009-0000-3313-7343

Alexander Ecker

Project Senior Scientist

Institut für Stahlbau

Technische Universität Graz, Lessingstraße 25 III, 8010 Graz, Austria

ORCID 0000-0003-0952-8867

Wolfgang Richter

Project Senior Scientist

Institut für Wasserbau und Wasserwirtschaft

Technische Universität Graz, Stremayrgasse 10, 8010 Graz, Austria

ORCID 0000-0001-8430-5853

Antonella Frigerio

Deputy Director

Department of Environment and Sustainable Development

Energy Research Center RSE S.p.A., 54 Via Rubattino, 20134 Milan, Italy

ORCID 0000-0001-5497-4386

EurCOLD bulletins on penstocks, pressure shafts and tunnels: Selected aspects of fatigue evaluation of welded steel parts

Alpine hydropower plants are vital for grid stability but increased ancillary service demands to address even elevated fatigue risk in welded steel penstocks. This is critical for high-strength steel designs and retrofitted plants facing unforeseen load spectra. This paper summarizes work by the EurCOLD "Penstocks, pressure shafts and pressure tunnels" Working Group. It critically reviews fatigue design standards and engineering concepts, addressing specific needs of welded steel penstocks. Aggregated insights and design examples provide a practical framework for design and structural life-cycle management of existing plants.

KEYWORDS: Hydropower; Penstocks; Pressure shafts and tunnels; Fatigue; Steel welds; Fracture Mechanics

INTRODUCTION

Alpine hydropower plants act as highly flexible "batteries" for the European power grid. This flexibility is essential for balancing and efficiently exploiting the volatile supply of new renewable energy sources such as solar and wind energy and ensuring the power grid stability. However, the provision of ancillary services within a rapidly evolving electricity market significantly increases load variations and raises the issue of fatigue evaluation of welded hydraulic steel structures, such as penstocks (Cassano et al., 2020). This requirement extends to both newly designed power plants and existing or retrofitted plants subjected to operational load spectra that were not foreseen in the original design criteria. Moreover, the utilisation of high-strength steels, which facilitate more slender designs, may amplify fatigue-related vulnerabilities (Pachoud, 2017), rendering fatigue a critical and even decisive parameter in

structural design, evaluation, and life-cycle management (Pollak-Reibenwein & Akgun, 2016).

In this context, the European Working Group "Penstocks, pressure shafts and pressure tunnels" has been established by the European Regional Club (EurCOLD) of the International Commission on Large Dams (ICOLD). It has committed to publishing technical bulletins providing a comprehensive overview of good practices (Richter et al., 2025). The series of bulletins is provisionally foreseen to be published in four parts, including good practices and recommendations for design of new projects and safety assessment of existing structures.

This paper introduces selected key aspects of fatigue evaluation of steel penstocks, highlighting some of the valuable insights expected from the forthcoming EurCOLD bulletins. Published standards and recommendations for fatigue design are first critically reviewed. Subsequently, engineering approaches for fatigue design concepts are summarised. Reference is also made to recent research addressing needs of steel-lined pressure shafts and tunnels (e.g., fatigue strength of typical penstock welds and grouting openings). Finally, examples of published fatigue designs of penstocks and special parts are reviewed, providing aggregated insights to practitioners.

REVIEW OF STANDARDS AND RECOMMENDATIONS

The methods of fatigue assessment of welded structures can be classified into two broad categories (see, e.g., Fuštar et al., 2018):

1. ***S-N* approaches**, where the *S-N* curves (or so-called "Woehler" curves) are derived based on experimental fatigue testing. *S-N* curves provide a direct relationship between the fatigue life and the load cycles *N*, against the applied stress amplitudes *S* (in terms of nominal, structural, and notch stresses). The *S-N* curves implicitly account for initiation and propagation stages.
2. **Crack propagation approaches**, based on Linear Elastic Fracture Mechanics (LEFM) and the Paris-Erdogan crack propagation law (or derivates). In this approach, it is assumed that an initial crack is present in the welded joint, and only the propagation stage is modelled.

Standards and recommendations for the design of steel structures commonly used in Europe adopt various variations of these approaches. In general, *S-N* approaches are relevant for fatigue assessment of new projects, assuming initial flawless structures, whilst LEFM

approaches allow to perform fitness-for-service assessment for existing structures where specific flaws have been detected at a certain stage of the lifecycle.

S-N curves are characterised by their fatigue strength at 2×10^6 cycles with an associated probability of survival, so-called FAT classes. Tab. 1 proposes a comparison of standards or recommendations for fatigue assessment based on *S-N* curves and FAT classes for *local* stresses (i.e., structural and notch stresses), of particular interest for penstock design. Comparing documents such as ASME B&PVC (2023), FKM-Guideline (2023), Eurocode 3 (EN 1993-1-9:2013), EN 13445-3:2021, recommendations of the International Institute of Welding IIW (Hobbacher, 2016) or CODETI Div.3 (2014) may be challenging as they rely on different safety concepts. For example, the FKM-Guideline (2023) explicitly accounts for mean stress effects, whereas the current version of Eurocode 3 (EN 1993-1-9:2013) does not. Nevertheless, Tab. 1 hereinafter attempts to summarise the key differences in the underlying safety concepts and local stress estimation. Similarly, a direct comparison between *S-N* curves issued from the ASME Code and, for instance, the FAT classes proposed in the recommendations of the IIW is not straightforward, as they are based on different stress definitions. It is noteworthy that all listed standards and recommendations provide FAT classes for the nominal stress approach (*global* stress). Nominal stresses are typically determined using analytical formulas, whereas structural and notch stresses generally require the use of finite element analysis (FEA), particularly for complex structures (see, e.g., Pollak-Reibenwein et al., 2013).

Tab. 1. Standards and recommendations commonly used for fatigue evaluation

Standard or recommendations	**Structural stress calculation**	**Notch stress calculation**	**Safety factors**	**Survival probability**
ASME B&PVC, Section VIII, Div.2, Part 5 (2023)	Linearized stress obtained by post-processing (as welded)	No standardized notch stress definition	Embedded in *S-N* curves	99%
	Peak stress directly from FEA (smooth weld)		Embedded in *S-N* curves	Not provided
FKM-Guideline (2023)	Extrapolated and linearized stress obtained by post-processing	R1-concept	1.0 to 1.4, depending on damage severity	97.5% + safety factor
EN 1993-1-9:2013 (current version)	No structural stress concept mentioned, but structural stress FAT classes	N/A	Partial safety factors: Load: 1.0 Material: 1.0 to 1.35 depending on damage severity	95% (with a 75% confidence interval)

prEN 1993-1-9:2023 (preliminary version, expected publication of final version 2027/2028)	Extrapolated stress obtained by post-processing	R1-concept	Partial safety factors: Load: 1.0 Material: 1.0 to 1.35 depending on damage severity	95% (with a 75% confidence interval)
IIW (Hobbacher, 2016)	Extrapolated stress obtained by post-processing	R1-concept	Partial safety factors: Load: no explicit value but to be considered Material: 1.0 to 1.4 depending on damage severity	95% (with a 75% confidence interval)
EN 13445-3 (2021)	Extrapolated stress obtained by post-processing	N/A	Embedded in *S-N* curves	97.7%
CODETI Div.3 (2014)	No structural stress concept mentioned, but structural stress FAT classes	N/A	Embedded in conservative fatigue classes	Not stated

ENGINEERING APPROACHES FOR FATIGUE ASSESSMENT

Welded steel penstocks typically consist of multiple fatigue-relevant structural components, including a large number of welded pipe sections joined both in the workshop and on site, as well as a reduced number of geometrically more complex elements such as reinforced bifurcations, transitions, or manholes. Typical circumferential and longitudinal welds at cylindrical pipes constituting a straight penstock stretch are sketched in Fig. 1. An overview of the main engineering methods for fatigue assessment of welded steel structures is provided hereinafter.

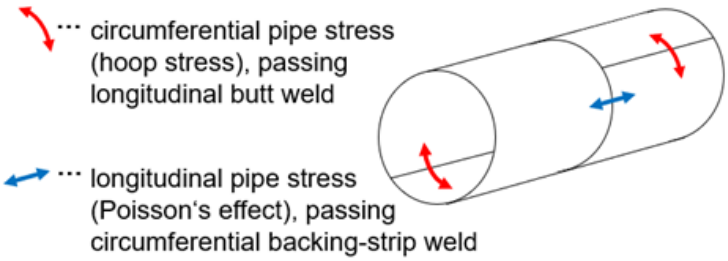


Fig. 1. Typical cylindrical penstock welds

S-N approaches

The *nominal stress* approach is the simplest method, linking fatigue strength to the range of applied nominal stress cycles. In this method, local stresses are disregarded (see Fig. 2) and *S-N* curves are provided for a various structural detail category in *as-welded* conditions,

possibly both for constant and variable amplitude loadings. Where nominal stress can be estimated with closed-form analytical solutions, this approach can be implemented without modelling efforts. Typical examples on penstocks include the circumferential (hoop) stress for thin-walled pipes at longitudinal welds, and the axial stress at circumferential welds (in general due to Poisson's effect). Stress concentrators such as geometrical imperfections and weld profile are implicitly considered within prescribed limits of the classification of the structural details. Nominal stress approaches are provided in most structural codes.

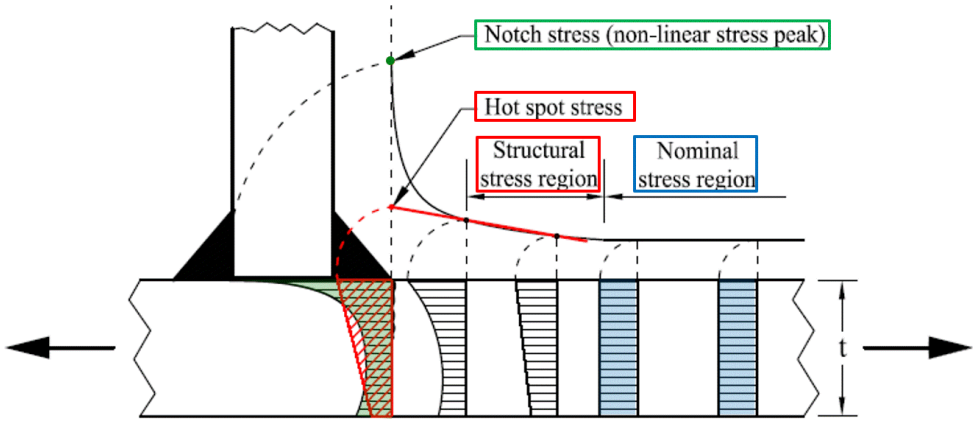


Fig. 2. Stress components approaching weld toe

Geometrically more complex structural details that cannot be classified in the frame of the nominal stress approach generally require fatigue assessment based on FEA to estimate local stresses. In some cases, analytical formulas for stress concentration factors may be available in literature (e.g., roof-topping effect at a longitudinal butt weld of a cylindrical pipe). Local approaches are categories in two approaches: the *structural (hot spot) stress* approach, and the *effective notch stress* approach. See the evolution of stress components in Fig. 2.

The *structural stress* approach includes the effect of the structural configuration but excludes stress concentrations due to the weld profile itself. This approach enables the treatment of structural details where a nominal stress cannot be defined meaningfully. It also reduces the number of FAT classes (typically FAT 90-100 for steel), i.e., hot-spot *S*-*N* curves (as a function of structural stress ranges). The structural stress is composed of membrane and bending components, excluding the nonlinear peak caused by the weld toe. Standards prescribe various approaches to determine structural (hot spot) stresses, i.e., via extrapolation from reference points away from the weld (see Fig. 3), or via direct stress linearization (see

Fig. 4, left). Note that these stresses are physically different, but both aims at removing the nonlinear peak component. The weld root fatigue, however, is not covered by the structural stress approach (e.g., for partial penetration and fillet welds, see Fig. 4). The membrane σ_m and bending σ_b components can be determined from FEA results, for instance as follows (Dong, 2001):

$$\sigma_m = \frac{1}{t}\int_0^t \sigma_x(y)\cdot dy \tag{1}$$

$$\sigma_m \cdot \frac{t^2}{2} + \sigma_b \frac{t^2}{6} = \frac{1}{t}\int_0^t \sigma_x(y)\cdot y\cdot dy + \delta\int_0^t \tau_{xy}(y)\cdot dy \tag{2}$$

where the nomenclature is described in Fig. 4 (right).

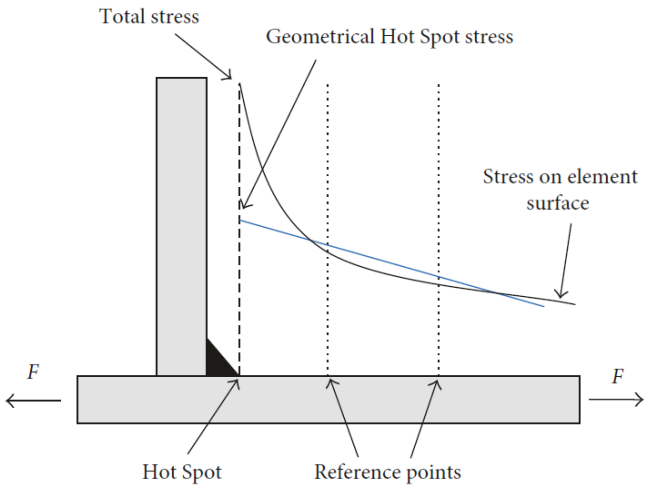


Fig. 3. Illustration of hot-spot stress calculation via extrapolation (from Fuštar et al., 2018)

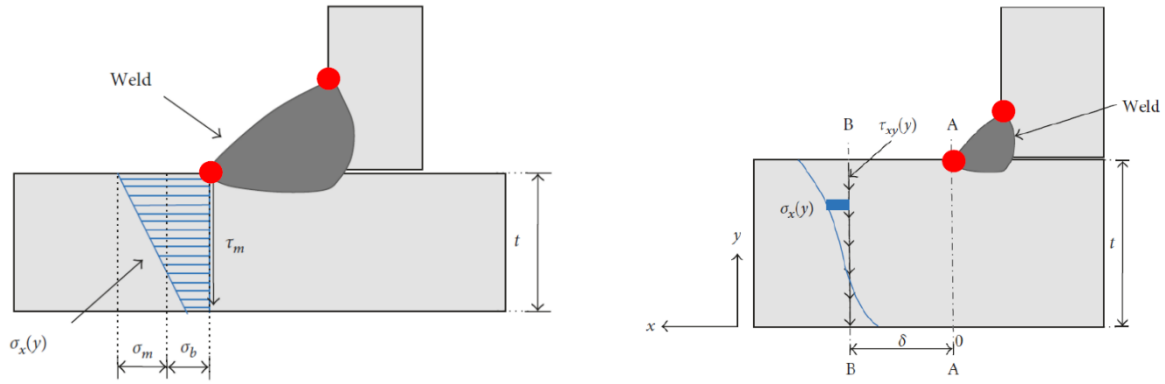


Fig. 4. Description of structural stress components (left) and of structural stress calculation procedure (right) (modified from Fuštar et al., 2018). Structural stress evaluation applied only to weld locations marked in red

Finally, the *notch stress* approach considers the nonlinear peak induced by the weld profile (at weld toes or roots). The R1-concept (see Fig. 5) is the state-of-the-art approach for assessing notch stress fatigue, and it is also applicable to weld roots. R1 involves modelling weld root and toe with a 1 mm *reference* radius. Comprehensive details on local stress approaches can be found, e.g., in (Hobbacher, 2016).

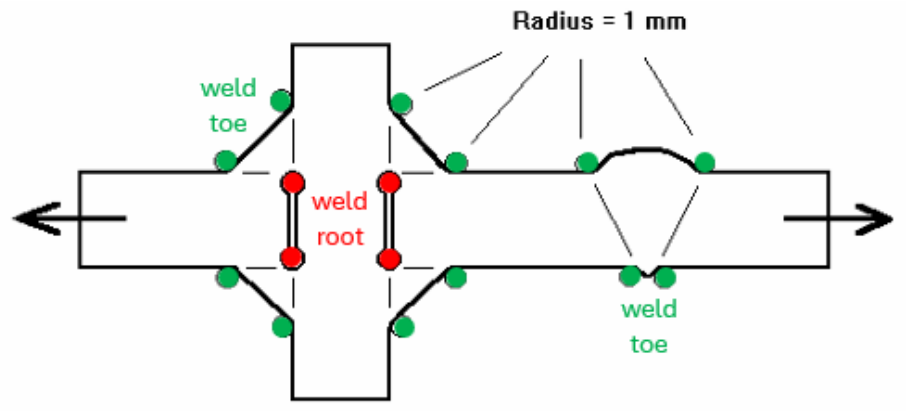


Fig. 5. R1-concept: fictitious rounding of weld toes and roots (modified after Hobbacher, 2016)

For smooth or ground welded joints, fatigue assessment according to EN 1993-1-9:2013 or IIW (Hobbacher, 2016) may be based on nominal or structural stress ranges obtained from FEA without explicit modelling of the weld geometry. In this case, local weld-toe notch effects are not included in the stress definition but are implicitly covered by the selected FAT class, which may be increased for improved weld quality.

In ASME B&PVC (2023), smooth or ground welded joints may be assessed for fatigue using elastic stresses obtained from a linear elastic FEA that represent the overall structural stress state of the component, without explicit modelling of the weld geometry. Fatigue evaluation is performed using the ASME smooth-bar fatigue curves, with weld effects accounted for by applying fatigue strength reduction factors defined by the code.

LEFM approach

In the fracture mechanics (LEFM) approach, the fatigue crack growth per applied load cycle da/dN is a function of the applied stress intensity range ΔK_I. It follows the so-called Paris-Erdogan law (Paris & Erdogan, 1963), expressing a linear relation between da/dN and ΔK_I in a log-log space:

$$\frac{da}{dN} = C(\Delta K_I)^m \tag{3}$$

where C and m are the fatigue coefficient and exponent, respectively, and are material-dependent constants, determined experimentally. In this approach, the crack-like flaw is explicitly considered. The crack only propagates during cycle *N* if the applied ΔK_I is greater than a threshold, also depending on the material.

For welded plated structures such as penstocks, the general formulation for the stress intensity factor (SIF) K_I at a crack tip is a function of the structural stress components and can generally be expressed as:

$$K_I = [M_m(\sigma_m + p_{cr}) + M_b\sigma_b] \cdot \sqrt{\frac{\pi \cdot a}{Q}} \tag{4}$$

where a is the crack depth, M_m and M_b are shape correction factors, p_{cr} is the pressure applied on the crack face (if any), and Q is the flaw shape parameter. Various closed-form analytical solutions to estimate SIFs at surface and embedded cracks in welded plates or cylinders exist in the literature (see, e.g., Pachoud et al., 2017). Where not available, they can be obtained by means of FEA.

The LEFM approach, combined with non-destructive testing to characterise the possible presence of crack-like flaws, is of particular interest to estimate the remaining life of a structure under given foreseeable loading spectra where stable crack propagation governs the fatigue assessment, and can also be implemented, e.g., within the frame of a *Damage Tolerant Design* approach (Zerbst et al., 2007).

RECENT RESEARCH ON PENSTOCK FATIGUE

Special parts (manifolds, manholes, grouting holes)

Fatigue is of particular concern in parts of penstock with stress concentrators, such as bifurcations, fixed supports, mitred bends or transitions at manifolds (Unterweger et al., 2024), access openings (manholes) or grouting holes. For manifolds, the structural (hot-spot) stress should be estimated at welded hot spots to identify governing locations and to guide targeted inspection and monitoring. To capture the smoothing effect of fatigue-relevant pressure fluctuations, geometric nonlinearity should be included, and the fatigue load case is evaluated using two static pressure load cases. The first represents the upper bound, defined

by the static internal pressure increased by half of the pressure fluctuation range. The second represents the lower bound, defined by the static internal pressure decreased by half of the same range. The difference between the resulting stress states is then taken as the stress range for the fatigue assessment.

Fig. 6 illustrates, as an example for an exposed manifold (Unterweger et al., 2024), the fatigue utilization (%) and highlights where pressure fluctuations govern fatigue demand. In this example, the critical location occurs at a sliding bearing positioned at a mitred bend.

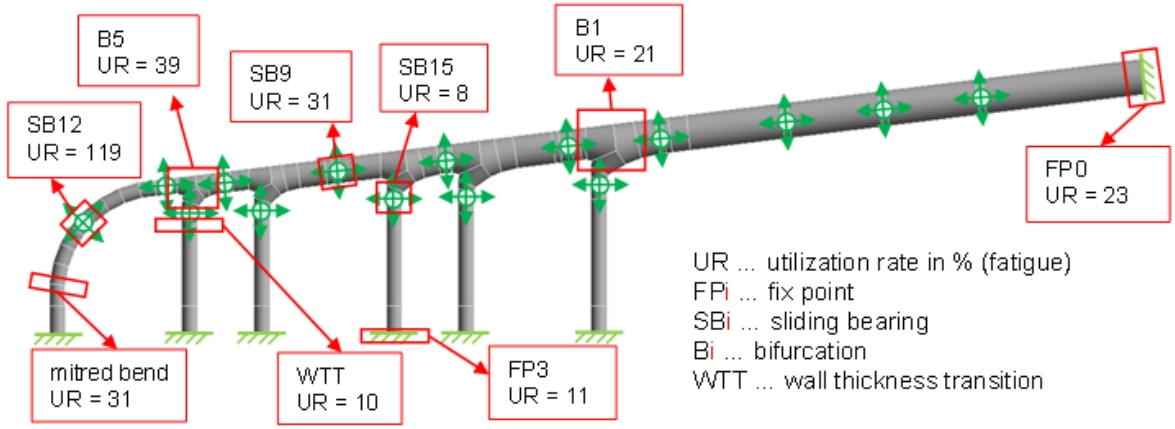


Fig. 6. Fatigue utilisation (%) at various locations on an exposed manifold

For access openings (AOs) with nozzles and flanges, the local behaviour of the nozzle-to-pipe region and the flange-bolt system under internal pressure must be investigated for fatigue assessment (Unterweger et al., 2025). Both plates and bolts must be incorporated in the FEA. This level of modelling is needed to obtain reliable structural (hot-spot) stresses for fatigue assessment. In pressure-driven load cases, the dominant membrane action is the hoop stress, while longitudinal components must reflect the specific restraint and load combination considered in the global system. At access openings, the maximum stress under design pressure occurs at the inner edge of the cut-out, at the apex (hot-spot HS1 at $\alpha = 0°$, see Fig. 7). Consequently, nozzle-to-pipe welds are often decisive for fatigue. Increasing the nozzle wall thickness or reinforcing the pipe wall in the cut-out zone most effectively lowers the hot-spot stresses in this weld.

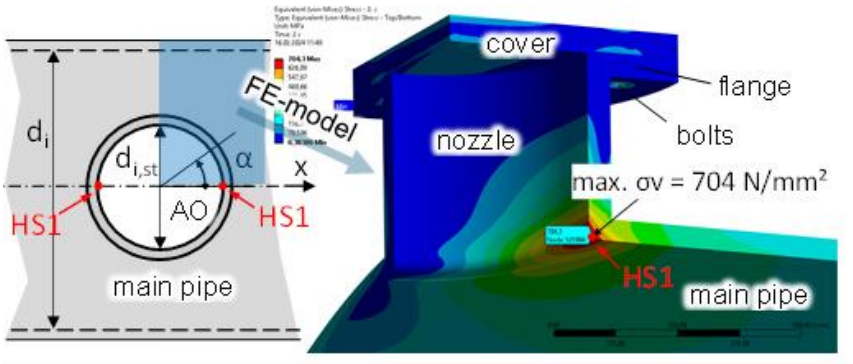


Fig. 7. Access Opening (AO) Von Mises equivalent stresses σ_v with maximum at Point HS1; internal pressure loading

A three-year research project, integrating fatigue testing and parametric FEA, aimed at improving the design of grouting openings in steel linings (Greiner & Lechner, 2013). A total of 35 specimens covering existing and optimized grouting opening shapes in high-strength steels (S690Q, S690QL1, Alform 700M) were tested. Failures initiated either at outside weld toes or at stress peaks in threads or drilled holes, depending on the detail and grinding condition. The fatigue evaluation consistently supports using *S-N* curves with slope $m = 5$ for welds, threads, and drilled holes, with specific characteristic resistances and mean stress compensation where applicable. The outcome provides new design *S-N* curves and confirms that, with strict manufacturing quality, the grouting openings can reach fatigue resistances comparable to those governing longitudinal welds in steel liners (Greiner & Lechner, 2013).

Experimental strength analysis of typical penstock welds

Most fatigue assessment standards or recommendations do not distinguish fatigue strength as a function of steel grade for welded structures. This hypothesis was recently investigated for typical penstock high-strength steel welds (Pollak-Reibenwein, 2024). The impact of material strength on the fatigue resistance of typical penstock welds was investigated, specifically comparing full penetration butt welds and backing-strip welds fabricated from high-strength steels S500ML and S690QL. The results demonstrated that backing-strip welds utilising S690QL exhibited a markedly enhanced fatigue life (Fig. 8). Both material grades of butt weld specimens showed much higher fatigue strength than standard recommendations for this structural detail (Fig. 9).

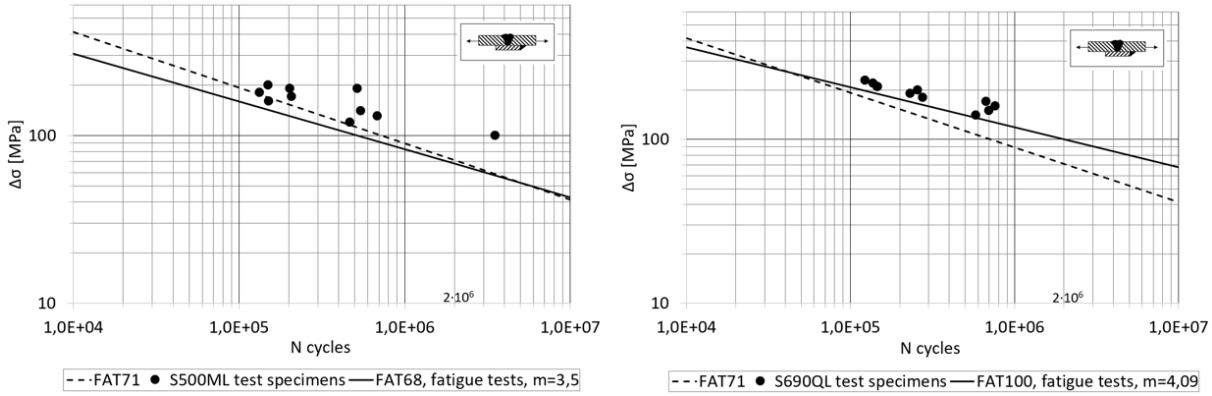


Fig. 8. *S-N* curves for backing-strip weld specimens made of S500ML (left) and S690QL (right) (after Pollak-Reibenwein, 2024)

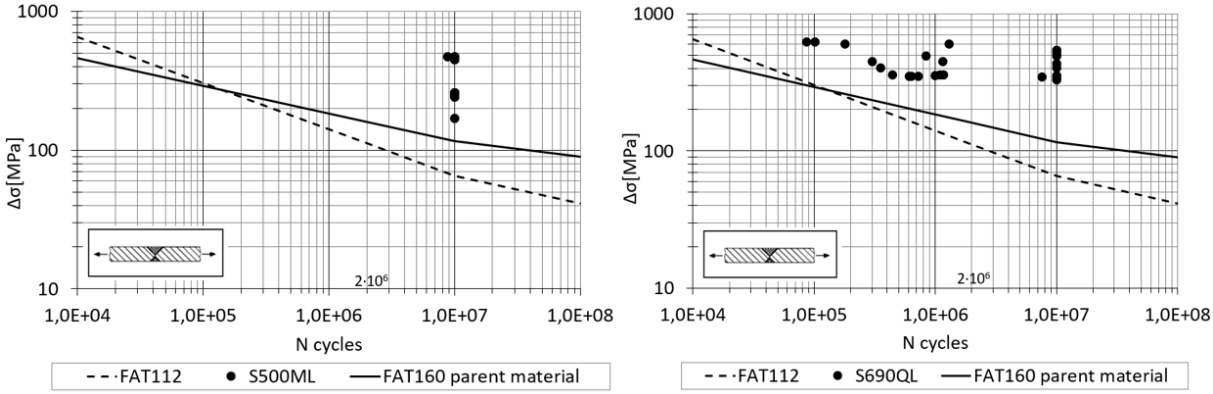


Fig. 9. *S-N* curves for butt weld specimens made of S500ML (left) and S690QL (right) (after Pollak-Reibenwein, 2024)

These findings suggest that the application of higher-strength steels can improve reliability and extend service life or inspection intervals, if welding quality is guaranteed at best practices' levels. Strict adherence to approved procedures, meticulous control of heat input, and comprehensive inspection protocols as per relevant welding standards are imperative to guarantee these benefits.

CASE STUDIES FROM LITERATURE

Whilst fatigue assessment of welded steel structure is the subject of a vast body of literature, practical applications to steel penstocks remain seldom. Specific recent applications to steel penstocks are reviewed hereinafter.

Examples of application of *S-N* approaches

(Demal & Moser, 2013) used the notch stress approach (following the recommendations of the IIW) together with FEA to estimate the effective notch stresses for various weld geometries and geometrical imperfections such as roof-topping or linear misalignments. The results were integrated into a linear damage calculation using the Palmgren-Miner rule (see, e.g., Maddox, 1991), comparing accumulated stress ranges from operational manoeuvres against the FAT 225 resistance class. The study specifically highlighted how manufacturing imperfections, such as roof topping and linear misalignment, significantly increase local bending stresses and reduce the expected lifetime of the penstock.

(Dreyer et al., 2019; Dreyer et al. 2021) have conducted fatigue assessment of a penstock in Switzerland based on the implementation of a calibrated digital twin (*Hydro-Clone*). The digital twin replicates the real-time hydraulic behaviour of the hydropower plant based on in situ measurements. Applying the *rainflow cycle counting algorithm* on the transient pressure time series, the authors obtain a reliable estimate of the loading spectrum. Fatigue assessment is performed with the nominal stress approach computing damage with the Palmgren-Miner rule. Stress ranges are calculated based on analytical formula, FEA and comparison against in situ measurement (strain gauges). The use of digital clones generally gains increased interest for fatigue assessment of hydraulic steel structures (Condemine et al., 2023).

(Pachoud, 2017) performed fatigue assessment through a parametric study of fictive penstock designs, varying parameters such as pressure head and slenderness. Steel thicknesses were determined as if the penstocks would be designed following the C.E.C.T. (1980) recommendations assuming rock mass participation, for various steel grades. The author used the notch stress approach in combination with the Palmgren-Miner rule. Normalised loading spectra (with respect to mean pressure) were determined applying the *rainflow cycle counting algorithm* on the pressure transient data collected by (Hachem & Schleiss, 2012) on a Swiss pumped-storage scheme and scaled-up to each fictive case.

(Pollak-Reibenwein & Akgun, 2016) analyse two benchmark examples of fatigue assessment of welded joints of complex hydraulic steel structures by means of the structural stress approaches. The authors provide practical insights to calculate structural stresses via FEA and assess fatigue strength according to a selection of standards and refer to applications to complex structures such as the gate housing of a recently built hydropower pumped-storage plant in Switzerland, see Fig. 10.

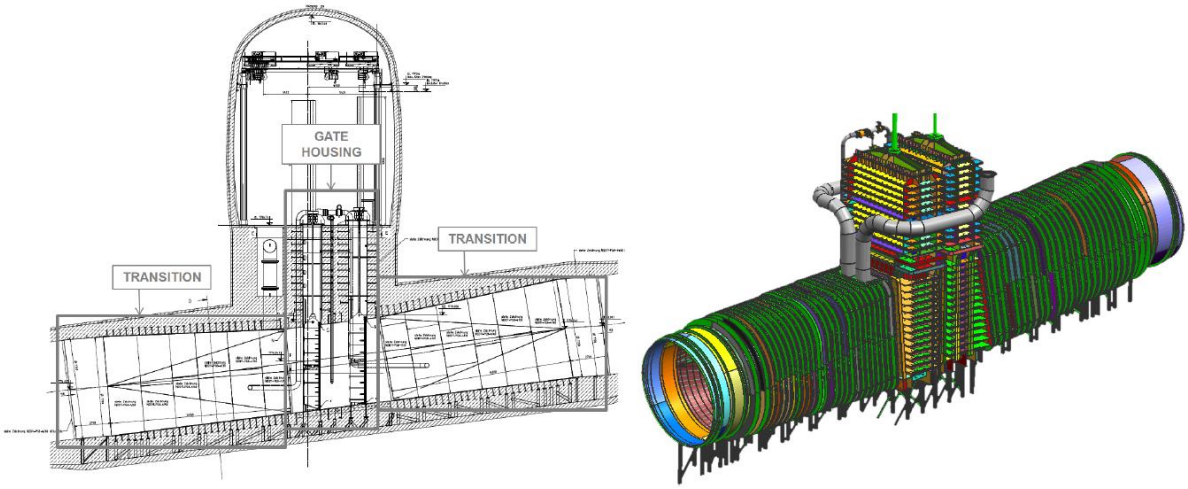


Fig. 10. Cross section (left) and 3D model of the gate housing and transition lining (from Pollak-Reibenwein et al., 2013).

Examples of application of LEFM approaches

(Pachoud, 2017; Pachoud et al., 2018; Adamkowski et al., 2021) performed fatigue life analyses of steel penstocks based on the LEFM approach. These studies specifically explore solutions to estimate stress concentration factors and stress intensity factors, both via analytical solutions and FEA.

(Pachoud, 2017; Pachoud et al., 2018) also proposed a comprehensive framework to develop probabilistic models for fatigue crack growth assessment in penstocks using the Monte Carlo simulation technique. Whilst the application focused on longitudinal butt-welded joints of cylindrical penstocks including geometrical imperfections, the provided insights can be used to establish procedures for any complex structural details.

SUMMARY

The growing need for operational flexibility in hydropower plants to integrate variable renewable energy sources into the power grid significantly increases fatigue loading in welded steel penstocks, thereby making fatigue a governing design and assessment criterion.

The review of existing standards and recommendations shows that fatigue evaluation methods can generally be grouped into two main families: *S-N* approaches, mainly suited to the design of new structures assuming defect-free conditions, and crack propagation approaches, based on Linear Elastic Fracture Mechanics (LEFM), particularly effective for the assessment of existing structures where defects are present. While these approaches are

widely adopted in different formulations, their comparison highlights the need for greater harmonisation and clearer, application-oriented guidance for penstock design and assessment.

The paper outlines that nominal, structural (hot spot) and effective notch stress concepts offer increasing levels of accuracy for fatigue assessment. While nominal stress methods remain suitable for simple geometries, local approaches supported by Finite Element Analysis (FEA) are essential for complex components and welded joints. Advanced methods, including digital twins and probabilistic approaches, enable more realistic loading assessment and improved life prediction.

Fatigue behaviour of special components (manifolds, manholes, grouting openings etc.) is strongly influenced by local geometry, stress concentrations, manufacturing and material quality. High-strength steels can improve performance, provided that strict fabrication and welding quality control procedures are ensured. Manufacturing imperfections significantly increase local stresses and reduce the expected lifetime of penstocks.

The work carried out within the EurCOLD Working Group "Penstocks, pressure shafts and pressure tunnels" provides a comprehensive framework for fatigue evaluation of welded steel penstocks, combining existing standards, recent research findings and practical engineering experience. The forthcoming EurCOLD technical bulletin is expected to consolidate these insights, supporting both the safe design of new hydropower schemes and the reliable life-cycle management of existing infrastructures.

REFERENCES

[1] Adamkowski, A., Lewandowski, M., Lewandowski, S. 2021. "Fatigue life analysis of hydropower pipelines using the analytical model of stress concentration in welded joints with angular distortions and considering the influence of water hammer damping." *Thin-Walled Structures* 159:107350. DOI:10.1016/j.tws.2020.107350.

[2] ASME 2023. *B&PVC (Boiler & Pressure Vessel Code) Section VIII-Rules of Construction for Pressure Vessels, Division 2-Alternative Rules*. New York, NY: The American Society of Mechanical Engineers.

[3] Cassano, S., Nicolet, C., Sossan, F. 2020. "Reduction of penstock fatigue in a medium-head hydropower plant providing primary frequency control." In *Proceedings of the 55th*

International Universities Power Engineering Conference (UPEC), Turin, Italy 1-4 September 2020. DOI: 10.1109/UPEC49904.2020.9209857.

[4] CODETI Division 3 2014. *Code for Construction of Penstocks*. SNCT Publications.

[5] Comité Européen de la Chaudronnerie et de la Tôlerie (C.E.C.T.) 1980. *Recommendations for the Design, Manufacture and Erection of Steel Penstocks of Welded Construction for Hydro Electric Installations*. Paris, France.

[6] Condemine, C., Grau, L., Masson, Y., Aubry, S. 2023. "Live digital twin for hydraulic structures fatigue estimation." In *Proceedings of PIANC Smart Rivers 2022 (PIANC 2022)*, Li, Y., Hu, Y., Rigo, P., Lefler, F.E., Zhao, G. (eds). *Lecture Notes in Civil Engineering* 264. Singapore: Springer. DOI: 10.1007/978-981-19-6138-0_43.

[7] Demal, R., Moser, C. 2013. "Fatigue assessment of hydropower plants – Penstocks using IIW-notch stress concept." In *Proceedings of the 3rd International Conference on High Strength Steels for Hydropower Plants*, Graz, Austria, 18-20 September 2013.

[8] Dong, P. 2001. "A structural stress definition and numerical implementation for fatigue analysis of welded joints." *International Journal of Fatigue* 23(10):865-876. DOI: 10.1016/S0142-1123(01)00055-X.

[9] Dreyer, M., Nicolet, C., Gaspoz, A., Biner, D., Rey-Mermet, S., Saillen, C., Boulicaut, B. 2019. "Digital clone for penstock fatigue monitoring." *IOP Conference Series: Earth and Environmental Science* 405:012013. DOI: 10.1088/1755-1315/405/1/012013.

[10] Dreyer, M., Nicolet, C., Gaspoz, A., Gonçalves, N., Rey-Mermet, S., Boulicaut, B. 2021. "Monitoring 4.0 of penstocks: digital twin for fatigue assessment." *IOP Conference Series: Earth and Environmental Science* 774:012009. DOI: 10.1088/1755-1315/774/1/012009.

[11] EN 13445-3:2021. *Unfired pressure vessels – Part 3: Design*. Brussels: European Committee for Standardization.

[12] EN 1993-1-9:2013 04 01. Eurocode 3 - *Design of steel structures – Part 1-9: Fatigue*

[13] prEN 1993-1-9:2023 04 01. Eurocode 3 - Design of steel structures Part 1-9: Fatigue; (Preliminary European Norm)

[14] FKM-Guideline 2023. *Analytical strength assessment of components in mechanical engineering.* Forschungskuratorium Maschinenbau.

[15] Fuštar, B., Lukačević, I., Dujmović, D. 2018. “Review of fatigue assessment methods for welded steel structures.” *Advances in Civil Engineering*. DOI: 10.1155/2018/3597356.

[16] Greiner, R., Lechner, A. 2013. “Fatigue strength of high-strength steel linings with different types of grouting opening.” *Steel Construction* 6(4):287-293. DOI: 10.1002/stco.201310040.

[17] Hachem, F.H., Schleiss, A.J. 2012. “Online monitoring of steel-lined pressure shafts by using pressure transients signals under normal operation conditions.” Journal of Hydraulic Engineering 138(12):1110-1118.

[18] Hobbacher, A.F. 2016. *Recommendations for fatigue design of welded joints and components*, Second Edition. In *IIW Collection*, IIW document IIW-2259-15 ex XIII-2460-13/XV-1440-13. Switzerland: Springer International Publishing AG.

[19] Maddox, S.J. 1991. *Fatigue strength of welded structures*. Abington Publishing.

[20] Pachoud, A.J., Manso P.A., Schleiss, A.J. 2017. “Stress intensity factors for axial semi-elliptical surface cracks and embedded elliptical cracks at longitudinal butt welded joints of steel-lined pressure tunnels and shafts considering weld shape.” *Engineering Fracture Mechanics* 79:93-119. DOI: 10.1016/j.engfracmech.2017.04.024.

[21] Pachoud, A.J. 2017. *Influence of geometrical imperfections and flaws at welds of steel liners on fatigue behavior of pressure tunnels and shafts in anisotropic rock*. PhD Thesis No. 7305, Ecole polytechnique fédérale de Lausanne EPFL, Switzerland, 2017; and in *Communication of the Laboratory of Hydraulic Constructions* LCH, EPFL, no. 69, Editor Schleiss, A.J. DOI: 10.5075/epfl-thesis-7305.

[22] Pachoud, A.J., Manso, P.A., Schleiss, A.J. 2018. “Advanced design of high strength steel-lined pressure shafts accounting for fatigue crack growth.” In *Proceedings of the ATCOLD Symposium Hydro Engineering*, Vienna, Austria, 2-3 July 2018.

[23] Paris, P., Erdogan, F. 1963. “A critical analysis of crack propagation law.” *ASME Journal of Basic Engineering* 85(4):528-533. DOI: 10.1115/1.3656900.

[24] Pollak-Reibenwein, C., Ralón-Rosales, R., Zsak, P. 2013. “Nant de Drance transition lining and gate housing: A challenge for FEA based stress evaluation.” In *Proceedings of the 3rd International Conference on High Strength Steels for Hydropower Plants*, Graz, Austria, 18-20 September 2013.

[25] Pollak-Reibenwein, C., Akgun, E. 2016. “Fatigue weld assessment in FEA by means of local stresses.” In *Proceedings of the 10th ICOLD European Club Symposium*, Antalya, Turkey, 25-30 October 2016.

[26] Pollak-Reibenwein, C. 2024. “Experimental and computational fatigue strength analysis of typical penstock welds.” In *Proceedings of the 77th IIW Annual Assembly and International Conference on Welding and Joining*, Rhodes, Greece, 7-12 July 2024.

[27] Richter, W., Bacchus, F., Frigerio, A., Giudici, R., Marence, M., Pachoud, A., Pollak-Reibenwein, C. 2025. “EurCOLD bulletins on penstocks, pressure tunnels and shafts: Selected overview.” *Geomechanics and Tunnelling* 18(5):507-516. DOI: 10.1002/geot.70009.

[28] Unterweger, H., Ecker, A., Langwieser, M. 2024. “Trag- und Verformungsverhalten von Verteilrohrleitungen.” *Stahlbau* 93(10):678-693. DOI: 10.1002/stab.202400008.

[29] Unterweger, H., Ecker, A., Langwieser, M. 2025. *Bemessung von Einzelstutzen und Einstiegsöffnungen mit Flanschen und Deckeln im Druckrohrleitungsbau*. Report FFG-Projektnr. F099 911839 und F099 925121 (683 pages).

[30] Zerbst, U., Schödel, M., Webster, S., Ainsworth, R.A. 2007. *Fitness-for-service fracture assessment of structures containing cracks*. London: Elsevier.

Pumped storage power plants in Poland

1. Agata Lethel
2. Kamil Jabłoński
3. Andrzej Sowiński

affiliationsList

1. M.Eng., Energoprojekt-Warszawa SA, al. Niepodległości 58, 02-626 Warszawa, Poland, 0009-0002-6294-4317
2. M.Eng., Energoprojekt-Warszawa SA, al. Niepodległości 58, 02-626 Warszawa, Poland, 0009-0006-5731-8425
3. M.Eng., Energoprojekt-Warszawa SA, al. Niepodległości 58, 02-626 Warszawa, Poland,

keywords

Pumped storage power plants, hydropower, hydroelectric power plants

abstract

Plans to build pumped-storage power plants in Poland date back to the 1930s, but the first one of this type, with a capacity installed power of 167 MW was not commissioned until 1971. Currently, the total installed capacity of Polish pumped-storage power plants, amounts to approximately 1.8 GW. In response to the needs of the power system, as well as new conditions arising from the growing share of renewable energy sources in recent years, the topic of constructing additional pumped-storage power plants in Poland has resurfaced and as the share of renewable energy has risen, creating new operational challenges for the power system, the concept of constructing further pumped storage plants in Poland has been revisited. Four new facilities with a combined planned capacity of around 3.25 GW are currently under consideration. Among them, the most advanced project is the Młoty pumped-storage power plant, with an expected capacity of about 1 GW, which is now undergoing environmental assessment procedures.

The Młoty project stands out not only because construction work had already begun in the past and was later suspended, but also due to its unique concept of creating a lower reservoir by damming a natural river. Such an undertaking would be a rare event in Polish hydrotechnics over the last 40 years, especially in the context of current environmental requirements. The remaining three planned pumped-storage power plants would rely on existing reservoirs. This article provides an overview of both existing and planned pumped-storage power plants in Poland, with particular emphasis on the Młoty project.

Nicolas ULRICH, M Eng., ARTELIA, 4 rue Germaine Veyret-Verner, 38130 Échirolles, France; nicolas.ulrich@arteliagroup.com
Frédéric Andrian., M Eng., ARTELIA, 4 rue Germaine Veyret-Verner, 38130 Échirolles, France; frédéric.andrian@arteliagroup.com
Thierry Vincent, M Eng, ARTELIA, 4 rue Germaine Veyret-Verner, 38130 Échirolles, France; thierry.vincent@arteliagroup.com
Pierre Agresti, M Eng, ARTELIA, 4 rue Germaine Veyret-Verner, 38130 Échirolles, France; pierre.agresti@arteliagroup.com

Checking the vibration risks in civil works structures of PSP powerhouses: leveraging on-site investigations to support numerical analysis

ABSTRACT

In hydropower and pumped-storage HPP powerhouse, the design of the unit shaft line model by the electromechanical (EM) equipment supplier usually relies on a numerical model in which the civil works foundations are represented as spring supports of arbitrary stiffness at different levels. In practice, these stiffness values are rarely verified. This paper presents a graded methodology for assessing vibration risk, from pseudo-static stiffness checks to modal and time-history analyses. As the dynamic modulus of concrete governs the results, a non-destructive geophysical method for measuring it directly on reinforced concrete is introduced and tested on the rehabilitation of a 1,700 MW pumped-storage plant.

KEYWORDS

Hydropower; pumped storage; powerhouse vibration; dynamic stiffness of civil works structure; numerical analysis; in-situ test

INTRODUCTION

Hydropower plants and pumped-storage schemes are increasingly used as flexible assets in modern power systems. Their role is no longer limited to renewable energy production. They are also expected to provide storage, rapid power modulation, frequency control and support to grids with a high share of intermittent renewable generation. This change in operating philosophy has a direct consequence on the civil works supporting turbines, pump-turbines and generators: they are exposed to more frequent transient regimes, more starts and stops, and operation over a wider frequency range than in conventional operation.

In a typical design process, the electro-mechanical equipment supplier generally provides loads, guide drawings and stiffness criteria for the civil works supports. As far as the authors are aware of, the stiffness criteria are rather arbitrary values which were generally assumed or accepted. The stiffness criteria are expressed in the form of support stiffness over a range of frequencies. It is understood that when the criteria are satisfied, both structural integrity of the EM equipment and the absence of deleterious vibrations related to their rotating parts are guaranteed. Most probably, the said criteria were satisfied under the older civil structure design principles, generally involving bulky members with limited openings and built on favorable founding conditions. More and more, due to operational constraints, large openings are created, e.g. around the draft tube for surveillance or storage purposes. Besides, the economical constraints have gradually led to thinner slabs and walls. The resulting structures are more slender and consequently more prone to vibrations.

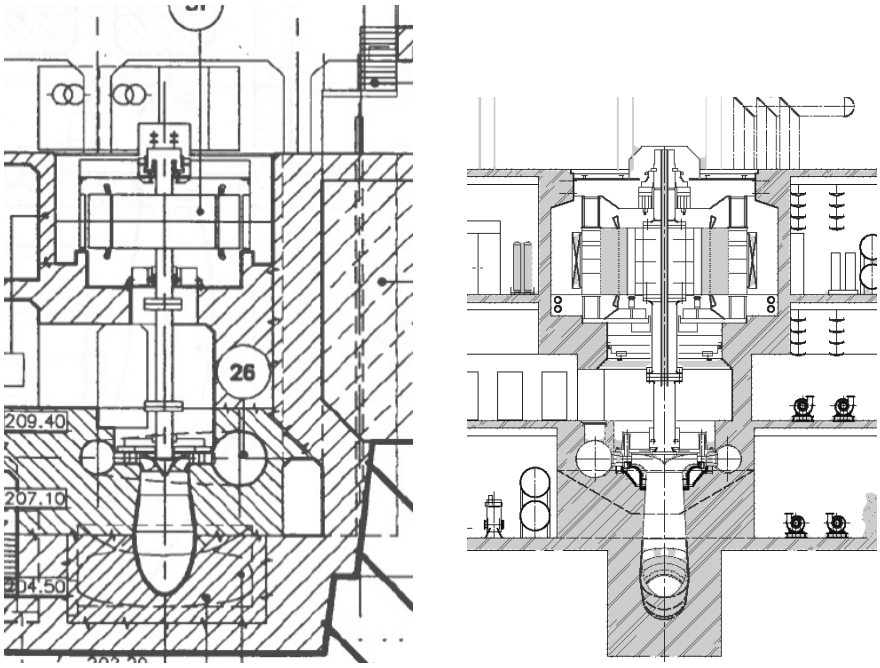


Fig. 1. Illustration of typical design layouts of powerhouse: older design (left), contemporary design (right)

Rys. 1. Ilustracja przedstawiająca typowe układy konstrukcyjne elektrowni: starsza konstrukcja (po lewej), współczesna konstrukcja (po prawej)

These new operating conditions increase the relevance of vibration risk assessment. However, the civil works structure of a powerhouse is rather complex so that it is not straightforward to determine a unique stiffness parameter. In addition, in refurbishment projects, the issue is amplified by uncertainties related to the real stiffness of existing

concrete, contact conditions, historical cracking and load redistribution mechanisms that are rarely known at the beginning of the design stage.

This paper proposes a practical and progressive methodology for vibration risk assessment in hydropower and pumped-storage powerhouses. The approach is intentionally graded: it starts with simple pseudo-static stiffness checks and moves progressively toward modal analysis, and dynamic response analysis. For each type of analysis, the advantages and limitations are discussed and preliminary criteria are proposed.

The approaches used highlight the prevalence of some parameters in the results of the analysis. Consequently, it has been decided to perform in-situ dynamic characterization in order to reduce uncertainties for an ongoing refurbishment project.

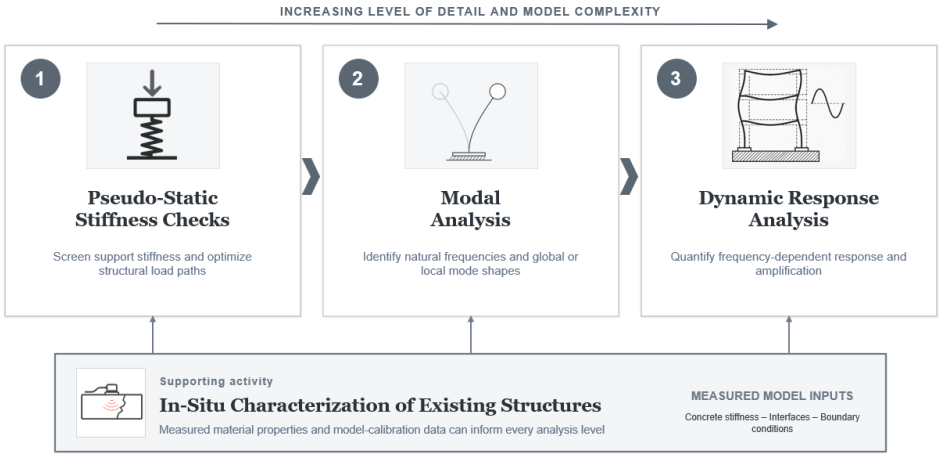


Fig. 2. Flow chart of the proposed methodology

Rys. 2. Schemat blokowy proponowanej metodologii

The proposed methodology is illustrated by means of feedback from several projects: 3 recent PSP schemes ranging from 250 to 350MW, one existing 1700MW PSP scheme and one recent 160MW HPP. All PSP schemes involve reversible Francis units whereas the HPP scheme includes vertical Pelton units.

1 NUMERICAL MODELS

The EM equipment suppliers' numerical models, whether they are simple 1D shaft lines or more elaborate 3D models, usually include only the effect of the civil works structure by means of spring supports at several levels: upper and lower generator, stator and turbine levels (Zou, et al. 2026).

Such models usually assume that the stiffness of civil works structure is a fixed value, even under dynamic conditions. This fixed value is used as criterion to be achieved on the civil works structure's side.

Depending on the supplier, the said required stiffness may actually include some parts of the EM equipment itself, e.g. stiffness of the oil film in the bearing and the brackets, arranged in series with the civil works structure. While the stiffness parameter of oil film is a major uncertainty, the inclusion of brackets in the stiffness criteria from the EM supplier's side poses some challenge in the civil works structure's stiffness evaluation's side. This will be discussed further in the current article.

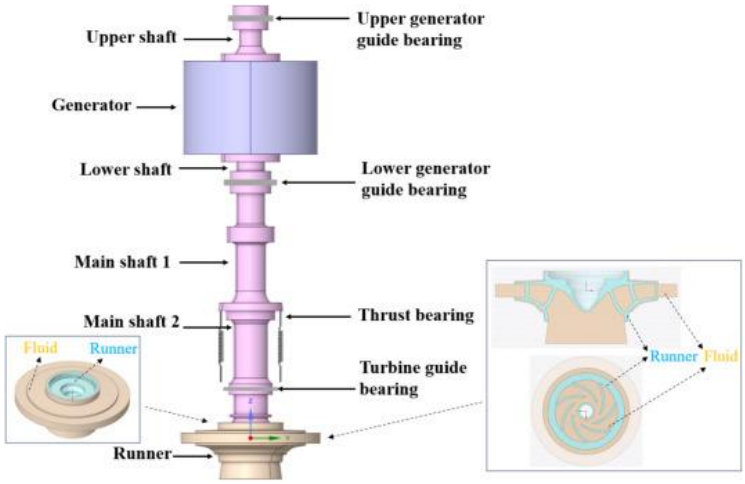


Fig. 3. Typical schematic shaft line model from EM equipment supplier (Zou, et al. 2026)
Rys. 3. Typowy schematyczny model linii wału dostarczony przez dostawcę sprzętu EM (Zou, et al. 2026)

The real behavior of civil structure is quite different: it is a complex network of structural members, some of them being rather bulky, while some being rather slender, supported by a foundation material, most of the time being competent rock for large HPP or PSP scheme. The consequence is that for a static load applied at each support of the EM equipment, the civil structure of the powerhouse will act as a spring. But, for an applied dynamic load, its reaction is not straightforward, being that of a complex network of springs, masses and dashpots. The main purpose of the present paper is to propose an approach for assessing a realistic behavior/reaction of the above complex system. Hence, it has been demonstrated that there may be minimum requirements for the numerical model used to simulate the system so as to reach an acceptable accuracy.

A typical numerical model as suggested in the current methodology includes the overall civil works structure of the powerhouse including the turbine pits, the surrounding members (slabs, beams, columns) extending up to the contact with the foundation or any free surface. Several sensitivity analyses have shown that truncating the model to a certain extent may lead to unrealistic results, depending on the adopted equivalent boundary conditions.

Consequently, if one intends to truncate the model, a demonstration of the relevance of the extent to which it is truncated shall be made. Besides, the same analyses highlighted the need to use 3D elements for modelling the turbine pits due to their bulky nature (Reddy 2007). The authors have chosen to use 3D solid elements for the overall structure as it is believed to be always more accurate than shell or 1D elements for the simulation of bending stiffness. For example, in a 300MW PSP scheme, when mixed shell/solid elements were used, the authors have encountered calculated civil works support stiffness at the generator level 30% lower than the one calculated in a model including only 3D solid elements.

For all case studies analyzed here, the powerhouse structures are constructed above sound rock or in rock cavern. Consequently, for some of them, the effect of the foundation is considered by means of Winkler springs whereas for the others, some extent of the foundation as well is included in the model as a massless linear elastic material. According to the authors, should a powerhouse be founded in less favorable founding conditions, the simulation of the interaction with the foundation should be addressed with greater care (Pecker 2010).

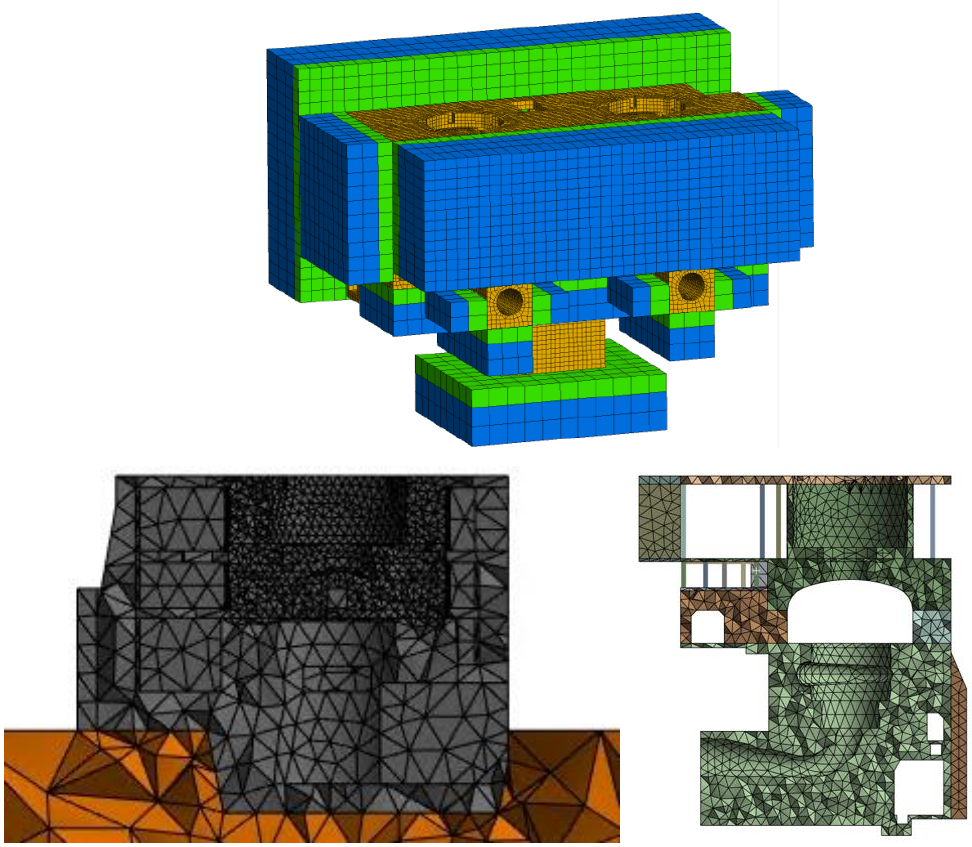


Fig. 4. Examples of numerical models with (top and bottom left) and without the bedrock displayed (bottom right, cross section along the shaft line axis)

Rys. 4. Przykłady modeli numerycznych z uwzględnieniem podłoża skalnego (u góry i u dołu po lewej) oraz bez niego (u dołu po prawej, przekrój wzdłuż osi szybu)

2 CONSTITUTIVE LAWS AND MATERIAL PARAMETERS

Given the assumptions/criteria on civil works structures and the load applied by the EM equipment parts, the displacements are not expected to exceed a few tenths of mm under normal operating conditions. In addition, the frequency of the loadings is relatively high: usually several Hz for large PSP schemes and high head HPP.

Consequently, all the involved materials involved on the civil works support side are assigned dynamic moduli parameters i.e., they are ideally derived from geophysical surveys. This raises questions regarding the cracking state of the concrete for existing facilities and has been handled in several ways as described later in this paper.

The densities of the materials are considered as well except for the foundation bedrock in order to avoid spurious modes due to the artificial reflection of waves due to the boundary conditions. When more advanced soil-structure interaction boundary conditions are adopted, i.e. ones allowing the absorption of outward waves, then the mass of the foundation bedrock needs to be considered as well. For the time history analysis, a damping of 1 to 2% is considered given the low strain expected.

The case studies on which the present paper is based have mostly used linear elastic constitutive laws for the materials and without any interface elements allowing for gap opening or sliding at any specific location the model. For one case, where there was doubt about the good contact between the slabs and the rock face of an underground powerhouse, several sensitivity analyses were carried out by the addition of contact elements allowing opening without tensile strength.

3 PROGRESSIVE METHODOLOGY FOR VIBRATION RISK ASSESSMENT

3.1 Step 1: Pseudo-static support stiffness checks

3.1.1 Description of the approach

The principle of the pseudo-static approach is relatively straightforward. Arbitrary forces are applied to the structure at the EM equipment support locations, and the resulting displacements are used to derive the corresponding stiffness. As the supporting structure is generally not symmetrical, the calculation is repeated in each relevant direction, and the lowest calculated stiffness is retained for comparison with the criteria specified by the equipment supplier. This somewhat covers the rotation of the shaft line imbalance along with

the rotation of the EM equipment: if the level of interest has 6 supports, then 6 calculations are performed, times the directions to be assessed, usually radial, tangential and vertical.

From the authors' experience, the vibration risk can be considered sufficiently low when the minimum calculated stiffness is at least three times greater than the supplier's requirement. Although this factor may appear arbitrary, it can be related to the decrease in reinforced concrete's Young's modulus when cracking and creep is considered (CEN 2004). Besides, based on the authors' feedback, this covers the maximum decrease in stiffness encountered when time-history simulation was also performed with several frequencies being tested (§3.3). As so far, the calculations were only carried out with rather homogeneous sound rock foundation, the value of this arbitrary factor shall be re-considered for more complex configurations. In any case, the pseudo-static analysis is considered to be relevant only at early stage of design.

Despite its conceptual simplicity, this approach requires careful definition of the interface between the equipment manufacturer model and the civil works model. The steel brackets used to support and position the shaft line act as structural stiffeners of the turbine pit. So, the bracket should be included in the civil works finite element model to obtain a realistic representation of the structure stiffness. However, the bracket being designed by the EM equipment supplier, it is commonly already represented explicitly in the supplier's dynamic shaft-line model, together with spring elements representing the civil works supports. Therefore, including the bracket again in the civil works stiffness calculation may result in its stiffness contribution being considered twice.

As an example, Fig. 5 compares the displacements calculated at the upper bracket level under equivalent loading, with and without a simplified explicit modeling of the bracket. Including the bracket reduces the calculated displacement by approximately a factor of two, corresponding to an equivalent increase in support stiffness. Here, as can be noticed, a diffusion of the loads is applied between the mainly loaded support and its two adjacent supports when the bracket is not explicitly modelled in order to attempt to consider its effect. The model, including directly a simplified bracket, considers a unique load as the bracket distributes the load by itself to all the supports. One may notice that in the latter case, the slab in the opposite direction to the load is contributing to the stiffness of the support.

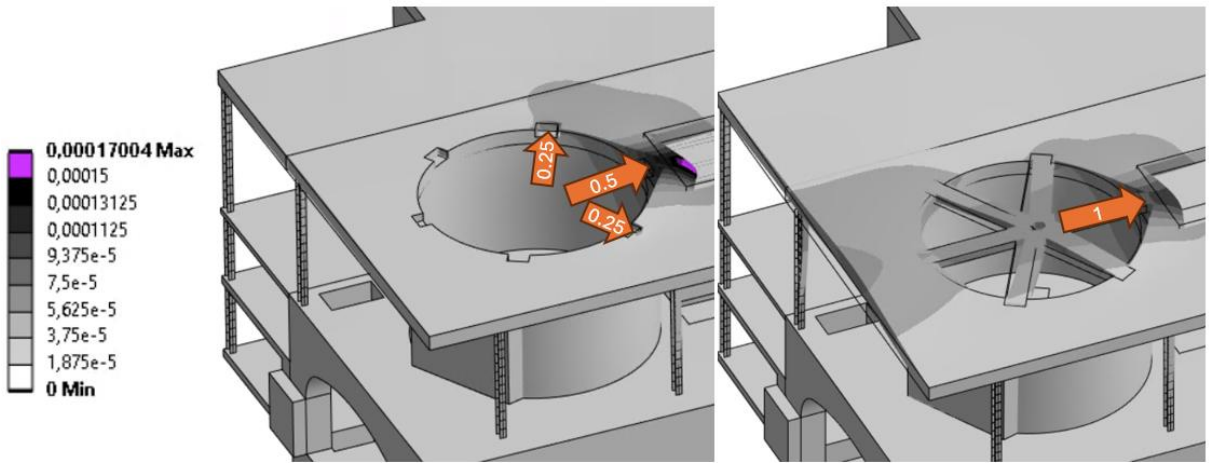


Fig. 5. Example of a stiffness calculation for an upper bracket with (right) and without (left) explicit modeling of the bracket

Rys. 5. Przykład obliczeń sztywności górnego wspornika z uwzględnieniem oraz bez uwzględnienia jawnego modelowania wspornika

The preferred modelling arrangement is for the equipment supplier to exclude the bracket stiffness from the equipment-side support representation and to specify a stiffness criterion for the combined bracket–concrete structure system. Civil works calculation can then explicitly include the bracket when determining the effective support stiffness. This approach provides a more representative assessment of load distribution while maintaining consistency between the EM equipment and civil works models.

If the above preferred modelling arrangement cannot be implemented, the authors recommend the following alternatives:

- Bracket included only in the equipment supplier's model: if the bracket cannot be represented in the civil works model, the applied load should be manually distributed among several concrete support points to approximate the load-distribution effect of the bracket (Fig. 5, left).
- Bracket included in both models: when the bracket is represented in both the equipment and civil works models, the stiffness-assessment load should be applied at a single bracket–concrete interface. The bracket then distributes the load among the remaining concrete supports. (Fig. 5, right).

3.1.2 Limitations

Pseudo-static analysis provides a simple and effective first screening of support stiffness by comparing the force-to-displacement ratio with the equipment supplier's criterion.

However, it does not capture dynamic amplification. A structure satisfying the static criterion may exhibit a lower effective stiffness when an excitation frequency approaches an eigenmode of the structure. Pseudo-static verification should therefore be regarded as the first stage of a risk-based assessment. Further modal or dynamic analyses are required when the stiffness margin is limited.

3.2 Step 2: Modal analysis

3.2.1 Description of the approach

The second step consists in calculating the natural frequencies and mode shapes of the structure and comparing them with the relevant excitation frequencies. Ideally, the model should include the brackets described previously, together with the static masses and rotational inertias of the EM equipment.

For complex powerhouse structures comprising numerous slabs, columns and walls, the number of calculated modes can be very large. More than 1,000 modes can be required to reach a cumulative modal mass participation of 95%. The modes must therefore be screened to retain only those relevant to the vibration assessment. Modal mass provides an objective selection criterion, but in the case of powerhouse vibrations, turbine pits vibration is believed to be more deleterious than simple slab/beam/column vibration. Unfortunately, modal mass analysis does not explicitly separate the parts of the structures which contribute to a given eigenmode. Hence, engineering judgement remains essential to exclude modes that do not significantly affect the turbine pits or equipment supports. Conversely, local modes affecting the turbine pits should not be disregarded solely because their contribution to the total modal mass is low.

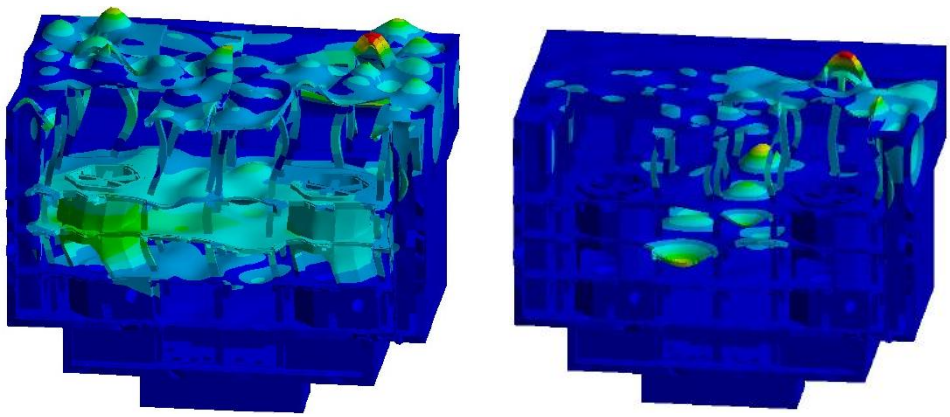


Fig. 6. Eigenmodes of the powerhouse – turbine pits modes (left) – slabs and columns modes (right)

Rys. 6. Tryby własne elektrowni – tryby własne studni turbinowych (po lewej) – tryby własne płyt i słupów (po prawej)

The selected natural frequencies are then compared with the equipment excitation frequencies, which may originate from several hydraulic, mechanical or electromagnetic phenomena. These typically include the rotational frequency and its harmonics, runner blade-passing and rotor–stator interaction frequencies, draft-tube vortex rope frequencies, and electrical frequencies associated with the generator and grid. The frequency ranges covered during start-up, shutdown and runaway should also be considered.

Fig. 7 illustrates a typical interpretation of modal analysis results. The red frequency range extends from start-up to the nominal rotational speed. Within this range, natural modes involving significant deformation of the turbine pits should be avoided. The orange bands represent other excitation frequencies considered less critical, as they generally transmit less energy to the structure. The figure also identifies modes with a modal mass participation greater than 1%, distinguishing turbine-pit modes from modes affecting other parts of the powerhouse.

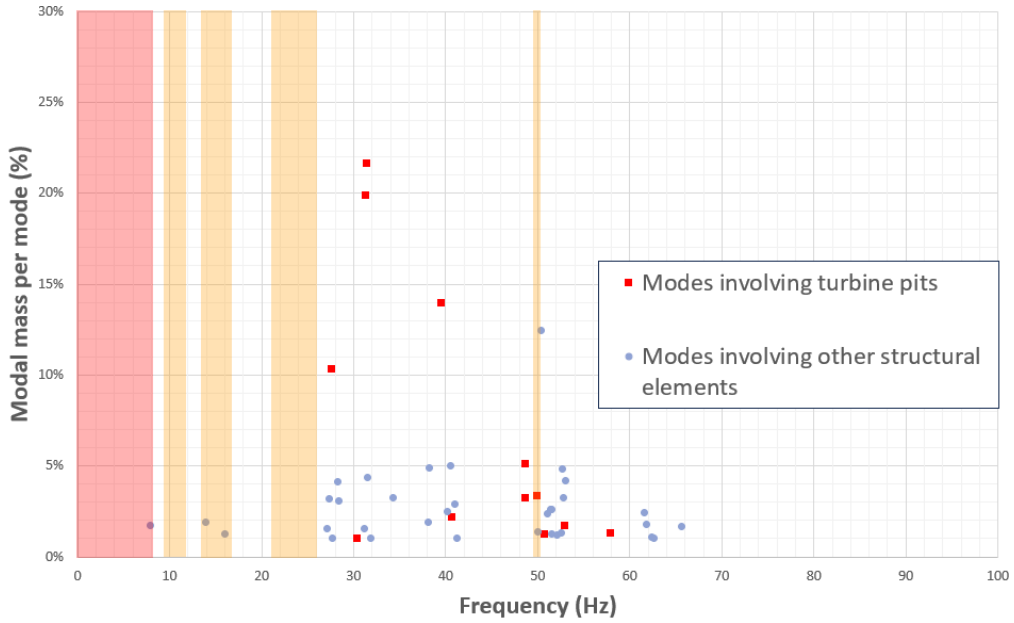


Fig. 7. Example of results interpretation of a modal analysis

Fig. 7. Przykład interpretacji wyników analizy modalnej

3.2.1 Limitations

Contrarily to the case of the pseudo-static and dynamic analyses, a modal analysis does not directly deal with stiffness, which is the main criterion from the EM equipment supplier.

Consequently, the authors, in collaboration with a few EM suppliers have identified the frequencies at which turbine pits natural frequencies may be critical.

All the case studies presented in this paper have exhibited turbine pits natural frequencies out of critical frequencies. This only means that the risk of dynamic resonance is reduced. However, it does not imply that the stiffness criteria are fulfilled.

On the other hand, should one natural frequency involving the turbine pits fall within critical frequency ranges, this does not imply that the stiffness criteria will not be fulfilled. However, most probably the risk of dynamic resonance is required.

Therefore, in the author's opinion, modal analysis is a useful tool to assess the risk of dynamic resonance, but it is not self-sufficient to state whether the system complies with the stiffness criteria or not.

3.3 Step 3: Time-history dynamic analysis

3.3.1 Description of the approach

When the first two steps do not provide sufficient confidence, time-history dynamic analysis can be used. The objective is to compute the actual displacement response of the support points under rotating loads, still of arbitrary intensity. These analyses allow the designer to derive dynamic stiffness as a function of frequency and to identify amplification peaks.

The proposed method consists of applying rotating forces at the support locations, with phase shifts representing equipment motion, while gradually sweeping the excitation frequency across the relevant operating range (Fig. 8). Since frequency varies over time, the resulting displacements and stiffness values can be expressed as functions of frequency.



Fig. 8. Typical time history of loads applied to a 6-support upper bracket – zoom on the 1st second

Rys. 8. Typowy przebieg czasowy obciążeń przyłożonych do górnego wspornika 6-podporowego – powiększenie pierwszej sekundy

The raw result of the analysis is the time history of displacements (Fig. 9). This parameter is still dependent on the applied load. However, one can notice that higher displacements are calculated at frequencies around 45 to 65Hz for the example shown with

fixed load intensity but with increasing frequencies. The dynamic stiffness is consequently expected to reduce at those frequencies.

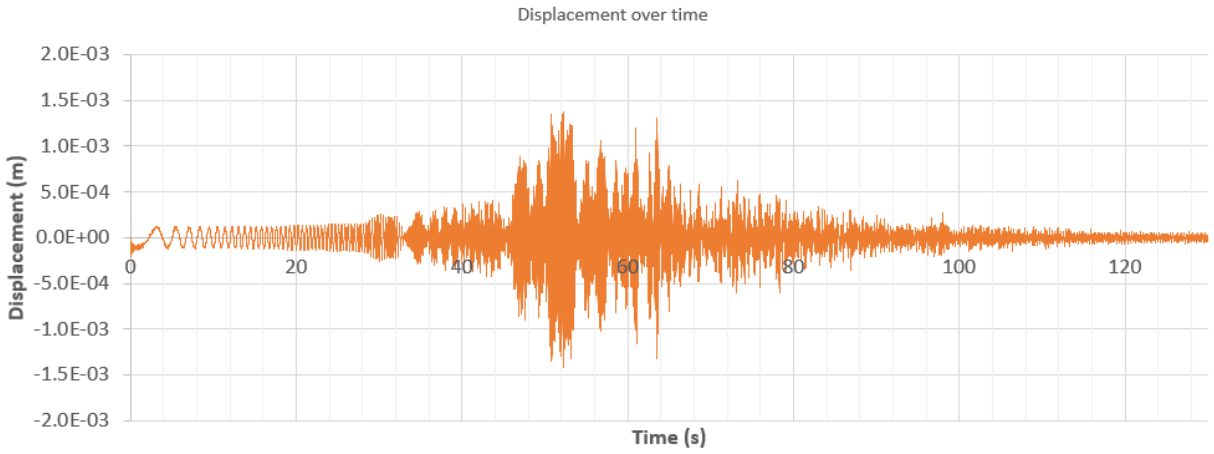


Fig. 9. Example of primary result of the dynamic analysis showing the displacement at a support location over time

Rys. 9. Przykład podstawowego wyniku analizy dynamicznej przedstawiający przemieszczenie w punkcie podparcia w funkcji czasu

Fig. 10 illustrates the frequency-dependent dynamic stiffness calculated at an equipment support with a zoom on the first 20 Hz. In this example, the stiffness at 12.5 Hz is approximately one-third of the pseudo-static value, indicating some dynamic amplification near this frequency. However, within the operating frequency range associated with the equipment supplier's criterion, the calculated stiffness remains sufficient.

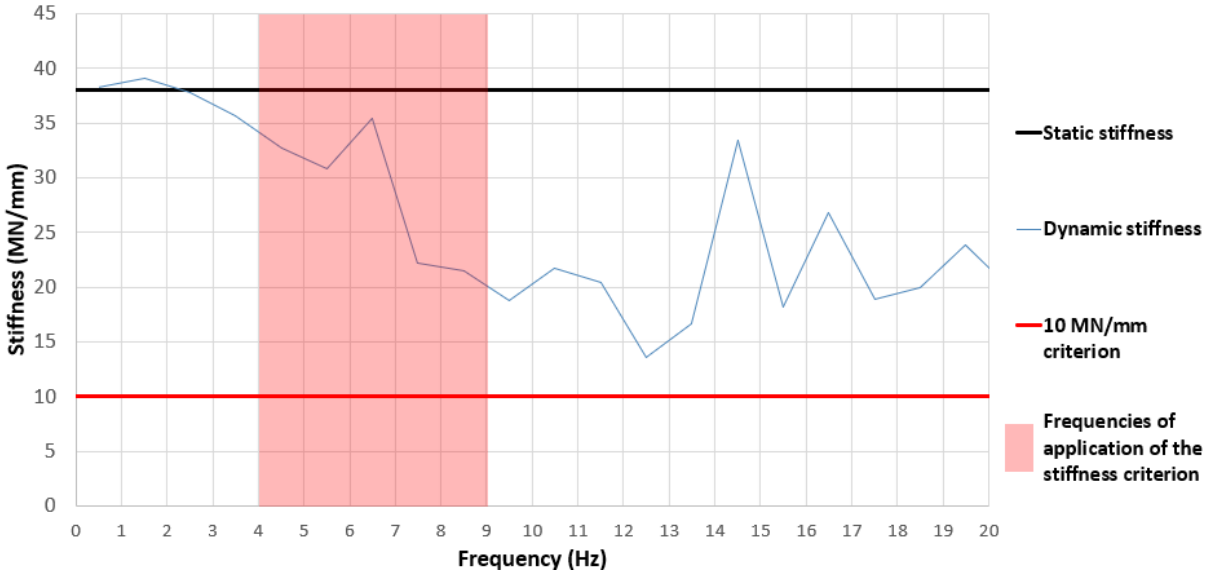


Fig. 10. Dynamic stiffness calculated at an equipment support

Rys. 10. Sztywność dynamiczna obliczona w punkcie podparcia urządzenia

3.3.1 Discussions

According to the authors, this approach is the most comprehensive among the three presented in this paper as it is the only one which deals explicitly with both stiffness and frequencies.

The results have shown some consistency with the simpler approaches for the cases studies addressed in this paper: up to the nominal frequency, the calculated civil works support stiffness yields the values assessed with the pseudo-static approach as long as the modal analysis has not highlighted any turbine pit-related eigenmode. Besides, the drop in stiffness is highlighted where the modal analysis has already identified some turbine pit-related eigenmodes. For all the case studies, the decrease in stiffness around those frequencies has never exceeded a factor equating 3, which is also the one used as a preliminary criterion for the pseudo-static analysis.

Still this approach also has some limitations as some excitation frequencies are not directly related to shaft rotation or rotor imbalance: the speed of a shaft line is not supposed to exceed the runaway speed although the proposed approach covers up to 120 Hz. The purpose is rather to capture some insight into the dynamic response of the civil works structure.

Besides, there may be some inaccuracy related to the loading histories: the applied duration may be not long enough to highlight clear decrease in stiffness. In addition, the effect of asynchronous rotation of all the shaft lines may also need to be investigated.

3.4 Supporting activity: in situ characterization for existing structures

In refurbishment projects, the uncertainty on material properties can become the governing issue. The dynamic modulus of existing concrete is often estimated from the static modulus using empirical factors. This assumption may be acceptable in preliminary design, but it may be difficult to justify for concrete that has been subjected to decades of operation, cyclic loading, cracking, repairs or ageing processes.

In situ non-destructive investigations can reduce this uncertainty. Geophysical methods, vibration measurements or other dynamic testing techniques may be used to characterize the actual dynamic properties of the powerhouse structure. These measured properties can then be introduced into numerical models and used to refine sensitivity analyses.

In the case of a refurbishment project, a preliminary test campaign was carried out to assess whether acoustic measurements could be used to characterize the dynamic properties of existing reinforced concrete directly within an operating hydropower powerhouse. The

method is based on measuring the travel time of an acoustic pulse between an emitting transducer and a receiving transducer. During the test campaign, 54 kHz transducers connected to a Pundit PL 200 acquisition unit were used, and the first arrival of the compression wave was identified from the recorded signal.

Three measurement configurations were investigated: direct, semi-direct and indirect transmission. They differ mainly in the relative positions of the emitter and receiver and, consequently, in the wave path through the concrete. Direct transmission provides the most clearly defined path, and consequently a more reliable measure, whereas semi-direct and indirect measurements are easier to implement, at the cost of a slightly more difficult interpretation.

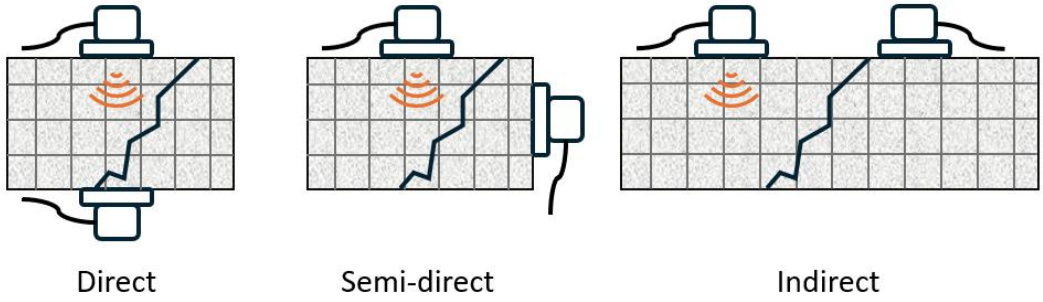


Fig. 11. Measurement configuration

Rys. 11. Konfiguracja pomiarowa

For this preliminary interpretation, the measured velocity was taken as the P-wave velocity, and the dynamic Young's modulus was calculated using constant values for density and Poisson's ratio. Regardless of the measurement configuration, the estimated dynamic modulus ranged from approximately 22 to 35 GPa across the investigated areas. These values appear reasonable for concrete that is about 50 years old and remains in relatively good apparent condition. Based on the available design data, the original intact concrete was expected to have a static elastic modulus of approximately 30 GPa.

Additional observations from the test campaign support the practical feasibility of the method. The first P-wave arrival remained clearly identifiable while a nearby unit was operating, indicating that low-frequency operational noise did not prevent signal picking. Clear acoustic signals were also obtained throughout the investigated reinforced concrete areas, including potentially heterogeneous or locally cracked zones. No significant increase in P-wave velocity attributable to the rebars was observed. Local cracking may, however, have

increased the wave travel time and contributed to the lower dynamic moduli estimated in some areas, consistently with a possible local reduction in concrete stiffness.

Overall, the test phase supports the feasibility of using acoustic measurements as a practical input for the dynamic assessment of existing powerhouse structures. Direct transmission should remain the reference configuration whenever access conditions permit.

Further measurement campaigns are planned to expand the dataset and improve the reliability of the results. Ideally, these investigations should be complemented by concrete sampling and laboratory testing to calibrate the in-situ acoustic measurements and validate the estimated dynamic moduli.

A further source of uncertainty may concern the quality of the contact between the concrete structure and the rock along the cavern sidewalls. Concrete shrinkage may lead to partial opening of this interface, thereby reducing the overall structural stiffness and increasing the risk of harmful powerhouse vibrations. A sensitivity analysis carried out using the pseudo-static method showed that the stiffness could decrease by a factor of 2 to 3 depending on the assumptions regarding contact between the concrete and the rock (bonded – compression only – no contact). This issue was considered for 300MW underground powerhouse, where a contact grouting system was initially envisaged. However, the first investigation cores indicated that the natural convergence of the cavern had compensated for the initial concrete shrinkage and maintained contact between the concrete and the surrounding rock. Consequently, the rather complex construction provisions initially planned was abandoned.

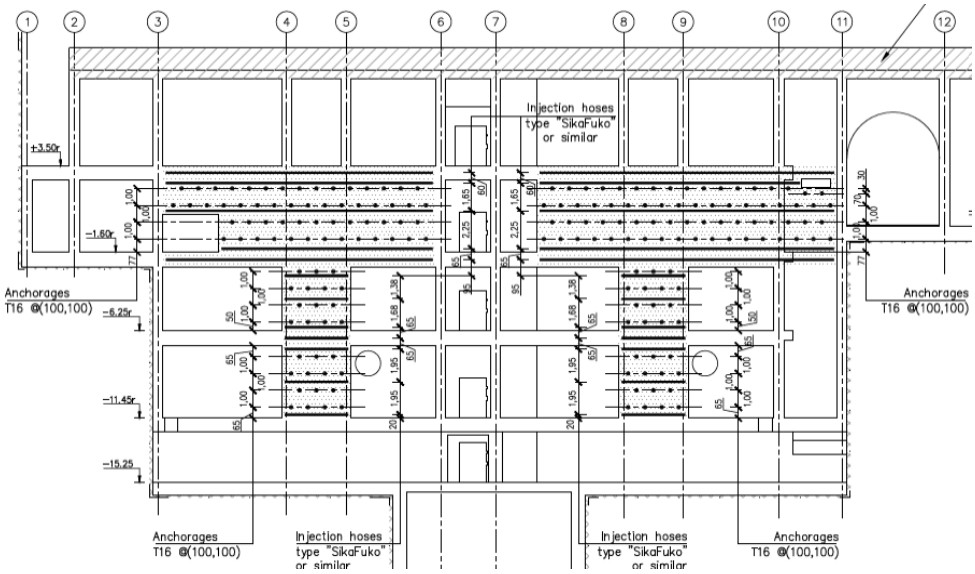


Fig. 12. Concrete-rock grouting and anchoring system originally planned for a 300MW PSP

Rys. 12. System iniekcji betonu i skały pierwotnie zaplanowany

4 CONCLUSIONS AND DISCUSSIONS

In the context of more stringent operation constraints and increased need in saving material quantities compared to the design of powerhouses and EM units a few decades ago, the arbitrary criteria adopted on the EM equipment supplier's side related to the stiffness support of the shaft line may have become less representative of the civil works structure's layout nowadays. This has made the checking of the actual stiffness on civil works support's side necessary.

As far as the authors are aware of, there is still not any standardized method for that purpose. Consequently, this paper proposes a graded approach for assessing the stiffness of civil works support of the powerhouse of large PSP scheme and high head HPP based on 5 case studies for which ARTELIA has been involved as designer. The applied gradation aims at speeding up the design stage and avoids carrying out sensitivity analysis based on the time-consuming approaches. In all the 5 case studies, checking the stiffness in the initial layout of the civil works structure has resulted in the need for increased thickness of the structural members, the need to change some materials toward stiffer ones (2^{nd} stage concrete at the bracket ends) or even the need to secure the contact between the powerhouse slabs with the rock face of the underground cavern. For some of them, the EM equipment supplier has agreed to a lower stiffness assumption after several unsuccessful attempts to achieve the initially prescribed values. Most of the design adjustment stages have been supported by the pseudo-static and modal analysis while the final verification stage has been the purpose of a more detailed time-history analysis as described in this paper. To date all the 5 case studies are under operation without any deleterious vibrations being reported.

The authors are aware of the economical consequences of the abovementioned design changes, but there are still several uncertainties related to the assessment of the behavior of the system which have led to the selection of rather conservative assumptions in the evaluation of the civil works structure dynamic stiffness. The concrete stiffness parameters, the effectiveness of the contact between the slabs and the rock face for underground powerhouses are among the main uncertainties on the civil works structure side. The paper proposes additional investigations, whether destructive or not, in order to reduce those uncertainties.

On the EM equipment's side, the main uncertainty is borne by the oil film at the bearings. On top of that, the authors have encountered some cases where the contribution of the oil film was considered by the EM supplier to be part of the shaft line support's stiffness i.e., to be assessed by the designer of the civil works structure.

The works carried out in this paper also highlight the need to address carefully the interaction between EM equipment and civil works structure. Here, the focus made on the brackets shows that neglecting its effect may significantly affect in an overconservative way the stiffness of the civil works structure stiffness. As in some cases, the brackets are already considered in the EM equipment supplier's model, its additional consideration in the civil works structure model needs to be addressed with care. Behind this specific case lies the necessity to define the appropriate boundaries between the EM equipment supplier and the civil works structure models. According to the authors, in order to refine and increase confidence in the use of the approach suggested in the current paper, a unique and comprehensive model i.e., including both EM equipment and civil works structures, would be much helpful. Such model could benefit from time histories of displacements measured from the real structure which will allow the model to be calibrated and to reflect the actual dynamic behavior. Having at hand that calibrated comprehensive model, then it is possible to come back to the simpler models and identify the governing parameters which need to be better evaluated in order to keep an acceptable accuracy.

5 REFERENCES

CEN. 2004. *EN 1992 - Eurocode 2: Design of concrete structures.* Brussels.

Pecker, A. 2010. "Soil Behavior: Dynamic Soil-Structure Interactions." *Dynamic Behavior of Concrete and Seismic Engineering.*

Reddy, J.N. 2007. "Theory and Analysis of Elastic Plates and Shells, second edition." *CRC Press (Taylor & Francis).*

Zou, Jiamin, Alexandre Presas, Yuejiang Han, David Valentín, Mònica Egusquiza, and Eduard Egusquiza. 2026. "Investigation of the added mass effect and bearing stiffness on the rotordynamics of pump-turbine shaft systems." *Journal of Energy Storage.*

Alireza Farhadi, PhD[1]*, Hans-Martin Leitner, PhD[2]

[1] Hydraulics Lead, Baucon International ZT GmbH, Austria. ORCID: 0000-0001-7311-0567.
[2] CEO, Baucon International ZT GmbH, Austria.

*Corresponding Author: alireza.farhadi@baucon.at.

Numerical Optimization of an Integrated Fish Passage System in a High-Capacity Run-of-River Hydropower Plant

Numeryczna optymalizacja zintegrowanego systemu przepławki dla ryb w przepływowej elektrowni wodnej dużej mocy

ABSTRACT

This study presents a 3D CFD optimization of an integrated upstream and downstream fish passage system in a high-capacity run-of-river hydropower plant. FLOW-3D® Hydro simulations were performed for multiple discharge–head scenarios using the RNG k-ε turbulence model. Initial optimization satisfied ecological criteria, including attraction flows and fish passage velocities, but exceeded allowable head-loss limits. Subsequent geometric modifications reduced hydraulic losses while preserving ecological performance. The final design met both environmental and energy production requirements.

Key words: Fish Migration, Hydropower, CFD, Head Loss, Environmental Flow

INTRODUCTION

Large run-of-river hydropower developments increasingly require the integration of effective fish migration facilities to preserve ecological connectivity while maintaining high levels of hydraulic and energy performance. The design of such systems presents a multidisciplinary engineering challenge, as ecological requirements for fish passage must be satisfied without compromising the operational efficiency of the hydropower scheme.

The considered project is a high-capacity run-of-river hydropower development (~1400 MW) equipped with multiple generating units and dedicated auxiliary units supplying flow to an integrated fish migration system. The fish passage facilities are intended to provide both

upstream and downstream migration routes for fish across a wide range of life stages and body sizes, while ensuring safe passage of drifting eggs and larvae during high-flow periods.

The fish migration concept comprises an upstream passage system consisting of an integrated passage within the hydraulic structure and a supplementary bypass channel, together with a downstream passage system embedded within the dam structure. The hydraulic performance of these facilities is governed by attraction flow requirements and by operational criteria established to ensure effective fish guidance and passage.

The design is subject to ecological performance requirements derived from regional fish passage guidelines (MRC, 2020), including minimum attraction flow allocations, limits on flow velocity within migration corridors (maximum 0.5 m/s), minimum flow depths (i.e. 3 m), and the establishment of clear hydraulic pathways guiding fish from attraction zones to passage entrances. In parallel, the hydraulic system must satisfy engineering requirements related to energy dissipation, cavitation-free operation, erosion prevention, ventilation, and overall hydraulic stability.

A particular challenge arises from the dependence of the upstream fish migration system on auxiliary generating units operating under a gross head range of approximately 22-34 m. Flow supplied by these units is conveyed through an extensive network of galleries, chambers, and hydraulic transitions before reaching the fish collection facilities. While these conveyance systems are necessary to generate adequate attraction flows, they also introduce hydraulic losses that directly affect the available operating head of the auxiliary units (see Fig. 1).

In addition to ecological requirements, the project is constrained by contractual power production obligations. The head losses occurring throughout the fish migration waterway must therefore remain within allowable limits to ensure compliance with the Energy Target Value (ETV) assumed during the detailed design phase and incorporated into the power purchase agreement. Consequently, the design problem requires simultaneous optimisation of ecological performance and hydraulic efficiency.

To address this challenge, a comprehensive three-dimensional Computational Fluid Dynamics (CFD) investigation was undertaken. The numerical model was used to evaluate flow behaviour under representative operating conditions, quantify hydraulic losses throughout the system, assess compliance with fish passage criteria, and support iterative geometric optimisation. The objective was to develop a configuration capable of satisfying both fish migration requirements and energy production constraints within a single integrated design.

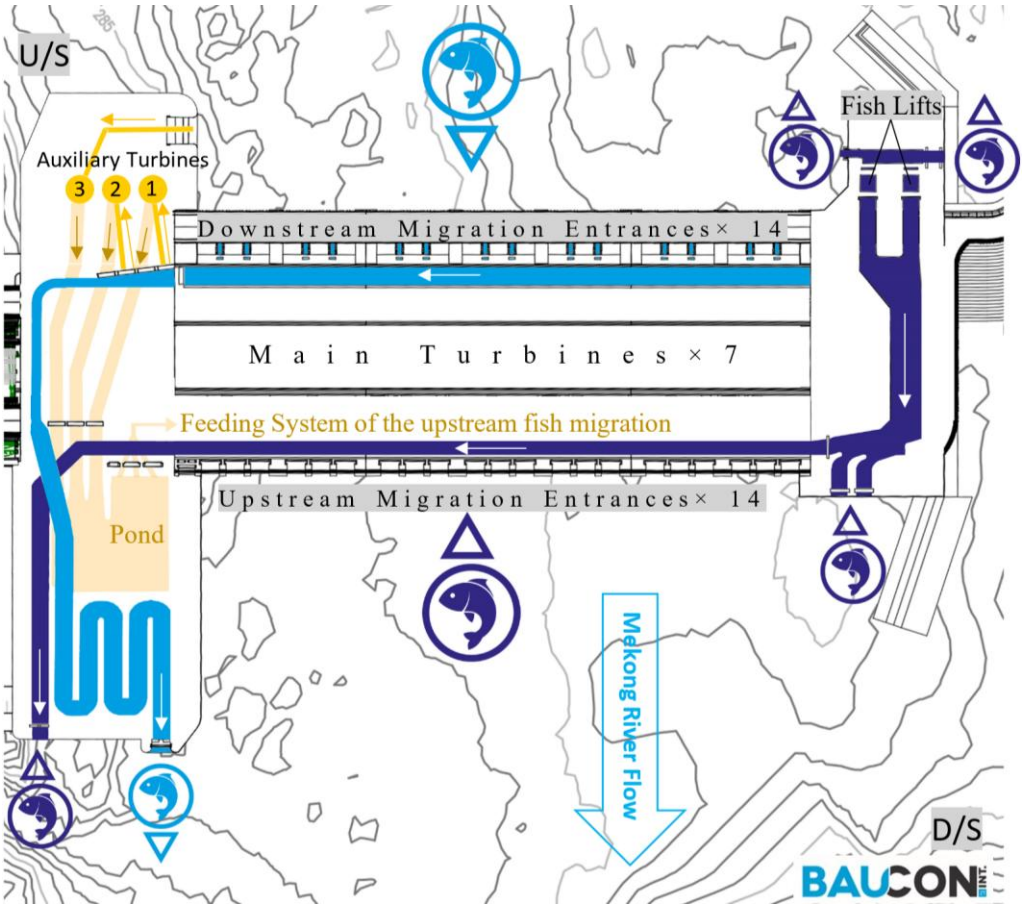


Fig. 1: Overview of the integrated fish migration (FM) system. Fish migration's upstream passage shown in dark blue, downstream passage in cyan blue (Author).

NUMERICAL APPROACH AND METHODOLOGY

CFD-Tool and Model Strategy

A three-dimensional CFD model was developed to determine hydraulic performance and required discharges for the integrated fish migration system. Simulations were carried out using FLOW-3D® Hydro (Flow Science, 2021), enabling full representation of complex free-surface flow conditions across interconnected hydraulic structures.

The computational domain was divided into upstream and downstream fish migration systems. To ensure computational efficiency while maintaining numerical accuracy, each system was further subdivided into smaller subdomains. In total, nine discharge–head operating points were evaluated to represent the full operational envelope of the facility, covering low-flow, partial operation, and high-flow conditions.

The model was used to quantify flow distribution, velocity fields, and head losses (Meusburger, 2002), with particular focus on attraction flow performance through auxiliary unit operation. The possible attraction flow range considered in the preliminary design extends from

approximately 70 to 210 m³/s, depending on operational configuration of the auxiliary units and hydraulic head conditions The attraction flow must be sufficient to satisfy ecological performance criteria; however, the discharge diverted to fish passage facilities represents water that is unavailable for power production. The CFD analyses therefore supported the development of a hydraulic configuration that achieves the required attraction flow performance while maximising the volume of water available for energy generation.

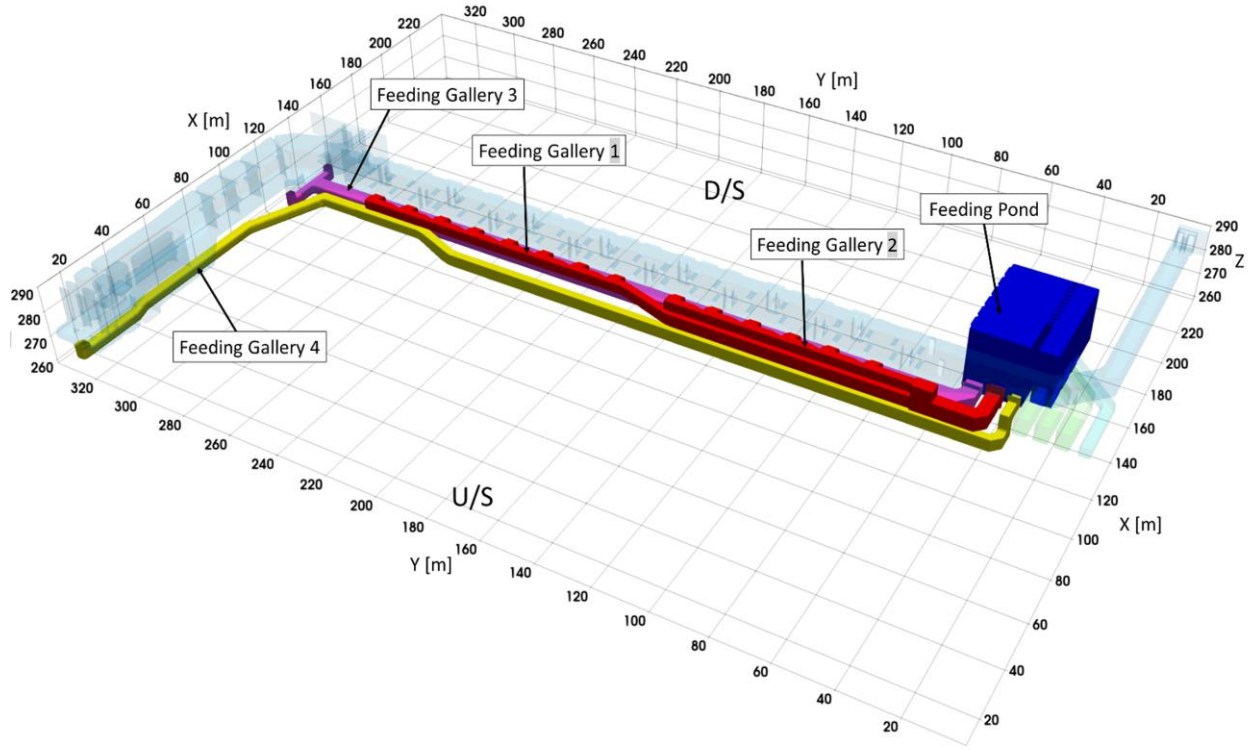


Fig. 2: Isometric view of the feeding galleries in the upstream FM system (Author).

Spatial Discretization and Turbulence Modelling

All simulations were performed using a structured multi-block mesh approach. Grid independence was assessed separately for each hydraulic subsystem.

For the upstream fish migration system, two mesh resolutions were tested: a coarse grid consisting of 10.48 million cells and a refined grid consisting of 45.19 million cells. Comparison of key hydraulic parameters (water levels, discharge distribution, and flow patterns) showed negligible differences, with deviations below 0.01 m for water levels and below 0.01 m³/s for discharge. Consequently, the coarse grid was adopted for the full parametric study, while local mesh refinement (0.75 m to 0.25 m) was applied in regions of strong velocity gradients and geometric complexity.

For a partial model of the auxiliary unit No. 3 waterway, a coarse grid of 4.79 million cells and a refined grid of 6.90 million cells were evaluated. Given the limited sensitivity to mesh refinement and the manageable computational cost, the refined grid was retained for final simulations, with element sizes ranging from 0.25 m to 0.125 m.

For the downstream fish migration system, grid independence was similarly confirmed using meshes of 8.39 million and 44.09 million cells. As in the upstream system, differences in hydraulic results were negligible, confirming mesh adequacy. Local refinement was applied in zones of hydraulic transition and near attraction structures.

All simulations employed the RNG k–ε turbulence model, which provides a robust representation of turbulent shear layers and recirculation zones typical of fish passage hydraulics.

Boundary Conditions and Hydraulic Representation

Boundary conditions were defined to replicate realistic hydraulic operating scenarios of the integrated system.

For the upstream fish migration system, the computational domain includes the feeding reservoir, distribution galleries, collecting chambers, fish lock structures, and downstream tailwater section. A constant inflow discharge was imposed at the upstream boundary, while the downstream boundary was defined by a fixed tailwater level derived from the system rating curve, incorporating contributions from main turbines, spillway discharge, and fish migration flows (see Fig. 2).

For the downstream fish passage system, the model includes the upstream reservoir approach zone, entrance structures, collecting gallery, small unit intakes, downstream chute, and tailwater region. The hydraulic boundary conditions were varied according to the operational matrix defined in Tab. 1, covering a range of unit configurations and environmental flow conditions.

Tab. 1 Simulation matrix for downstream fish migration system (Author).

Case	ETV						FM		
	Max. all units	2 units	1 unit (3)	1 unit (2 or 1)	min. 2 units	min. case	low	Extreme	Mean Annual
Inflow rate [m³/s]	194	140	70	70	79	35	80	188	180
Tailwater [m asl]	283.50	280.50	277.50	277.50	275.80	279.14	276.80	286.00	288.40

The modelling framework includes a detailed representation of surface roughness to capture energy losses across different hydraulic materials. Concrete surfaces were assigned a roughness height of 1.0 mm, sediment-covered or substrate-lined areas were assigned 20.0 mm, and steel-lined penstocks of the small unit intakes were assigned 0.03 mm. This differentiation ensures physically consistent estimation of frictional losses throughout the system.

Numerical Convergence and Solution Strategy

All simulations were conducted under steady-state conditions. Numerical convergence was assumed when inlet and outlet discharges were balanced and stabilized, and when no further significant variations were observed in water levels and velocity fields within the main hydraulic zones of interest.

The solution approach relied on the Volume of Fluid (VOF) method to capture the free-surface behaviour throughout the complex hydraulic system. This formulation enabled accurate representation of multiphase flow conditions in open-channel and pressurised transition zones.

No physical model or field data validation was available for this specific study. The numerical results therefore represent a design-stage predictive analysis used for comparative evaluation of design alternatives and hydraulic optimisation rather than calibrated prototype reproduction.

Hydraulic performance indicators, including discharge distribution, velocity fields, and head losses, were evaluated at both global system level and within individual subsystems of the fish migration network. System-level head loss was used as the primary constraint for compliance with energy production requirements, while local hydraulic behaviour was assessed to ensure ecological performance of fish passage routes.

RESULTS

First stage of optimisation (fish migration)

The initial optimisation phase focused on achieving compliance with ecological fish passage requirements defined by regional guidelines. These requirements establish the operational boundary conditions for the system, including a minimum utilisation of available flow corresponding to low-flow and flood conditions, as well as constraints on hydraulic velocities to ensure safe fish movement.

Within the fish migration system, flow velocities must remain below 0.5 m/s in main channels, while locally higher velocities up to 1.4 m/s are permitted over short distances (<0.20 m) in controlled acceleration zones. These limits, together with minimum flow depth and

continuous flow requirements under low tailwater conditions, define the hydraulic envelope for effective fish guidance and passage.

CFD-based simulations were used to adjust the hydraulic layout to satisfy these ecological criteria. The resulting configuration achieved acceptable velocity distributions and ensured that continuous attraction flow pathways were established throughout the system.

However, although ecological performance criteria were met, the resulting hydraulic configuration led to excessive head losses within the waterway. When evaluated against the Energy Target Value (ETV), which defines the allowable range of contracted hydraulic performance for the auxiliary units, the system did not satisfy the required energy production constraints.

Fig. 3 illustrates the distribution of hydraulic head losses obtained from the first-stage optimisation. The results clearly indicate that, while the system is hydraulically functional from an ecological perspective, the cumulative energy dissipation along the flow path exceeds the allowable limits for operational compliance.

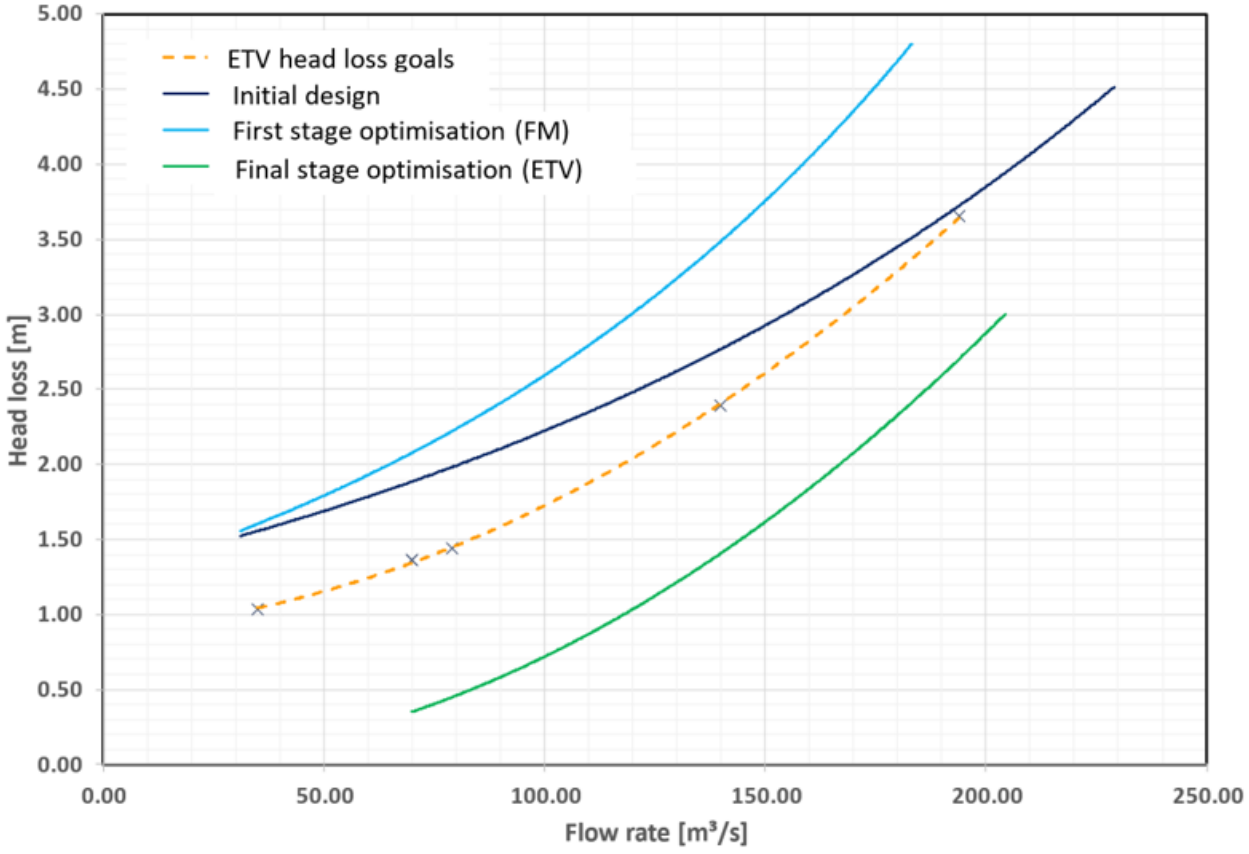


Fig. 3. Head losses calculated from numerical simulations during the initial stage of optimization (Author).

Final stage of optimisation (ETV)

Following the identification of excessive head losses in the initial design, a second optimisation phase was conducted with the objective of restoring compliance with the Energy Target Value (ETV) while maintaining the previously achieved ecological performance.

CFD results were systematically analysed to identify zones of concentrated energy dissipation, flow separation, and local hydraulic inefficiencies. Based on this analysis, targeted geometric modifications were implemented across the system. These included enlargement of hydraulic conduits, smoothing of abrupt transitions, and refinement of flow control and screening elements in order to reduce local resistance and improve overall hydraulic continuity.

An example of these improvements is shown in Fig. 4 for the feeding galleries of the upstream fish migration system, where modifications resulted in a measurable reduction in hydraulic losses and improved flow distribution towards the attraction zones. Equivalent optimisation measures were applied throughout the remaining components of the system.

The final configuration achieved a significant reduction in total head losses, bringing the system into compliance with the ETV constraints while preserving the hydraulic conditions required for fish migration. The results confirm that iterative CFD-based redesign is an effective approach for reconciling ecological performance requirements with strict energy production constraints in complex hydropower waterway systems.

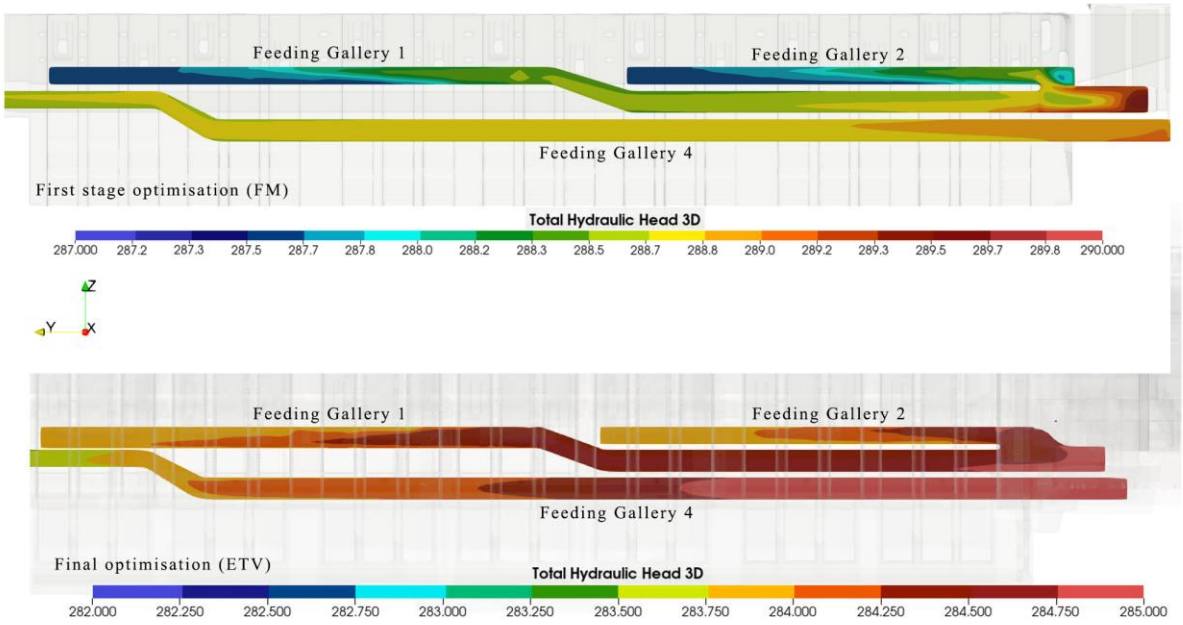


Fig. 4. Comparison of hydraulic head in the feeding galleries of the upstream fish migration system between the first stage optimization (FM) and the final optimization (ETV). The colour scale varies in both cases to improve visibility and clarity.

SUMMARY AND CONCLUSION

This study presented a CFD-based numerical investigation of an integrated fish migration system within a large run-of-river hydropower scheme, focusing on the interaction between ecological performance requirements and hydraulic constraints associated with energy production.

The results demonstrate that it is possible to achieve compliant fish passage conditions in terms of velocity distribution, attraction flow provision, and hydraulic connectivity through targeted hydraulic design. However, the initial design phase revealed that fulfilling ecological requirements alone leads to excessive hydraulic head losses, which are incompatible with operational energy performance constraints defined by the Energy Target Value (ETV).

A subsequent optimisation phase, based on detailed analysis of CFD results, enabled the identification and mitigation of critical hydraulic inefficiencies. Localised geometric refinements, including improved conduit transitions and reduced flow separation zones, resulted in a significant reduction of system head losses while maintaining the hydraulic conditions required for effective fish migration.

The study highlights the importance of coupled ecological–hydraulic optimisation in modern hydropower design. It further demonstrates that three-dimensional CFD modelling is a powerful tool for evaluating complex flow behaviour and guiding iterative design improvements in integrated waterway systems.

The proposed methodology provides a transferable framework for reconciling environmental requirements with strict energy production constraints in large-scale hydropower developments, particularly where fish migration facilities are embedded within primary hydraulic structures.

REFERENCES

- [1] Flow Science, Inc. 2021. *FLOW-3D® Version 2021R1 User's Manual.* Santa Fe, NM: Flow Science, Inc.

- [2] Mekong River Commission (MRC). 2020. *Technical Review Report on the Prior Consultation for the Proposed Luang Prabang Hydropower Project under the Procedures for Notification, Prior Consultation and Agreement.* Vientiane: Mekong River Commission Secretariat.

- [3] Meusburger, H. 2002. *Energieverluste an Einlaufrechen von Flusskraftwerken.* Doctoral dissertation, ETH Zurich.

SESSION C (part I). Dam Engineering and Construction		
1	Rico Senti	Alkali–silica reaction (ASR) in Dams – Mitigation of concrete swelling by cooling
2	Miroslav Spano	Challenges in conceptual design of the Skalička dam
3	Thomas Konow	Pore Pressure under Concrete and Buttress dams Methods for Rock Mechanics mapping and Discussion of design assumptions
4	Jonathon Reid Hristo Stanchev Ben Jones	Resilience by Design: Access and Maintenance at Havant Thicket Reservoir

Rico Senti, Axpo Power AG, Parkstrasse 23, 5400 Baden, Switzerland,
rico.senti@axpo.com

Bastian Otto, Axpo Power AG, Parkstrasse 23, 5400 Baden, Switzerland,
bastian.otto@axpo.com

Alkali-silica reaction (ASR) in dams – Mitigation of concrete swelling by cooling

Abstract

This paper examines the temporal evolution of the alkali-silica reaction (ASR) in two concrete dams in Switzerland operated by Axpo Power AG. Intensive instrumentation led to new insights into the complex ASR process, which is strongly influenced by temperature. The findings from the long-term strain measurement campaigns in the Runcahez and Roggiasca dams revealed the existence of a unique, dam-specific ASR swelling curve that follows an Arrhenius law and does not change with time. The kinetics of ASR can be represented by an exponential function of the concrete temperature, with the curve shape governed by the petrography and grading of the aggregates as well as the cement type and content. The predominant factor influencing the ASR swelling is the concrete temperature in summer (hot period). In the cold period of the year, measurements show no increase of swelling when the concrete temperature falls below 3 °C. Therefore, it is obvious that active cooling of dam concrete must have a beneficial effect by significantly slowing down the ASR process. In the present paper, the effectiveness of active cooling of the Roggiasca dam for the mitigation of concrete swelling is demonstrated and verified.

Keywords: Dam aging, Alkali-silica reaction (ASR), Concrete cooling, Mitigation of swelling

1 Introduction

It is well known that concrete dams can suffer from alkali-silica reaction (ASR). In Switzerland, a survey presented in [1] showed that 40% of concrete dams are affected by ASR. In most cases, it is reported that, after a period of ASR initiation, the dam becomes permanently deformed in both the vertical and horizontal directions. This is attributed to the swelling of concrete due to ASR, which is a slow chemical process, especially in the colder climate of the Swiss Alps. Such deformations have also been observed in two dams operated by Axpo Power in the central Alps: the slender 68 m high Roggiasca arch dam situated at an elevation of 955 m asl and the Runcahez gravity dam with a height of 30 m located at an elevation of 1280 m asl (see **Fig. 1**). Both the dams were commissioned in the mid-1960s.

In the publications [2], [3] and [4], it was shown that the distributions of ASR-induced strains and strain rates in a concrete dam are mainly governed by the concrete temperature in summer. It should be noted here that each of the two dams discussed in this paper was built using a single concrete mix (i.e. without any variation of cement content, aggregate type and aggregate grade in the whole dam) and the normal operating loads produce only small to moderate stresses. The

analysis of the measurement data of the swelling history collected over the last 10 years from intensive in-situ instrumentation revealed the existence of a unique characteristic ASR swelling curve for each dam.

Since the concrete temperature in summer was identified as the main driving force behind the ASR reaction, Axpo Power started to investigate if concrete cooling could slow down the ASR swelling. This paper presents the results of this investigation and discusses the influence of temperature on the ASR swelling rates as well as the extent of mitigation that can be achieved by cooling. The validation of all the findings is based on intensive in-situ temperature and strain monitoring in both the dams over the last decade.

2 Previous findings from in-situ measurements in the two dams

Axpo Power operates two concrete dams, which are among the dams most severely affected by ASR swelling in the central Alps in Switzerland. These dams have been monitored since their commissioning with geodetic measurements, levelling and plumb lines, providing a record of the concrete deformation over the entire life span of the dam. While the cyclic deformations due to the seasonal loads on the dams stay the same over the years, the dam shows increasing irreversible deformations due to ASR swelling.

In **Fig. 2,** the development of the vertical strains in Block 8 of the Roggiasca dam is illustrated. The data is derived from the geodetic measurements at 3 elevations (A, B and C). The strain in the top 20 m of the dam (between elevations A and B) is much higher than in the lower part (between elevations B and C). This is due to differing temperature conditions in these two parts, as discussed in [2] and [3]. The strain has increased to 1600 μm/m in the top 20 m to date, compared to only 200 – 600 μm/m in the lower part.

Figure 3 illustrates the vertical strain development in two blocks of the Runcahez dam. The strain has grown to as much as 4100 μm/m, which is the highest value recorded to date.

The swelling histories of both the dams show very similar ASR kinetics. They had both an initiation time of around 25 years after being commissioned in the mid-60s. In the early 1990s, permanent displacements were first noticed. The starting phase of swelling lasted for 10 to 12 years, resulting in a strain of up to 150 to 200 μm/m. The starting phase was followed by a transition phase with an increasing strain rate, leading eventually to the linear phase of ASR swelling. This phase has lasted for the last 8 to 10 years and still governs the current ASR behaviour.

The following discussion examines the current kinetics of swelling of concrete in the two dams. The details of the analysis carried out to determine the characteristic ASR swelling curve can be found in [2] and [3]. This analysis was based on the detailed data of temperatures and strains measured continuously for several years at the same locations in the dam concrete. The general approach is illustrated in **Fig. 4** with an example of application to a measurement location in the Roggiasca dam. From the strain data, the irreversible component of the dam deformation was evaluated. The strains were measured using either extensometers with 5 m measuring sections or sliding micrometres with a base length of 1 m. In winter, it was observed that no further swelling occurred when the concrete temperature dropped below a cutoff temperature of 3 °C. The strain was observed to increase mainly in summer. This insight inspired the engineers of Axpo Power to look for a unique function to relate the rate of ASR swelling observed in each dam to the concrete temperature. A suitable solution was found in the form of an Arrhenius function, which could also be approximated by a second-degree polynomial function.

Figure 5 depicts the best-fit curves of the relationship between the daily mean concrete temperature above 3 °C and the daily strain rate. In the Roggiasca dam, 6 measuring sections were fitted

over a 5-year period, compared to 9 sections over an 8-year period in the case of the Runcahez dam. The individual curves deviate only slightly from the mean characteristic ASR curve for each dam, which can be explained by measuring accuracy and some variability of concrete. In contrast, there is a significant difference in ASR kinetics between the two dams. For example, at a concrete temperature of 15 °C (i.e. 12 °C above the cutoff temperature of 3 °C), the swelling rate is 0.45 µm/m/day in the Roggiasca dam, compared to 1.7 µm/m/day in the Runcahez dam, a factor of around 4.

For all practical purposes, it can be assumed that ASR swelling is suppressed under cold climatic conditions. This was observed in both the Roggiasca and Runcahez dams, which show almost the same cutoff temperature of 2 to 3 °C. Above the cutoff temperature, the strain rate increases more than linearly with increasing concrete temperature. This is not surprising, since the chemical ASR reaction follows the Arrhenius law, which is an exponential function of the following form:

$$k = k_0 \, e^{\left(\frac{E_a}{R}\right)\left(\frac{1}{T_0} - \frac{1}{T}\right)}$$

where k_0 = reaction rate at the reference temperature T_0; E_a = activation energy; R = gas constant; T = temperature in Kelvin (K). In a simplified approach for ASR swelling of dams, the Arrhenius function can be assumed to be a quadratic function of the type

$$k = a(T - 3\,°C)^2 + b(T - 3\,°C)$$

where T is the concrete temperature in °C at a specific location. All the strain measurements in the Roggiasca and Runcahez dams were subsequently fitted with such a function, leading to two distinct characteristic ASR swelling curves.

Figure 6 shows an example of the comparison of the prediction based on the characteristic ASR swelling curve with the measurement of the elongation of an extensometer section in the crest region of the Runcahez dam. Over a period of 8 years, the same pattern is observed every year: no swelling in winter and accelerated swelling in summer. The prediction line based on the characteristic ASR swelling curve for the Runcahez uses a sinusoidal time function to simulate the mean seasonal variation of concrete temperature at the location of the strain measurement. Despite the simplified sinusoidal approach for the temperature effect, the quality of prediction is excellent. This indicates that the kinetics of ASR does not change over the 8-year period, supporting the findings from the geodetic measurements showing that the dam concrete in the crest region is in the linear phase of ASR swelling.

Figure 7 presents another example of a similar fitting for an extensometer section in the Roggiasca dam for an observation period of 5 years. The first 2 years, which was a period of normal operation, show again a very good fit when a sinusoidal fluctuation of the concrete temperature is assumed. However, in the last 3 years (i.e. from 2021 to 2023), the measured elongation in summer is significantly smaller than the prediction. This discrepancy is due to the cooling of the dam by sprinkling, as will be explained in detail later. Also here, the kinetics of ASR does not change over time.

The findings from the long-term intensive strain measurement campaigns in the Runcahez and Roggiasca dams reveal that there is a dam-specific unique ASR swelling curve that follows an Arrhenius law and does not change with time. All the locations within the top 20 m of each dam follow the same curve, which expresses the kinetics of ASR as an exponential function of the concrete temperature. Its shape is governed by various other factors influencing ASR, namely aggregate type (petrography), aggregate size (sieve curve), cement type and content, and relative moisture. It is evident from **Fig. 5** that the predominant factor governing ASR swelling in a dam is the concrete temperature in summer (hot period). In winter, the measurements do not show any

further increase of swelling once the concrete temperature falls below 3 °C, irrespective of how cold it is. Hence, ASR swelling depends only on how hot it is during the rest of the year. This insight led to the idea of active cooling of the dam concrete in summer to slow down or even stop the ASR swelling.

3 Cooling Roggiasca dam to reduce ASR

After gaining a fundamental understanding of the ASR kinetics through the analysis of the strain and temperature data from the two dams, engineers of Axpo Power decided to try to cool the dam concrete in summer to mitigate the negative effects of ASR on the dam structure. To the best of the authors' knowledge, this has never been tried before on any existing concrete dams.

A very simple, fast and cost-effective cooling system was installed at the Roggiasca dam, as shown in **Fig. 8**. Using a system similar to that used to water the gardens, the upstream and downstream faces of the dam were sprinkled from mid-May to the end of October. The setup was optimized several times over the 4 years of operation. The water for the cooling was taken from a small nearby creek.

In 2024, the reservoir could not be operated normally after a devastating flood on 21 June 2024. The reservoir remained completely full throughout the summer until mid-November 2024. During this period, the concrete was additionally cooled by the cold reservoir water.

As can be seen from **Fig. 9,** concrete on the sunny upstream side warms up to 27 °C or more in the top part of the dam, while the air temperature reaches a maximum of around 20 C in summer. The concrete on the shaded downstream side has usually about the same temperature as the air. In summer, the maximum water temperature is around 14 °C in both the river and the very small reservoir. During the cold period from December to the end of March, all the temperatures are usually below 5 °C.

Using the simple sprinkling system mentioned earlier, the maximum concrete temperature could be brought down to 20 °C, effectively eliminating the effect of radiation. During the summer of 2024, the full reservoir further reduced the concrete temperature to just 14 °C.

The concrete temperatures measured at the locations of the extensometers on the upstream side of the dam clearly showed the effect of cooling. Based on these measured temperatures and the characteristic ASR curve for the Roggiasca dam, the variation of the daily ASR swelling rates with time were calculated, for example, at the 3 locations of the extensometers in Block 8. The calculated strain rates presented in **Fig. 10** show that the swelling increases in summer, pauses in winter and the swelling rate reduces in the dam with increasing depth below the crest. Moreover, the distinct effects of the two different cooling mechanisms are evident from this figure. In the upper part of the dam, cooling by simple sprinkling reduced the swelling rate at a depth of 2.5 m below the crest to around 73% of the maximum value of 1.3 μm/m/day. The additional cooling by contact with water in the full reservoir during the summer of 2024 reduced the swelling rate further to just 34% of the maximum.

In **Fig. 11**, the predicted and measured ASR-induced elongations of the extensometer sections in Block 8 of the Roggiasca dam are compared over an observation period of 7 years. Each prediction curve in this graph consists of 2600 values of daily strain rates calculated using the characteristic ASR curve and the measured concrete temperatures. In contrast, the prediction shown earlier in **Fig. 7** was based only on a sinusoidal function to represent the seasonal variation of the concrete temperature. The reason for the substantially improved agreement between the predicted and measured ASR behaviour in **Fig. 11** was the use of the actually measured concrete temperatures in the computation of the prediction based on the characteristic ASR curve. This

high level of predictive accuracy could be achieved not only for all 9 extensometer sections, but also for the various periods with markedly different temperature conditions with and without cooling.

Figure 12 compares the measured and predicted ASR-induced elongations of the extensometer sections in Blocks 5 and 8 of the Roggiasca dam over the period 2023-2025, which includes the summer of 2024 with the full reservoir. This graph illustrates once again the excellent agreement between the measured and predicted ASR behaviour. It also shows that the strain rate was very low during the summer of 2024 because of additional cooling by the full reservoir.

Figure 13 demonstrates the impressive effect of cooling on the elongations measured in Block 5 of the Roggiasca dam. The upper part of the dam (up to a depth of 5 m below the crest) expanded by 8 mm in 7 years, while the lower part (between depths of 5 m and 10 m below the crest), which is usually partially submerged, swelled by only 4 mm (see the yellow and blue points, respectively). This indicates that contact with cold reservoir water reduces the ASR swelling by about 50%. The upper part swells in a normal year by 1.3 to 1.4 mm. When cooled by sprinklers, the annual swelling is reduced to between 0.9 and 1.25 mm, i.e. on the average to around 80% of the normal value. When additionally cooled by contact with water in the full reservoir, the swelling decreases further to 0.5 mm, which is only about 40% of the normal value.

If concrete could be cooled to 6 °C in summer (mid-May to the end of October), the swelling would reduce to just 0.12 mm or less than 10% of the normal value. That implies that the lifetime of a dam suffering from ASR would be increased by a factor of about 10.

4 Conclusion

In [4], the effect of ASR swelling on the initiation and development of structural cracks in the Roggiasca dam was described and discussed.

In the present paper, it is shown that cooling is by far the most effective and controllable way to reduce ASR swelling in existing dams for the mitigation of the negative consequences like the initiation and growth of structural cracks. The beneficial effect of cooling starts almost immediately after the installation of a cooling system, as proven by the in-situ measurements in the Roggiasca dam.

The ASR-induced cracks in the Roggiasca dam could indeed have been largely prevented by cooling. If the Roggiasca dam would have been cooled from 2005 onwards to the temperature level of the reservoir water, today's cracks in the dam would have developed only in the year 2060. If it had been cooled further down to 6 °C in summer, these structural cracks would have occurred only in the year 2205, i.e. 200 years later.

5 References

[1] Amberg F., Bremen R., Droz P., Leroy R., Maier J., Otto B. 2017 “Concrete Swelling of Dams in Switzerland.”, *Swiss Committee on Dams*

[2] Otto B., Senti R. 2025 “ASR strain rate distribution in a Swiss arch dam.”, *The International Journal on Hydropower & Dams, Issue 4, 78-82.*

[3] Otto B., Senti R., Panduri R. 2025 “Unique dam-specific ASR swelling curve and the effect of dam cooling.” *The International Journal on Hydropower & Dams, Issue 5, 80-84.*

[4] Otto B., Senti R., Panduri R. 2025 “Structural crack formation in a Swiss dam affected by swelling due to ASR.” Challenges in Hydraulic Engineering: Proceedings of the 21st Technical Dam Control International Conference, 2025

Authors

Dr. Bastian Otto, Age 66

PhD, JCU Queensland Australia, dipl. Civil Engineer ETHZ Switzerland

Senior dam engineer at Axpo Power AG in Switzerland. Engaged in the fields of dam engineering, dam safety, seismic analysis, geomechanics and underground works. Responsible engineer for the Muttsee dam and environmental issues during the construction of the 1000 MW Limmern pumped storage plant.

Rico Senti, Age 54

MSc Engineering Geology, EPFL Switzerland

Head of dam department at Axpo Power AG in Switzerland. Engaged in the fields of dam safety, geomechanics and underground works. Responsible engineering geologist during the construction of the Muttsee dam.

Figure 1: Roggiasca arch dam and Runcahez gravity dam

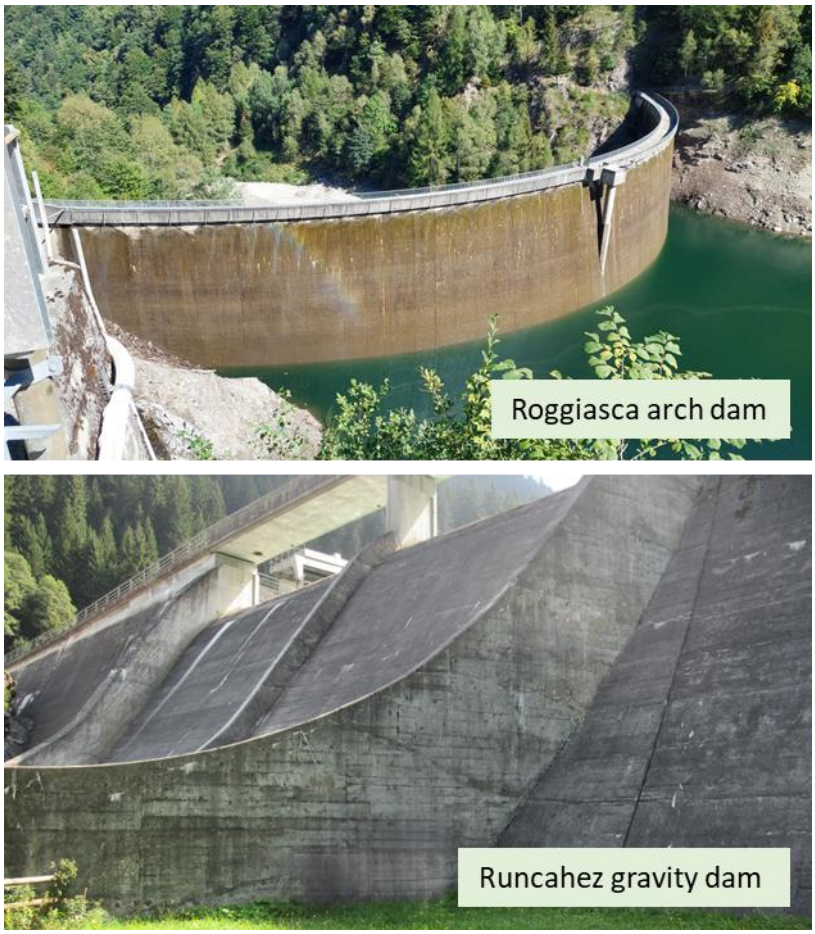


Figure 2: Development of vertical strains over the height of the dam as determined by geodetic measurements (Roggiasca Dam, Block 8)

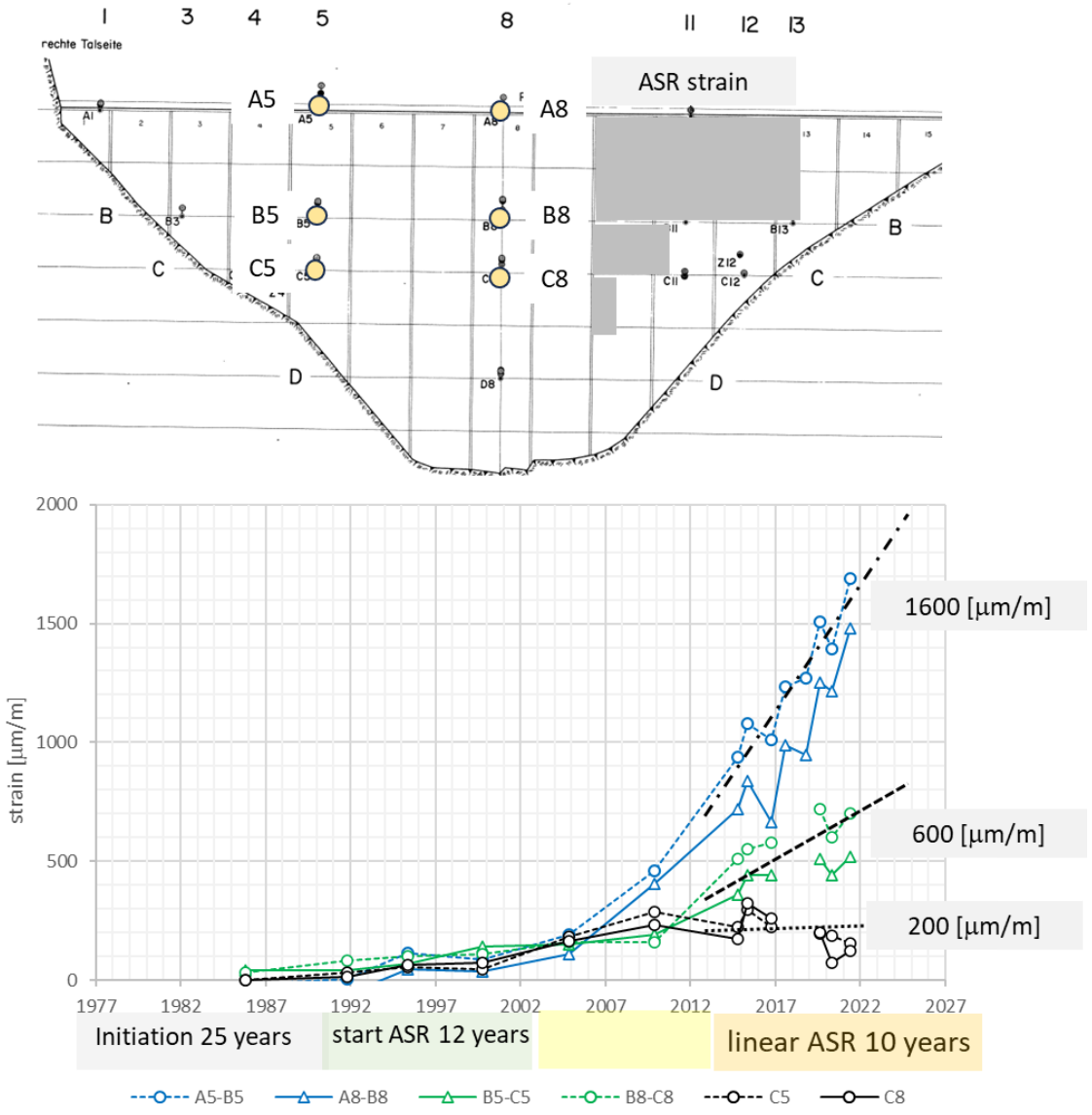


Figure 3: Development of vertical strains as measured by levelling (Runcahez Dam, Blocks 3 and 11)

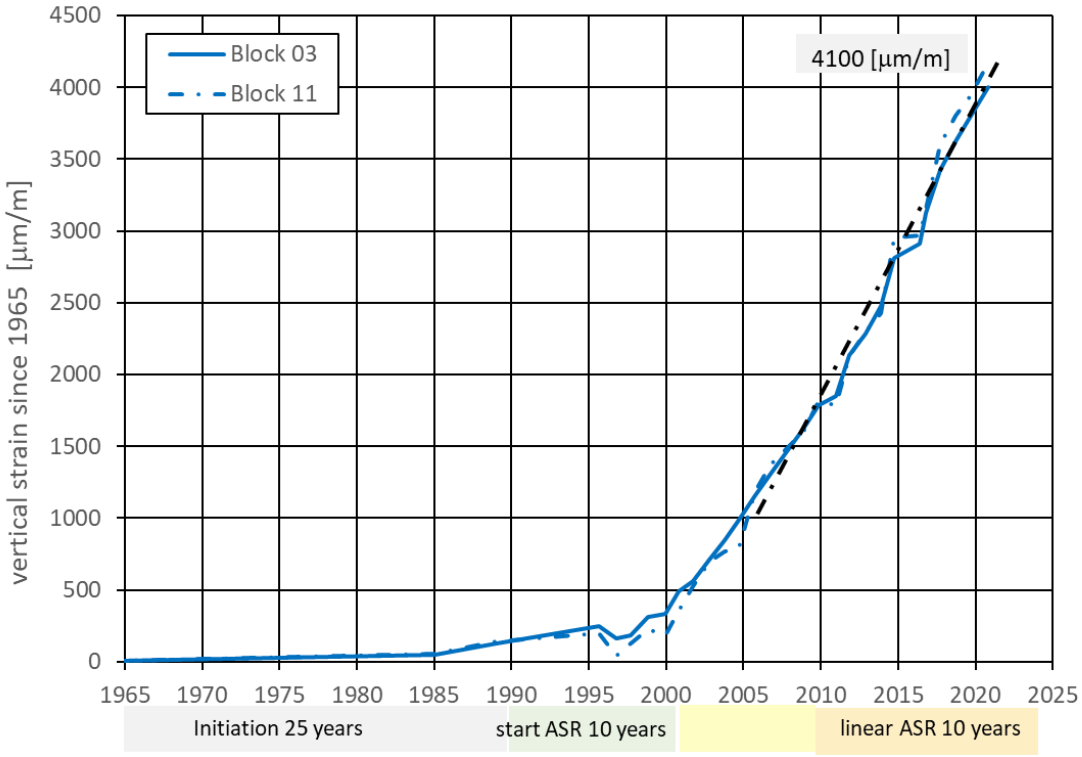


Figure 4: General approach to determine the characteristic ASR swelling curve

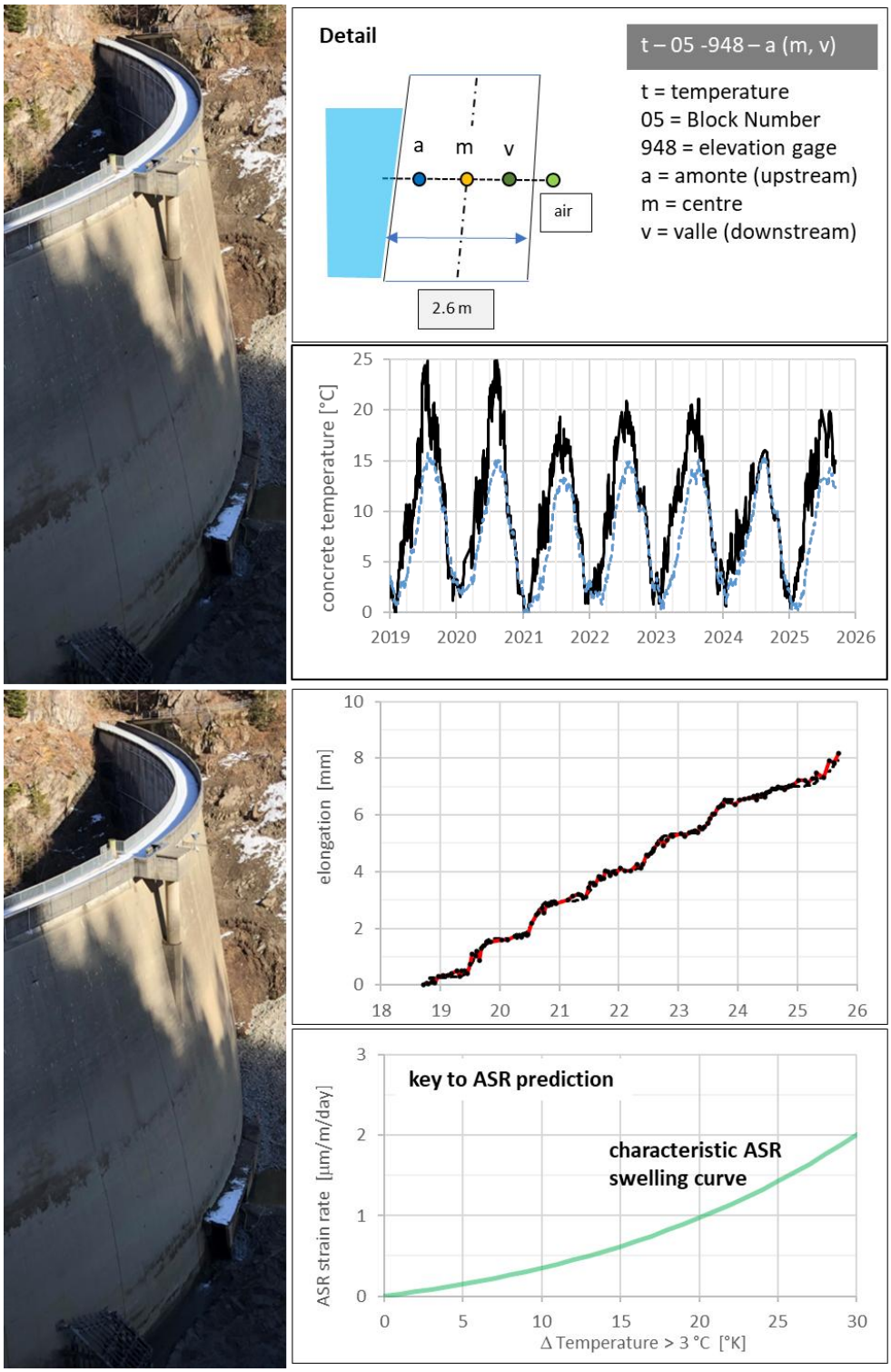


Figure 5: Characteristic ASR swelling curves for Roggiasca and Runcahez dams

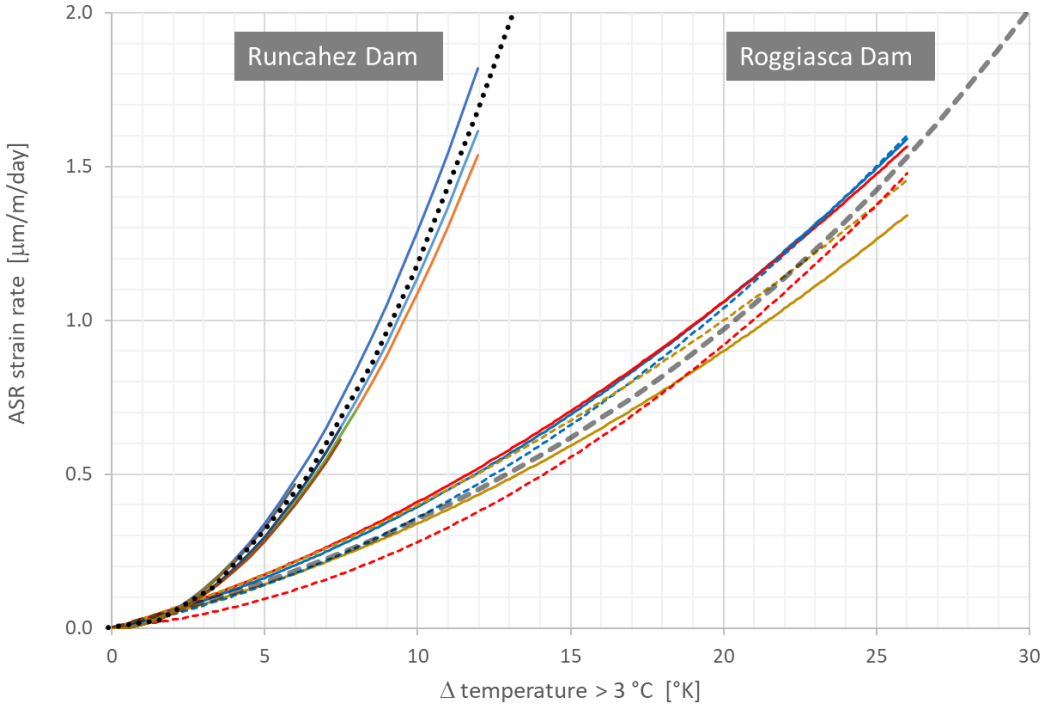


Figure 6: Comparison of measured elongation of extensometer section with prediction based on characteristic ASR swelling curve (Runcahez dam, near the crest)

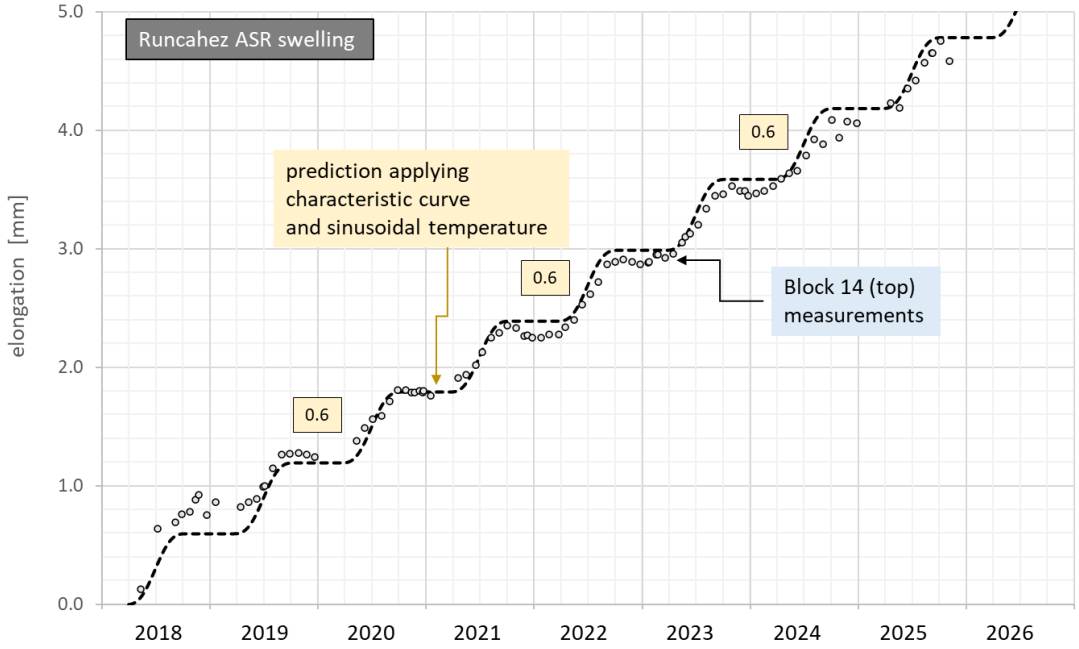


Figure 7: Comparison of measured elongation of extensometer section with prediction based on characteristic ASR swelling curve (Roggiasca dam, near the crest)

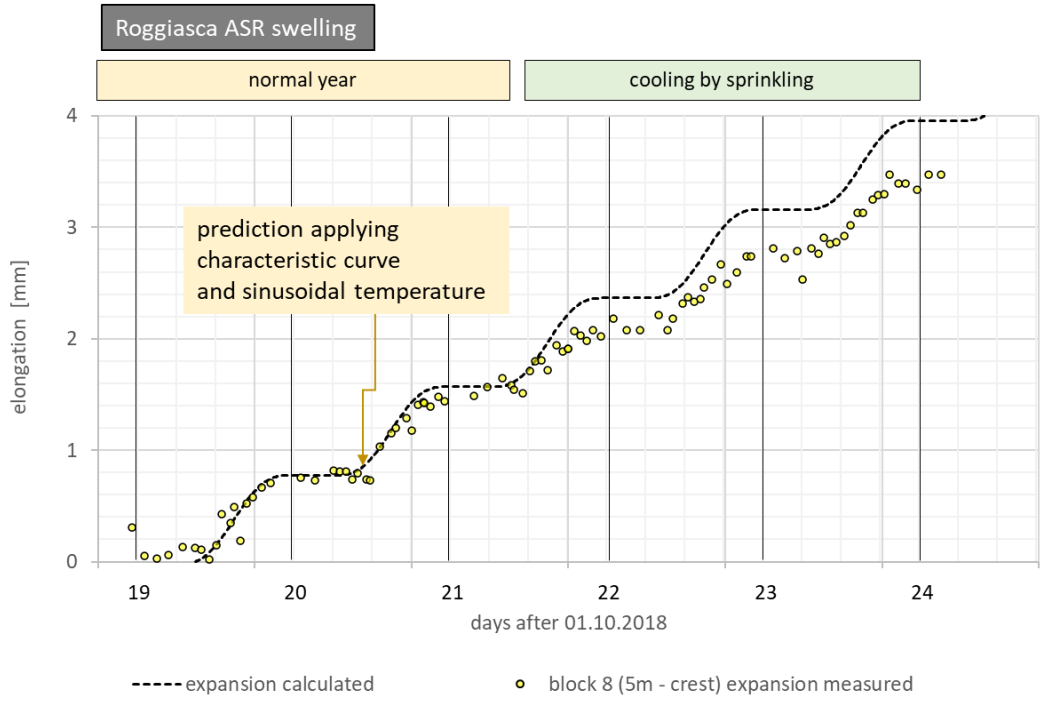


Figure 8: Cooling system installed at Roggiasca dam



upstream face

downstream face

Figure 9: Comparison of concrete temperatures in Roggiasca dam with water and air temperatures

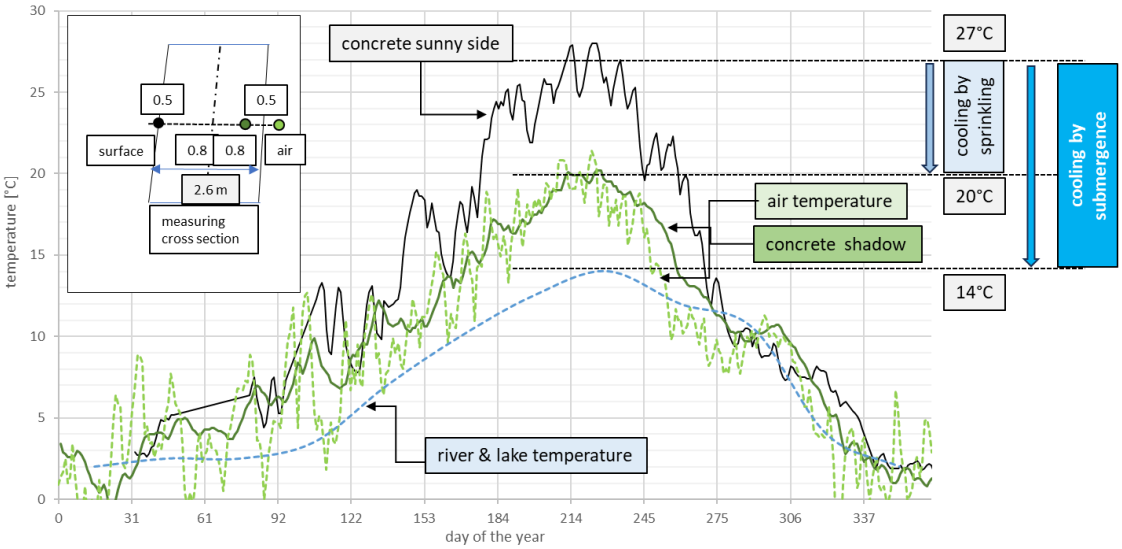


Figure 10: Strain rates calculated based on characteristic ASR curve and measured concrete temperatures at three extensometer locations in Block 8 of Roggiasca dam

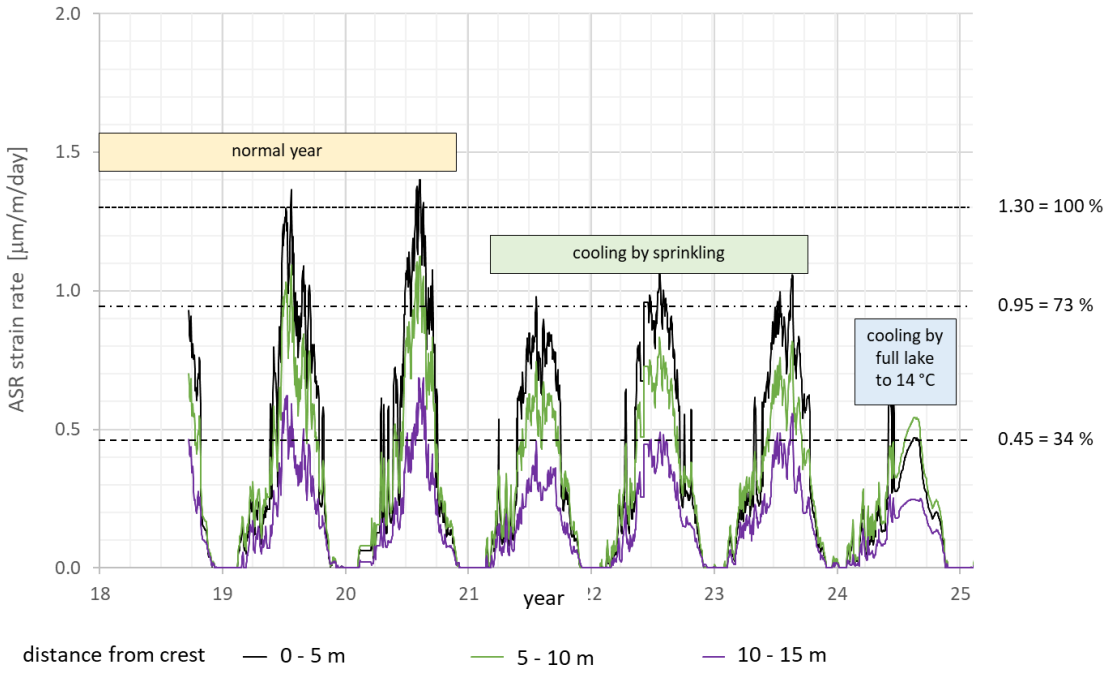


Figure 11: Comparison of measured and calculated ASR-induced elongations of extensometer sections in Block 8 of Roggiasca dam with and without cooling

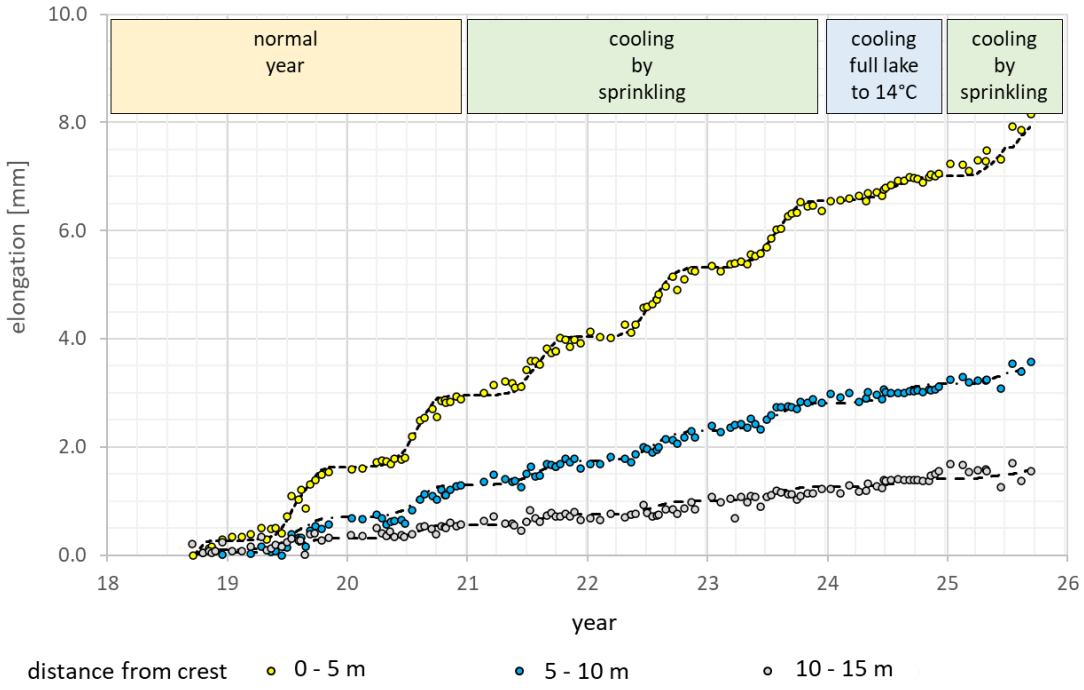


Figure 12: Reduction of ASR-induced elongations of extensometer sections in Blocks 5 and 8 of Roggiasca dam in the summer of 2024 with additional cooling by contact with water in the full reservoir

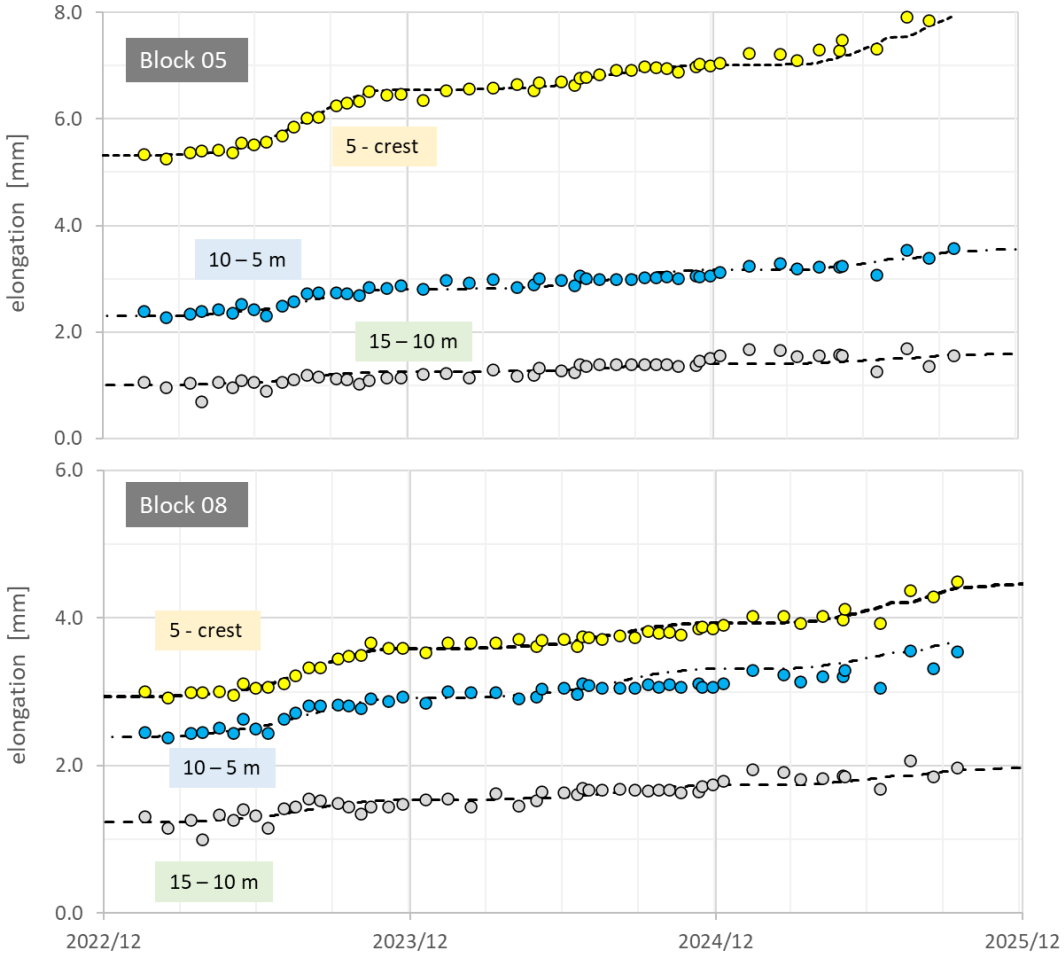
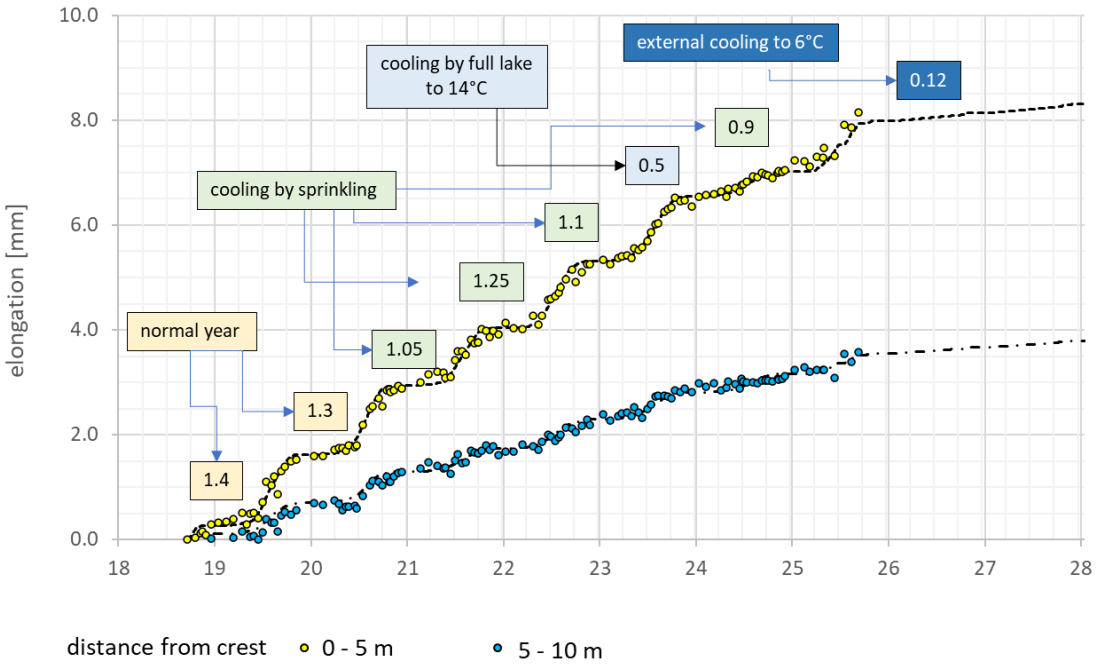


Figure 13: Effect of cooling on ASR-induced elongations of extensometer sections in Block 5 of Roggiasca dam



Challenges in conceptual design of the Skalička dam

Miroslav Spano

Jaromír Říha

Affiliations List

Assistant professor, Brno University of Technology, Faculty of Civil Engineering, Veveri 95, 602 00 Brno, Czech republic, ORCID: https://orcid.org/0000-0001-6299-4440
Professor, Brno University of Technology, Faculty of Civil Engineering, Veveri 95, 602 00 Brno, Czech republic, ORCID: https://orcid.org/0000-0002-1362-5769

keywords

Skalička dam, conceptual design, multi-criteria analysis

abstract

The paper focuses on the pre-design phase of the Skalička dam, which was based on the development of four conceptual design variants and their evaluation using a multi-criteria analysis. The aim was to identify an optimal solution with respect to technical, environmental, operational, hydrogeological, and social aspects. The proposed variants differed primarily in the conception of the dam location (across valley or lateral) and operation (multipurpose or dry reservoir). The assessment included the design of lateral reservoir filling and its impact on dam safety and operational performance. Particular attention was paid to the potential influence of reservoir impoundment on the regime of karst groundwater within the Devonian aquifer and on groundwater levels in the Quaternary aquifer in the adjacent area. The multi-criteria analysis enabled a systematic comparison of the individual variants, identification of their main advantages and risks, and selection of the preferred concept. Key partial issues addressed during the pre-design phase and the applied approaches to their resolution may also be applicable to the preparation of similar water management projects in hydrogeologically complex settings.

AUTHORS

Thomas Konow, Dam Safety Officer, Å Energi Hydropower, Skippergata 23, 4611 Kristiansand, Norway, E-mail: thomas.konow@aenergi.no

Bjørn Nilsen, Professor Emeritus, NTNU - Norwegian University of Science and Technology, S.P. Andersens veg 15a, NO-7031 Trondheim, Norway, E-mail: bjorn.nilsen@ntnu.no

Simon G. Bjønness, Senior Specialist Concrete dams, Dr.techn. Olav Olsen, Strandveien 18, 1366 Lysaker, E-mail: sgr@olavolsen.no

ARTICLE TITLE

Pore Pressure under Concrete- and Buttress dams
- Rock Mechanics mapping and Design assumptions

KEYWORDS:

Concrete dams, Buttress dams, Rock Mechanics mapping, Pore pressure, Design assumptions, Instrumentation

INTRODUCTION

This paper is based on a report from 2026, with the title: “Pore pressure and concrete dams”. The report was financed by Norwegian dam owners through Renewables Norway (Fornybar Norge) and the ongoing dam safety project DSHP.

The report evaluates results from 87 piezometers of five buttress dams, and the main findings are:

- Drainage directly downstream the buttress slab will eliminate the pore pressure under the buttresses downstream the slab, even for very wide buttresses. There was no sign of pore pressure connected to the reservoir in any of the piezometers installed in the buttress dams with an upstream drainage gallery.
- Stability calculation of foundations should be based on a geologic evaluation of the rock mass. Stereographic projection and rock mass classification according to the RMR system have been found to be best suited technique for geological characterization of dam foundations.
- Drainage curtains are the most efficient way to control pore pressures in the foundation. It is important to note that drainage holes in a drain curtain will need to be checked and cleaned/flushed at regular intervals, as the holes can be clogged by fines and minerals in the bedrock.
- If piezometers are to be installed, the installation should be based on a geologic evaluation. The placement, inclination and depth of the borehole and placement of the piezometer must be carefully identified from a geological mapping. Random instrumentation of rock foundation is of little value.

The report is also available in English and can be downloaded here: DSHP - Pore Pressure and concrete dams

PORE PRESSURE AND DAM TYPES

Pore pressure is normally a significant design load for gravity dams, while for buttress dams a reduced pore pressure is normally assumed. Definition of dam types is therefore important to understand assumptions for pore pressure when calculating dam stability.

The dam types covered by this article are:

- Gravity dams, and include these dam types:
  i. Concrete gravity dams
  ii. Masonry dams
- Buttress dams, and include these dam types:
  i. Slab buttress dams (including Ambursen dams and slab buttress dams)
  ii. Multiple-arch dams
  iii. Solid head buttress dams

Definition of pore pressure

It is worth noting that pore pressure is normally used to describe water pressure in voids in soil. However, the Norwegian regulations also use the term “pore pressure” for joint water pressure in rock foundations and therefore the same definition is used in this article.

Assumptions for pore pressure

Assumptions of pore pressure generally consider the following two design situations:

- Dam stability: This applies for the stability of the dam structure and the contact zone between concrete and rock foundation.
- Foundation stability: This applies for the overall stability of the rock foundation and the dam structure, with pore pressure in rock joints giving uplift (i.e. pore pressure perpendicular to the rock surface).

The pore pressure must cause uplift, in order to be of concern for structural stability. This means that the pore pressure must form in a joint that is parallel or sub-parallel to the dam foundation.

NORWEGIAN REGULATIONS

There are different safety requirements for gravity dams and buttress dams. The main difference is assumptions for pore pressure distribution and safety requirements for overturning. Safety requirements are summarized on the table below.

Table 1. *Design requirements for Norwegian dams (NVE 2026).*

Safety requirements for Norwegian dams	Overturning		Sliding	
	Gravity dam **Resultant** (*1)	**Buttress dam** **SF** (*2)	**Gravity dam** **SF** (*2)	**Buttress dam** **SF** (*2)
Ultimate limit state (ULS)	1/3 B (*3)	1.4	1.5	1.4
Accident limit stat (ALS)	1/6 B (*3)	1.3	1.1	1.1

*Comments:

*1 - Resultant: Safety requirement is defined as the distance from the overall resultant force and to the downstream toe of the dam.

*2 - SF = Safety Factor: The ratio between the resisting forces and the driving forces affecting dam stability.

*3 - B = Foundation Width: The width of dam section at the foundation, measured from the downstream toe to the upstream heel.

Assumptions for pore pressure

Gravity dams

In Norway pore pressure assumptions depends on the type of gravity dam, as listed below:

i. Concrete gravity dam: Linearly decreasing pore pressure is assumed in areas with compressive load transfer to the foundation, and a full pore pressure in areas with no compressive stress. Example in **Figure 1** shows pressure distribution in ALS, with compressive stress only in the downstream part.

ii. Drained gravity dam: The pore pressure can be reduced to 33% of the upstream water head in the drainage section. However, full pore pressure should be considered in all parts of the cross-section where there is no calculated compressive load transfer to the foundation.

iii. Masonry dams: These dams are constructed of dry laid stone blocks without any mortar in the joints. The dam type is considered as drained, and the drainage is placed at a distance of 25% of the upstream water head from the upstream side. Drainage is assumed also when there is no compressive stress in parts of the foundation.

The figure below illustrates pore pressure under a concrete gravity dam and a drained concrete gravity dam.

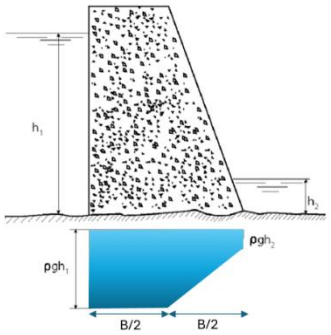
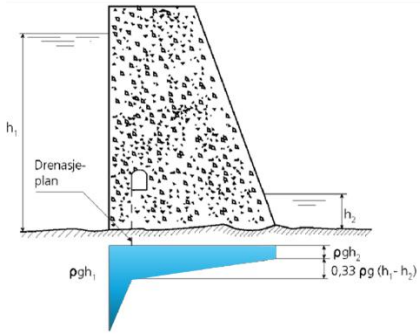
Gravity dam:	Drained Gravity dam.
	
Linearly decreasing pore pressure in areas with compressive stress to the foundation	Reduced pore pressure can be assumed. The pore pressure can be reduced to 33% of the upstream water head in the drainage section.

Figure 1. *Pore pressure distribution for concrete gravity dams according to Norwegian regulations.*

Buttress dams

About 10 % of the Norwegian dams are Slab Buttress dams, while there are only a few Solid Head Buttress dams. There are no multiple arch dams.

Pore pressure assumptions for Solid Head Buttress dams are therefore taken from international literature, while the pore pressure under Slab Buttress Dams are based on normal practice in Norway, as described here:

i. Solid Head Buttress: Each buttress consists of a buttress head and a buttress support that form one monolithic structure. The entire buttress must be lifted in order to open a crack between the rock and the concrete. In this situation, the safety against overturning will be < 1.0. For higher safety factors, a linear decreasing pore pressure under the buttress head is the normal assumption. On the downstream side of the buttress head, the dam is freely drained, and therefore no pore pressure can develop here.

ii. Slab Buttress Dams: Slab buttress dams have a movement joint between the upstream slab and the buttress support, that allows movement between the slab and the support. The slab can thus be lifted up from the foundation and from the support. In theory there can be a full pore pressure under the slab. On the downstream side of the slab, the dam is freely drained, and therefore no pore pressure can develop here.

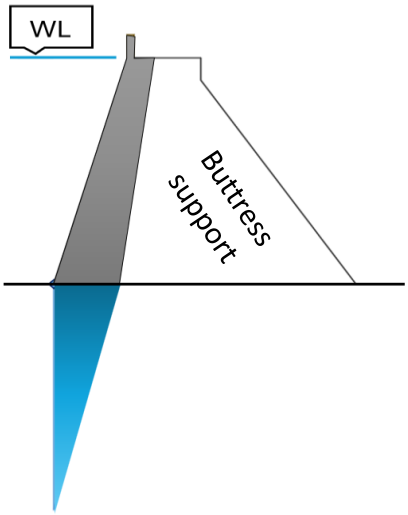
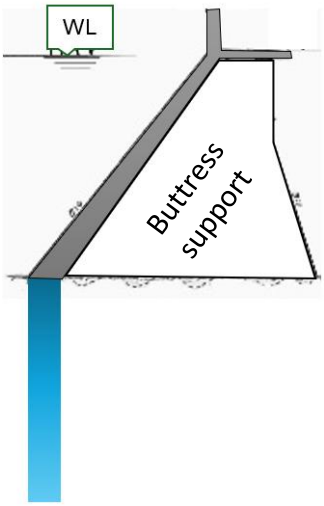
Solid Head Buttress dams	Slab Buttress dams
	
General pore pressure assumptions for Solid Head Buttress dams from international literature.	Pore pressure assumptions for Slab Buttress Dams based on general practice in Norway

Figure 2. *Pore pressure under Solid Head Buttress dams and Slab Buttress Dams*

ROCK FOUNDATIONS AND PORE PRESSURE

The general assumption for pore pressure distribution used in the regulations (see previous chapter), is valid in homogeneous materials, but not in heterogeneous foundations with discontinuities such as joints and fractures in the bedrock. The discontinuities can be any defect that separates the rock mass and is characterized by zero or very small tensile strength and therefore may easily deform and displace.

In general, pore pressure distribution in the bedrock will therefore be a nonlinear distribution of the uplift pressure.

Joint water pressure

The “joint water pressure” causing uplift in the foundation is the main concern when evaluating foundation stability. Uplift can occur when joints are oriented parallel or sub-parallel to the surface. The joints located close to the rock surface are those of most concern. This implies that increasing depth of the rock fracture reduces the adverse effects of uplift (M. Abdi (KTH) 2022).

The most common assumption regarding pressure build-up for dam foundation is that the aperture (opening) remains constant along the joint, which results in a linear distributed uplift pressure beneath the dam according to the figure below.

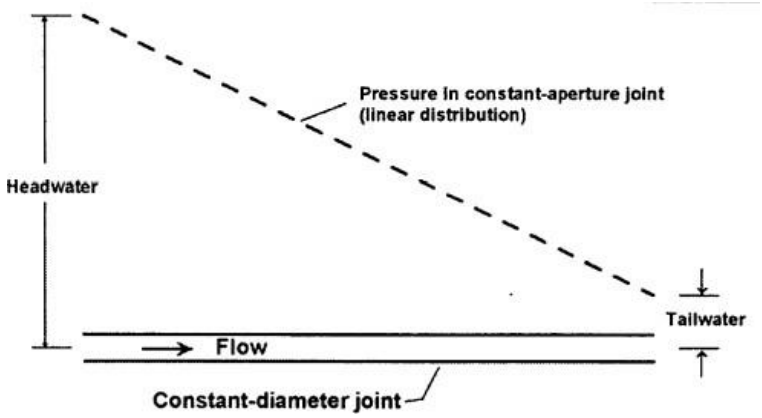


Figure 3. *Linearly distributed pressure from the heel to the toe of a dam (USACE/ERDC March 2002)*

The degree of interconnection between the joints and their length can change the distribution of the uplift pressure, as shown in the figures below. A joint with varying aperture will in theory result in a nonlinear uplift distribution. Consequently, the joint can for example be modelled with a large aperture starting from the heel and a smaller aperture in the downstream side, as shown in figure (b) below. If the aperture is small on the upstream side and increases to the downstream side, this will result in a reduced pore pressure, as shown I figure (a).

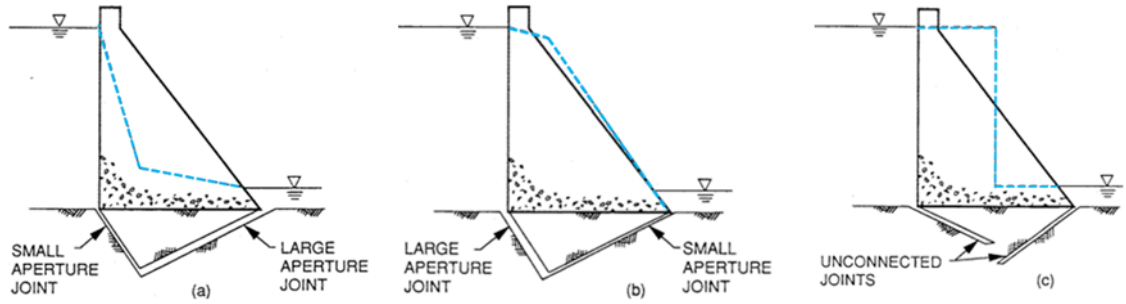


Figure 4. *Influence of joint aperture and interconnectivity on uplift. (EPRI, 1992). The pore pressure is illustrated with dotted blue line.*

Experience with joint water pressure

Experience from a large number of rock slopes indicates that the real, in-situ water pressure is much smaller than what should be caused by the triangular distribution. This has been found to be mainly due to the fact that most fractures do not convey water in the entire fracture plane, and that considerable amounts of water may escape along secondary, intersecting fractures. Similar effects may also influence joint water pressure at dam foundations, resulting in considerable exaggeration of joint water pressure if configuration like shown in Figure 3 and Figure 4 is used in calculation.

The loads transferred from a dam structure will be higher at the downstream toe as the load from the water pressure on the upstream face results in an overturning force. High rock stress has the effect of compressing the joint fracture walls and thus reducing permeability. This effect may result in decreased permeability towards the downstream toe. Change in aperture in the direction of flow may cause uplift pressure to follow a

curved rather than a linear distribution. However, the effect is highly dependent on the rock properties and the size of load transfer to the foundation.

This effect is illustrated in the figure belove. As this effect is load dependent, it is more visible for higher dams and will change with water levels in the reservoir – as shown I the figure below.

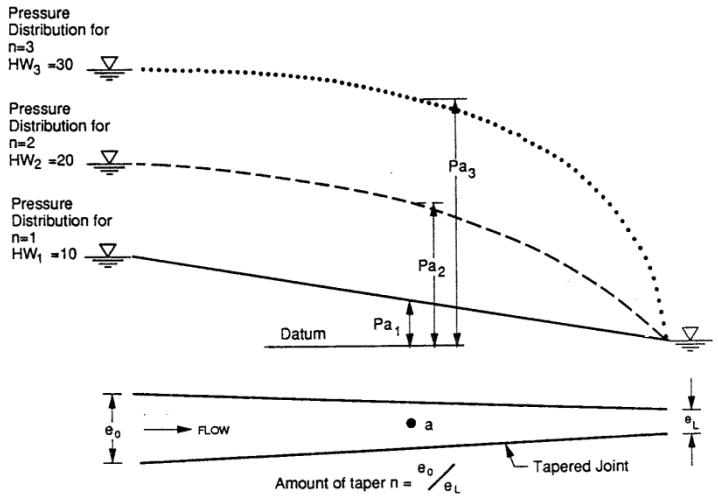


Figure 5. *Uplift distribution in a deformable rock joint with increasing headwater and thereby increasing rock stress (EPRI 1992).*

This implies that the pore pressure can be of greater concern for high dams compared to lower dams. One of the dams evaluated in this report had indications of this effect. At this dam the ratio between pore pressure and upstream water pressure had a linear correlation up to normal operating water level. However, during a large flood where the water level raised 1 m, one piezometer indicated that the pore pressure increased more than expected from the linear relation below normal operating water level.

Hydraulic jacking and Hydraulic fracturing

Undesired pore pressure and uplift affecting structural stability can develop only if there is an open crack with no bonding along the crack. In general, this will occur only if the pore pressure exceeds the potential bonding plus the weight of the overlying mass (dam weight and /or rock mass). This will result in hydraulic jacking if there is no bonding, or hydraulic fracturing in a solid material (ie. with bonding) where a new crack will develop due to the force from the pore pressure.

The 186 m high Zillergound dam in Austria is one example where hydraulic fracturing was suspected. Here a crack formed at an upstream water pressure of 16 bar just above the base joint. Fracture mechanical studies at the dam showed that initial cracks up to a length of about 1 m remained stable up to a difference between water pressure and vertical stress of about 10 bar (P. Obernhuber 2009).

Pore pressure reduction – Drainage

It seems that drainage is the most effective method to reduce uplift pore pressure. According to cases given in (EPRI 1992) a curtain grouting can reduce the quantity of flow, but several of the cases showed that a grout curtain did not control the uplift flow. All the

examples, however, had only a single row of grout curtain, which represents an older practice. Modern practice, using two or three rows of grout curtains, provides substantially better sealing and will probably have a much better performance.

The cases referred to in this paper show that drainage gallery directly downstream the buttress slab will eliminate the pore pressure under the downstream buttress support, even for very wide buttresses. The piezometers installed in these dams, did not measure pore pressure that was influenced by the reservoir.

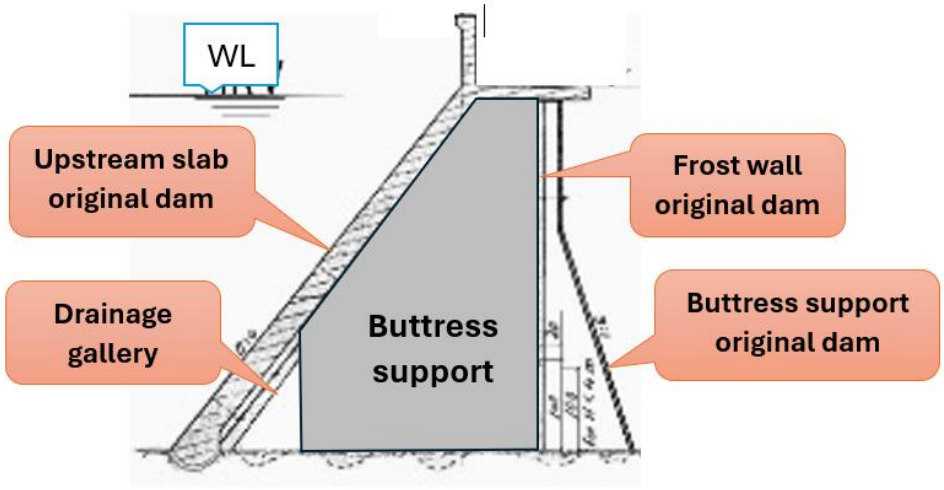


Figure 6. Typical section of 3 of the dams included in the study. Piezometers installed show that the drainage gallery eliminates pore pressure under the buttress support. A drainage curtain in the bedrock would also control pore pressure in the foundation.

MEASUREMENTS OF PORE PRESSURE IN THE ROCK FOUNDATION – CASE STUDIES

The cases in this paper, refer to the report (Dr. techn. Olav Olsen 2026) with evaluation of five buttress dams with a total of 87 piezometers installed in the foundations to monitor pore pressure. The dams are referred to as dam A, B, C1 and C2 and D.

Dam A has a bottom gate between the 2 highest buttress supports. The bottom gate is placed on a concretes slab cast on the rock foundation in the highest section. Although the dam is a traditional Norwegian slab buttress dam, the gated section with the bottom slab can be compared to a solid head buttress dam with a “very wide” buttress support in terms of the rock-/concrete interface, as the bottom slab is continuous from upstream heal to downstream toe.

Dams B, C1, C2 and D have buttresses that have been strengthened and are therefore defined as “Heavy Buttress Dam” according to the Norwegian Dam Safety Regulations (Energidepartementet 2009). The main features of the dams are listed below:

- Buttress support - Contact sone of the rock-/concrete interface:
  - Dam A: Slab under bottom gate is 6 m wide
  - Dam B: 2 m wide buttress support
  - Dam C and D: 6 m wide buttress support

- Drainage gallery:
  - Dam A: Gallery to each side of the bottom gate.
  - Dam B: Gallery between buttress supports
  - Dam C and D: Gallery upstream the buttress support
- Drainage curtain: Dam D
- Grout curtain: Dam A

Table 2. *Key information of the dams and sensor output (total 87 sensors).*

Dam	Dam height	Foundation according to RMR	Grout curtain?	Drainage	Total leakage	No. of piezometers	Correlation PP and WL*?
A	21 m	Fairly good to good/very good	Yes	No	Not visible	16	Yes – for 1 piezometer
B	19 m	Fairly good to good	No	Drainage Galley	<0.2 l/s	24	No
C1, C2	12 m	Good to very good	No	Drainage Galley	< 0.1 l/s	28	No
D	14 m	Very good	No	Drainage Galley and Drain Curtain	Not visible	19	No

* Explanation: PP = Pore Pressure, and WL = water level

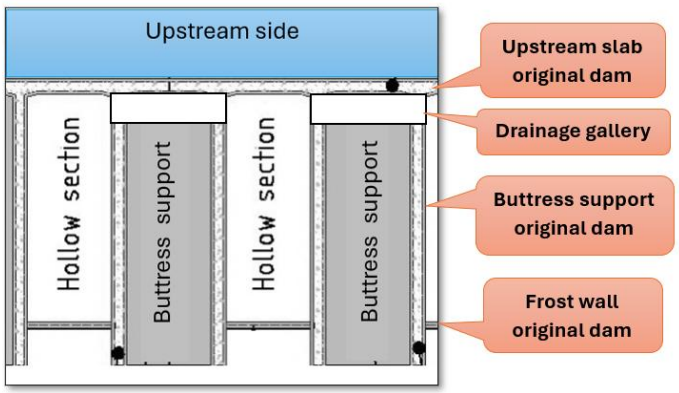


Figure 7. Plan view - typical outline of Dam C and D

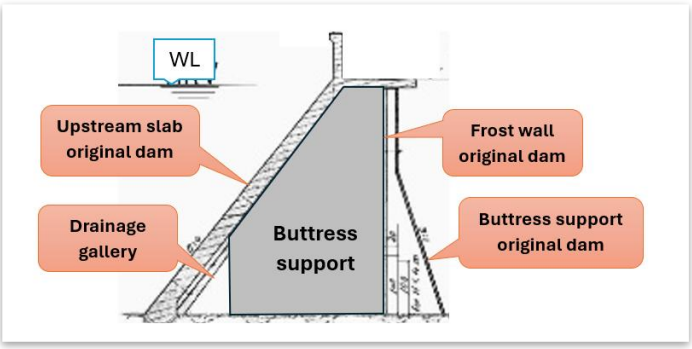


Figure 8. Dam C and D; Section through the buttress (cast between the supports in the old dam)

Placement of piezometers

Dam A

Under the bottom gate of dam A, the sensors were placed in a grid as shown below. The grid consists of 2 lines (L1 and L2) along the dam axis, and 3 lines perpendicular to the dam axis (B1, B2 and B3). In general, the sensors were placed to measure the pore pressure in the rock-/concrete interface (0-0,5 m under the foundation). In each end of Line L1 there were also 3 piezometers at the depth 1,5 m, 3,0 m and 4,5 m.

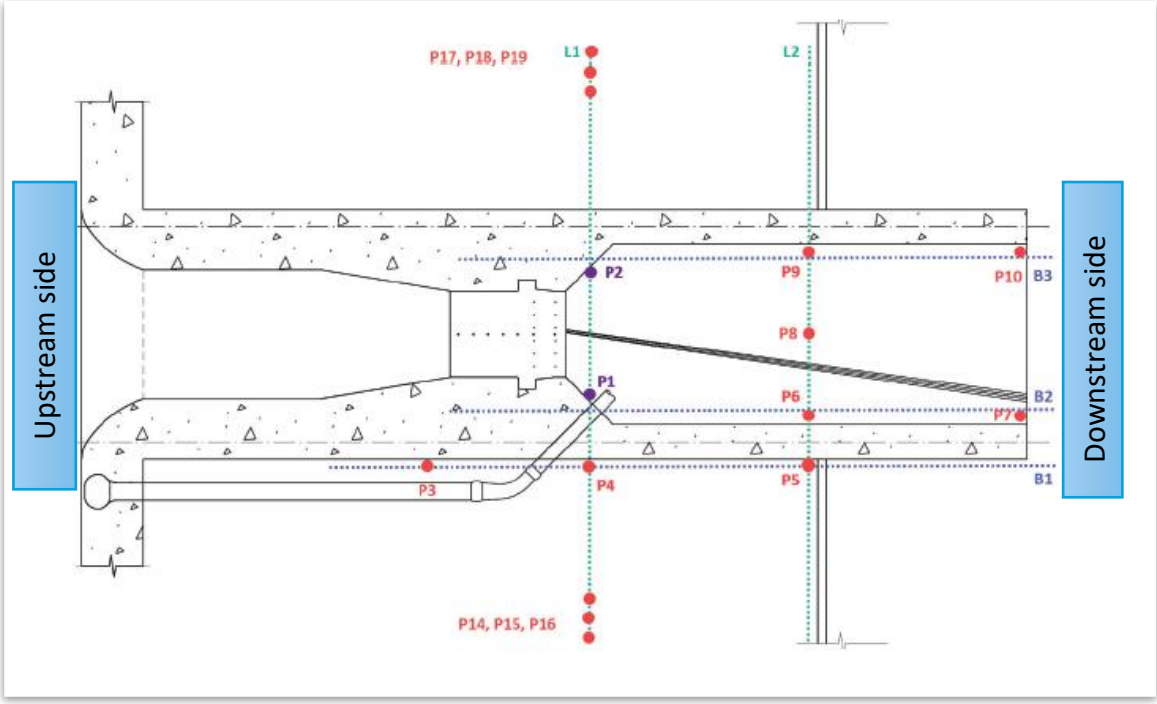


Figure 9. *Plan view of the bottom gate section with the 16 sensors along 5 axes, B1, B2, B3 and L1 and L2. Upstream side is to the left and bottom gate in the middle.*

Dam B, C and D

Installation of the sensors are similar for dams B, C and D.

All the sensors were placed 1 m under the bedrock surface and under the buttress support. The pore pressure measured can therefore be considered as representative for the upper part of the foundation close to the rock-/concrete interface. There number of piezometers under each support are in general 2 or 3. The placement of sensors in all the dams was done without a geological mapping which would have increased the likelihood for intersecting a joint with pore pressure.

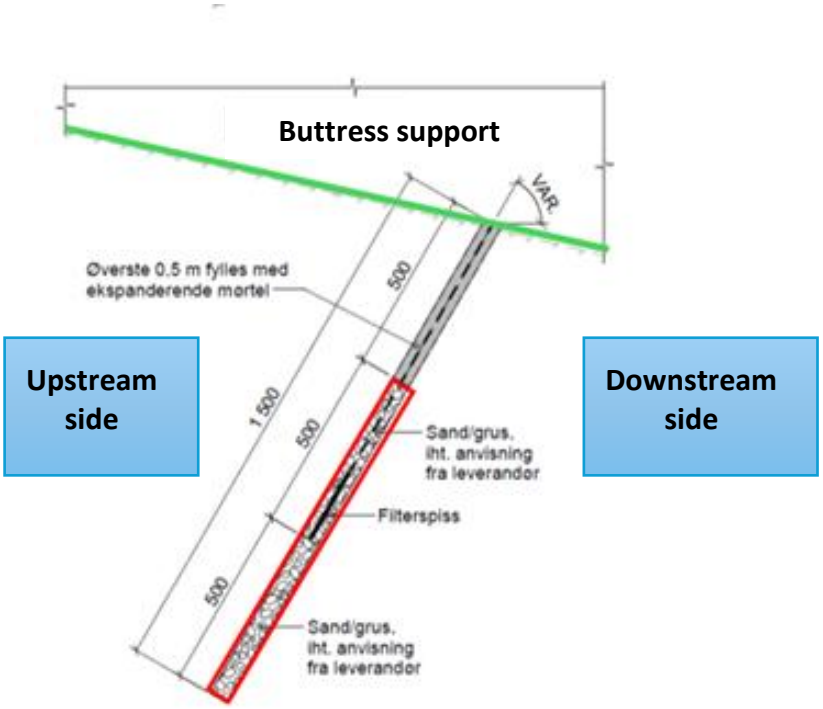


***Figure 10**. General layout of boreholes in foundation for piezometers in dam B, C and D. The pizometers are placed in 1,5 m deep boreholes is tilted 45^{o} to the upstream side.*

Assessment of the measurements

Water flow in rock a joint is rarely evenly distributed, but rather concentrated in certain sections (flow channels). This means that monitoring of a borehole intersecting a fracture with water does not necessarily display any joint water pressure. It also means that estimating the resultant joint water pressure based on the maximum monitored value will give a gross over-estimation. On the other hand, if a piezometer borehole does not intersect a water leading section of a fracture, no water pressure will be measured.

Drainage gallery directly downstream the buttress slab eliminates pore pressure under the buttress support. This also applies for very wide buttress support. This is shown by the measurements from dam B, C and D;

- No pore pressure was detected by the 71 piezometers installed in the dams with an upstream drainage gallery.
- This applies to dam B with a slender buttress supports and dam C1, C2 and D with a “very wide” buttress supports (6 m wide).

The decision to install piezometers in rock foundations should be based on an evaluation of the rock mass and should only be installed if this evaluation concludes that pore pressure can be a potential issue regarding stability. If piezometers are deemed necessary, their placement should be guided by geological mapping conducted by an engineering geologist to ensure the sensors are positioned in cracks that may cause unwanted uplift.

Given the potential for errors associated with piezometers and sensor data, structural safety should not rely solely on instrumentation. However, instrumentation can be highly valuable for assessing long-term structural behavior.

ENGINEERING GEOLOGICAL MAPPING

Based on literature reviews and experience from rock mapping, the investigation procedure for the foundations of the case dams, was based on the following steps:

1) Mapping of rock types and discontinuities like faults, joints and fractures, with subsequent plotting of discontinuities and analysis in stereographic projection.
2) Schmidt hammer testing for subsequent rock strength estimation.
3) Classification of rock mass quality based on the RMR-method (Rock Mass Rating).

This procedure is believed to be a good option for dam foundations in general. Regarding classification of the rock mass, the RMR-method is believed to be the best alternative for dam foundations because of its high number of relevant parameters included in the mapping, and its correction factor for foundations. RMR classification provides an objective characterization and may also be used as a guideline for what should be considered as “good bedrock” according to the Norwegian Dam safety Regulations (Energidepartementet 2009).

The stereographic projection technique is very useful for many purposes related to dam foundation considerations, such as evaluation related to stability/risk of sliding and finding optimum direction of boreholes, i.e. for grouting, drainage and piezometer-placement. Illustration of the stereographic projection technique is shown below

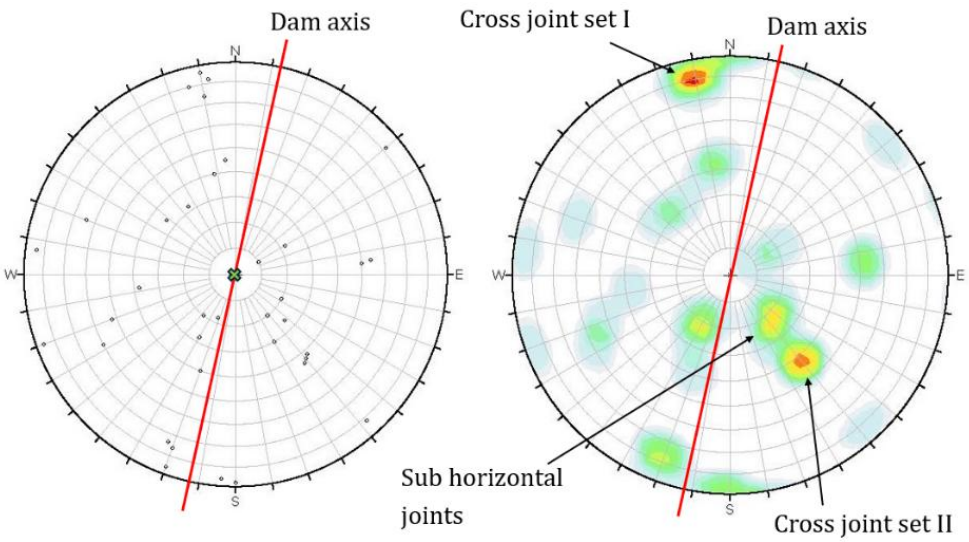


Figure 11. *Illustration of stereographic presentation. Indication of the dam-axis is important, as the orientation of joints relative to the dam axis is important to identify critical joints.*

A summary of the engineering geological conditions of the five damsites is shown below. The green line shows the orientations of piezometer drillholes.

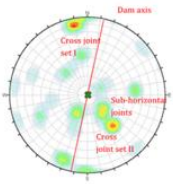
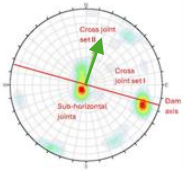
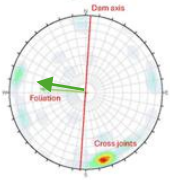
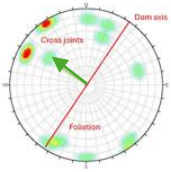
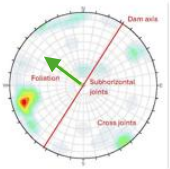
Pole plot / Direction of piezometer BH	A	B	C-1	C-2	D
					
Rock type	Gneiss, granitic and migmatitic	Syenite	Amphibolite/ gabbro	Amphibolite/ gabbro	Rhyolite
R_L => ~UCS (MPa)	140-300	220-280	As for C-2 approx.	110-155	Approx.100-250
RMR	44-82	51-76	78-83	88-94	82-83
Designation	Fairly good to good/very good	Fairly good to good	Good til very good	Very good	Very good

Figure 12. Summary of engineering geological investigations of the 5 dams. Green arrows indicate direction and inclinations of piezometer drillholes.

For the main joint sets illustrated in the above figure**Błąd! Nie można odnaleźć źródła odwołania.**, it can be concluded that the orientations of the piezometer drillholes have been quite favorable for dam A, B and C2 (i.e. fairy perpendicular to a main joint set), and less favorable for dam C1 and D. The stereographic projection technique will be particularly valuable in connection with planning of new piezometer holes. The lengths of the monitoring sections of piezometer boreholes have been only 0,5 m in most cases. This is short when the typical fracture spacing for most of the dam sites is in the range of 0,6-2,0 m.

Thus, with short piezometer drillholes and orientations as shown in Figure 10, the probability of intersecting water bearing fractures has been quite small, and it is not surprising that so many of the holes have been dry. To increase the probability of intersecting water bearing joints, the direction of boreholes should be based on data from joint mapping, and the lengths of piezometer drillholes should be increased beyond 2 m.

SUMMARY

The paper is based on a report from 2025, with the title: “Pore pressure and concrete dams”. The report was financed by Norwegian dam owners through Renewables Norway (Fornybar Norge) and the ongoing dam safety project, DSHP.

The report evaluates results from 87 piezometers of five buttress dams, and the main findings are:

- Drainage immediately downstream the buttress slab will eliminate the pore pressure under the buttresses downstream the slab, even for very wide buttresses. There was no sign of pore pressure connected to the reservoir in any of the piezometers installed in the buttress dams with an upstream drainage gallery.
- Stability calculation of foundations should be based on a geologic evaluation of the rock mass. Stereographic projection and rock mass classification according to the

RMR system have been found to be best suited technique for geological characterization of dam foundations.

- Drainage curtains are the most efficient way to control pore pressures in the foundation. It is important to note that drainage holes in a drain curtain will need to be checked and cleaned/flushed at regular intervals, as the holes can be clogged by fines and minerals in the bedrock.
- If piezometers are to be installed, the installation should be based on a geologic evaluation. The placement, inclination and depth of the borehole and placement of the piezometer must be carefully identified from a geological mapping. Random instrumentation of rock foundation is of little value.

The report is also available in English and can be downloaded here: DSHP - Pore Pressure and concrete dams

REFERNCES

Dr. techn. Olav Olsen. 2026. «Fornybar Norge.» *Fornybar Norge/Forskning og utvikling/DSHP/Rapporter for poretrykk under betongdammer.* 19 January. https://www.fornybarnorge.no/forskning/forskningsprosjekter/produksjon/dshp/rapporter-for-poretrykk-under-betongdammer/.

Energidepartementet. 2009. *Forskrift om sikkerhet ved vassdragsanlegg (Damsikkerhetsforskriften).* Oslo: Energidepartementet.

EPRI. 1992. *Uplift Pressures, ShearStrengths and Tensile Strengths for Stability Analysis of Concrete Gravity Dams, Vol. 1.* Denver, Colorado: Electic Power Reserch Institute.

M. Abdi (KTH), D. Nitzimanis (KTH). 2022. «Numerical simulations of pore pressure on concrete buttress dams.» Stockholm: KTH.

NVE. 2026. «nve.no/energi/tilsyn/damsikkerhet/regelverk/.» *nve.no/energi/tilsyn/damsikkerhet/regelverk/.* https://lovdata.no/dokument/SF/forskrift/2009-12-18-1600.

P. Obernhuber, F. Perner. 2009. «Arch Dam Analysis Using the Zillerground Dam as an Example.» *ICOLD Congress 2009.* Brasilia: ICOLD. Q90 - R 25.

USACE/ERDC. March 2002. *Assessment of Geology as it Pertains to Modeling Uplift in Jointed Rock: A Basis for Inclusion of Uncertainty in Flow Models.* US Army Corps of Engineers, WilliamL. Murpy, Robert M. Edeling, John M. Andersen.

Sarah Thomas, Project Director, GHD, Sarah.Thomas@ghd.com

Justin Hodgkinson, Design Manager, GHD, Justin.Hodgkinson@ghd.com

Ben Jones, Associate Engineer, AtkinsRéalis, Ben.Jones@atkinsrealis.com

Resilience by Design: Access and Maintenance at Havant Thicket Reservoir

Odporność przez projektowanie: Dostęp i konserwacja przy zbiorniku Havant Thicket

Abstract

Portsmouth Water's Havant Thicket Reservoir — the first new UK reservoir in several decades — provided a rare opportunity to embed long-term operational resilience directly into the design of a major water asset.

The project team drew on lessons learned from operational sites across the region, prioritising future maintainability, adaptability, and safe access.

These insights informed a systematic, innovation-led approach that integrated access, lifting, and maintenance considerations throughout all design stages.

Keywords: Reservoir, access, maintenance, design, resilience, 3D modelling

INTRODUCTION

Havant Thicket Reservoir is an environmentally-led project designed to protect two world-renowned chalk streams, the Rivers Test and Itchen, in Hampshire, on the south coast of England. It is being delivered by Portsmouth Water, to provide water storage for supply to Southern Water customers in times of drought.

It is the first major new UK reservoir to be delivered in over 30 years. Under current plans, the reservoir capacity of at least 8,700Ml will be filled with water from the Bedhampton Springs and will enable up to 21Ml/d to be supplied to Southern Water customers.

Outline design phase for planning application

AtkinsRéalis was appointed Principal Designer for the outline design of Havant Thicket Reservoir by Portsmouth Water (PW) in summer 2019, with a programme to provide a design for inclusion in a planning application in August 2020. This process began with a set of Inception Reports, which were similar to desk studies but which outlined the options for variations to a previous feasibility design produced by Arup in 2009.

These options included re-alignment of the embankment, development of a secondary embankment to retain a wetland within the reservoir, the relocation of the main embankment culvert away from the valley bottom to be founded on London Clay, and the rearrangement of the control house layout to allow better access for maintenance of pipes and valves within the culvert.

Each set of options was presented as an approval request for a Key Technical Decision to a Working Group, which was formed of the PW Engineering Manager, PW Operations leads including network managers, and PW environmental managers. These presentations included 3D models in CAD and Navisworks, outline design drawings and architects' models, especially for the latter element of the control house layout.

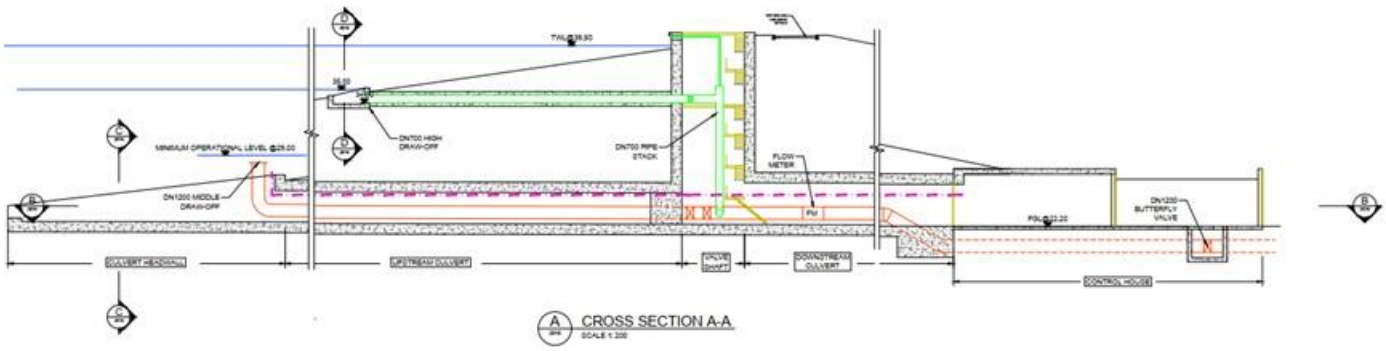


Figure 1. AtkinsRéalis outline design reservoir culvert, valve tower and control house: cross section

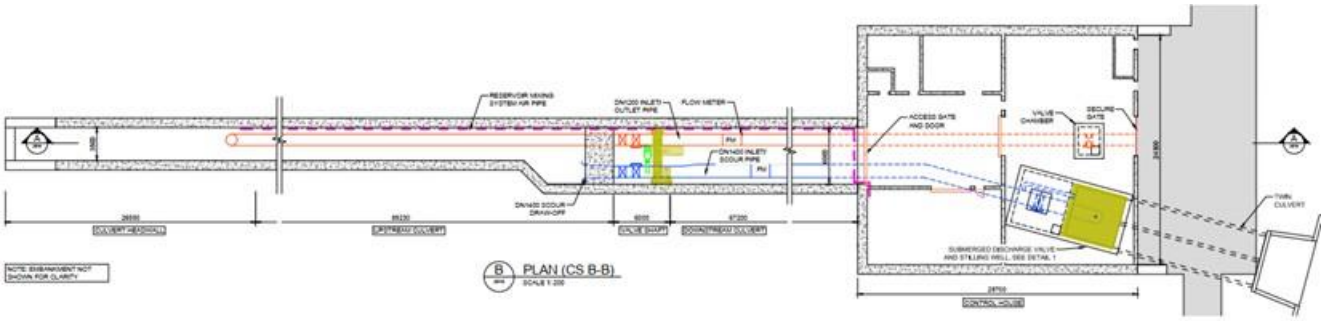


Figure 2. AtkinsRéalis outline design reservoir culvert, valve tower and control house: plan GA

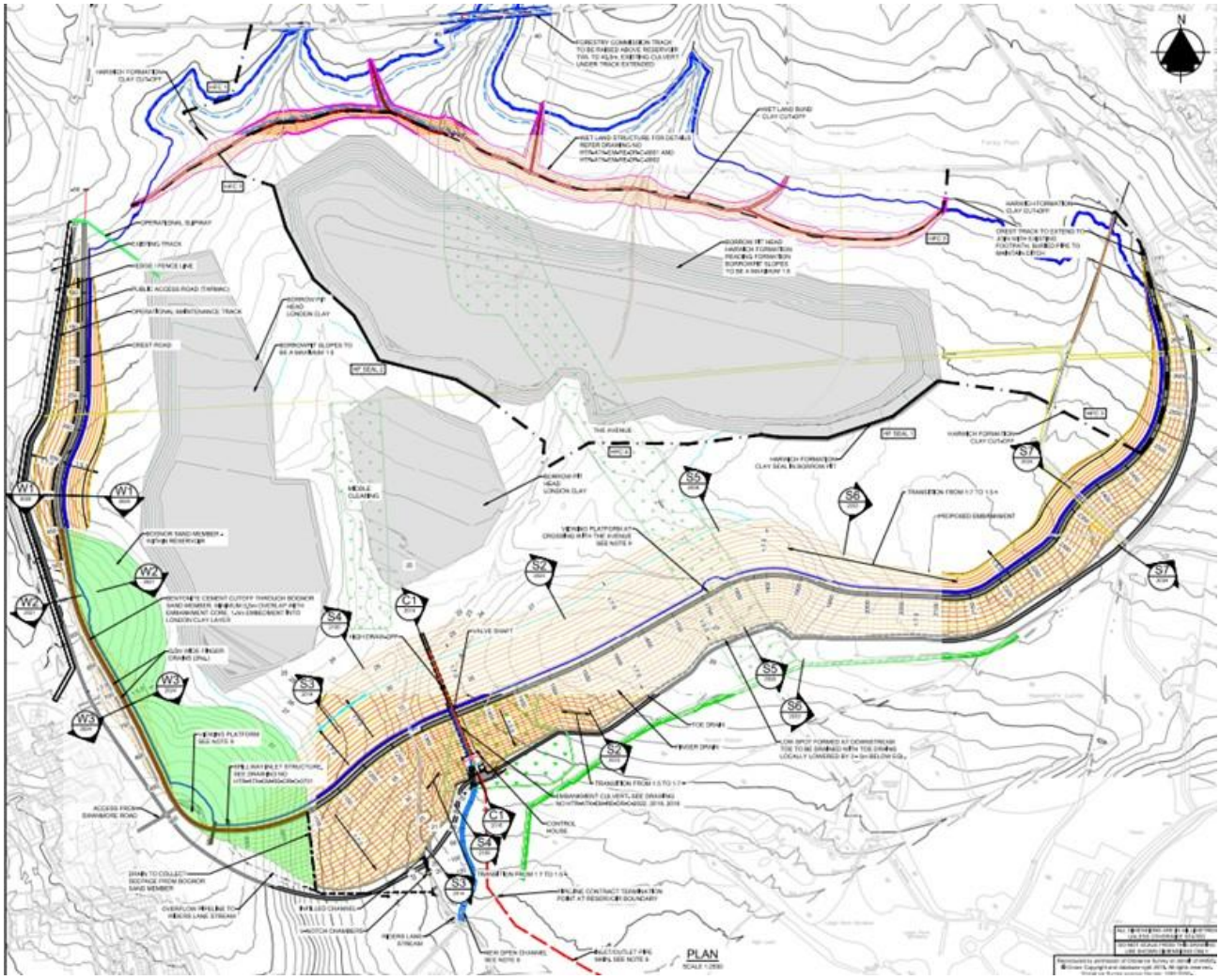


Figure 3. Outline design reservoir GA plan by AtkinsRéalis, showing main embankment, culvert (section C-1), wetlands retaining embankment and borrow pits (in grey)

These Working Group sessions, along with early Hazard and Operability Studies (HAZOPS) and Access, Lifting and Maintenance (ALM) Strategy sessions, were used to agree maintenance, access and lifting strategies, the key parts of which were:

– **Pipes sections / spools could be lifted from inside culvert using a trolley.** The culvert invert was to slope downstream to merge with the control house courtyard access level, which was to be level with the existing ground at that area. The concept for this was that a Hi-Ab (a truck-mounted crane) could be driven into the CH courtyard area from the access road outside of the dam slope, and get as close as possible to the culvert end, from where pipes sections would be brought out. (The sizing of the Hi-Ab, with an extended crane arm, therefore determined the

height to the control house roof slab soffit, so that the Hi-Ab could be driven inside the building and lift pipes.)

- The use of a ceiling-mounted gantry, for lifting out pipe sections within the culvert, was discounted at this point, due to the extra requirement for regular maintenance of the gantry which would be rarely used. (This decision was changed later in the detailed design phase for reasons discussed in the section on detailed design.)
- **Valves could be lifted out of the valve shaft by a large mobile crane** to be seated on the embankment crest. (This led to inclusion of the embankment loading condition of the crane, plus a large diameter gate valve, in the client's requirements in the Scope.)
- **The submerged discharge valve (SDV)**, **could be lifted out of the deep chamber in the control house courtyard by another crane sat outside the control house compound walls.** (The SDV is for controlling and dissipating the energy of emergency drawdown discharge flows, is likely to weigh over 21 tonnes, and is located in the control house courtyard.)

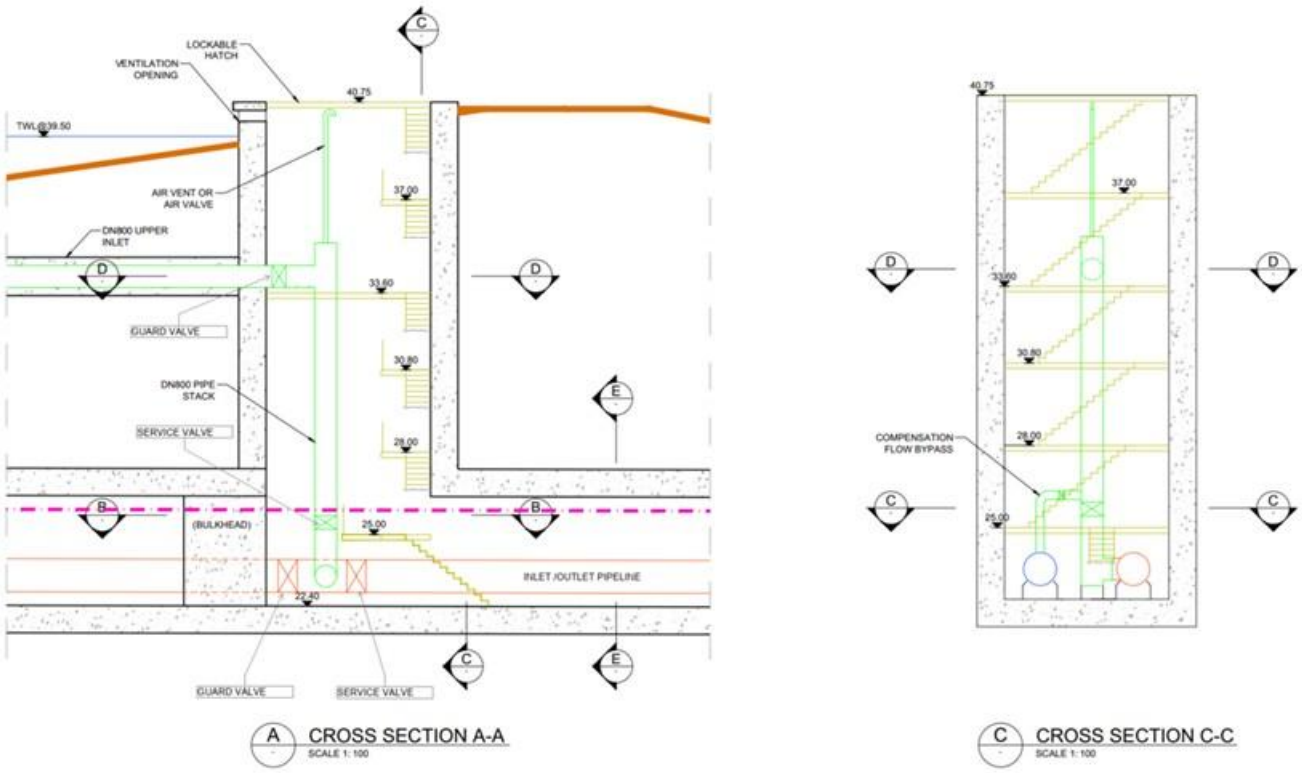
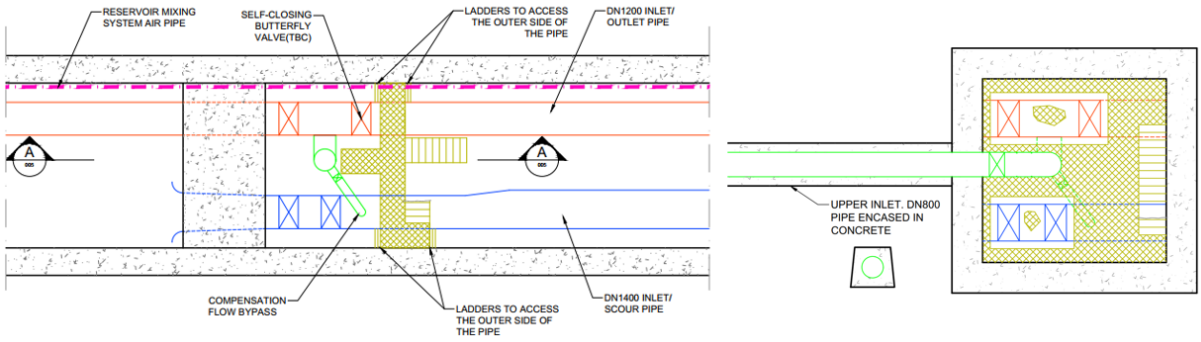


Figure 4. Valve access shaft sections



Plan at base (culvert invert level)
Section B-B

Plan at landing at upper outlet level
Section D- D

Figure 5. Valve access shaft plans

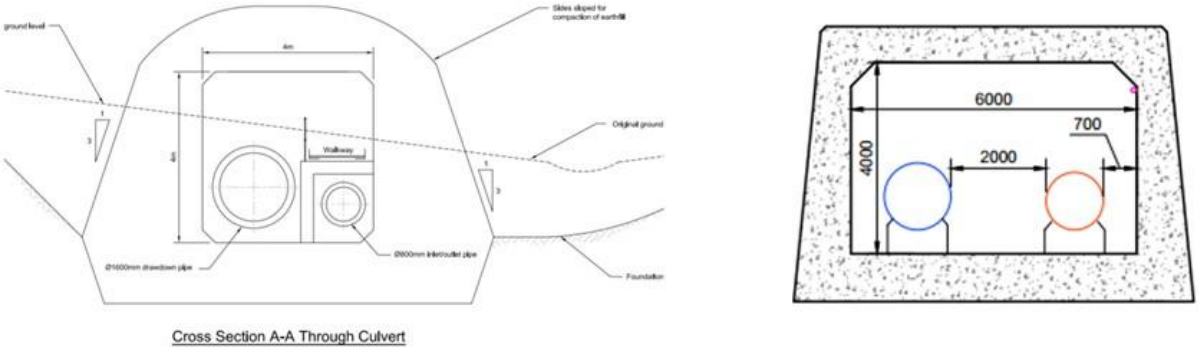


Figure 6. Proposed change from Arup design culvert 4m x 4m (left) to 6m x 4m allowing pipe sections to be moved between scour and inlet/outlet pipe (right)

Isolation of upstream guard valves in the valve tower, to allow their replacement or refurbishment, was considered during the outline design. It was acknowledged that this operation would be difficult, especially with the reservoir remaining full, although likely to be very rare (potentially once in the 100 year design life of the reservoir). It was assumed that, as the upstream half of the culvert was level with the existing ground level, any future valve isolation /replacement works could be planned to include a ROV operated by a diver, following the recent example of Talybont Reservoir, Wales (for the client, Dyr Cymru Welsh Water, 2019 [i]) where a bespoke robot was specially designed to run inside the flooded upstream culvert to the bulkhead to place a 'top hat' (isolation box) against the bellmouth of the outlet intake.

(In the detailed design phase, the culvert level has had to be dropped around 5m below natural ground level, with a raised intake / box structure at the upstream end. This has necessitated a rethink of how the upstream guard valves can be isolated, to improve

operational resilience. This process is currently ongoing and may lead to a change in design of the top half of the lower intake structure.)

The outline design informed the planning application, which was produced by AtkinsRéalis for Portsmouth Water to submit to the two local planning authorities in August 2020.

The outline design by AtkinsRéalis was included in the Invitation to Tender ITT package for the Main Reservoir Works (MRW) contract along with a Reservoir Design and Operations Report which explained the various decisions made up to that point including the access and maintenance strategy. Sections / summaries from the RD&OR, and the Embankment Stability Design Report, were then taken into the client's requirements document, which became known as the Scope Support Document and included performance specifications. This document was appended to the MRW Scope.

The outline design drawings then became known collectively as the 'reference design' which was assessed and incorporated into a tender submission by the MRW contractor in January 2022, with one major change to the reservoir structural layout, to be outlined in the next section.

[1] **Cotter, Bush, Woollcombe-Adams and Edwards, 2019, "Talybont Reservoir – innovations in pipework replacement", British Dam Society evening meeting presentation, at the Institution of Civil Engineers, London.**

Detailed Design

The Construction and Detailed Design phase of Havant Thicket progressed from an initial opportunity pursuit in early 2021 and Future Water MJJV (Mackley Jones Brothers Joint Venture) was appointed as the Design & Build contractor by 2022. Following this, GHD was first engaged to deliver the enabling works package. This enabling works package was key as design was able to begin whilst mobilization from FUW was occurring. In 2023, GHD's role expanded significantly with appointment to deliver the detailed design for the main reservoir works, forming the core of the project's design phase.

During the enabling works and detailed design phases, GHD undertook a comprehensive review of the outline design in alignment with Future Water (FUW), Portsmouth Water (PW) and AtkinsRéalis. This review coupled with additional investigations carried out post mobilization resulted in some key design changes.

Key design changes from the outline design to the current design are attributed to unfavourable geotechnical conditions identified during further ground investigations. The key changes include:

- Slackening of the embankment slopes resulted in overall lengthening of the upstream and downstream culvert.
- The culvert's founding levels had to be lowered, resulting in a control building with a basement level where it intersected with the culvert.
- The valve tower had to be located further away from the clay core into the reservoir basin, resulting in a significant change to the proposed access for maintenance and personnel.
- The overall profile of the culvert was changed from square to an arch and the valve tower was changed from square to circular to lower the geotechnical/structural interface stresses.

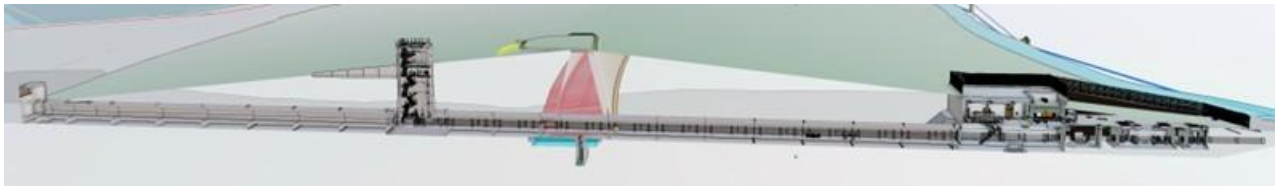


Figure 7. Slackened embankment resulting in longer culverts

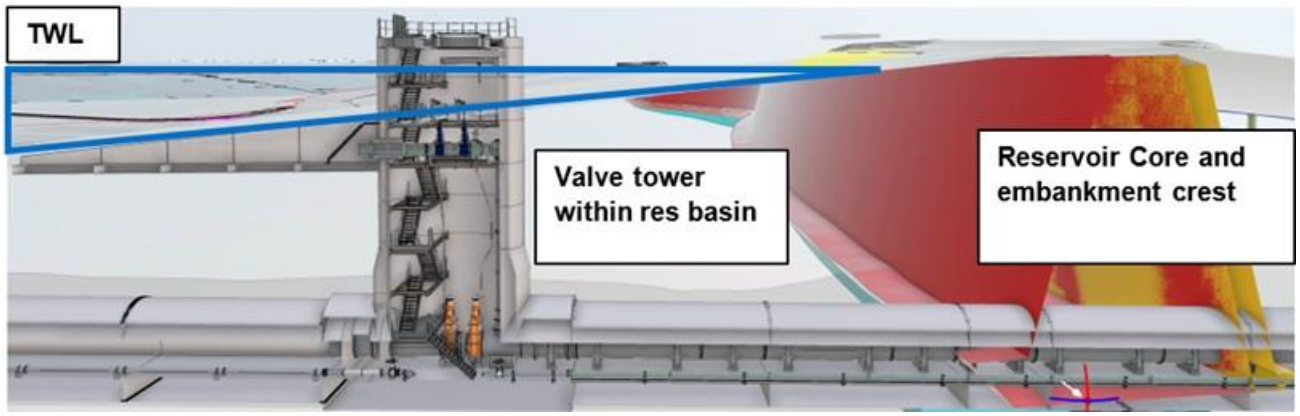


Figure 8. Valve tower relocation further within basin (reservoir to the left, embankment core on the right)

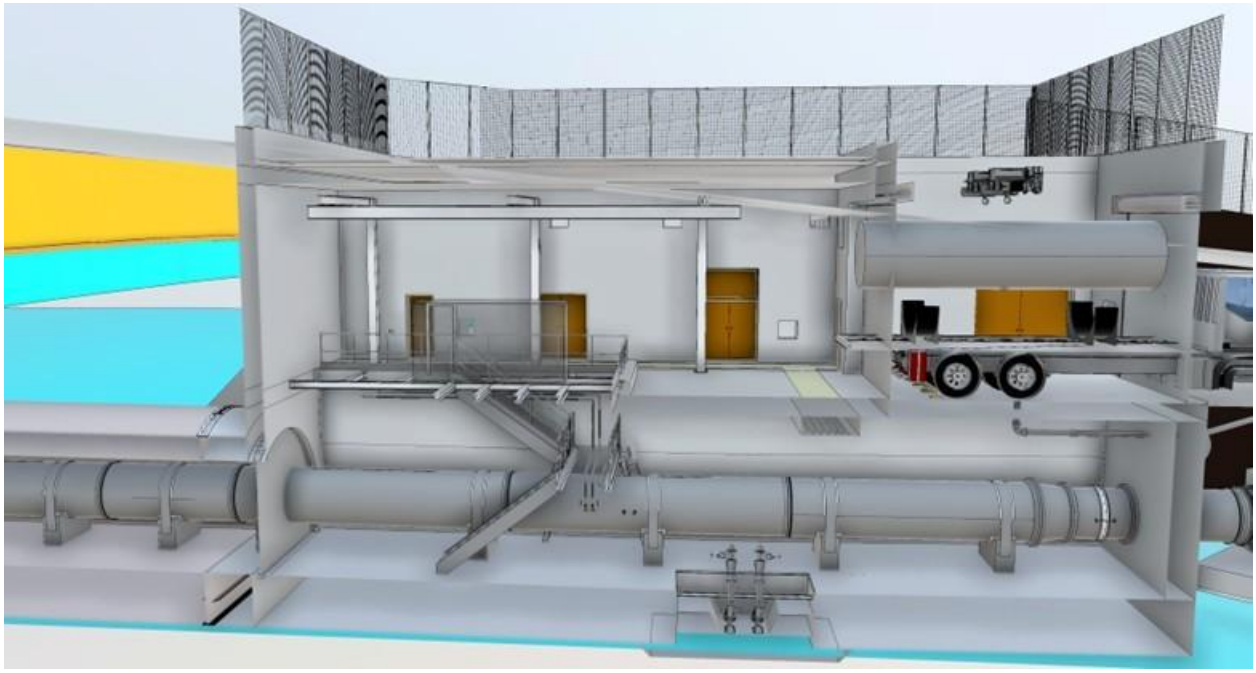


Figure 9. Two storey control building with culvert intersection within a lower basement

With the significant amount of change, the primary focus was to ensure the new arrangement would meet modern safety, access, lifting, and maintenance requirements. Extensive hazard and operability (HAZOPs), and access lifting and maintenance (ALMs) workshops were held to systematically ratify the design. The key focus is to eliminate hazards where reasonably practical by reduction through design, minimising the reliance on procedural controls.

The key tool in meeting the risk reduction requirements is the federated Revit model which served two core purposes:

1. Design tool allowing spatial analysis of structure and full interdisciplinary co-ordination and clash detection.
2. Visualisation tool during HAZOPs, ALMs and other key studies to allow stakeholders a deeper understanding of the design in a short duration.

Based on the numerous studies the following key design changes were implemented to ensure safety in design and ease of maintenance asset near the end of their design life.

– Removing pipework from the abstraction culvert to eliminate submerged pipework within the basin, eliminating maintenance on submerged pipe work.
– Introducing a means to isolate the upstream culvert to allow safe removal of guard valves while the reservoir is still full. This included redesigning the lower intake to facilitate the installation of an isolation plate (from a boat, and potentially using either divers and/or robots) and then mechanical means to both drain and then fill the culvert before and after maintenance.
– Moving the valve tower further into the reservoir basin complicated access to remove the critical guard valves. A platform was incorporated within the embankment to allow a suitable crane to park on the embankment and lift the 11 tonne valves through strategic openings in the valve tower top.
– A gantry crane was reintroduced, into the control building, that can lift a pipe section from the lower basement directly onto a reversed truck, and similarly a new pipe section can be lowered onto the trolley system in the lower basement to be transported to repair site.

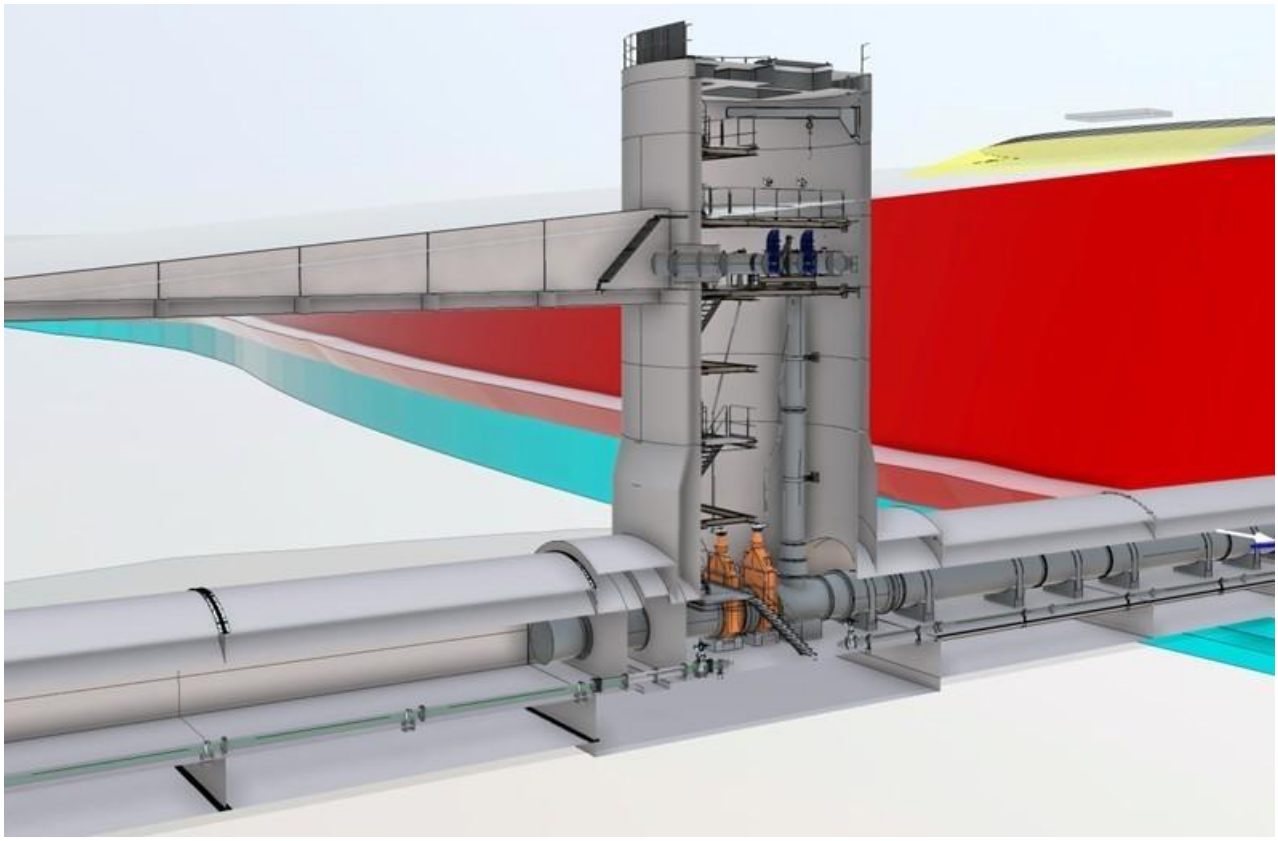


Figure 10. All mechanical pipework was removed from upstream culvert reducing maintenance requirements.

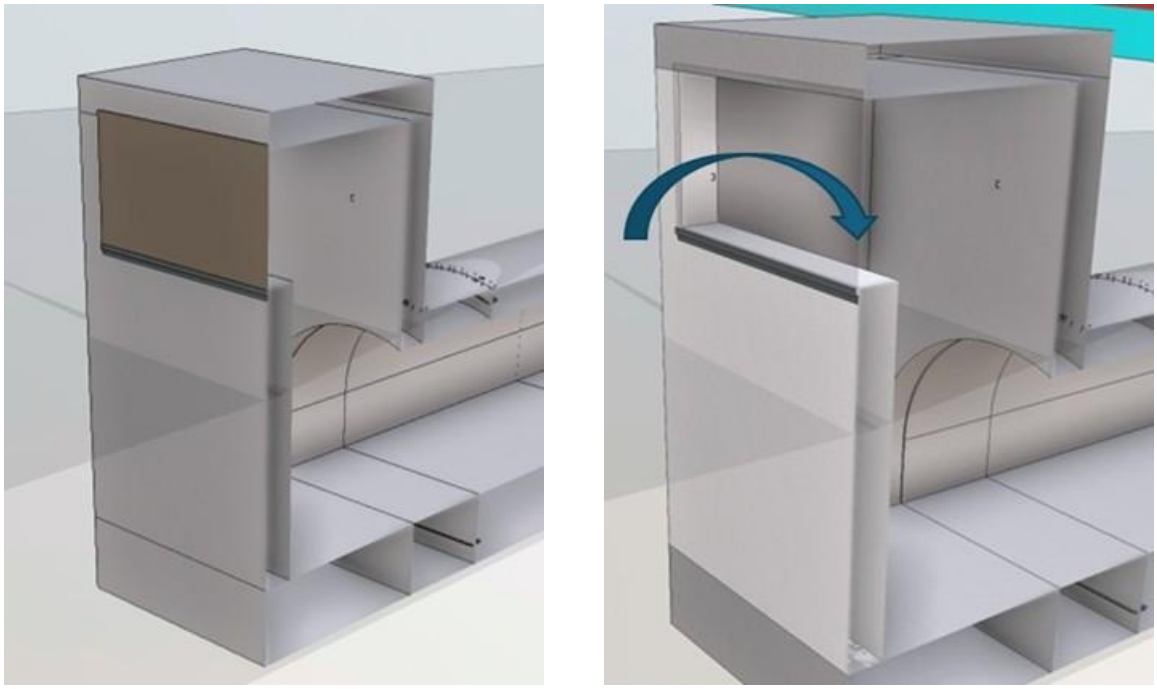


Figure 11. Redesigned lower intake to simplify installation of isolation plate by divers

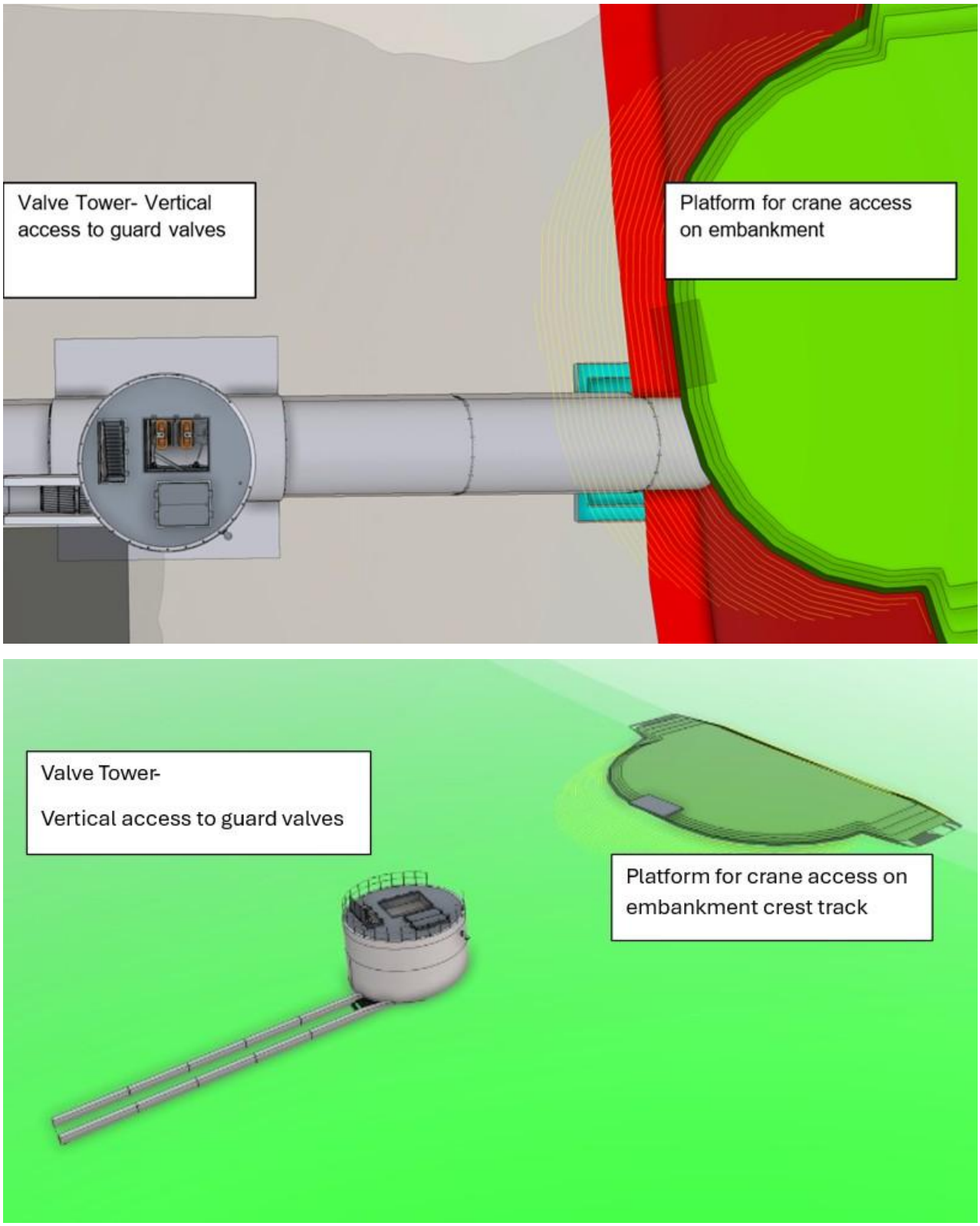


Figure 12. Crest track platform for crane to facilitate removal of key guard valves if required

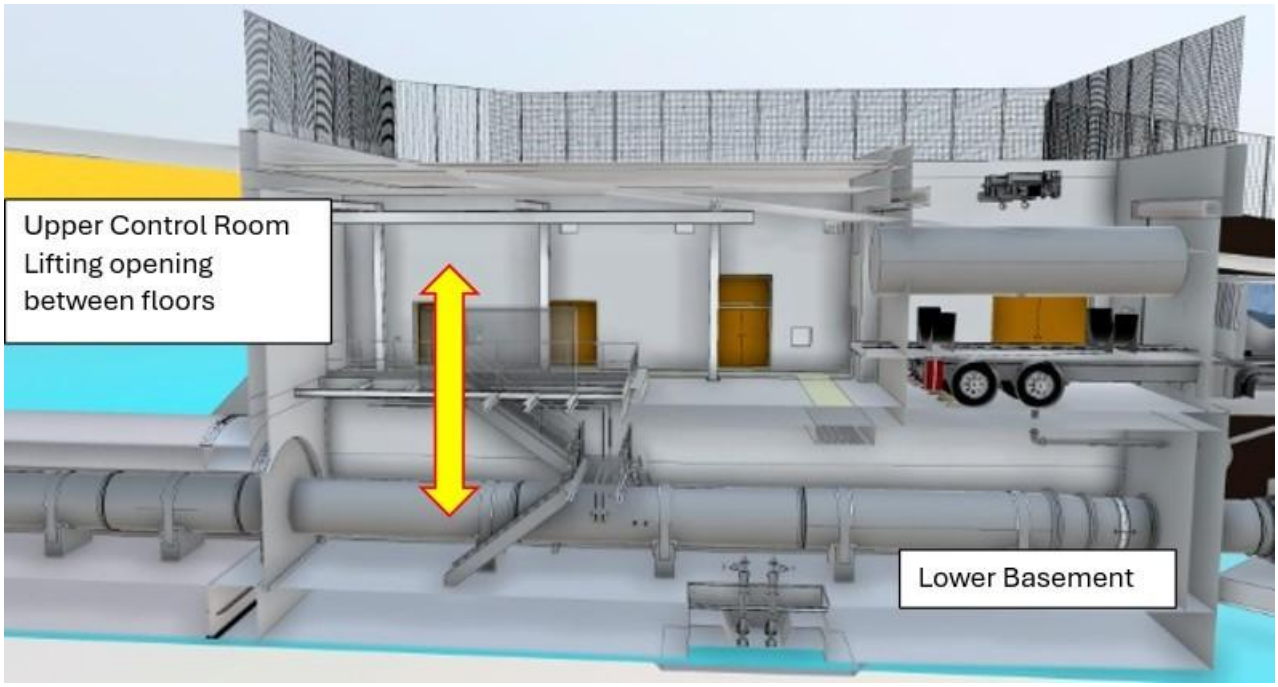


Figure 13. Gantry crane to simplify lifting from lower basement into upper control room

Conclusion

The design of the Havant Thicket Reservoir ultimately demonstrates how robust, adaptable engineering can respond to uncertainty while strengthening long-term operational performance. Faced with significant geotechnical constraints and fundamental layout changes, the project team did not simply adapt the design to accommodate these challenges—they used them as an opportunity to re-test and enhance the asset's maintainability, safety, and resilience over its full design life.

The detailed design also reflects a clear shift towards designing for end-of-life interventions from the outset. Features such as embankment-integrated crane platforms, accessible valve removal strategies, and maintainable culvert configurations demonstrate a practical understanding of the realities of operating large water assets over decades. These solutions go beyond compliance, embedding operational foresight directly into the infrastructure.

Importantly, the iterative collaboration between GHD, Future Water, Portsmouth Water, the Construction Engineer (from Binnies) and AtkinsRéalis ensured that lessons from both legacy assets and the evolving site conditions were captured and translated into tangible design improvements. This integrated approach has resulted in a safer, more maintainable and more resilient reservoir than originally envisaged at outline stage.

In summary, Havant Thicket Reservoir sets a strong precedent for future reservoir schemes by demonstrating that detailed design is not simply a process of refinement, but a critical stage for embedding long-term asset performance. By prioritising operational resilience, maintainability, and safety through design-led solutions, the project establishes a benchmark for how complex infrastructure can be delivered with a clear line of sight to its whole-life requirements.

SESSION C (part II). Dam Engineering and Construction		
1	Fredrik Tunberg, Ludvig Emgård	Lighting the way: Sub-millimeter crack detection through high-resolution texture mapping in GPS-denied dam structures
2	Krzysztof Radzicki	Innovative Polish Solutions for Monitoring, Seepage Control, and Foundation Engineering of Earth Dams
3	Emmanuel Robbe	Monitoring Strategies for Swelling Concrete Dams: Practices and Perspectives

Katarina Nylander, MSc in Computer Science, Spotscale AB, Storgatan 42, 582 23 Linköping, Sweden, katarina.nylander@spotscale.com

Pär Ljustell, PhD in Solid Mechanics, Kiwa Technical Consulting AB, Box 7178, 170 07 Solna, Sweden, par.ljustell@kiwa.com

Lighting the way: Sub-millimeter crack detection through high-resolution texture mapping and AI in GPS-denied dam structures

Abstract: Internal dam inspections face lighting and access hurdles, causing fragmented data. This paper presents a methodology using high-resolution 3D digital twins for desktop inspections. At the Storfinnforsen dam, 300,000 images were processed to reconstruct surfaces with sub-millimeter precision. Integrating photogrammetry and AI allowed experts to annotate cracks down to 0.2 mm over 3,100 m². Documenting all surfaces, including intact concrete, creates a comprehensive baseline for future analysis, supporting a proactive and non-destructive asset management strategy.

Keywords: Structural Health Monitoring, Unmanned Aerial Vehicle (UAV), Deep learning, Photogrammetry, Crack detection, Concrete dam

INTRODUCTION

Structural Health Monitoring (SHM) plays a crucial role in ensuring the safety and longevity of critical infrastructure. The global inventory of large dams is experiencing a notable aging trend, with over 26% of the world's registered large dams constructed before 1975 (Fell 2015). This demographic shift introduces progressive degradation mechanisms, including concrete carbonation, reinforcement corrosion, and freeze-thaw erosion. Historically, dam

safety evaluation has relied upon manual visual inspections and discrete contact-based instrumentation. However, these conventional methods are labor-intensive, time-consuming, and pose severe safety challenges, particularly when accessing steep concrete faces, high spillways, and confined internal galleries that necessitate risky fieldwork involving scaffolding (Choi et al. 2023). This often results in fragmented, paper-based reporting that makes tracking structural integrity over time challenging (Leite et al. 2025).

To address these operational bottlenecks, there has been a paradigm shift toward automated SHM utilizing Unmanned Aerial Vehicles (UAVs) equipped with multi-modal sensor payloads (Villarino et al. 2025; Liang et al. 2023; Simplicio and Pereira 2025). UAVs act as a disruptive innovation, offering a flexible, non-contact data acquisition platform that captures high-resolution visual data across vast and complex hydraulic surfaces. Rotary-wing platforms, in particular, are preferred for close-range inspections of steep dam faces and confined spaces due to their hovering capabilities and maneuverability. Coupled with advancements in computer vision, specifically close-range photogrammetry and Structure from Motion (SfM) algorithms, UAV-acquired imagery can be transformed into metrically accurate, high-resolution 3D point clouds and digital twins (Khaloo et al. 2018).

Processing the massive imagery datasets collected by UAVs requires robust analytical tools. Before the rise of deep learning, traditional image processing techniques such as Canny and Sobel edge detection algorithms, were widely used to identify discontinuities in pixel intensity. While straightforward, these methods are highly sensitive to noise, lighting variations, and complex surface textures, often leading to unreliable results in real-world environments (Khan et al. 2024). Recently, deep learning architectures, particularly Convolutional Neural Networks (CNNs) and object detection models, have demonstrated strong proficiency in analyzing the complexity of dam surfaces. These models can effectively distinguish actual structural cracks from complex background noise, such as mineral staining, shadow patterns, and the seams between formwork boards (Han and Gu 2025; Kannan et al. 2026).

Despite these advancements, applying standard CNNs to dam surfaces can still result in high rates of false positives. This highlights the need for synergistic workflows where AI acts as a highly sensitive detection tool that is subsequently verified by human experts (Zhao et al. 2024). In this project, the Storfinnforsen dam in Sweden was used as a case study to validate such a new digital inspection workflow. Commissioned in 1954 and operated by

Uniper, it is Sweden's largest concrete dam, consisting of an 800-meter-long buttress structure supported by 74 concrete monoliths with a maximum height of 40 meters. Over time, seasonal temperature shifts and fluctuating pressure from the water and bedrock cause the dam sections to tilt slightly back and forth. To counter these environmental variables and prevent stress patterns from causing surface cracks, the dam sections have been encased in protective cladding. While this weatherproofing creates a more stable internal climate with controlled temperature and humidity, it also forms the dark, confined gallery environments that make traditional visual inspections challenging.

To overcome these logistical hurdles and establish a reliable digital baseline for future monitoring, a remote sensing approach was adopted. This methodology enables a complete transition to desktop-based visual inspections without direct human contact with the highest-risk areas of the structure.

DATA CAPTURING IN CONFINED SPACES

To achieve detailed visual coverage in the GPS-denied and dark environments of the dam's interior, advanced robotics and drone technology were utilized. A photogrammetry-ready Scout 137 Drone System from ScoutDI, equipped with its own lighting and a tethered power supply, was deployed to navigate the confined spaces. The tether system provided both continuous power for prolonged operational endurance and a stable data transfer link.

Operators from Kiwa Technical Consulting successfully captured 300,000 high-resolution, location-tagged images of the internal concrete walls. The inspection specifically targeted two monolith bays (sections 41-42 and 42-43), covering a concrete surface area of approximately 1,550 square meters each, totaling 3,100 square meters.

To ensure high image quality, the drone utilized its integrated camera payload, featuring an 8.3-megapixel sensor with a 3.5x optical zoom and autofocus capabilities, optimally designed for confined space inspections. In photogrammetric applications, the spatial resolution of the digital model is fundamentally determined by the Ground Sampling Distance (GSD). The theoretical GSD can be calculated using the following equation:

$$\mathrm{GSD} = \frac{\mathrm{D} \cdot \mathrm{p}}{f} \tag{1}$$

where D represents the object distance, p is the physical pixel pitch of the camera sensor, and f is the focal length of the lens. Operating at a consistent distance of approximately 0.4 meters from the structure, the system achieved a sub-millimeter GSD of 0.2 mm. A summary of the key flight and sensor parameters is presented in Tab. 1.

Tab. 1. UAV flight and sensor parameters for the Storfinnforsen inspection (source: authors' study).

Parameter	**Specification**
UAV Platform	Scout 137 (Tethered)
Camera Model	ScoutDI Integrated Camera
Image Resolution	8.3 Megapixels
Lens	3.5x Optical Zoom with autofocus
Object Distance (D)	~0.4 m
Image Capture Frequency	~0.25 Hz
Ground Sampling Distance (GSD)	0.2 mm

To optimize the 3D reconstruction and damage detection, the data acquisition was divided into two distinct flight patterns. The Damage Detection Flight (DDF) focused on capturing fine details at the target GSD, while the 3D Flight (3DF) was conducted at two to four times the distance of the DDF to capture the broader structural context. The flights were conducted using automated lawn-mower paths with an image overlap of approximately 80% in the vertical direction and approximately 67% in the horizontal direction. To further increase the accuracy of the spatial reconstruction, frequent loop closures returning to previously captured points, were integrated into the flight paths, and continuous camera movement was maintained around corners to ensure stereoscopic overlap.

Since the internal galleries are completely GPS-denied, absolute scaling of the digital model was achieved using physical marker plates placed on the concrete walls. By measuring the exact distance between the circle centers on these plates, a reliable geometric reference was established for the photogrammetry software. Finally, proper camera parameter calibration, balancing ISO, aperture (f-stop), and shutter speed, combined with the drone's onboard lighting, ensured an exposure without severe motion blur or high-contrast shadows.

By deploying automated drones for this extensive documentation, the need for erecting scaffolds and performing work at height was eliminated.



Fig. 1. The tethered Scout 137 Gen 2 drone system deployed in the confined and GPS-denied gallery of the Storfinnforsen dam (*source: ScoutDI AS*).

DATA PROCESSING AND 3D RECONSTRUCTION

The captured imagery was systematically processed using Spotscale's proprietary photogrammetry pipeline, which employs advanced Structure-from-Motion (SfM) and dense matching algorithms. These algorithms are specifically optimized for handling massive high-resolution inputs and generating metrically accurate 3D point clouds. The 300,000 images were aligned to reconstruct the dam's internal surfaces into a continuous, spatially correct digital twin.

The resulting 3D model is built from a total of 93 billion pixels of high-resolution texture data. This resolution ensures that fine surface anomalies become clearly visible in the digital environment, making the models suitable for expert inspection and annotation on standard workstation computers.



Fig. 2. High-resolution 3D reconstruction of the targeted monolith bays, rendering the complete spatial context of the concrete surfaces (*source: authors' study*).

AI-ASSISTED DAMAGE DETECTION AND HUMAN VERIFICATION

Following the generation of the 3D model, an AI-based damage detection system utilizing Convolutional Neural Networks (CNNs) was applied to the original images. The machine learning algorithms analyze all available views of each pixel on the surface to detect structural features such as cracks and spallings. Modern CNN architectures have demonstrated strong proficiency in analyzing complex dam surfaces and effectively distinguishing actual structural cracks from complex background noise (Feng et al. 2025).

The system is designed with a core principle: an existing defect must not be missed, as overlooking a structural flaw carries a significantly higher risk than over-detecting non-existent ones. Because of this sensitivity, the AI may flag "false positives" triggered by specific surface characteristics, such as the texture of shotcrete or the seams between formwork boards used during the original casting.

This is where the synergy between artificial intelligence and human expertise becomes essential. The AI acts as a detection tool rather than a replacement for the engineer. The concrete expert navigates the 3D model on their screen and effectively filters out the false positives based on their understanding of damage mechanisms and concrete pathology. Each verified crack is then interpreted as a separate object and represented either as a projected raster on the geometry or as a 3D polyline along the center line (medial axis) of the crack. This allows the software to automatically determine the width over the crack's length, establishing its dimensions in 3D space with sub-millimeter accuracy.

RESULTS AND DESKTOP ANALYSIS

A significant advancement of this combined workflow is that structural experts can perform their comprehensive analysis entirely from their workstations, navigating the 3D model rather than the physical galleries. During the Storfinnforsen project, the expert successfully identified and annotated structural cracks down to 0.2 millimeters in width.

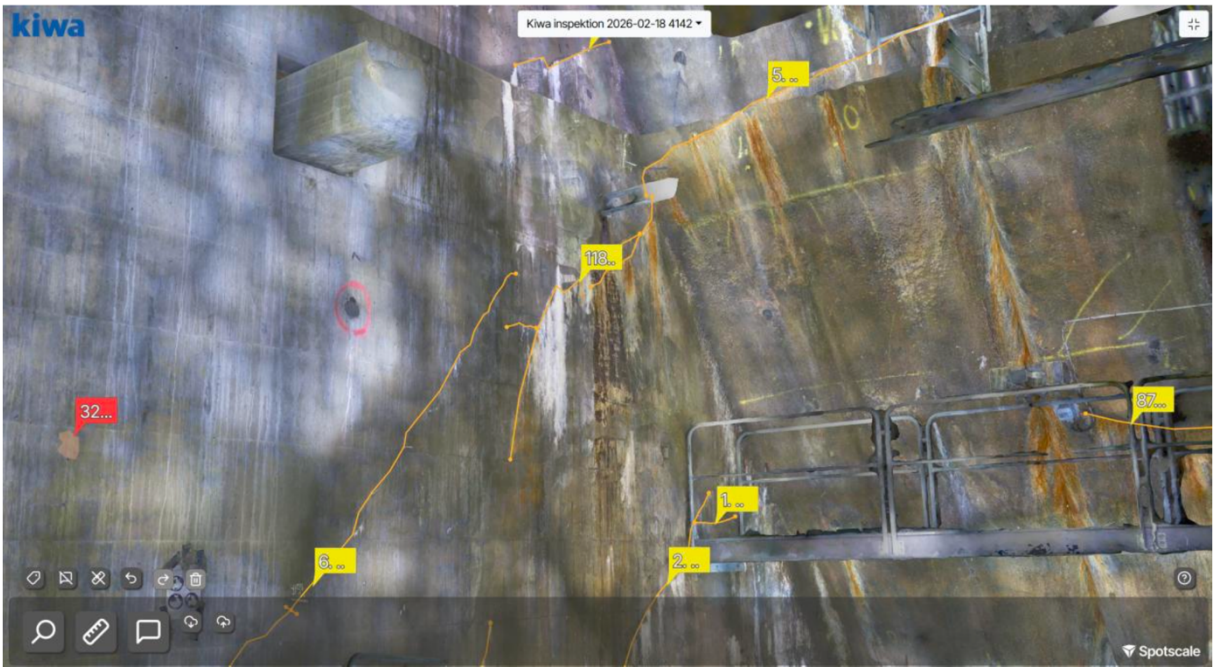


Fig. 3. The digital inspection interface displaying the high-resolution 3D model, enabling the structural expert to navigate the concrete surfaces, verify AI-detected anomalies, and log georeferenced annotations with associated metadata (*source: authors' study*).

Every observation is saved as a geospatial data point at its exact coordinate on the dam's surface within the model. Furthermore, annotations were enriched with metadata such as damage type, origin, structural component, and characteristic measurements.

A crucial advantage of this digital methodology is the complete documentation of all concrete surfaces within the sections, including the areas without detectable defects. Documenting the intact concrete creates a comprehensive "zero measurement" or reference baseline for the asset, establishing a reliable foundation for all future inspections.

DISCUSSION

The transition to UAV-based photogrammetry and digital 3D-models offers substantial operational advantages over conventional techniques. Traditional inspections of large dams are labor-intensive, time-consuming, and pose severe safety challenges, particularly in difficult-to-access areas. By deploying automated drones for extensive internal documentation, the need for erecting scaffolds and performing dangerous work at height was completely eliminated, significantly reducing operational risk.

Furthermore, the methodology addresses the inherent subjectivity of paper-based reporting. By anchoring every observation digitally within a spatially correct 3D model, engineers can return to the exact same coordinates during subsequent inspections. This enables the use of change-detection algorithms to accurately assess crack propagation or the formation of new defects over time.

Despite the clear advantages, the methodology presents certain technical challenges that must be managed. The massive imagery datasets, in this case resulting in 93 billion pixels, demand significant computational resources for both photogrammetric reconstruction and AI processing. Additionally, enclosed dam galleries are GPS-denied environments. To ensure accurate metric scaling, physical marker plates with known dimensions had to be deployed on the concrete walls to provide absolute references. Proper lighting is also critical; uneven exposure or high-contrast shadows can severely degrade the performance of both the 3D reconstruction and the AI damage detection, necessitating careful integration of onboard illumination.

From a long-term perspective, this data-driven approach contributes to a more sustainable built environment. With precise data on structural health, maintenance and repair efforts can be localized based on actual structural behavior rather than estimations. This precision minimizes material waste and maximizes the lifespan of the critical infrastructure.

SUMMARY

The combination of high-resolution drone imaging, advanced 3D photogrammetry, and AI-assisted human verification provides a complete and reliable overview of the structural condition of internal dam galleries. By anchoring every observation digitally, the methodology provides a spatially correct baseline for future comparative analysis. This level of precision significantly reduces the ambiguity previously caused by manual paper documentation. The ability to safely assess critical components without erecting scaffolds or disrupting operations broadens the application of this technology to other assets, such as highway bridges, retaining walls, and confined spaces in industrial facilities.

ACKNOWLEDGMENTS

The authors would like to acknowledge the engineering and technology partners Kiwa Technical Consulting, Spotscale, ScoutDI, and Uniper who collaborated on this project.

REFERENCES

Choi H., Kim H., Kim S., Na W. 2023. "An Overview of Drone Applications in the Construction Industry." *Drones* 7(8): 515. DOI: 10.3390/drones7080515.

Fell R. 2015. *Geotechnical Engineering of Dams*. Leiden: CRC Press.

Feng W., Cao S., Fang L., Du W., Ma S. 2025. "Crack Detection and Displacement Measurement of Earth-Fill Dams Based on Computer Vision and Deep Learning." *Sustainability* 17(22): 10186. DOI: 10.3390/su172210186.

Han F., Gu C. 2025. "Surface Damage Detection in Hydraulic Structures from UAV Images Using Lightweight Neural Networks." *Remote Sensing* 17(15): 2668. DOI: 10.3390/rs17152668.

Kannan A., Narasimhan G., Subburaj M., Sivaraman A., Sivaraman A., Velayutham K. 2026. "Automated Dam Crack Detection Using YOLOv10 and UAV Imagery for Structural Health Monitoring." *Journal of Physics: Conference Series* 3191: 012103. DOI: 10.1088/1742-6596/3191/1/012103.

Khaloo A., Lattanzi D., Jachimowicz A., Devaney C. 2018. "Utilizing UAV and 3D Computer Vision for Visual Inspection of a Large Gravity Dam." *Frontiers in Built Environment* 4: 31. DOI: 10.3389/fbuil.2018.00031.

Khan U., Ishfaque M., Khan S., Xu F., Chen L., Lei Y. 2024. "Comparative Analysis of Twelve Transfer Learning Models for the Prediction and Crack Detection in Concrete Dams, Based on Borehole Images." *Frontiers of Structural and Civil Engineering* 18(10): 1507–1523. DOI: 10.1007/s11709-024-1090-2.

Leite D., Marcelino J., Guerra N., Manso J., Marques N. 2025. "Structural Health Monitoring and Inspection of Dams Based on Unmanned Aerial Vehicles Photogrammetry with 3D Model Reconstruction." *Soils and Rocks* 48(4): e2025002225. DOI: 10.28927/SR.2025.002225.

Liang H., Lee S., Bae W., Kim J., Seo S. 2023. "Towards UAVs in Construction: Advancements, Challenges, and Future Directions for Monitoring and Inspection." *Drones* 7(3): 202. DOI: 10.3390/drones7030202.

Simplicio P., Pereira G. 2025. "Multi-resolution UAV Path Replanning for Inspection of Tailings Dams." *2025 International Conference on Unmanned Aircraft Systems (ICUAS)*.

Villarino A., Valenzuela H., Antón N., Domínguez M., Méndez Cubillos X. 2025. "UAV Applications for Monitoring and Management of Civil Infrastructures." *Infrastructures* 10(5): 106. DOI: 10.3390/infrastructures10050106.

Zhao S., Kang F., He L., Li J., Si Y., Xu Y. 2024. "Intelligent Structural Health Monitoring and Noncontact Measurement Method of Small Reservoir Dams Using UAV Photogrammetry and Anomaly Detection." *Applied Sciences* 14(20): 9156. DOI: 10.3390/app14209156.

Krzysztof Radzicki

PhD Eng; Cracow University of Technology, Faculty of Environmental and Energy Engineering

ul. Warszawska 24, 31-155 Kraków, Poland

e-mail: krzysiek.radzicki@gmail.com

ORCID: 0000-0002-1302-9799

Innovative Polish Solutions for Monitoring, Seepage Control, and Foundation Engineering of Earth Dams

Abstract

This paper presents selected Polish innovations in monitoring, seepage control, and foundation solutions for earth dams, addressing key challenges related to seepage, internal erosion, and overall structural safety. The monitoring system is based on Multi-Point Thermal Sensors (MPointS), which enable detection and continuous monitoring of concentrated seepage paths, including leakages, by means of temperature measurements. The system provides quasi-continuous temperature profiling along the entire length of the dam body and its foundation, allowing for highly detailed spatial identification of seepage zones. By using integrated heating elements, the sensors can also perform active thermal tests, enabling reliable leakage localization and quantification of seepage velocity. The second solution is a hybrid seepage barrier used in dam rehabilitation. It consists of PVC sheet piles installed within trench-mixed soil–cement barrier. A key advantage of this approach is the possibility to construct an effective seepage barrier without lowering the reservoir water level, making it particularly suitable for rehabilitation of operating dams under normal service conditions. The third innovation is an advanced foundation system in the form of a spatial grid constructed from trench-mixed elements. The grid is composed of intersecting soil–cement panels forming a lattice structure, which enables the safe foundation of earth dams on very weak subsoil layers of considerable thickness (up to 8 m in the presented case). As a result, these solutions contribute to risk minimization, reduction of operation and maintenance costs, and extension of the service life of existing dam infrastructure.

Keywords: earth dams, renovation, hybrid seepage barrier, trench-mixed grid foundation

1. INTRODUCTION

Earth retaining structures — earth dams, levees, and canal embankments — form the backbone of numerous water management objectives, including water supply, hydropower generation, and flood protection. Throughout their service life, from construction through decades of operation to rehabilitation, these structures present a range of engineering challenges. This paper discusses three innovative engineering solutions developed and implemented in Poland, each addressing a different stage in the life cycle of a retaining structure and a different engineering need. The author of this paper was involved in the development or implementation of each of these solutions. They are: a grid foundation composed of a network of longitudinal and transverse soil–cement panels produced by deep trench mixing, enabling dam construction on weak subsoil; Multi-Point Thermal Sensors (MPointS) for early detection of seepage and internal erosion in earth retaining structures and their foundations; and a hybrid seepage barrier, allowing relatively rapid construction of a new vertical sealing element from the dam crest without lowering the reservoir level.

The first solution concerns the construction stage and consists of an intermediate foundation in the form of a grid of soil–cement panels beneath an earth dam. New earth retaining structures continue to be built, increasingly — due to site constraints — under difficult ground conditions. In the case discussed here, the dam had to be founded on a weak, highly compressible subsoil of considerable thickness. Conventional pile or column-based solutions did not provide sufficient bearing capacity under these conditions, while soil replacement would have been time-consuming and uneconomical. This prompted the search for an alternative foundation approach. The soil–cement panel grid solution described in greater detail below has been used with increasing frequency, particularly in Poland, in geotechnical applications such as landslide stabilisation and intermediate foundation of various civil engineering structures (Szczygielski, 2025). However, in the case presented in this paper, it is the first application of this solution as a foundation for a retaining structure.

The second solution discussed is the Multi-Point Thermal Sensor (MPointS) technology, designed to optimise and simplify the application of the thermal method, particularly its active variant, for early leakage detection in existing dams, levees, and canal embankments, while minimising costs. A significant proportion of retaining structures worldwide, including in

Poland, are already several decades old, their technical condition has deteriorated substantially, and the fundamental challenge lies in early and accurate detection of destructive processes that may be occurring within them (Radzicki et al., 2024). For earth retaining structures, one of the most critical threats is the development of seepage and erosion processes. Thermal monitoring using linear temperature sensors is a recommended and effective method for their detection (ICOLD, 2017). For several decades, fibre-optic cables have been the sensors of choice for this purpose (ICOLD, 2025). However, this method has numerous limitations when applied to existing earth dams and levees (Radzicki et al., 2021). These limitations are either eliminated or significantly reduced by MPointS technology, which has been deployed on numerous retaining structures in recent years.

The third solution relates to the rehabilitation stage. When the development of destructive processes necessitates repair of a retaining structure, this frequently poses a major financial and organisational challenge, carried out under severe constraints. Environmental considerations, water supply requirements, or energy production often limit or altogether preclude a significant drawdown of the reservoir water level. Such a situation arose in 2025 at the Cedzyna dam, where intensified seepage processes began to compromise structural safety, while at the same time there was strong pressure to minimise the cost and duration of repairs and to avoid lowering the reservoir level. In response, for the first time worldwide, a hybrid seepage barrier was implemented on a retaining structure, combining a trench-mixed soil–cement barrier with PVC sheet piles installed within it, thereby restoring the dam's sealing element without drawing down the reservoir.

The following sections provide a concise overview of these innovative solutions.

2. SPATIAL GRID OF SOIL–CEMENT PANELS AS A DAM FOUNDATION

A nearly eight-metre-thick layer of weak, highly compressible subsoil beneath a roughly seven-metre-high hydraulic embankment presents a formidable engineering challenge. This was the situation faced by the Cracov-based design office AdEko when designing the earth dam of a dry flood-retention reservoir on the Młynówka River upstream of Trzcinica (Jasło district) — a structure 187 m long, impounding up to 6.76 m of water under extreme conditions. The site investigation revealed complex ground conditions: weak, highly compressible cohesive soils with low strength parameters extending locally to approximately 7–8 m below ground level, in places so soft that undisturbed sampling was infeasible. The structure was classified as Geotechnical Category III (the highest).

The foundation solution for the Młynówka dam was developed by a three-person team comprising Dr Krzysztof Radzicki, Dr Krzysztof Podleś, and Dr Witold Bogusz. Extensive three-dimensional numerical modelling of a representative dam section in the zone of highest hydraulic loading and most unfavourable subsoil configuration was carried out for various foundation arrangements. Numerous subsoil improvement and foundation variants were analysed: soil replacement proved uneconomical and difficult to execute, while pile- and column-based solutions did not provide adequate bearing capacity given the thickness of the weak stratum.

Ultimately, an innovative intermediate foundation was adopted, employing a spatial grid of intersecting soil–cement walls. This represents the first known application of such an arrangement as a dam foundation worldwide. Trench-mixed grids had previously been used in Poland primarily for landslide stabilisation and intermediate foundation of various civil engineering structures, including road embankments (Szczygielski, 2025). As a dam foundation, however, this solution was applied for the first time.

The grid consists of continuous soil–cement walls produced by continuous deep mixing, at least 0.6 m thick, arranged in two mutually perpendicular directions — transverse and parallel to the dam axis — at a centre-to-centre spacing of 3.4 m in both directions (Fig. 1).

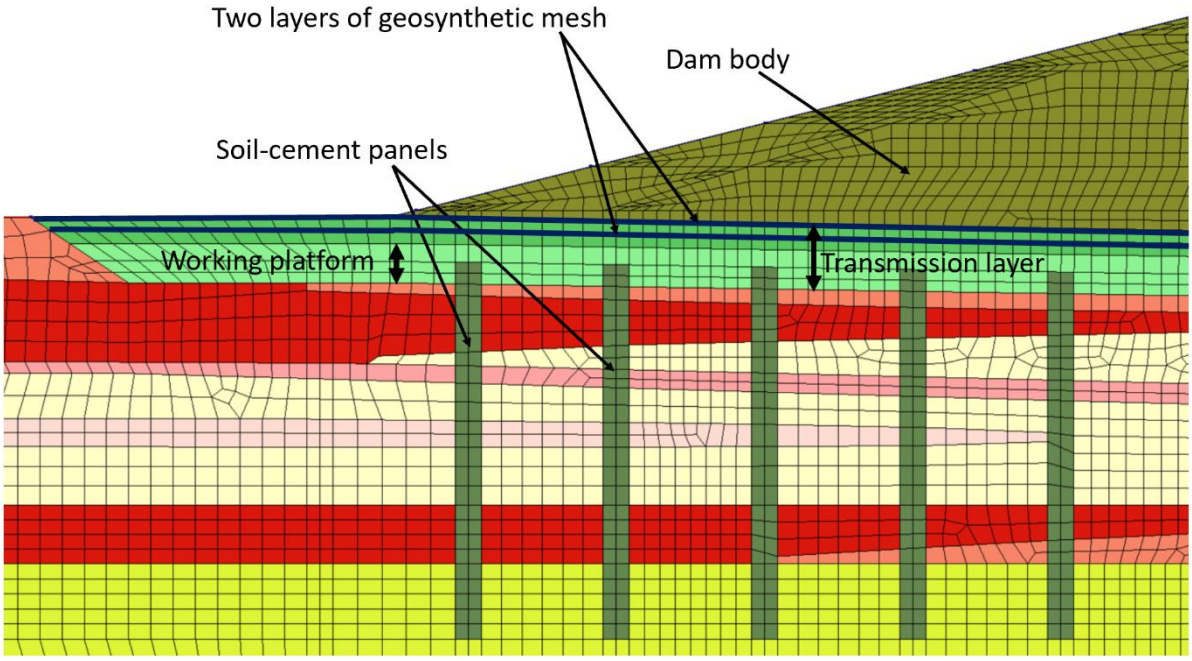


Fig. 1. Dam foundation designed as an intermediate foundation comprising a grid of soil–cement panels with a transfer layer above (source: Radzicki, Podleś, 2026)

Loading is transferred from the dam body into the grid through an intermediate transfer layer at least 1.5 m thick, reinforced with two layers of geosynthetic mesh — one placed at the top of the layer, the other 30 cm below — which distribute the embankment loads more uniformly between the soil–cement panels and the soil confined between them. An integral part of this layer is a working platform, constructed first, which allows heavy plant to operate on the weak subsoil during panel installation.

Below the transfer layer, the grid panels penetrate the weak subsoil stratum and are embedded in the competent bearing layer beneath it. This arrangement transmits loads from the dam body, through the transfer layer and the panels, to deeper subsoil layers of adequate bearing capacity, while partially mobilising the bearing capacity of the soil enclosed between the panels.

One of the panels beneath the upstream toe of the dam, running parallel to its axis, was utilised as a sealing element in the dam foundation. A geomembrane was attached to this panel and routed up the upstream slope. Together with the panel, it forms a continuous sealing element extending through the foundation and the embankment (Fig. 2).

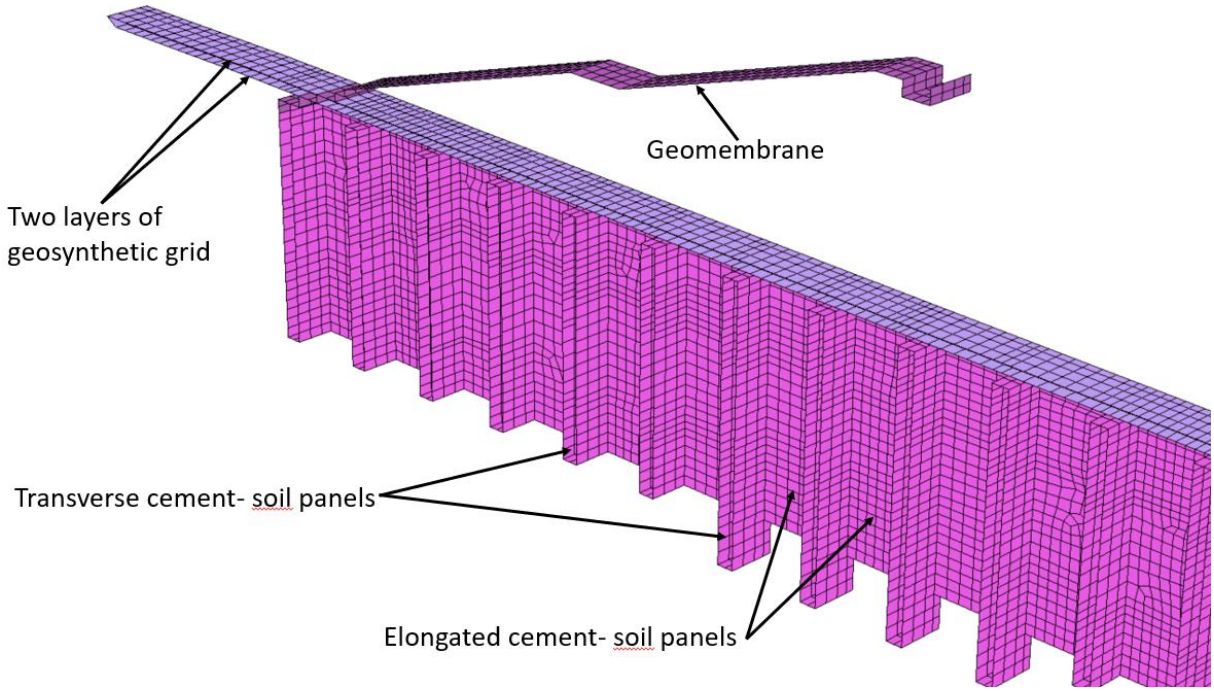


Fig. 2. Three-dimensional detail of the arrangement of soil–cement panels, geosynthetic meshes, and geomembrane (source: Radzicki, Podleś, 2026)

3. MULTI-POINT THERMAL SENSOR (MPOINTS)

3.1. Operating principle and monitoring concept

The thermal method exploits the coupled transport of heat and water in soil: in zones of intensified seepage, flowing water carries heat by advection, producing characteristic temperature anomalies relative to the surrounding ground. Analysis of these anomalies enables direct investigation of seepage processes and indirect inference about the occurrence of internal erosion. In active mode, the degree of heating of a sensor integrated with a heater element is measured — the higher the seepage velocity, the more intense the cooling and the smaller the temperature rise. Calibration of the sensor's thermal response in the laboratory enables quantitative determination of local seepage velocity in-situ, whether in periodic field surveys or in permanent monitoring systems installed in earth retaining structures and/or their foundations .

The Multi-Point Thermal Sensor (MPointS) was developed in a collaboration between Cracow University of Technology, represented by the author of this paper, and the company Neostrain, headed by its President, Marek Stoliński. Its implementation is intended to facilitate widespread adoption of linear thermal monitoring of seepage and erosion processes on existing earth retaining structures, where installation of fibre-optic cables — the sensor type used for this purpose until now — is costly, technically difficult, or even poses a risk to the safety of the retaining structure (Radzicki et al., 2021). With MPointS technology, individual sensor units are driven vertically from the surface without excavation, spaced closely enough to produce a quasi-continuous horizontal sensor line. The key advantage of this approach is its minimal invasiveness — in particular, the absence of post-installation ground disturbance that could create preferential seepage paths. Additional benefits include rapid installation without the need for heavy plant, and the ability to install sensors at greater depths within the foundation. Furthermore, a damaged individual sensor can be readily replaced with a new one (Radzicki, Stoliński, 2024a).

The system most commonly comprises two or more sensor lines at different depths, building a quasi-planar monitoring zone for seepage and erosion processes (Fig. 3) (Radzicki, Stoliński, 2024). Sensors are typically located at the downstream toe of the structure — an arrangement that reduces costs and, most importantly, enables early detection of erosion processes, which typically develop from this zone towards the upstream side (Radzicki et al., 2021; Radzicki, Stoliński, 2024a).

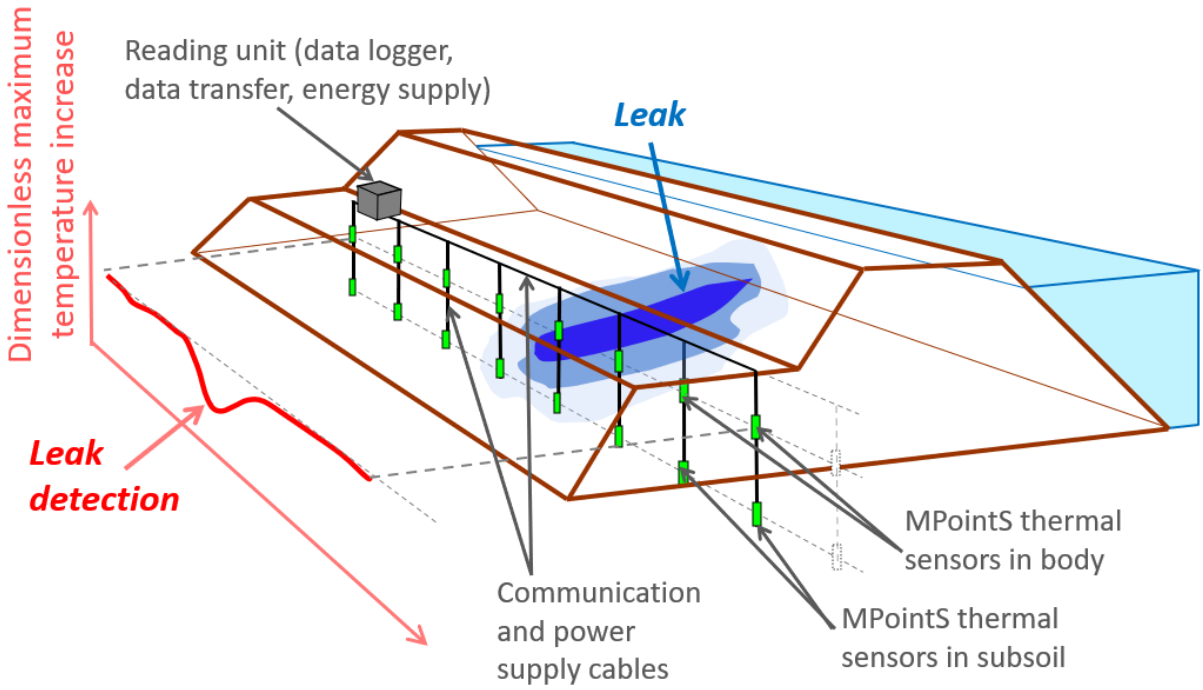


Fig. 3. Schematic of MPointS system installation with two sensor lines (A) and its application for quasi-linear monitoring of seepage through the body and foundation of an earth retaining structure (B) (source: Radzicki et al., 2021)

3.2. MPointS deployments

MPointS technology has been deployed on various types of retaining structures both in Poland and abroad. The world's first application of MPointS sensors took place in 2014 on the existing Kozłowa Góra earth dam and was simultaneously the first installation of seepage and erosion thermal monitoring on any retaining structure in Poland.

The Kozłowa Góra dam on the Brynica River (Silesia voivodeship) is 1300 m long and 8 m high; its body was built from heterogeneous local material, and the highly permeable alluvial foundation reaches a thickness of up to 11 m locally. Following the 2010 flood, alarming symptoms of intensified seepage were observed on a section of the right-bank dam, including local failure of the toe drain slope. After analysing the limitations of fibre-optic cable installation — in particular, the risk of triggering erosion during earthworks given the high phreatic surface — the decision was taken to deploy the newly developed MPointS technology (Radzicki et al., 2015).

A single sensor line was installed at a depth of 2.5 m with a spacing of 1 m, covering the section exhibiting the most pronounced symptoms. Active thermal measurements enabled

determination of local seepage velocities along the entire monitored reach. The results showed that seepage was occurring throughout the section, and clearly identified two zones of particularly intensified seepage (Fig. 4). The deployment confirmed that MPointS sensors enable not only detection of seepage zones and leakage locations, but above all in-situ determination of local seepage velocities — the parameter most critical for assessing the severity of seepage processes and the risk of internal erosion (Radzicki, Stoliński, 2024b).

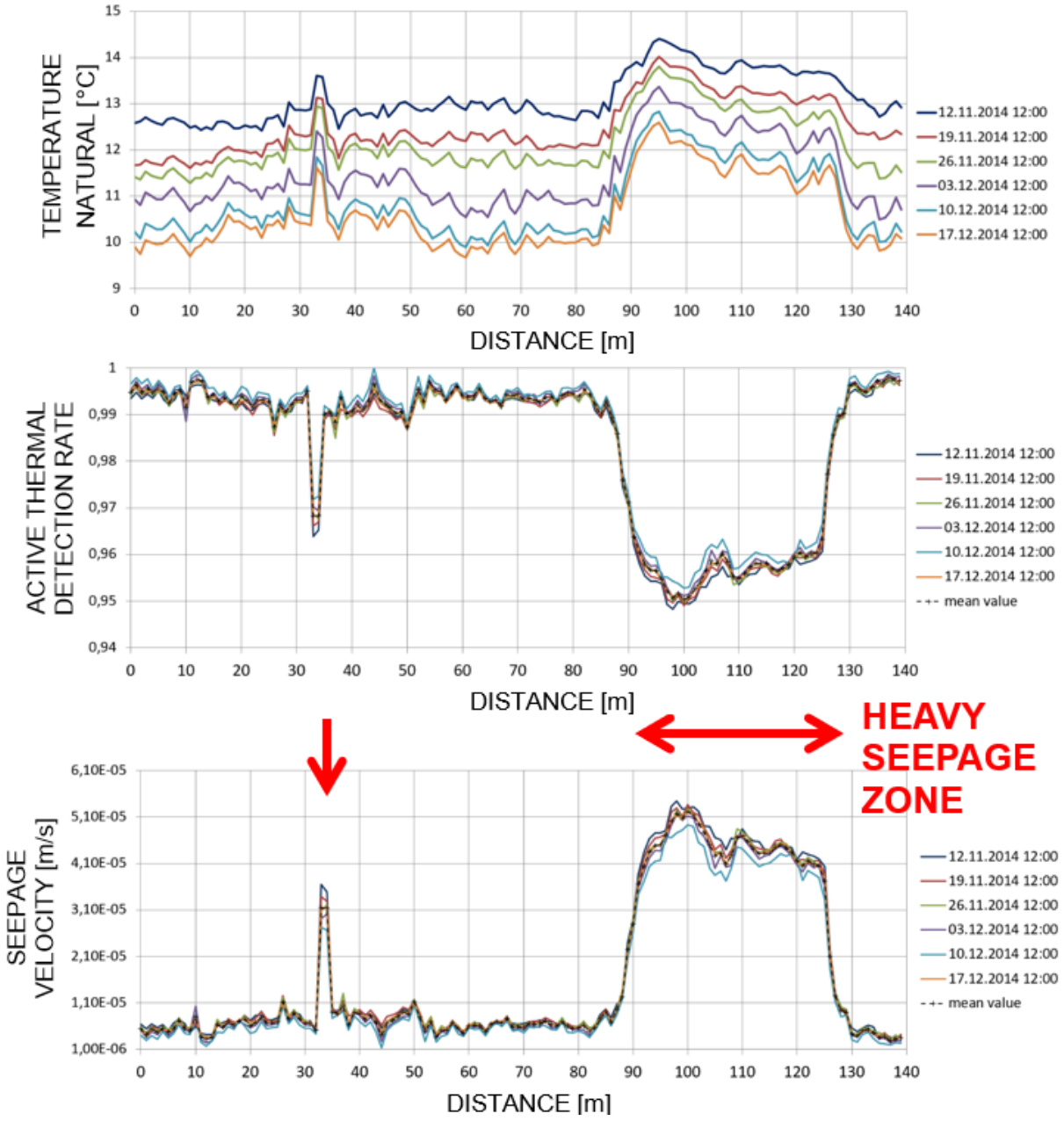


Fig. 4. Seepage velocities determined in 2014 using thermo-active MPointS sensors installed along the Kozłowa Góra dam at a depth of 2.5 m in the downstream berm (source: Radzicki, Stoliński, 2024b)

The effectiveness of the technology was further validated by a second reference deployment — the first thermal monitoring system on an existing levee in Poland, installed in 2017 on the left-bank Vistula levee at Wawrzeńczyce, where seepage and early-stage erosion at the downstream toe had been observed during the 2010 flood. During a relatively low flood event in 2019, the MPointS sensor line installed in the levee foundation detected a leakage zone and enabled determination of seepage velocities within it. This became a key argument for carrying out remedial works on the monitored section (Radzicki et al., 2021).

A subsequent MPointS deployment was carried out on a section of the Elbląg Canal near the Całuny lock (2020), representing the first thermal monitoring system on this type of structure in Poland. MPointS sensors have also been used abroad: for leakage monitoring on a North Sea levee in the Netherlands (2018) and for monitoring the development of erosion tunnels in the foundation of one of the largest earth dams in Central Europe, in Ukraine (2021) (Radzicki, Stoliński, 2024b).

4. HYBRID SEEPAGE BARRIER

4.1. Engineering concept

Seepage barriers constructed by continuous deep mixing (CDMM) using a trench cutter are becoming an increasingly common solution for rehabilitating sealing elements in earth dams, owing mainly to speed of installation and competitive cost relative to other technologies. This is the same family of technology described in Section 2 of this paper, used there to construct the grid foundation. When CDMM is employed to construct a seepage barrier, however, it has a fundamental limitation under reservoir conditions that generate seepage through the barrier zone. While the soil–cement panel is curing under a hydraulic gradient from the reservoir side, seepage flow may degrade the still-unset mix and reduce the design impermeability of the barrier. The same difficulty applies to barriers constructed in a slurry-supported trench (Radzicki, Stoliński, 2024a).

The hybrid seepage barrier concept (HPP — Hybrydowa Przesłona Przeciwfiltracyjna) overcomes this limitation by combining two elements within a single barrier. First, a CDMM soil–cement panel is formed; then, while the mix is still fresh and unset, PVC sheet piles are driven into it. The soil–cement body provides structural continuity and holds the sheet piles in position, while the PVC sheet piles — whose interlocks are factory-fitted with gaskets — form a low-permeability membrane that governs the overall impermeability of the barrier. Testing of

this solution indicates a hydraulic conductivity of the order of $k \approx 10^{-11}$ m/s. Crucially, the sealing function is performed by the gasketed PVC sheet-pile interlocks rather than the curing soil–cement, meaning the barrier maintains its impermeability even during installation, under an active seepage gradient (Radzicki et all., 2026).

The most important practical consequence of this feature is the ability to construct an effective sealing element at normal reservoir operating levels, without interrupting the operation of the structure and without the need to draw down or empty the reservoir. This is of decisive importance for dams with water intakes or those serving hydropower generation, for which emptying the reservoir would mean ceasing operation. It also helps to limit adverse environmental impacts and disruption to other reservoir users, such as recreational or fishery activities.

4.2. Implementation: Cedzyna dam

The HPP barrier was implemented during the rehabilitation of the Cedzyna earth dam near Kielce. This was the first known application worldwide of a hybrid seepage barrier with PVC sheet piles installed in a trench-mixed soil–cement panel on a retaining structure.

The technology was jointly developed by the companies Soley and Pietrucha. The design for its implementation at Cedzyna was prepared by the Kraków-based hydrotechnical design office AdEko, with the involvement of the author of this paper, on behalf of the Regional Water Management Authority (RZGW) in Kraków. PVC sheet piles were supplied by Pietrucha (www.pietrucha.pl), while all installation works — construction of the soil–cement barrier and insertion of the sheet piles — were carried out by Soley (www.soley.pl).

Construction works were carried out from September to December 2025, covering a total barrier length of 400 m (150 m and 250 m in the right-bank and left-bank dam bodies, respectively), constructed along the crest axis to a depth of 16 m, with a panel width of 0.4 m. Each section was executed in two steps: first, the soil–cement panel was mixed in the ground along the designed alignment; then PVC sheet piles were driven into the still-fluid mix, with interlock continuity being monitored throughout (Fig. 5). The recycled-PVC sheet piles used at Cedzyna carry a durability guarantee of up to 50 years — a service life commensurate with the rehabilitation horizon of the structure (Radzicki et all., 2026).



Fig. 5. Schematic of Hybrid Seepage Barrier (HPP) construction.

5. CONCLUSIONS

The three solutions presented address critical needs at different stages in the life cycle of an earth dam. Their common value lies in the fact that each closes a significant gap in the existing state of engineering practice and the state of the art — respectively in the fields of foundation design, monitoring, and rehabilitation of earth retaining structures.

The trench-mixed grid concept addresses the longstanding challenge of founding earth dams on thick layers of weak cohesive soils. Its first-ever application as a dam foundation demonstrates that modern deep-mixing techniques can be reconfigured to solve foundation problems hitherto regarded as extremely difficult to execute.

The development and deployment of the MPointS sensor removes significant barriers to the application of a highly effective thermal monitoring method for seepage and erosion detection on existing dams and levees. Installation of the fibre-optic cables used previously could cause ground disturbance, and was further hampered by slow installation rates and high costs. Numerous pilot deployments of MPointS sensors have confirmed that their quasi-continuous, minimally invasive installation not only provides early leakage detection, but above all enables in-situ determination of seepage velocity along the structure — the parameter most closely linked to the assessment of internal erosion risk.

Combining gasketed PVC sheet piles with a trench-mixed soil–cement barrier in the form of a hybrid seepage barrier achieved high impermeability while eliminating the need to draw down the reservoir — a decisive advantage for dams serving water supply or energy production, and one that also reduces environmental impact and operational disruption.

Collectively, these solutions contribute to a more cost-effective and lower-risk approach to the life-cycle management of earth dams.

References

ICOLD (2017). *Internal erosion of existing dams, levees and dikes, and their foundations*, Bulletin 164 vol. 1, pp. 292.

ICOLD (2025). *Internal erosion of existing dams, levees and dikes, and their foundations*, Bulletin 164 vol. 2, pp. 501.

Pietrucha International sp. z o.o. www.pietrucha.pl [accessed: July 2026].

Radzicki K., Gołębiowski T., Ćwiklik M., Stoliński M. (2021). „A new levee control system based on geotechnical and geophysical surveys including active thermal sensing: a case study from Poland". *Engineering Geology*, vol. 293, p. 1–24. DOI: 10.1016/j.enggeo.2021.106316.

Radzicki K., Podleś K. (2026). „Innovative Polish rehabilitation and construction solutions for earthfill dams and their numerical modeling". *XXXVI National scientific conference computer methods in design and analysis of hydraulic structures*, 2–5 March 2026, Korbielów, Poland.

Radzicki K., Sieinski M., Gołębiowski T., Zelaya-Wziątek D., Dmitruk Z. (2024). „Stan budowli piętrzących w Polsce. Cz. 1, Zagadnienia problemowe i wyzwania". *Inżynier budownictwa* 6/2024 (nr 228), s. 66–72. https://inzynierbudownictwa.pl/stan-budowli-pietrzacych-w-polsce-cz-i/

Radzicki K., Siudy A., Stoliński M. (2015). „An innovative 3D system for thermal monitoring of seepage and erosion processes and an example of its use for upgrading the monitoring system at the Kozłowa Góra dam in Poland". *Q. 99 – R. 7, 25th International Congress on Large Dams*, 17–19 June 2015, Stavanger – Norway, p. 85–101.

Radzicki K., Stoliński M. (2024a). „Development of thermal leak detection method and monitoring of seepage and internal erosion processes in earth dams, levees and dikes and their

implementation in Poland". *Materiały Budowlane* 12/2024 (nr 628), s. 55–77. DOI: 10.15199/33.2024.12.08.

Radzicki K., Stoliński M. (2024b). „Seepage monitoring and leaks detection along an earth dam with a multi-sensor thermal-active system". *Bulletin of Engineering Geology and the Environment*, 2024, vol. 83, nr 9, s. 1–15. DOI: 10.1007/s10064-024-03826-3.

Radzicki K., Sołtysik R., Zaremba T. (2026). „Seepage monitoring and leaks detection along an earth dam with a multi-sensor thermal-active system". *Energetyka Wodna*, 2026/1, vol. 57, s. 34–35.

Soley sp. z o.o. www.soley.pl [accessed: July 2026].

Szczygielski M. (2025). „Niekonwencjonalne wykorzystanie paneli CDMM do posadowienia estakady kolejowej". *Materiały Budowlane* 6/2025 (nr 634), ss. 6. DOI: 10.15199/33.2025.06.

Monitoring Strategies for Swelling Concrete Dams: Practices and Perspectives

Emmanuel ROBBE

Expert Barrages
EDF Hydro
DTG - Département Génie-Civil
Service Auscultation Surveillance Ouvrages Hydrauliques
134, Chemin de l'Etang
38950 Saint Martin le Vinoux

Abstract

Monitoring concrete dams affected by swelling serves two key objectives.

First, it enables the surveillance of failure mechanisms—particularly those triggered by swelling—to extend the operational lifespan of the dam while maintaining safety. Second, it supports the evaluation of swelling kinetics and spatial variability, including vertical displacement and localized concrete deformation, to improve understanding of both the swelling process and the dam's structural behavior. Monitoring also plays a critical role during remedial interventions, helping to validate their effectiveness.

The paper will present an overview of current monitoring practices applied to EDF dams affected by swelling, aligned with the objectives outlined above. Typical displacement rates and estimated cumulative amplitudes will be provided based on data from several impacted structures.

Looking ahead, the paper highlights two promising techniques for enhancing local insight into swelling kinetics: automated planimetric and altimetric measurements using prisms, and deformation monitoring via optical fiber sensors. Initial results from pilot implementations on two arch dams will be discussed.

SESSION D. Levees and tailing dams		
1	Tomasz Zaremba	Hybrid Cut-Off Wall – Modern Hydraulic Engineering Solutions by the Pietrucha Group
2	Rémy Tourment	Lessons learned from the operation of safety spillways in flood protection levee systems in France
3	Jonathan Simm	The International Handbook on Emergency Management of Flood Defences
4	Jarosław Ajdukiewicz	Effective renovation and sealing of hydraulic structure beds and slopes using controlled underwater concreting with synthetic formwork: practical implementation insights

Hybrid Cut-Off Wall – Modern Hydraulic Engineering Solutions by the Pietrucha Group

Tomasz Zaremba
Pietrucha Group

Abstract

The rehabilitation of existing dams and reservoirs requires reliable seepage-control solutions that can be adapted to existing structures and site conditions. This paper presents the Hybrid Seepage Barrier (HPP), a geocomposite solution developed by Grupa Pietrucha for hydraulic and flood-protection structures. The HPP combines interlocking EcoLock PVC sheet piles with integrated sealing joints, embedded in a hardening suspension or a soil–suspension mixture. This configuration provides a continuous seepage barrier while combining the properties of the mineral barrier and the mechanically interconnected polymer profiles.

The paper describes the concept of the HPP system, its main components and construction principles, with particular attention to the use of vinyl sheet piles installed in the freshly formed barrier. The technical properties of the solution are discussed with reference to the national technical assessment ITP-PIB-KOT-2023/0052, including a declared permeability coefficient of 10^{-11} m/s after 28 days of hardening.

The practical application of the technology is presented through a case study of the Cedzyna Reservoir in Poland, where the HPP was used to seal the dam body and foundation over approximately 450 m. The case study demonstrates the applicability of the technology to the rehabilitation of existing water-retaining structures.

Keywords

Hybrid seepage barrier; HPP; seepage control; hydraulic structures; dam rehabilitation; vinyl sheet piles; Cedzyna Reservoir; Pietrucha Group

Lessons learned from the operation of safety spillways in flood protection levee systems in France

B. Beullac[1], R. Tourment[1], S. Patouillard[2], Damien Kuss[3], B. Tourlonnias[4]

[1]INRAE, RECOVER, Aix Marseille Univ, Aix-en-Provence, France, remy.tourment@inrae.fr
[2]PONSOH, French Ministry of Ecology, Paris, France
[3]SYMBHI, Saint-Martin-d'Hères, France
[4]France digues, Saint-Martin-d'Hères, France

Abstract: Safety spillways, increasingly adopted by French levee managers to protect against overtopping breaches, offer significant advantages for flood risk reduction in protected areas. This paper presents various hydraulic designs (free, fusible or gated weirs), their advantages and limitations, and analyses several recent and historic French cases based on flood events or risk assessments. It shares lessons on design, hydraulic behaviour, management, and how these structures influence flood risk in protected areas.

Keywords: safety spillways, lessons learned, levee systems, hydraulic design, morpho dynamics of watercourses, risk management.

INTRODUCTION

The integration of safety spillways into flood protection systems, when effective, presents significant advantages, ultimately enhancing flood risk reduction in protected areas. As a result, this approach is increasingly adopted by French levee managers to safeguard their systems from breaches caused by overtopping and to have the hydraulic behaviour of the system predictable. While older safety spillways exist in France—particularly along the Loire River levees—and several new structures have been constructed over last decades on other waterways, feedback on their operational performance remains relatively undocumented and poorly disseminated.

After a short history of spillways in France, this article examines the various hydraulic functions for safety spillways, and different types of design including fixed weirs, fuse plugs and movable weirs, along with their respective advantages and limitations. The links between spillways and emergency management in leveed areas are also discussed. The article then provides a detailed description and analysis of both recent and historical case studies, focusing

on flood events that triggered spillway operation or specific risk assessments. The insights drawn from these experiences highlight key considerations for the design, hydraulic behaviour, and management of these structures, as well as the potential risks they may pose to areas protected by flood defence systems.

1/ HISTORY OF SPILLWAYS IN FRANCE

In France, the history of spillways was, until recently, closely linked to the one of levees and the major floods they have withstood.

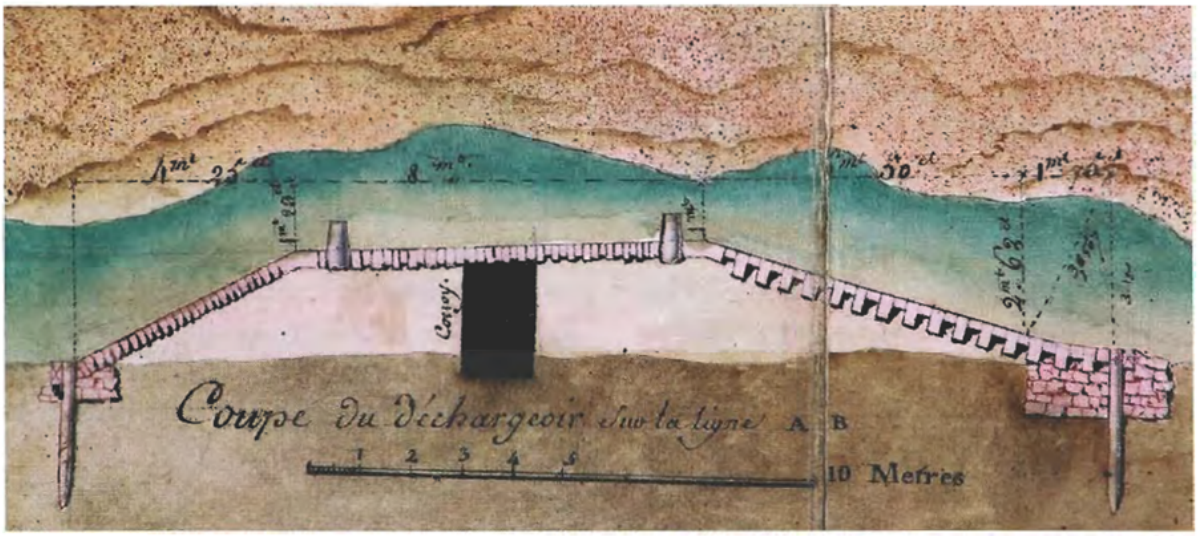


Fig. 1. La Bouillie spillway in Blois *(source: F. De Person, 2001)*

For the Loire River, this history dates back at least to the 16th century with the construction of spillways—known as "déchargeoirs"—built to divert the river's waters upstream of towns and thus bypass inhabited neighbourhoods *(Maurin, 2013)*. One example presented in figure 1 is the La Bouillie spillway in Blois, which was built in 1584 *(de Person, 2001)*. Given its effectiveness, the structure has been preserved, expanded, and improved over the centuries in response to flood events. The last flood to trigger the operation of this spillway was in 1907, illustrated in figure 2 *(Rivière, 2007)*.



Fig. 2. The last flood to trigger the operation of La Bouillie spillway in 1907 *(source: Rivière, 2007)*

Following the numerous breaches caused by four "rare" floods in the early 18th century, a program to manage the Loire River—including the systematic construction of similar spillways—was implemented under the authority of king Louis XIV along all the levees between Giens and Tours *(Patouillard, 2024)*. During the devastating floods in 1733, most of these spillways proved ineffective in terms of flood damage and were removed, except for two structures that had been proven effective in the past, including the one in La Bouillie. It is therefore important to note that, from the outset, the construction of a spillway does not appear to guarantee its effectiveness until it has been tested by one or more floods.

On the Vidourle River, engineer Henry Pitot built ten masonry spillways (1764–1773) to avoid breaches, significantly reducing downstream flow during floods.

Following the three "rare" floods of the late 19th century, a new program established under the authority of emperor Napoleon III provided for the construction of 19 spillways along the Loire River (1867) called Comoy's spillways from the name of the engineer who led the program. The Comoy's spillways are large masonry structures, often equipped with fuseplugs (see §2.2.2). Finally, only eight were built including the Jargeau spillway of Orléans levee system *(Dion, 1961)*.

During the 20th century, spillway construction remained scattered: two spillways on the Divatte (Loire-Atlantique, 1917), three concrete spillways on the Aude River after the 1952 floods (effective in 1996 and 1999), and a fusible spillway on the Reyran River (1962). Along the Rhône River, the Compagnie Nationale du Rhône (CNR) developed 18 spillways and overflow-resistant levees, with overflow return periods ranging from 2 to 20 years that feed

into flood expansion areas to mitigate the consequences of the CNR run of the river dams on the aggravation of floods.

The 21st century has seen accelerated development: reconstruction of the Aramon spillway (2003) after the 2002 flood, at the junction of the Gardon and Rhône rivers, new spillways on the Durance (Les Mées, 2006, and Rochebrune, 2011), Gardon (Comps, 2006), Lez (Lattes, 2008, diverting floods to the Lironde River), Vidourle (Lunel, 2009), Seine (Sartrouville, 2012), Isère (30 safety spillways and 16 diversion spillways, 2012-2022), Romanche (5 spillways, 2015-2018) and Rhône (2 spillways,2016-2021) rivers. The design of these spillways was facilitated by numerical hydraulic modelling, which must take into account uncertainties inherent in the models themselves, as well as variations in water levels along the spillways (due to hydrology and variations in riverbed morphology), in order to produce spillways that perform effectively under real-world conditions.

These structures, featuring diverse designs (free weirs, fusible plugs, or gated weirs), reflect a shift toward more resilient flood management, combining protection and flow regulation. Their effectiveness, tested during recent flood events for some of them, underscores their critical role in reducing flood risks.

2/ GENERAL INFORMATION ON SPILLWAYS IN LEVEE SYSTEMS

2.1/ Hydraulic functions in levee systems

A spillway may perform one or more of the hydraulic functions *(Degoutte, 2021)* described in this section.

2.1.1. Protect the levee system itself (resilience to overflow)

By its impact on flow lines a spillway located upstream of a levee system will delay the critical levee overflow and reduce load on all or part of the levee system. Thus, such a safety spillway protects the levee system itself by increasing the return period of the safety flood[1] on all or parts of it. Indeed, downstream the spillway, the diverted flow will be taken out of the river

[1] The safety flood is the flow line for which the levee will maintain a margin of safety in response to various failure modes (once the safety flood is exceeded, the levee may fail). The safety flood has to be higher than the protection flood which corresponds to the elevation of the spillway crest.

flow and the flow line will be lowered (figure 3), in principle up to the sea, or up to where the diverted flow comes back into the watercourse. Upstream, if the flow comes from the river, the flow line will be lowered by backwater effect. Such effect will gradually decrease upward as head losses along the watercourse will "consume" the benefit of downstream lowering. By being designed to resist overflow erosion, spillways allow, up to their flood design level, controlled discharge of water into areas of relatively low vulnerability, or where actions can be undertaken to lower the consequences of flooding.

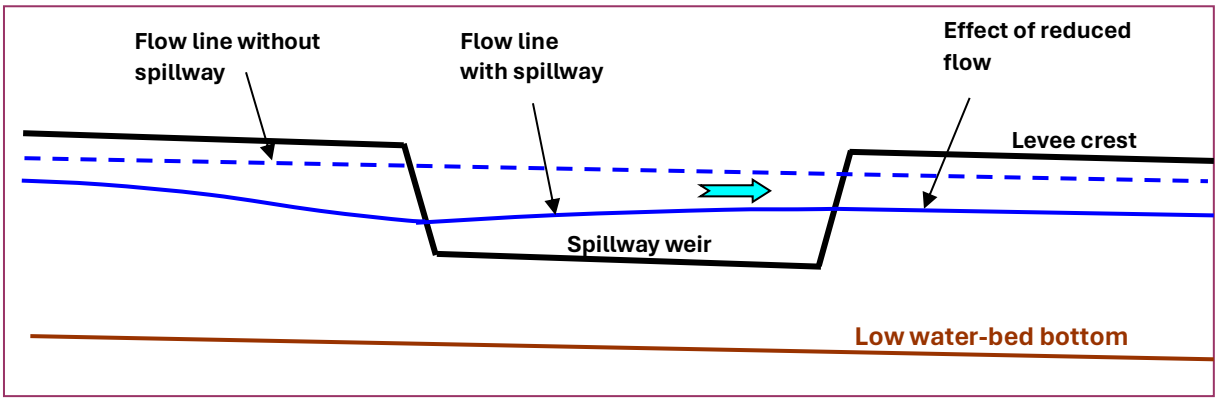


Fig. 3. Theoretical effect of a spillway on the flow line of a river in steady flow conditions *(source: Degoutte, 2021)*

Spillways are more suitable for slow-flowing rivers with low sediment transport. Indeed, in torrential conditions, experience in France shows that the activation of a spillway drastically reduces the bed's capacity to transport sediment, which can lead to the bed becoming completely filled with sediment during a flood and a total diversion of the flow through the spillway.

2.1.2. Mitigate flooding effects downstream

a. Spillway feeding into a flood expansion area:

If the return in the watercourse of the flow diverted by a spillway can be controlled and delayed, the area where is diverted this flow can be considered a flood expansion area which mitigates the effects of flooding downstream. Indeed, flood hydrograph peaks are attenuated and flood volumes in the watercourse downstream are reduced. In certain situations where the downstream section of the levee system is subjected to higher water levels on the protected side – due to water flowing from the spillway – than on the river side, the installation of a return spillway in this levee section, that lets water flow from the leveed area back to the river, can reduce the risk of this levee breaching.

b. Bypass spillway:

A bypass spillway water supplies a diversion canal to locally lower a watercourse's downstream water level. The canal compensates for the watercourse's insufficient flow capacity over a certain section and rejoins the watercourse downstream of that section; for example: the Coursan diversion canal (Department of Aude, France, the Bouillie secondary channel of the Loire River in Blois (Department of Loir-et-Cher, France). One of the limitations of a diversion canal hydraulic efficiency, the maximum flow that can be diverted, is its section, among other topographic factors.

c. Partitioning spillways:

A partitioning spillway also supplies a diversion canal but diverted water doesn't join the same watercourse downstream, but another outlet such as a lagoon, a lake, the sea, or another watercourse. It then mitigates the effects of flooding downstream the spillway. Such is the case for the Lez diversion spillway in Lattes (Department of Hérault, France), which flows into the Méjean lagoon via the Lironde River channel. This outlet imposes its own limits to water levels in the canal, from downstream, as it may be temporarily elevated by an exterior factor (its own flooding, abnormally exceeding high tide levels...).

2.2/ The different types of spillway designs

Flood water from the river is usually derived in a spillway via a weir which also controls the water discharge in function of the hydraulic head. The weir is then followed by a chute and often by an energy dissipation area; the water then flows into a protected area, a flood expansion area (2.1.2 a) or a channel (2.1.2 b and c). Various types of weirs can be mentioned *(Degoutte, 2021; Goutx, 2005)*.

2.2.1. Fixed weir spillways

A spillway is typically fed by a fixed weir that functions passively.

The weir's flow rate is always an important criterion for flood expansion areas and often for protected areas as well. Contrary to the situation on most of dams, the discharge head is rarely very high since there is no point in discharging water too frequently or creating levees with crests much higher than the weir's crest. As a result, most weirs need to be very

long, which can be prohibitive because of the site's conditions or financial considerations. Nevertheless, in some particular situations spillways on levees can be similar to dams' spillways with a higher H/L ratio. These considerations also apply to fuse plug weirs (2.2.2) and movable weirs (2.2.3).

2.2.2. Fuse plug weirs

To maximise the flow per linear metre, in the case of land constraints, an option is to place fuse plugs above the fixed weir that collapse above the protection level, releasing an initial flow rate per metre that is much higher than with fixed weirs. Compared to a fixed weir, flooding of a protected area can be delayed and the capacity of a flood expansion area can be increased. These benefits should be weighed against higher cost and potential dysfunctions of the fusible device and having a quicker flooding of the protected area when the plug fuses.

Different kind of fuse plugs:

- Erodible fuse plug embankment: earth, sand or gravel embankment placed on fixed weir (figure 4). This kind of fuse plug must erode and disappear under the action of the overflowing water. Depending on their designs, the collapse time of these devices cannot always be guaranteed, and it can be assisted by human action *(CIRIA, 2013)*. Once eroded, it must be rebuilt.

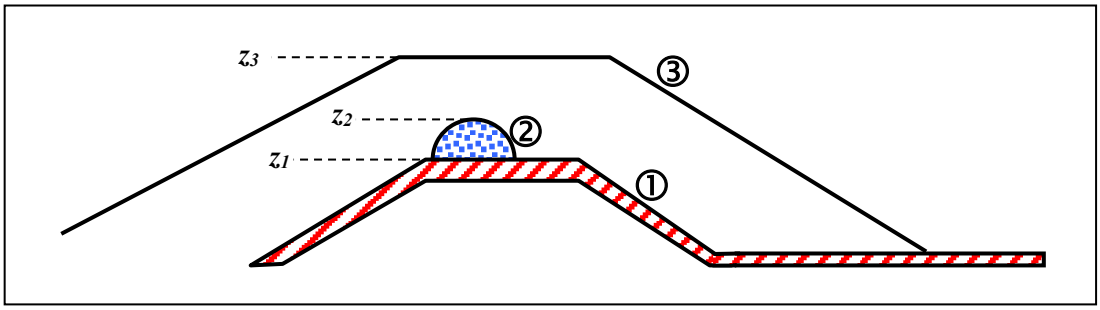


Fig. 4. General section for erodible fuse plug embankment spillway: ① fixed spillway section ② erodible fuse plug ③ section of levee continuous section *(source: Degoutte, 2021)*

- Gravel ribbon topped by concrete slabs placed side-by-side behind a fixed weir, that tilt when water discharge erodes the gravel ribbon (figure 5). Once toppled, components generally cannot be reused and must be replaced by new ones.



Fig. 5. Fuse plug spillway formed with gravel ribbon topped by concrete slabs, on the Aa river in Engelberg, before and after operating *(source: OFEN)*

- Free-standing fusegates placed side-by-side on a fixed weir, that automatically topple under water pressure, when a specific water level is exceed, flooding a base chamber. This kind of spillway, which was, for example, built on the Allan levee system in France (figure 6), is rather expensive. Once toppled, components often cannot be reused and must be replaced by new ones.

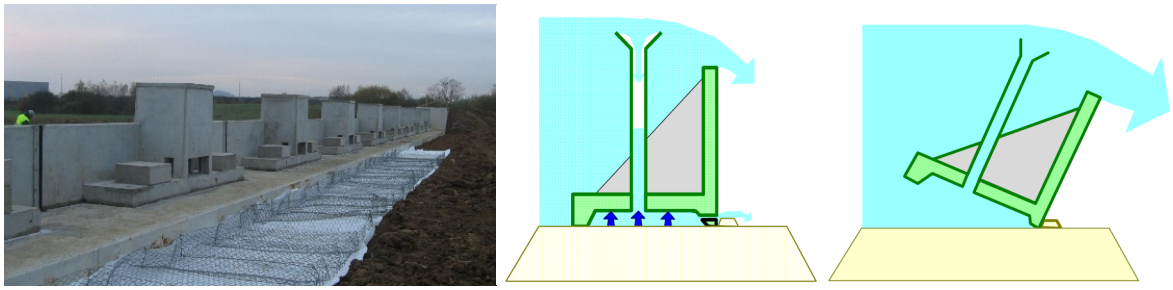


Fig. 6. Allan spillway and principle of free-standing fusegates (upon introduction of uplifts and during tilting) *(source: Hydroplus)*

2.2.3. Movable weirs

A weir with an adjustable movable device, flap gate, or inflatable weir, etc. (figure 7) presents quite same interests than fuse plug weirs but in addition can be adjusted and operated according to the water level. Contrary to fuse plug weirs, partial lowering is possible. After the spill, the weir can return to its initial position. The cost is generally higher for this kind of spillways than for fuse plugs.

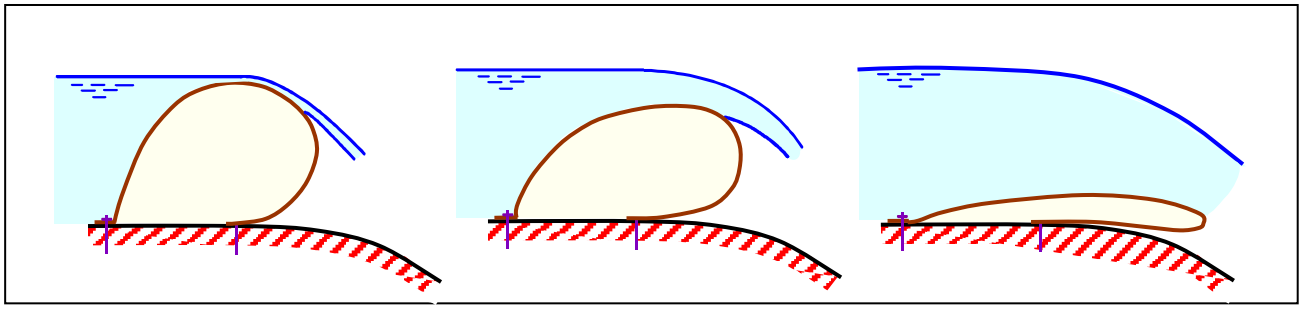


Fig. 7. Principle of movable weir by inflatable structure *(source: Degoutte, 2021)*

2.2.4. Regulated sluices and pumps

Regulated sluices and pumps are alternative solutions designed to achieve the same hydraulic objectives than spillways. They can allow to divert water from the very start of a flood event, without waiting for the water level to reach a spillway weir level. They generally allow for relatively low flow rates compared to weirs.

2.3/ Complements to spillway solutions

Levee managers should pay close attention to spillways during a flood event that is likely to activate them. Levee managers should warn authorities in charge of emergency management (mayors, prefects, ...) if they think the spillway will be activated by the expected flood and should warn the same authorities once the spillway begins operating. In addition, where a flood forecasting service exists, it should be notified if a substantial part of the watercourse's flow will soon be diverted, in order to update forecast.

The emergency management strategy is developed with saving lives as the top priority. Emergency management cannot be improvised and must be carefully thought through. It is important to understand, test, and assess all necessary measures to get people threatened by flooding to safety, particularly in the case of spillway operating or levee failure. To achieve this, it is essential to have a thorough understanding of the behaviour and management of water discharged into the protected area and of how it is drained via gates, sluices or pumps.

These measures should include plans to evacuate and/or shelter people according to the expected flood level; such plans are easier to draw up, as flooding of the protected area is more predictable with a spillway than by breaches which are random.

3/ CASE STUDIES

3.1/ Orléans/Jargeau spillway

Following the 1866's flood on Loire River, the engineer Comoy led a program to build modern spillways. The Jargeau Comoy's spillway was built between 1878 and 1882, on the site of a breach in the levee upstream from Orléans. This 1866's breach, located upstream of the village of Jargeau, helped to protect the homes in the downstream part of the leveed area, at a time when the levee was in danger of overflowing in that area.

The Jargeau Comoy's spillway is 715 m long and is equipped with a 575 m sandy material fuse plug approximately 1.70 m high, raised above the fixed spillway (figure 8). In the case of a major flood threatening the integrity of the levees, when the water level rises above the crest of the fuse plug, this one is designed to erode under the force of the overflowing water *(Saussaye, 2024)*, and then to gives way, causing a high-intensity overflow (in terms of the height of the overflowing water and/or of duration). Nevertheless, the fuse plug must remain robust enough to withstand a low-intensity flood for a short time, thereby providing temporary protection for the population that would be affected if it open.

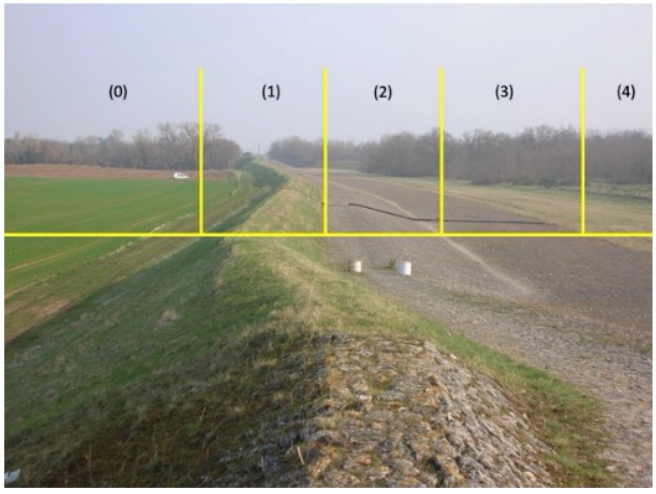


Fig. 8. Jargeau spillway, from left to right: (0) the unprotected floodplain; (1) the fusible embankment; (2) the overflow-resistant section; (3) the energy dissipation zone; (4) the natural ground *(source: R. Tourment)*

The fuse plug is reinforced with masonry stone (without grout joint) on the river side, acting both as revetment and sealing. Since its construction, vegetation has grown on the surface and the materials have evolved. For this reason, the erosion capacity of the fuse plug

must be reassessed (Saussaye, 2024). Furthermore, the Jargeau spillway was originally designed to operate for a 170-year return period flood but the riverbed has sunk as a result of sand extraction for post-war reconstruction. In 2010, it was estimated that Jargeau spillway operates only above the 500-year flood, whereas some sections of the levee of Orléans can overflow for less than the 200-year flood. For that reason, works to lower the Jargeau spillway fuse plug to operate 20 cm under the 200-year flood took place in 2023-2024 (Henry, 2024). The case of Jargeau spillway highlights the importance of changes in the river's morphology to the functioning of a spillway and the need to regularly check these changes and reassess the spillway actual role.

3.2/ Comps spillway

The Comps spillway (in the Gard department) is situated on a levee on the right bank of the Gardon River, upstream of the confluence with the Rhône River. This levee, whose crest is set at elevation 16 m NGF, was built in the 1970s to protect the Baisses agricultural plain which is also a flood expansion area. The Comps spillway was constructed over a length of 40 m at the upstream end of this levee, prior to its connection to the masonry 'Comps levee', built in 1925 to protect the village of Comps from flooding. The spillway fixed weir is set at elevation 13 m NGF and protected, at the crest and on both slopes, by a layer of loose riprap. It is fitted with a fuse plug of gravelly material set at elevation 13.8 m NGF.

This structure was put to the test for the first time during the Gardon flood of 9–10 September 2002, with little damage for the spillway fuse plug. The spillway fixed structure itself had not sustained any significant damage *(Royet, 2004)*. In the days following the flood, the fuse plug was rebuilt to its original specifications.

In December 2003, the spillway was again in operation for several hours due to a flood with a hundred-year return period on the Rhône, which reached a level of just over 14 m NGF at the spillway (figure 9). At the end of the flood, it has been observed that: the fuse plug was eroded over its entire height, but only over a length of 20 to 26 m; the loose riprap of the fixed weir was visible over a large area and extensively eroded at the weir level, exposing the compact silt of the spillway body.



Fig. 9. Comps spillway on December 3, 2003 *(source: Paul Royet)*

These two events highlight that the fusible device installed on the Comps spillway was not functioning as intended. Not only was the fuse mechanism not guaranteed to function, but the fuse plug malfunction caused damage to the spillway itself, due to increased stress (concentration of flow) compared to what it would have experienced in the absence of fuses, and to insufficient protection of the fixed weir.



Fig. 10. Current Comps spillways *(source: Gérard Degoutte)*

The design of the spillway has since been modified (figure 10) through the installation of concrete-bound riprap on the crest and downstream face and a concrete weir without fuse plug. The leveed system has also been modified (figure 11) with the construction of a new spillway between the Baisses plain and the town, and the reinforcement of Comps masonry

levees. Nevertheless, this example demonstrates the difficulty posed by this type of fusible structure, which is simple in principle but not always entirely reliable in operation.

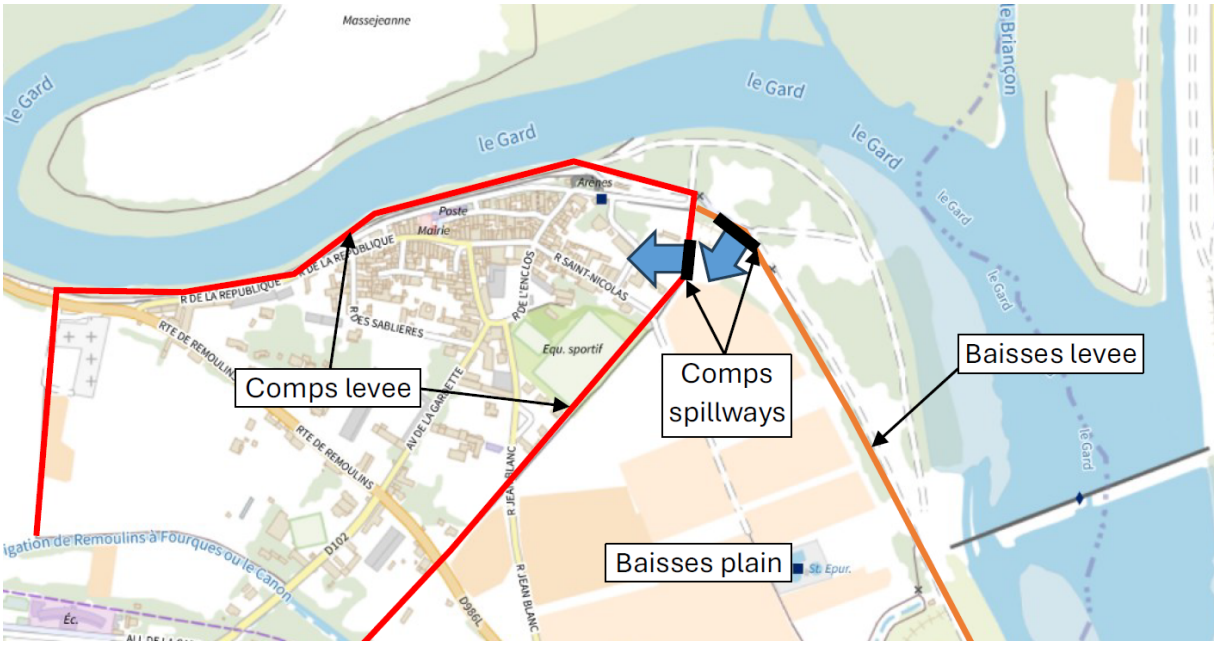


Fig. 11. Current configuration for Comps leveed system *(source: B. Beullac)*

3.3/ Aramon safety spillway

The village of Aramon, situated near the Rhône and Gard rivers junction, is protected against floods by a system of levees, with one dated from the 18th century. During September 2002 flood this levee, 1.8 km long, failed in several places, causing five fatalities. Post-flood diagnosis concluded to the need of completely rebuilding it.

Three principles guided the design of the new flood defences *(Mallet, 2004; Goutx, 2005)*:

- to maintain, for the municipality of Aramon, the same level of protection as that provided by the original levee;
- to design a scheme which, in the event of exceptional flooding, allows for a slow inundation of the village without the levee breaching;
- not to worsen, compared to the previous situation, the floodwater levels in the unprotected floodplain.

After comparing a range of solutions and modelling their hydraulic impact in various configurations, the following design parameters were proposed (figures 12&13):

- a 900 m long spillway at an elevation of 14.40 m NGF, in the north-western area, furthest from residential properties;
- a 900 m long levee at an elevation of 15.50 m NGF, in the southern area, where the embankment is close to houses.

The length of the spillway section has been calculated to ensure that, in the event of an exceptional flood reaching a level of 15.50 NGF, the Aramon protected area is sufficiently pre-filled so that the residual risk of breach at the point of overflow onto the non-submersible section is as low as possible.

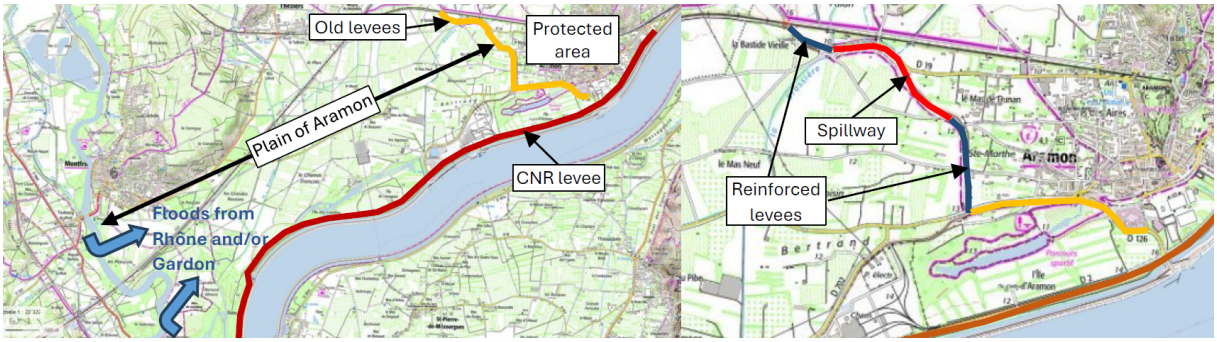


Fig. 12. Leveed system of Aramon: before and after spillway construction *(source: B. Beullac)*

In addition to the spillway, the municipality of Aramon has drawn up an emergency response plan providing for the evacuation of residents from the protected area. In the event of a slow-rising flood on the Rhône, the evacuation threshold has been set at 14.20 m NGF. In case of a rapid rise in the water level of the Gardon, the rate of rise at the levee (1 m/h in September 2002) means that decisions regarding the evacuation of the population must be taken on the basis of the levels observed – and their progression – further upstream along the river.

The Aramon spillway overflowed immediately after it was completed, during the Rhône River flood from 1 to 5 December 2003. The spillway functioned for about 5 hours with a maximum head of 15–20 cm *(Mallet et al., 2004)*. The structure was found to be performing satisfactorily and the levee system has not been breached. The only reinforcement required following the flood was to improve the watertightness of the riprap revetment on the spillway.

The emergency response plan, which provides for the evacuation of residents before the water reaches the spillway, was activated as a precautionary measure during the afternoon of 3 December to avoid a night-time evacuation. Residents were able to return to their homes the following day.



Fig. 13. Aramon spillway[2] *(source: R. Tourment)*

The difference of consequences between 2002 and 2003 (no impact on the levees or the local population), highlight that the combination of the spillway and the evacuation plan proved its effectiveness.

3.4 / Lattes partitioning spillway

For many years, the town of Lattes has been subject to significant flooding. In 2004, it was estimated that the Lez River's flow rate before the levees protecting Lattes at the time overflowed was 500 to 550 m^3/s, corresponding to floods with a return period of approximately twenty years (the levees could potentially break sooner due to their structural performance) *(Quévremont, 2006)*. These levees had been built or modified after the 1976 flood (between 1980 and 1986) to cope with a reference flood of 600 m^3/s, then estimated to be a 100-year event. During the Lez floods of 2002 (450 m^3/s in Lattes), 2003 (470 m^3/s in Lattes), and 2005 (487 m^3/s in Lattes), levees nearly overflowed. Under these circumstances,

[2] The spillway is in the background; in the foreground the levee not resisting to overtopping with a higher crest level

a project was launched to better protect the town of Lattes and its 18,000 inhabitants. The town adopted a development plan (figure 14) that involved installing a flow-diverting spillway upstream of Lattes to divert floodwaters exceeding the capacity of the Lez River's main channel into a secondary channel (dug to join and then follow the Lironde floodplain).

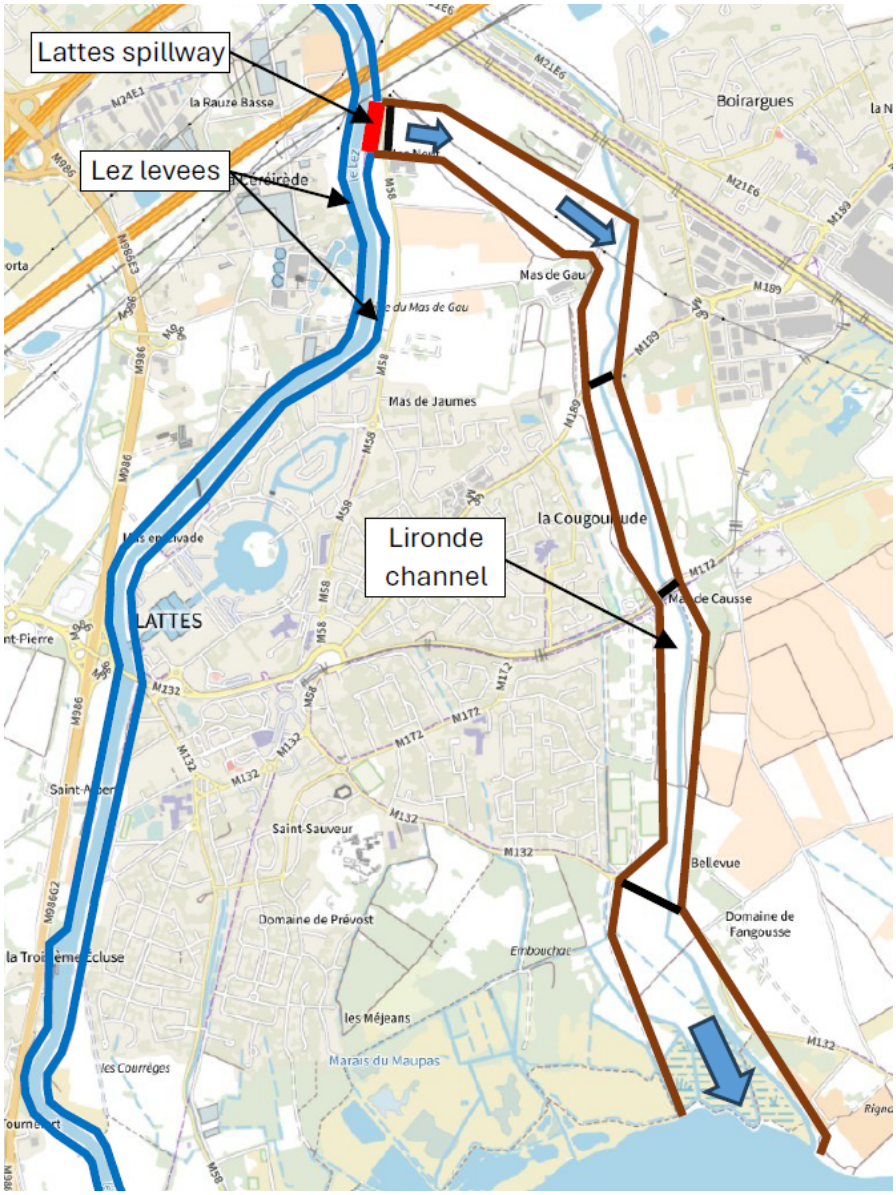


Fig. 14. Lattes protection system *(source: B. Beullac)*

Works began in 2007. It consisted of creating a 150-meter-long spillway (figure 15) designed to operate at a flood flow rate of 400 m^3/s, representing a return period of less than 10 years, the 100-year flood upstream of Lattes having been revised to 900 m^3/s during the project. A 900-meter-long channel was created downstream of the spillway to connect with the small stream La Lironde, whose bed was widened to 200 meters. The four roads and the railway line crossing this channel were reinforced to withstand overflow, and management

guidelines were established to control access during floods. La Lironde flows into the Méjean pond, which thus serves as a flood expansion area. In addition, 12 kilometers of Lez levees downstream of the flood control structure were reinforced or raised to allow a flow rate of 630 m^3/s in the Lez River, plus a safety margin. The materials extracted from the channel were used to strengthen or rebuild the dikes. The construction of the channel required 90 hectares of land, acquired from 195 landowners. In total, 1 million cubic meters of material were moved.



Fig. 15. Lattes partitioning spillway *(source: R. Tourment)*

Thus, with this flood protection system, Lez floods with a flow rate of less than 400 m^3/s in Lattes are contained within the Lez riverbed thanks to the levees. For floods with flow rates between 400 and 1,000 m^3/s in Lattes, part of the flow is diverted into the Lironde River to reach the Méjean pond, and no overflow occurs on the Lez levees. In the event of an exceptional flood with a flow rate exceeding 1,000 m^3/s, an overflow occurs upstream of the diversion spillway and ensures that the downstream flow in the Lez never exceeds 630 m^3/s. The Lattes diversion spillway was activated only once, during the flood of October 7, 2014, with a maximum overflow of approximately ten centimeters. No significant damage to the flood protection system and the protected area occurred. The organization plan worked as intended, in particular the closing of the roads affected by overflowing.

3.3/ Isère safety and diversion spillways

The Isère amont project (Kuss, 2024; Rossano, 2016), implemented by SYMBHI between 2012 and 2023 (€135 million), protects 29 municipalities in the Grésivaudan valley upstream of Grenoble - over 300,000 residents - against the 200-year design flood (Q = 1,890 m^3/s). The protection strategy relies on flood attenuation upstream of the Grenoble conurbation through 16 controlled flood storage areas (CFSAs, total storage capacity 33.5 Mm^3), achieving a 35% reduction in peak discharge at the entrance to the urban area.

The system comprises three categories of structures (figure 16). Sixteen diversion spillways feed the CFSAs from the 30-year flood onwards: 12 fixed weir spillways and 4 movable flap gate spillways. The latter equip the CFSAs closest to Grenoble, providing operational flexibility and maximising diverted discharge. Thirty safety spillways, distributed across both the primary levees lining the Isère and the setback levees enclosing the CFSAs, enable controlled overflow during the 200-year flood, preventing any uncontrolled breach of the system. Finally, levee removal sections (fuse plug spillways) supply the riparian forests reconnected to the Isère from the 5-year flood onwards. For the most critical structures, a continuous water-level monitoring system transmits stage data in real time to a supervisor, enabling remote surveillance and operational coordination during flood events.

To date, no flood has activated the system in full. The flood of 15 November 2023 (1,040 m^3/s at Grenoble, return period ~20 years) provided the first real-world test since the project's completion in early 2023. It triggered the diversion spillway of the Lumbin-Crolles CFSA, with a maximum overflow depth of 15-20 cm sustained over approximately 7 hours. Paradoxically, the observed return period (~20 years) falls below the design activation threshold (30 years). This early triggering should not be interpreted as a structural malfunction: Alpine rivers with high bedload transport are geomorphologically dynamic systems, whose longitudinal profile adjustments — incision/aggradation, bank erosion, lateral migration — alter stage-discharge relationships and therefore the effective activation thresholds of spillways. A spillway necessarily operates within a range of triggering discharges that reflects the natural variability of channel geometry within its hydraulic zone of influence. Regular bathymetric monitoring is therefore an integral and non-negotiable component of managing this type of system.

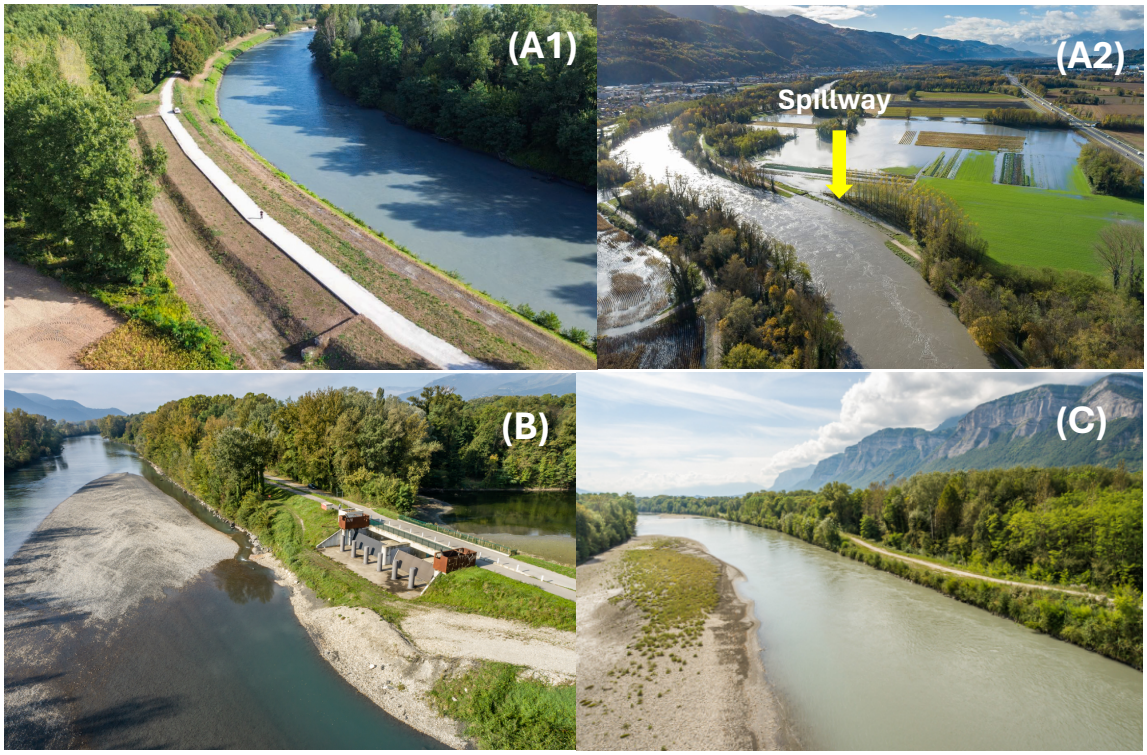


Fig. 16. Illustration of the different types of spillways found on the River Isère. (A1): fixed weir diversion spillway; (A2) fixed weir diversion spillway des Iles de Crolles on the 15 November 2023; (B) movable gates; (C) fuse plug weir. *(source: SYMBHI)*

The four movable spillways were not activated during this event. Their operational record highlights a fundamental challenge: these structures are called upon extremely rarely, yet must be fully functional on the day of a major flood. The investment in preventive maintenance, periodic testing and crew training is therefore substantial — and cannot be deferred.

4/ CONCLUSIONS

Lessons learned from the different case studies are the following:

- According to the local topographic and hydraulic situation, it is possible to optimize the inclusion of one or more spillways in a levee system, given the different possible types of spillways and weirs.
- The combination of a spillway and an emergency response plan is effective to manage flood risk in a protected area.
- Changes in the river's morphology can have significant impact on hydraulic operations of a spillway, even in steady flow conditions.

- A spillway necessarily operates within a range of triggering discharges that reflects the natural variability of channel geometry within its hydraulic zone of influence. Regular bathymetric monitoring is an integral and non-negotiable component of managing this type of system.
- Erodible fuse plug embankments, which are simple in principle but not always entirely reliable in operation, impact the hydraulic operation of spillways and thus levee systems, and possibly the safety of spillways themselves.
- The investment in assessments, preventive maintenance, periodic testing and crew training, for erodible and movable weirs is substantial and cannot be deferred.
- Partitioning spillways, which lower the water level along the entire downstream length of the river, may require specific measures for the diversion channel, both in structural terms and in terms of crisis management.

While in the past adding spillways in levee systems usually was done rather empirically after major flood events and catastrophic failures, the more recent inclusion of spillways in levee systems is facilitated by numerical modelling and the demonstration of their effect on flood consequences. Anyway, given the uncertainties related to the model itself, and also in some local situations the important variability in the different flood regimes leading to different slopes of the water lines along the spillway, different modelling situations have to be analysed to design a spillway able to perform in real conditions. Overall, the inclusion of spillways in rivers levee systems greatly improve their safety by improving their resilience to overtopping, and more and more systems are now designed including them.

REFERENCES

[1] CIRIA. 2013. *Chapter 9 Design*, in *The International Levee Handbook: 975-1191.* London: CIRIA. ISBN: 978-0-86017-734-0

[2] Degoutte G., Tourment R. 2021. *Spillways on river levees*. Versailles: Quae. DOI: 10.35690/978-2-7592-3285-7

[3] De Person F. 2001. *La Loire à Blois – Le déchargeoir de la bouillie en action ou le contrôle du chemin de l'eau de 1584 à 1907* – rapport interne Direction Régionale de l'Environnement (DIREN) Centre.

[4] Dion R. 1961. *Histoire des levées de la Loire*, CNRS éditions (2017).

[5] Goutx D., Tourment R., Mériaux P. 2005, « Eléments de conception hydraulique des déversoirs des endiguements de protection contre les inondations », *Ingénieries N°Spécial 2005*: 169-178.

[6] Henry E., Valenziano A., Kaboré A. 2024. « Hydraulics of the levee system of the "val d'Orléans", design and operation for managing the overtopping of the levees (Loiret) ». Colloque Digues 2024, Aix-en-Provence, France.
DOI: 10.5281/zenodo.10629083

[7] Kuss D., Body J.-L., Pinhas M., Koulinski V., Merlo A., Verdeil D., Henry J., & Milleret D. 2024. « River Isère upstream from Grenoble: solid transport management methods to ensure long-term protection of protected areas ». Colloque Digues 2024, Aix-en-Provence, France. DOI: 10.5281/zenodo.10604061

[8] Mallet T., Royet P., Cault J.-B. 2004. « Reconstruction de la digue d'Aramon après la crue de septembre 2002 », Colloque technique CFGB 2004.

[9] Maurin J., Patouillard S., Tourment R. 2013. « Les déchargeoirs au XVIIe siècle, les déversoirs au XIXe et quelles perspectives pour la gestion des surverses au XXIe siècle ». Congrès SHF Événements extrêmes d'inondation 2013, Lyon, France.

[10] Patouillard S., Pèpe Y., Grand V., Maurin J. 2024. « Putting into perspective the management of state-owned Loire River's levees from the 16 th century to the present day ». Colloque Digues 2024, Aix-en-Provence, France.
DOI: 10.5281/zenodo.10589971

[11] Quévremont P. 2006. *Expertise des projets d'action de prévention des inondations sur le bassin du Lez.* Rapport de l'Inspection générale de l'environnement. Ministère de l'écologie et du développement durable.

[12] Rivier J. 2007. Colères de Loire en 1907. Gien : Imprimerie Centrale.

[13] Rossano F. L. 2016. *Floodscapes-contemporary landscape strategies in times of climate change*. Doctoral dissertation. ETH Zurich.

[14] Royet P., Mériaux P. 2004. « Les déversoirs fusibles le sont-ils vraiment ? ». Colloque technique CFGB 2004.

[15] Saussaye L. Chevalier C. Patouillard S. Durand E. Bastien Bridoux B. 2024. « Erodibility assessment of one spillway's earthen fuseplug in the middle Loire using mobile jets erosion tests ». Colloque Digues 2024, Aix-en-Provence, France.
DOI: 10.5281/zenodo.10620098

Jonathan Simm, PhD, FREng, Independent Consultant, Wantage, OX12 8JT, United Kingdom jonathan.simm@gmail.com
Bart Vonk, BEng Rijkswaterstaat WVL, Postbus 2232, 3500 GE Utrecht, The Netherlands
Eric Huijskes, MSc, Huijskes Advies, Joelaan 1, 1217 GG Hilversum, The Netherlands
Marcel Bottema, PhD, Rijkswaterstaat WVL, Postbus 2232, 3500 GE Utrecht, The Netherlands

The International Handbook on Emergency Management of Flood Defences

ABSTRACT

The *International Handbook on Emergency Management of Flood Defences* (IHEMFD) was developed to address a critical gap in global flood risk management: the absence of comprehensive, operational guidance for managing flood defence systems during emergencies. While the *International Levee Handbook* (ILH) provided a strong foundation for design and long-term asset management, it did not sufficiently address the dynamic, time-critical challenges associated with emergency preparedness and response. This paper describes the development of the IHEMFD, outlines its structure and conceptual foundations, and reflects on the collaborative processes that enabled its creation. Key challenges included defining scope across diverse national contexts, harmonising terminology, integrating contributions from multiple authors, and ensuring international relevance. Success factors included a clear roadmap, iterative drafting, strong editorial oversight, and extensive virtual collaboration. The handbook has been widely disseminated, downloaded in 37 countries, and adopted by organisations including UNDRR and UNESCO. Its emphasis on continuous learning and organisational maturity positions it as a document that it is hoped will evolve with emerging insights and global needs.

KEYWORDS: Flood defence; emergency management; guidance

1. INTRODUCTION

Flood risk management has undergone significant transformation over the past two decades, driven by increasing climate variability, ageing infrastructure, and heightened societal expectations for safety. While substantial progress has been made in the design, assessment, and long-term management of flood defences, the operational dimension of emergency management has historically received less systematic attention. Specifically, there was insufficient information and guidance on this topic in the International Levee Handbook. The ILH, published in 2013, became a widely used reference for levee design and asset management, but it was not intended to provide detailed guidance for emergency situations. Given the increased frequency and severity of flood disasters (see Figure 1) and the aging and deterioration of flood defences in many parts of the world, it became apparent that there was a need to document and share good practice on emergency management from around the world. It was believed that this might also encourage the development of a community of practice around emergency management of flood defences.

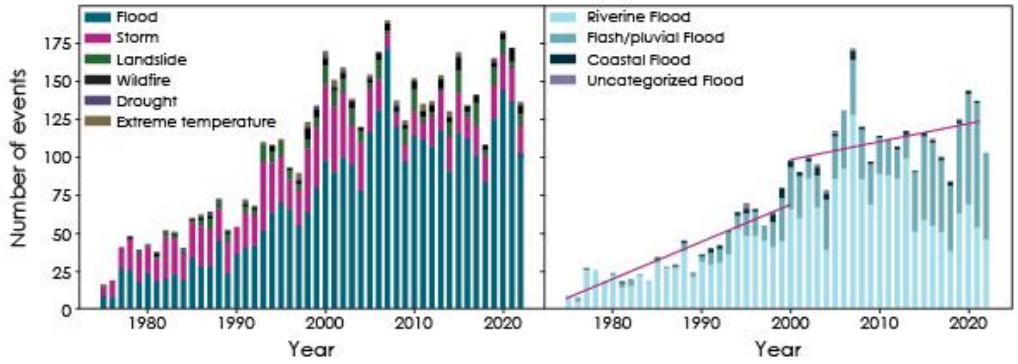


Figure 1. Number of disaster events (left) and flood events (right) with one or more fatalities as recorded in EM-DAT 1975-2022 *(after: Jonkman, S.N et al, 2024)*
Liczba katastrof (po lewej) i powodzi (po prawej) z jednym lub większą liczbą ofiar śmiertelnych odnotowanych w danych EM-DAT 1975–2022 (według: Jonkman, S.N i in., 2024)

Recognising this gap, four major national organisations—Rijkswaterstaat (Netherlands), the Environment Agency (England), the Ministry of Land, Infrastructure, Transport and Tourism (MLIT, Japan), and the US Army Corps of Engineers (USACE, USA)—initiated a collaborative effort to develop a new international handbook focused specifically on emergency management of flood defences. These organisations collectively manage extensive networks of flood protection infrastructure and have substantial experience responding to extreme events. Their shared recognition of the need for operational guidance provided the foundation for the IHEMFD.

The primary audience for the handbook (see Figure 2) is the flood defence manager, defined as the individual or organisation responsible for the operation, inspection, and emergency response of flood defence systems. Secondary audience members were their partners, e.g. forecasters, crisis managers, civil security, response personnel and the military. This reflects the multi-agency nature of flood emergency management, which requires coordination across technical, operational, and strategic domains.

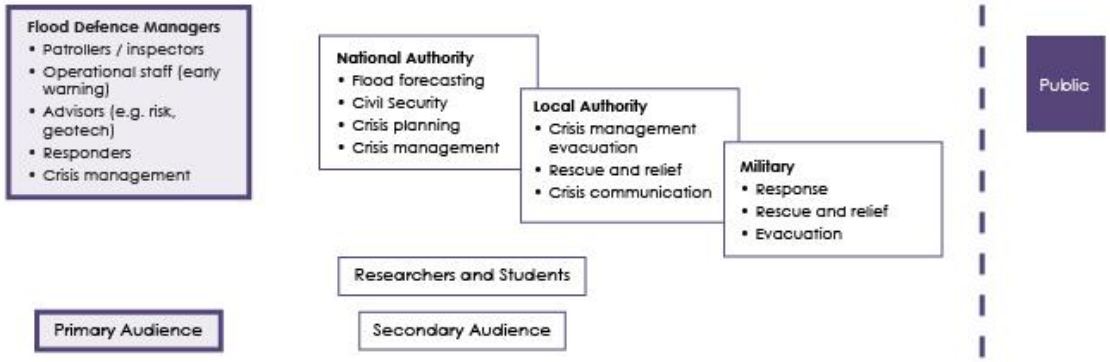


Figure 2. Primary and secondary target audience for the IHEMFD *(source: IHEMFD)*
Podstawowa i drugorzędna grupa docelowa IHEMFD *(źródło: IHEMFD)*

The authorship team was drawn from the partner organisations and their wider networks, including research institutes, consultancies, and universities. This collaborative authorship model was designed to ensure that the handbook reflected a broad range of expertise and international perspectives.

2. Development of the IHEMFD including role of the Polders 2C project

The development of the IHEMFD was significantly enabled by the **Interreg Polder2C's project**, a European initiative aimed at strengthening flood resilience through cross-border collaboration. The Polder2C's project was established to address shared challenges in flood risk management across the North Sea region. Its objectives included:

- Enhancing cross-border collaboration
- Improving emergency preparedness
- Testing and validating emergency measures
- Developing shared training and exercise programmes
- Strengthening the knowledge base for flood defence management

These objectives aligned closely with the needs of the IHEMFD, making the project an ideal platform for its development. The Polders 2C project provided not only financial

support but also created a shared understanding of the need for operational guidance based on a foundation of practical experience resulting in a structured framework for knowledge exchange, field experimentation, and community building. Thus, it enabled a transition from a community of the willing to a community of committed experts; this transition was essential for sustaining the multi-year effort required to produce the handbook.

One of the earliest achievements of the Polder2C's project was the development of the initial framework for the handbook. This included:

- Defining the scope and objectives
- Establishing the chapter structure
- Identifying authors and contributors
- Developing a roadmap and timeline
- Securing buy-in from partner organisations

The project facilitated workshops and meetings about the IHEMFD where experts from different countries could discuss their experiences, identify common challenges, and agree on shared principles.

A distinctive feature of the Polder2C's project was its emphasis on practical field trials, which provided valuable insights into the behaviour of flood defences and the effectiveness of emergency measures. These trials included:

- Controlled overtopping experiments, which tested the resilience of embankments and the effectiveness of reinforcement techniques.
- Rapid repair exercises, where teams practiced installing emergency measures such as sandbags, geotextiles, and temporary barriers.
- Inspection drills, which trained participants to identify early warning indicators under realistic conditions.
- Joint exercises, involving teams from multiple countries working together to respond to simulated flood events.

These activities generated empirical data and practical experience that informed the operational guidance in Chapters 7–14 of the IHEMFD - see Section 3 of this paper.

The Polder2C's project also played a crucial role in initiating and building a Community of Practice around flood defence emergency management. This community now includes government agencies, water authorities, research institutes consultancies, construction contractors and emergency responders. The community provides a platform for ongoing knowledge exchange, training, and collaboration, with the vision of sustaining the IHEMFD as a living document.

After the initial scoping activities under the Polders 2C project, various organizations and independent professionals provided input for the IHEMFD free of charge, contributing their expertise and knowledge, either as authors, reviewers or editors. Recognising that both governance and practical procedures would vary from country to county, authors were asked to focus on identifying underlying principles and challenges when writing up good practice and only give national practice as examples of implementation of these principles.

The handbook underwent extensive review and input from multiple authors and reviewers. This resulted in the handbook passing through several iterations as the content was fleshed out and made more precise.

3. CONCEPTS, STRUCTURE AND CONTENT OF THE HANDBOOK

Two central conceptual frameworks for the handbook are (1) the Source–Pathway–Receptor (SPR) model (Gouldby & Samuels, 2005) for flood risk management and (2) the emergency management cycle.

The SPR model (see Figure 3) distinguishes between:

- **Source**: The origin of the flood hazard
- **Pathway**: The route by which water travels
- **Receptor**: The people, property, and infrastructure at risk

The handbook focuses primarily on the **pathway**, specifically the flood defences that mediate the movement of water.



Figure 3. The Source–Pathway–Receptor Model *(source: IHEMFD) Model źródła-ścieżki-receptora (źródło: IHEMFD)*

In terms of the emergency management cycle (Figure 4), the focus is therefore on preparedness and response actions aimed at avoiding or at least delaying flood defence failure. This focus distinguishes the IHEMFD from broader flood emergency management

guidance, which often emphasises evacuation, public communication, and recovery. The handbook instead concentrates on the technical and operational measures required to maintain the integrity of flood defences during extreme events.

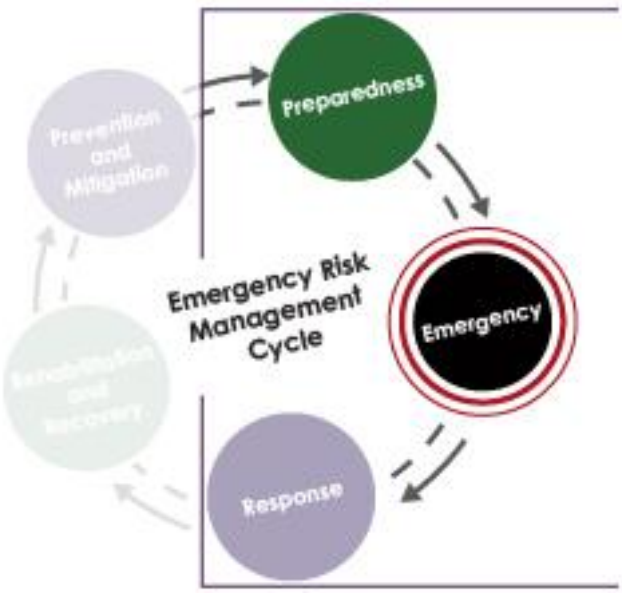


Figure 4. Emergency management cycle showing areas of focus in the IHEMFD *(source: IHEMFD).*
Cykl zarządzania kryzysowego pokazujący obszary zainteresowania w ramach IHEMFD *(źródło: IHEMFD)*

As well as these frameworks, it was also necessary to produce an agreed classification for both flood defences and for emergency response types.

The IHEMFD is intentionally structured to guide the reader from foundational concepts through to detailed operational processes and, ultimately, to organisational learning and implementation. The structure reflects the recognition that emergency management of flood defences is not a single discipline but a **system of interdependent activities**, each requiring clarity, coordination, and technical understanding. The handbook's architecture therefore mirrors the complexity of real-world emergency management, where governance, physical processes, operational decision-making, and organisational culture interact continuously.

Main themes of the handbook include:

- **Emergency Management**: The IHEMFD covers emergency management strategies, including logistics and implementation during flood emergencies. The handbook

provides numerous examples to help understand what is necessary for effective emergency management of flood defences.

- **Preparedness and Response**: The handbook emphasizes the importance of preparedness and response measures to manage risks of flood defence failure during extreme flood events. It outlines key principles and best practices for inspections, early warnings, how to understand failure mechanisms, and how to identify and deliver response measures.
- **Governance and Collaboration**: The IHEMFD delves into governance aspects, detailing processes and activities related to emergency management. The handbook highlights the importance of collaboration among various organizations and professionals to ensure effective flood defence management.
- **Identification and Understanding of Failure Processes**
- **Selecting, Designing and Installing Emergency Mitigation Measures** (including understanding their limitations)
- **Knowledge Sharing and Learning**: The handbook stresses the need for knowledge sharing and continuous learning. It aims to educate the next generation by transferring best practices from experienced flood fighters and documenting knowledge and experiences.
- **Funding and Resources**: The handbook discusses the justification for funding necessary capacities and competencies. It underscores the importance of securing adequate resources to support emergency management efforts.

The handbook is divided into 17 chapters (see Figure 5), grouped into four major components, plus an introduction and conclusion. This structure is not merely organisational; it reflects a conceptual progression from *why* emergency management of flood defences matters, to *what* must be understood, to *how* it must be done, and finally to *how organisations can embed and sustain these practices*. Table 1 provides more detail on the content of each chapter .



Figure 5. IHEMFD chapter structure (source IHEMFD)

Struktura rozdziału IHEMFD (źródło IHEMFD)

Table 1. Summary of Content of chapters of the IHEMFD *(source: authors' review of IHEMFD)*

Podsumowanie treści rozdziałów IHEMFD *(źródło: recenzja autorów IHEMFD)*

Chapter 1 – Introduction Chapter 1 sets out the purpose, scope, and intended audience of the handbook. It explains the need for operational guidance on emergency management of flood defences, noting that existing documents such as the International Levee Handbook do not address the dynamic conditions of emergency response. The chapter introduces the conceptual foundations used throughout the handbook, including the focus on defence behaviour under load and the importance of preparedness and coordinated action. It emphasises that

the handbook is intended for practitioners responsible for real-time decision-making and must be adapted to diverse national and institutional contexts.

Chapter 2 – Emergency Management of Flood Defences

Chapter 2 outlines the core principles that underpin emergency management for flood defences, including the SPR and emergency management cycle frameworks discussed in the previous section of this paper. It adapts general emergency management concepts to the specific challenges of defence systems, emphasising timeliness, proportionality, coordination, and uncertainty management. The responsibilities of different stakeholder organisations in setting policy and in developing plans and tactics are explained. The chapter highlights the need for situational awareness, clear escalation pathways, and pre-established triggers for action. It also stresses the importance of integrating technical understanding of defence behaviour with operational decision-making and action, setting out the roles of different stakeholder organisations at the operational level. The chapter also gives examples of how responsibilities for flood defences are distributed across agencies and levels of government, using examples from the Netherlands, England, Japan, and the United States, which illustrate different governance and funding arrangements. The chapter highlights challenges such as fragmented responsibilities, differing legal mandates, and the need for effective information sharing. It emphasises that successful emergency management depends on clear roles, coordinated structures, and well-defined decision-making authority.

Chapter 3 – Preparedness

Chapter 3 overviews some key elements of preparedness, emphasising not only the importance of developing emergency management plans but also the importance of capacity building and field exercises and of community engagement and awareness. A key part of preparedness is a proper understanding of hazards and risk (defence failure probability x consequence) and of sustaining the resilience (robustness, redundancy and recoverability) of the defences. Hazards such as high rainfall, river discharges and/or coastal storm surges and associated early warning systems are explained. In terms of the resilience of defences, the importance of regular inspections and record keeping linked to likely failure mechanisms is emphasised, explaining the role of fragility curves in describing the probability of failure in relation to the increasing water load. Trigger levels

for action during monitoring of loads and responses are recommended based on hydraulic models, fragility curves and/or other practical experience of performance.

Chapter 4 – Response

Chapter 4 provides an overview of operational planning, coordination and action during various types of emergencies. It describes decision-making processes, communication protocols, and escalation mechanisms that ensure timely and consistent action. It emphasises the importance of inspections and assessments carried out during the emergency in driving the nature and timing of responses. The chapter emphasises the importance of using and coordinating response resources from different geographies and from organisations not normally involved in flood risk management. Post response/emergency activities are also explained such as data collection, waste management and debriefing of personnel.

Chapter 5 – Flood threats

Chapter 5 provides an overview of the types of flood threats that challenge defence systems, including riverine, coastal, pluvial, groundwater, and combined events. The chapter is framed around two key tables. One table explains (for each type of water system) the characteristics of floods, including predictability/lead time, duration, rate of water level rise and wave action The other explains the direct threats to the flood defences which are relevant for each of these characteristics, including direct inundation erosion, movement of damaging debris, overflow and overtopping damage and water intrusion and soil weakening. The chapter emphasises that understanding the nature of the threat is essential for selecting appropriate emergency measures and for anticipating defence behaviour under load.

Chapter 6 – Flood defences

Chapter 6 provides an overview of the types of flood defences for which emergency management may be appropriate. Much of the IHEMFD is focussed on flood embankments and the various types of these are explained and their likely weaknesses. The installation and operation during a flood emergency of demountable and temporary defences and ancillary structures is also discussed. Less attention is given to flood walls, retention dams and flood diversion structures.

Chapter 7 – Communicating for emergency management

Chapter 7, the first of the more detailed chapters on processes and activities, explains the nature and importance of building an effective, professional and open risk communication framework which helps all involved to navigate the emergency 'vortex'. The process starts with developing a communications plan covering strategic, tactical and operational levels. The chapter discusses both communications between professional organisations, both nationally and internationally and also with the media. Systems for communicating directly with the public are also set out.

Chapter 8 – Assessing and inspecting

Chapter 8 focuses on structured inspections and assessments of flood defences during high-water conditions. It describes inspection objectives, team organisation, safety considerations, and the importance of repeatable observation methods. The chapter explains how priorities are set using known weakness of defences and available monitoring data. Approaches to inspection including equipment selection, inspection timing and preparation take account of the characteristics of the defence, the likely failure mechanisms and the flood prone area, together with the health safety and wellbeing of the inspectors involved. The relative benefits and risks of in person inspection vs remote/drone assessment to identify anomalies in defences are discussed.

Chapter 9 – Problem identification and diagnosis

Chapter 9 describes how flood defences behave under hydraulic loading and outlines the main failure mechanisms, including overtopping erosion, internal erosion, slope instability, and structural failure. A key table explains how each failure mechanism may or may not be relevant to each defence types. The chapter identifies early warning indicators for each mechanism such as boils, cracks, seepage, and deformation. The role of fragility curves in capturing the performance of defences with and without interventions is explained. The chapter explains how small defects can escalate into major breaches if not detected and addressed promptly.

Chapter 10 – Selecting and designing measures

Chapter 10 describes how emergency measures are selected once a problem has been diagnosed. It explains the factors influencing selection for the approach(es) to deal with each failure mechanism including available time, resource constraints, site accessibility, and expected hydraulic conditions during installation. The chapter provides an overview of common measures such as crest level raising to reduce overtopping, reducing the load on

the defence, strengthening the defence, providing erosion protection. It emphasises rapid but defensible decision-making supported by pre-established measure catalogues and engineering judgement. Approaches to closing breaches in flood defences (should they occur) are also discussed.

Chapter 11 – Techniques for emergency measures

Chapter 11 expands on the engineering considerations required to design and execute emergency measures in the field, stressing time and logistical constraints and the need to follow best practices even for simple techniques. It describes how material properties, geometry, anchoring, load paths, and expected duration influence design choices for each of the response approaches. The chapter emphasises simplicity, robustness, and adaptability, recognising the constraints of emergency conditions. A key table explains how each technique can be applied to deliver one of the measures set out in the previous chapter. Considerable attention is given to the commonly used approaches including the creation of structures using sandbags or big bags, mobile flood defence systems and pumping systems.

Chapter 12 – Logistics and implementation

Chapter 12 explains how logistics underpin all emergency management activities. It outlines mobilisation of personnel, equipment, and materials; site access; safety management; and coordination with other emergency services, making use of pre-identified resource depots, reliable supply chains, transport planning, and mutual-aid arrangements. The chapter highlights common bottlenecks—fuel shortages, equipment breakdowns, access constraints—and strategies to mitigate them. It emphasises balancing resource demand with availability, particularly during large-scale events. The chapter emphasises rehearsed procedures, clear leadership, and effective communication. It discusses operational challenges such as night-time work, unstable ground, and rapidly changing hydraulic conditions. Examples illustrate how implementation strategies vary depending on defence type and available resources.

Chapter 13 – Health, safety and wellbeing

Chapter 13 focuses on the health safety and welfare of personnel involved in emergency operations. It emphasises the need for a culture of health safety and welfare to be embedded in policies and plans and the importance of risk assessments and training.It outlines physical risks such as unstable ground, fast-flowing water, heavy machinery, and

adverse weather, as well as organisational measures required to manage them. The chapter emphasises safety briefings, protective equipment, supervision, and rest cycles. It also addresses psychological wellbeing, recognising the stress and fatigue associated with prolonged emergency work. Examples show how partner organisations involved with the IHEMFD have integrated safety management into flood response.

Chapter 14 – Reliability of emergency measures

Chapter 14 has been included because emergency measures cannot prevent all failures of flood defence and may still fail either by incorrect design and installation, failure to complete the required tasks within the available time or operational failure. Methods for quantifying the reliability of measures are explained, using case studies of known failures. Examples of training exercises incorporating assessment of reliability are given.

Chapter 15 – Sharing knowledge and collaborating

Chapter 15 highlights the importance of knowledge exchange across organisations, regions, and countries in helping to mitigate defence failures during floods. It describes collaborative mechanisms such as joint exercises, shared databases, training programmes, and communities of practice. The chapter emphasises learning from past events, near-misses, and innovations. It also discusses how international collaboration—such as that underpinning the IHEMFD—helps harmonise terminology, improve interoperability, and accelerate learning.

Chapter 16 – Justifying the required funding

Chapter 16 examines how organisations justify and secure funding for emergency preparedness and response. It explains the challenge of investing in capabilities that may be used infrequently but are essential when needed. The chapter discusses the importance of demonstrating value to policymakers and the public using tools such as cost–benefit and multi-criteria analysis. It highlights the need for sustained investment in training, equipment, and organisational capacity.

Chapter 17 – Making it work

Chapter 17 provides guidance on implementing the handbook within organisations. It introduces maturity levels for emergency management capability and offers a step-by-step tool for self-assessment and improvement planning. The chapter emphasises that the handbook is a living document and encourages users to contribute to future revisions

through the international Community of Practice. It highlights early examples of organisations using the maturity model to identify gaps and strengthen preparedness.

4. COMPLETION, IMPACT, AND EARLY APPLICATION

A comprehensive and coherent handbook was eventually completed and published at the end of 2024. Key success factors included:

- A clear roadmap, agreed by all partners
- Development of common language concepts and definitions
- Iterative drafting, beginning with skeleton chapters
- An ambitious timeline, which maintained momentum
- Extensive virtual collaboration, accommodating time zones
- A strong editorial team, with multiple reviewers per chapter

Subsequently, the handbook has been widely disseminated. As at the end of 2025, the handbook had already been downloaded more than 1800 times, covering 37 countries (see Figure 6). More than 640 individuals have joined the associated Community of Practice.



Figure 4. Map of showing countries which have downloaded the IHEMFD *(source: Bart Vonk).*

Mapa pokazująca kraje, które pobrały IHEMFD (źródło: Bart Vonk).

The handbook has attracted interest from international organisations, including UNDRR (United Nations Office for Disaster Risk Reduction) and UNESCO. UNDRR have provided a link to the handbook on their Prevention Web (see https://www.preventionweb.net/publication/international-handbook-emergency-management-flood-defences). UNESCO has adopted the handbook for educational purposes, and IHE-Delft is developing a two-week course based on it, financed by EU Interreg project BONSAI.

Early applications have included the following:

- Self-assessments by German water authorities and a fire brigade using the concept of maturity levels for emergency management organisations. These assessments were carried out using the tools for self-assessment and improvement planning provided in Chapter 17 of the IHEMFD and were deliverables for the EU Interreg project FlashFloodBreaker.
- A Japan–Netherlands collaboration on early warning systems
- Training and capacity-building initiatives

5. Conclusion

The *International Handbook on Emergency Management of Flood Defences* represents a significant advancement in global flood resilience. It fills a critical gap between long-term asset management and real-time emergency response, providing a practical, internationally informed guide for practitioners. Its development required extensive collaboration, negotiation, and editorial effort, but the result is a coherent, comprehensive, and widely applicable resource. As climate change increases the frequency and severity of extreme events, the handbook will play an increasingly important role in supporting safe, effective, and coordinated flood defence emergency management worldwide.

6. Acknowledgements

Rijkswaterstaat (Netherlands) managed the overall IHEMFD project and funded coordination and support. USACE (USA) funded the graphic design of illustrations, the Environment Agency (UK) funded the lead editor, and MLIT (Japan) managed the publishing.

References

CIRIA (2013) *The International Levee Handbook*. Report RP957, London: CIRIA. ISBN: 978-0-86017-734-0

CIRIA (2014) The International Levee Handbook training webinars, available at https://www.ciria.org/Resources/Free_publications/I_L_H/ILH_Chapter_overviews.aspx

Gouldby, B. and Samuels, P. (2005) *The language of risk*. FLOOD*site* document T32-04-01 available at https://www.floodsite.net/html/partner_area/project_docs/floodsite_language_of_risk_v4_0_p1.pdf

Jonkman, S.N., Curran, A., and Bower, L.M. (2024) "Floods have become less deadly: an analysis of global flood fatalities 1975-2022." *Natural Hazards* Vol 120: 6327–6342. DOI: 10.1007/s11069-024-06444-0.

Vonk, B., Huijskes, E., Simm, J., Helms, W., Thornely, B., Lilley, P. and Tsimopoulou, V (eds) (2024) *International Handbook on Emergency Management of Flood Defences*. Rijkswaterstaat, Utrecht, and Japan Bosai Platform, Tokyo. Available at www.rws.nl/en/handbook

Effective renovation and sealing of hydraulic structure beds and slopes using controlled underwater concreting with synthetic formwork: practical implementation insights

Jarosław Ajdukiewicz

INORA
Przedsiębiorstwo Realizacyjne INORA Sp. z o.o.
ul. Prymasa Stefana Wyszyńskiego 11; 44-100 Gliwice

Abstract

The presentation will discuss practical experiences gained during the renovation and sealing of hydraulic structures using controlled underwater concreting with temporary synthetic formwork. The talk will introduce the principles of the technology, explain how synthetic formwork enables precise concrete placement under water and illustrate its advantages through few case studies. The execution process will be outlined step by step, including installation of the formwork and controlled filling. Key challenges encountered during construction will be presented together with the solutions applied on site. The presentation will conclude with a summary of lessons learned, recommendations and guidance on when this technology provides the greatest technical and economic benefits.



PROCEEDINGS

